Natural Products and Their Derivatives in Cancer Prevention and Therapy: Inositol Phosphates and Illudin S

A DISSERTATION
SUBMITTED TO THE FACULTY OF THE GRADUATE SCHOOL
OF THE UNIVERSITY OF MINNESOTA
BY

Xiaodan Liu

IN PARTIAL FULFILLMENT OF THE REQUIREMENTS
FOR THE DEGREE OF
DOCTOR OF PHILOSOPHY

Shana J Sturla, PhD
Advisor

October, 2009

Acknowledgements

First and foremost, I would like to express my most sincere gratitude and appreciation to my advisor, Dr Shana J. Sturla, for her support, patience, encouragement and guidance throughout my graduate study. She was always willing to listen and ready to give her advice to help me out from many difficulties in my research and my life in Minnesota. Her energetic working style, enthusiasm to science, and scientific attitude will greatly influence my future scientific career.

I thank the other members of my dissertation committee — Professors Stephen S. Hecht, Robert Vince, and Phillippe Buhlmann for their feedbacks and suggestions on my research, which are valuable to improve the quality of this work. I also thank Dr Hecht and Dr Vince for their help with my job seeking.

I thank the former members of Dr Sturla's laboratory, Thu N.T. Nguyen, who was the first person I knew in Dr Sturla's lab and helped to get familiar with everything in the lab. A special thank you to Dr Jiachang Gong who encouraged me a lot on my study and research, I really appreciate the conversation with him that cheered me up and stimulated me thinking deeply on my research. I wish to acknowledge all the other members in Dr Sturla's lab, James Neels, Jolanna Norton, Dr Ganesan Vaidyanathan, Rahul Lad, Dr Marina Tanasova, Kathryn Peitsch, Hailey Gahlon, Heidi Dahlmann for useful suggestions and help. I enjoyed working and talking with them as they made the lab a fun place.

I thank Dr Patrick E. Hanna for the discussion, suggestions, and encouragements during the preparation of my paper manuscripts.

I thank all my friends in the department of medicinal chemistry, Xin Zhou, Li Liu, Tsui-Fen Chou, Qing Li, Yan Jia, Siyi Zhang, Swapna Bhagwanth and Xingnan Li for their friendship and support that have given so much fun and have carried me on through all the difficult time during my study here.

I gave many thanks to Dr Peter Villalta for his leading me into the area of Mass spectrometry. I also thank Brock Matter for his useful suggestions on characterizing protein adducts with ion trap mass spectrometer.

Last, I could not have completed all the requirements for my degree without the support of my family, especially my husband Zhibing Yang, and my parents, Shuhua Liu and Yuxi Liu.

Table of Contents

List of Tables

Chapter Two

Chapter Four

List of Figures

Chapter Four

Chapter Five

Chapter Six

Chapter Seven

List of Schemes

Abbreviations

Ins	*myo*-inositol
InsPs	*myo*-inositol phosphates
$InsP_1$	*myo*-inositol monophosphate
$InsP_2$	*myo*-inositol bisphosphate
$InsP_3$	*myo*-inositol triphosphate
$InsP_4$	*myo*-inositol tetrakisphosphate
$InsP_5$	*myo*-inositol pentakisphosphate
$InsP_6$	*myo*-inositol hexakisphosphates
AMP	adenosine 5'-monophosphate
ESI	electrospray ionization
LOD	limit of detection
TD-Ins(4,5)P_2S_2	1D-1,2,3-trideoxy-*myo*-inositol-4,5-bisphosphorothioate
DD-Ins(1,4,5)P_3S_3	1D-2,3-dideoxy-*myo*-inositol 1,4,5-trisphosphorothioate
CID	collision-induced dissociation
DTT	DL-Dithiothreitol
AMPS	adenosine 5′-O-thiomonophosphate
TEAB	triethylammonium bicarbonate
MS	mass spectrometry
GR	glutathione reductase
GSH	glutathione

AF	acylfulvene
HMAF	6-hydroxymethyl acylfuvlene
DMEM	Dulbecco's modified Eagle's medium
FBS	fetal bovine serum
GSSG	oxidized glutathione
NADPH	reduced nicotinamide adenine dinucleotide phosphate
EtOAc	EtOAc
AOR	NADPH-dependent alkenal/one oxidoreductase
TFA	trifluoroacetic acid
NWML	nominated molecular weight limit
BCA	bicinchoninic acid
Trx	thioredoxin
TrxR	thioredoxin reductase
DTNB	5,5'-dithio-bis(2-nitrobenzoic acid)
Cys	cysteine
BIAM,	biotin-conjugate iodoacetamide
Trp	tryptophan
TCA	trichloroacetic acid
Gpx	glutathione peroxidase
Se	selenium
Sec	selenocysteine

Chapter One: Introduction

1 Natural products and cancer

Data regarding death rates by diseases over the last fifty years indicate that only cancer death rates remain unaltered while the deaths caused by other major chronic diseases such as heart disease and influenza decreased significantly during that period (Figure 1).[1] Furthermore, if no urgent and effective actions are taken, cancer rates could further increase to 15 million new cases and 10 million new deaths in 2020.[2] Carcinogenesis is a multistage process consisting of initiation, promotion, malignant conversion, and progression.[3-5] Thus, the multistage sequence of events offers chances for intervention to prevent, inhibit, delay, or reverse the progress of carcinogenesis. One third of cancers are preventable and another third are treatable with early detection.[6] Nature provides us with a fertile pool of resources that have yielded effective agents to fight against human cancers in both preventive and therapeutic strategies.

Cancer prevention is gaining more attention with the increasing knowledge of cancer at epigenetic, genetic, molecular and cellular levels. There are at least two ways to reduce cancer risk: avoiding exposure to cancer-causing biological, chemical and physical agents, and consuming chemopreventive agents. Numerous dietary components from grains, nuts, cereals, spices, fruits vegetables, beverages and botanical agents from medicinal plants and herbs have been show to possess strong chemopreventive properties for a variety of cancers. Among them, *myo*-inositol, tea polyphenols, curcumin, resveratrol, genistein, and lycopene are in clinical trials with respect to their preventive activity against a variety of human cancers including lung, colon, prostate, cervical, skin, and breast cancer.[7-12] Dietary chemopreventive agents are divided into two broad classes on the basis of their window of effectiveness: blocking agents and suppressing agents. Blocking agents act concurrent with carcinogen exposure by preventing metabolic activation of carcinogens to reduce the likelihood of cellular DNA and protein damage. Suppressing agents suppress cell replication or induce apoptosis by inhibiting the inappropriate activation of cellular transcription factors such as NF-κB and AP-1.[13] Blocking agents have also been found to function by inhibiting carcinogen-activating phase 1 enzymes and/or inducing carcinogen-detoxifying phase 2 enzymes through Nrf2 activation, which facilitate the elimination of endogenous and environmental

carcinogens. As in the case of isothiocyanates that are abundant in cruciferous vegetables, the phase 2 detoxifying enzymes such as quinone reductase and glutathione transferase are induced.[14-16]

Extensive research on molecular targets and mechanism of action has blurred the boundary between cancer prevention and therapy. Many natural products possess not only cancer preventing properties, but also are active for cancer treatment, such as curcumin,[17-20] and *myo*-inositol hexaphosphate.[21-23] Humans have relied on nature for disease remedies for thousands of years. Even now, around 80% of the world's inhabitants take traditional plant-sourced medicines for their primary health care.[24] Over 60% of the currently used anticancer drugs originate from natural sources. Particularly in the area of cancer, from 1981 to 2006, 63 of 81 (77.8%) of approved anticancer drugs were either natural products or were derived or mimicked natural products.[25]

Progress in modern screening, extraction, and analysis techniques facilitates the detection, isolation, and characterization of bioactive ingredients from the natural matrix.[26-36] Conventional anticancer drugs mainly are capable of inhibiting cancer growth regardless of their chemical nature and underlying mechanism of action. In cancer cells, multiple signal transduction and gene expression pathways are dysfunctional.[37, 38] Extensive studies regarding molecular mechanisms of traditional chemotherapeutic compounds, such as curcumin and isoflavones, suggest that multiple cellular targets are involved in modulating different signaling pathways with an overall result of toxicity.[39, 40] Likewise, modern combination therapies also aim for modulating multiple targets.[41, 42] In contrast, targeted therapeutics are proposed to be promising for their potential as the basis of individualized therapies with fewer side effects. A potential drawback of the single target approach is whether the potency of the drug is adequate enough to reverse cancers and overcome drug resistance.[43] On either side of the controversy, it remains critical to understand mechanisms of action for chemopreventive and anticancer natural products with respect to cellular targets, and chemical and biochemical transformations.

2 *Myo*-inositol (Ins) and *myo*-inositol phosphates (InsP) in nutrition, biochemistry, and cancer

Ins is a hydroxylated cyclohexane scaffold for varying degrees of stereospecific phosphorylation, which results in 63 possible InsP isomers with different numbers of substituted phosphate groups and at different sites on the inositol ring.[44] Ins is also the structural basis for another group of cellular signaling molecules phosphatidylinositol phosphate (PtdInsP) which are the most abundant inositol lipid in mammalian membranes.[45] InsPs are intracellular second messengers in eukaryotic cells. Among them, Ins(1,4,5)P_3 has been extensively studied in the regulation of calcium signaling.[46] In response to extracellular stimuli, Ins(1,4,5)P_3 is released from the membrane-bound PtdIns(1,4,5)P_3. The binding of $InsP_3$ to its receptors located on the endoplasmic reticulum (ER) causes calcium release from the ER, which triggers various cellular responses.[47] $InsP_3$ is rapidly converted to other InsPs through reversible phosphorylation and dephosphorylation by corresponding phosphatases and kinases in a complex biochemical metabolism network participating in cell signaling regulation (Figure 2).[48] Knowledge regarding the functions of InsPs other than Ins(1,4,5)P_3 in cell signaling has accumulated significantly in the past twenty years,[46] and data suggest a critical role for Ins compounds in biochemical processes of living organisms.

Phytic acid ($InsP_6$), the principle phosphorus carrier for many plants, is the predominant InsP contained in substantial amounts in grains, nuts, and legumes. Compared to $InsP_6$, lower InsPs exist in relatively small amounts, and they can be formed from the degradation of $InsP_6$ by phytase or other phosphatases, gastrointestinal digestion, food processing, or storage.[49] Although studies regarding higher InsPs indicate that they impair the absorption of minerals including calcium, iron, and zinc by chelating and precipitating these cationic minerals.[50-55] InsPs in foods are regarded as a significant source of *myo*-inositol, which plays a critical role in the health of central nervous system as a natural precursor for InsPs and PtdInsPs.[56, 57]

Ins and InsPs have been shown to possess cancer chemopreventive and chemotherapeutic properties in cancer cells and animal cancer models.[58-62] Ins suppresses liver and lung carcinogenesis in mice,[63-65] and $InsP_6$ inhibits colon and breast

carcinogenesis.[66-69] Ins and InsPs were also found to be involved in Aβ aggregation in Alzheimer's disease.[70] $InsP_6$ have been shown to inhibit the proliferation of a variety of human cancer cells including colon, pancreatic, breast, large intestine, and prostate cancer when treated alone or in combination with other anticancer drugs.[22, 23, 71-78] In cancer and pre-cancerous cells, degradation of $InsP_6$ to Ins or $InsP_1$-$InsP_5$ could enhance its activity,[79] however the underlying mechanisms are poorly understood and lower InsPs are hypothesized to play a role.[73, 80]

Although Ins and InsPs are significant in so many different areas including nutrition, physiology, and pharmacy, their rapid enzyme-mediated interconversion in biological systems combined with a lack of selective and sensitive analysis methods suitable for complex biological sources limits advances in understanding relevant biological mechanisms and relative distributions. Thus enzyme-stable analogs as well as advanced analysis methods are, the topics addressed by the research described in Chapters 2 and 3 of this thesis, are expected to be helpful scientific tools for addressing these and other fundamental questions regarding Ins compounds in health and disease.

3. Cellular Redox Regulation and Cancer Chemotherapy

In response to stress, cellular enzymatic redox systems not only contribute to antioxidant defense but also influence the functional activity of various other enzymes that further regulate many vital cellular events including gene expression, cell proliferation, differentiation, and apoptosis.[81-83] Under physiological conditions, endogenous oxidants such as nitric oxide and hydrogen peroxide act as second messengers, reversibly modulating signaling pathways via redox enzymes to achieve their physiological functions.[84, 85]

Cysteine residues play important roles in the biochemistry of many proteins because of the unique chemical properties of this amino acid. The primary thiol possesses high reactivity, redox properties, and an ability to coordinate metal ions.[86] These features are even further potentiated when the sulfur is displaced by selenium to generate the selenocysteine.[87] Sec is incorporated into selenoproteins either during protein synthesis with UGA, a codon for translation termination, or through post-translational process.[88]

Cellular redox regulation in large part is maintained by a diverse group of thiol oxidoreductases through thiol/disulfide exchange or cysteine modification.[89] Thiol groups of redox-sensitive cysteines in proteins have lower pK_a values (4-6) than physiological pH, which therefore present as deprotonated, highly reactive thiolate anions.[90-92] The reversible thiol/disulfide exchange reaction is a sensitive switch for cells to transduce signals within the signaling cascades comprised of redox proteins, by which the proteins' conformation and activity are modulated in analogy to tyrosine phosphorylation in kinase signaling cascades.[93] Signaling by endogenous reactive oxygen species is mainly through reversible or irreversible modification of cysteine residues in proteins, such as S-nitrosylation by nitric oxide and conversion to sulfonic acid by hydrogen peroxide.[94, 95] In addition to redox signaling, thiol/disulfide homeostasis also is critical for proper protein function. Thus a disruption can impact downstream events involving the functions of various proteins including enzymes, chaperones, and transcription factors.[96-105]

The glutaredoxin (Grx) system, together with the thioredoxin (Trx) system forms the major regulator of cellular redox homeostasis and keeps a reducing thiol-rich intracellular redox state.[106] Both systems draw their reducing potential ultimately from NADPH.[107] The Grx system includes glutathione (GSH), the most abundant small molecule thiol in the cell (1-12 mM), glutaredoxin, and glutathione reductase (GR) which reduces oxidized GSH to regenerate GSH. The Trx system contains thioredoxin reductase (TrxR) and its protein substrate thioredoxin (Figure 3). Grx and Trx are both small thiol/disulfide oxidoreductases (9-16 kDa). Grx's usually have CPYC as the active site sequence and are able to catalyze reactions by a thiol/disulfide exchange mechanism in proteins and also catalyze the reduction of protein-GSH mixed disulfides.[106] Trx also has a similar active site motif WCGPCK and it has been established as having a critical role in DNA synthesis, DNA transcription, cell growth,[108] and cell apoptosis by reductively regulating key enzymes. GR and TrxR are both flavin enzymes and share great similarities with respect to structure and activity. However, the presence of selenocysteine at the C-terminus active site of TrxR makes it more reactive towards cellular electrophiles, and the flexibility of C-terminus active site broadens the range of TrxR substrates significantly.[109, 110] Although glutathione is the most abundant small

molecule thiol in the cell, the active redox pool comprised of protein thiol overwhelms glutathione (70% vs. 30%).[111] Consequently, protein thiol can be more directly involved in cellular redox signaling.[112] Especially, the alterations of redox signaling proteins play a significant role in the pathology of human diseases including cancer and cardiovascular disease, the two major death-causing chronic diseases in the U.S.[1, 113-116]

Increased Trx and TrxR levels have been detected in many human primary cancers compared to normal tissue including breast, prostate, cervical, ovarian, and pancreatic cancers.[114, 117-119] Knock-down of TrxR led to a remarkable reduction of tumor progression and metastasis and a significant decrease of cancer-related proteins in lung cancer.[120] The underlying mechanism for the participation of Trx systems in cancer initiation and progression is hypothesized to involve their role in redox signaling by inactivating tumor suppressors such as p53, increasing the supply of reducing equivalents for DNA synthesis from ribonucleotide reductase, and activating transcription factors such as NF-κB to over-stimulate cell growth and sensitize cells to growth factors.[121, 122]

As a consequence of the altered redox state in cancer cells, the regulation of thiol-dependent signaling cascades are dysfunctional. This situation offers an intervention opportunity for the development of anticancer therapeutics. Targeting redox-active cysteines of Trx or Grx system enzymes by anticancer compounds have been reported and linked to their anticancer mechanism. Due to the extraordinary reactivity of selenocysteine at the active site of TrxR, anticancer compounds such as cisplatin,[110] auranofin (a gold complex),[123] arsenic compounds,[124] curcumin (a polyphenol), and flavonoids[125, 126] are all potent TrxR inhibitors via reversible or irreversible interactions with active site cysteines. Similarly, there are various examples of GR inhibition as a therapeutic strategy: antimalarial agents,[127] agents to decrease drug resistance,[128] and agents with anticancer activity.[129] According to the quantitative analysis of global cellular thiol/disulfide status, intracellular Cys-containing proteins are not constitutively reduced, and instead may remain oxidized during redox signaling in response to oxidant diamide.[111] In accord with this, some potent inhibitors of redox-regulating enzymes are allosteric. For example the Trx inhibitor PX-12 inhibits Trx activity by covalent

modification on Cys^{73} which is important for the Trx dimerization by forming a disulfide bridge between two monomers.[86, 130]

4. Natural cytotoxin illudin S and its acylfulvene analogs

Acylfulvenes (AFs) are semisynthetic analogs derived from the mushroom toxin illudin S, but AFs possess better antitumor selectivity than illudin S. The AF and illudin S, based on preliminary data regarding bimolecular binding and impact on DNA synthesis are suggested to act as alkylating agents through electrophilic α,β-unsaturated ketone and/or cyclopropane ring. The structurally related sesquiterpene compound, natural product ptaquiloside which also has the key allylic cyclopropane, was found to produce DNA lesions by reacting at cyclopropane ring.[131-133] However, compared to other conventional alkyalting agents such as cisplatin and mitomycin, acylfulvenes display some unique features, which was hypothesized to be attributed to the specific bioactivation by cellular NADPH-dependent reductase.[134-138] Considering that AFs maintain the same scaffold as illudin S and they can also be catalyzed by the same enzyme, it is still unclear the underlying mechanism for their improved selectivity.[139] The studies on modulation of cell sensitivity towards illudin S by cellular GSH level and different reactivity of small thiols with illudin S and AFs suggest that reaction with cellular thiols may play a role for illudin S extreme toxicity.[140-142] A central hypothesis addressed in chapters 4, 5, and 6 of this thesis is that disruption of cellular redox homeostasis by inhibition of redox-regulating enzymes in part dictates selectivity patterns for AFs cytotoxicities.

5. Overview of the thesis

This findings described in this dissertation contribute to building our understanding of cancer prevention and therapy mediated by natural products and their derivatives, which is important for their clinical application and for design of more targeted synthetic compounds. The work described in Chapter 2 illustrates a novel bioanalytical approach for simultaneous analysis of naturally occurring inositol and inositol phosphates, which was applied to analyzing the distribution of these compounds in dietary samples and cancer cells. Furthermore, the method facilitates the biological evaluation of an enzyme-resistant inositol triphosphate analogue described in Chapter 3. The studies described in

Chapter 3 involve testing the biological and chemical reactivity of synthetic analogues that were designed and synthesized for the purpose of probing the role of second messenger Ins(1,4,5)P_3 in chemoprevention and other biochemical processes that cannot be realized due to its metabolic instability. The work described in chapters 4, 5 and 6 demonstrates the differential influences of small molecules on critical cellular redox-regulating enzymes including glutathione reductase, thioredoxin, and thioredoxin reductase. The focus of these studies was the antitumor natural product illudin S and its acylfulvene derivatives. The inhibition of enzyme reductase activity, influence on the protein conformation, interaction with the active site cysteines, and impact on corresponding cellular proteins by these compounds were evaluated and compared. Our results reveal reactivities of these compounds towards thiol-containing redox-regulating enzymes that are unexpected on the basis of reactivity patterns toward thiol-containing small molecules such as cysteine and glutathione. These data contribute to understanding mechanisms underlying acylfulvenes' improved anticancer selectivity, and, more broadly, for exploring the possibility of modulating redox-control systems in a selective manner for anticancer therapy. Finally, Chapter 7 provides a discussion of some related observations concerning the reactivity of acylfulvenes.

Figure 1. U.S. death rates by causes in 1900, 1950, and 2000. Rates are per 100,000 and are age-adjusted to the 2000 U.S. standard population[1].

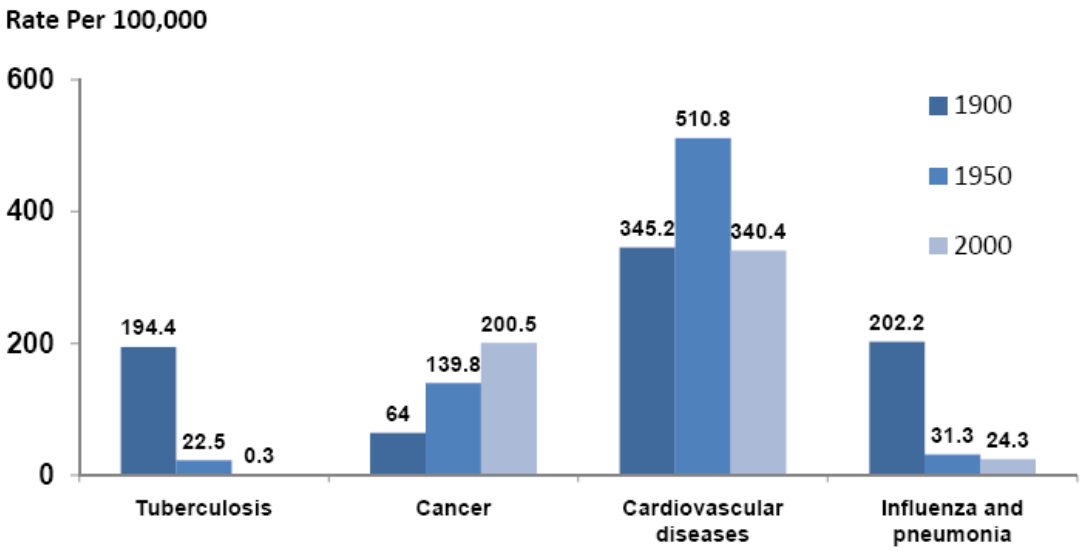

[1] *Source:* 1900-1970, U.S. Public Health Service, *Vital Statistics of the United States,* annual, Vol. I and Vol II; 1971-2001, U.S. National Center for Health Statistics, *Vital Statistics of the United States,* annual

Figure 2. Complex network of *myo*-inositol and different *myo*-inositol phosphates in biological systems. Adapted by permission from Macmillan Publishers Ltd: Nature Reviews Molecular Cell Biology[46], copyright (2001)

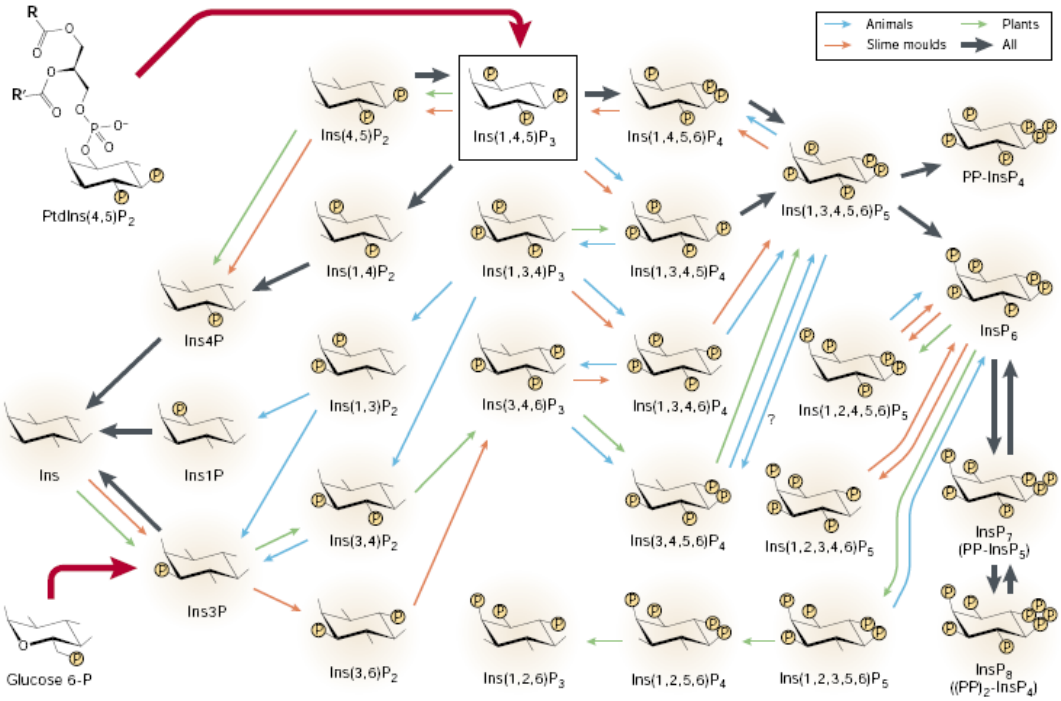

Figure 3. Redox cycles and mechanisms for Trx system.

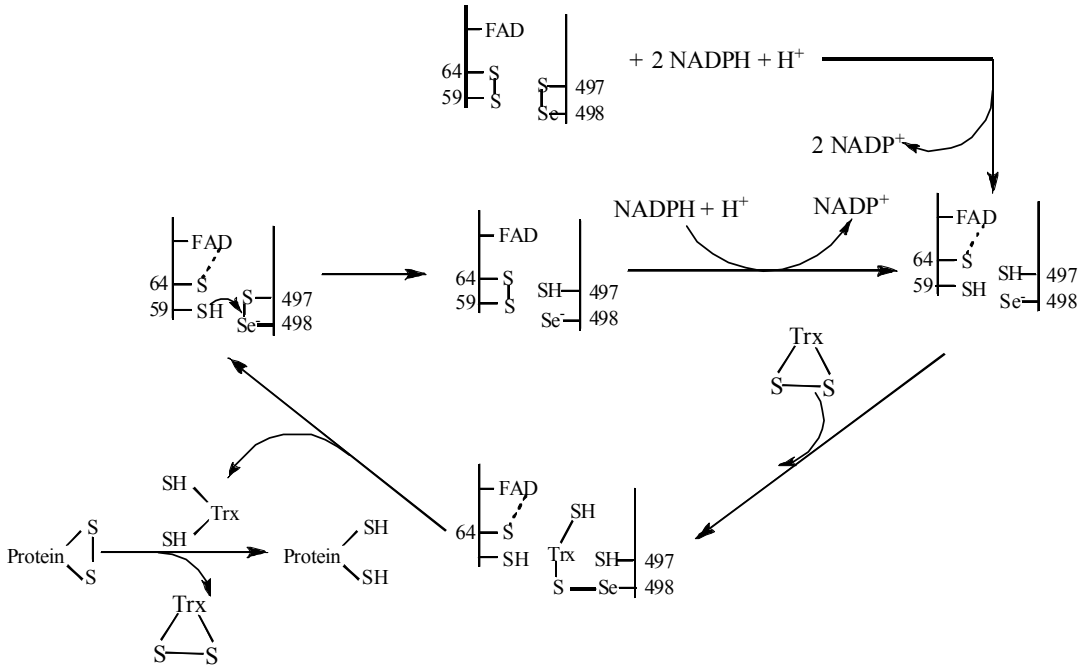

Part I. Analysis of inositol, inositol phosphates, and an enzyme-resistant analog

Myo-inositol (Ins) and *myo*-inositol phosphates (InsPs) are widely distributed in plants and animals. The evaluation of Ins and InsPs distribution in cells and plant sources can impact the understanding of their role in nutrition, cellular processes and diseases, and how they may be modulated by diet. We developed an anion-exchange chromatography-tandem mass spectrometry (HPLC-ESI-MS/MS) method for the separation and simultaneous quantitation of Ins and different naturally occurring phosphorylated inositol compounds. Chromatographic separation was achieved in 30 min on a commercial anion exchange column (150 × 0.5 mm) using a gradient of 200 mM ammonium carbonate buffer (pH 9.0) and 5% methanol in H_2O. Analytes were identified by selective reaction monitoring using a triple quadrupole mass spectrometer in negative ion electrospray mode. Adenosine 5'-monophosphate was used as a general internal standard for quantitation. Using this approach, Ins and InsPs were measured in three different plant samples and in cultured cell, illustrating significant differences in the distribution of inositol compounds in food sample compared to cells and between cell types.

Ins and InsPs are cellular second messenger with potential roles in cancer prevention and therapy. It typically is difficult to attribute specific pharmacological activity to a single inositol phosphate because they are rapidly metabolized by phosphatases and kinases. We designed stable analogs of Ins(4,5)P_2 and Ins(1,4,5)P_3 that maintain the biological activity, but are phosphatase and kinase-resistant LC/MS/MS analysis of the enzyme-catalyzed reaction products indicates the phosphorothioate analog of Ins(1,4,5)P_3 is stable towards alkaline phosphatase, and under the same condition, the natural ligand was extensively hydrolyzed. Analogs developed in this study are potential chemical probes for understanding mechanisms of inositol phosphate actions that may be elucidated by eliciting specific and prolonged activation of the Ins(1,4,5)P_3 receptor.

Chapter Two: Simultaneous determination of inositol and inositol phosphates in complex biological matrices: quantitative ion-exchange chromatography-tandem mass spectrometry[*]

[*] Portions reproduced with permission from Xiaodan Liu, Peter W. Villalta, Shana J. Sturla. (2008) Rapid Commu. Mass Spetrom. (23): 705-712.

1. Introduction

Myo-inositol (Ins) is a scaffold for varying degrees of stereospecific phosphorylation, which results in 63 possible inositol phosphate isomers (Figure 1).[44] Phytic acid (inositol hexakisphosphate, $InsP_6$), contained in substantial amounts (~ 1-20 μmol/g) in oilseeds, cereals, nuts and other crops, is the principle carrier of phosphorus and a precursor of inositol phosphates.[49, 143] In plants, the lower inositol phosphates ($InsP_1$-$InsP_5$) are widely distributed in relatively small and varying amounts and also can be formed from the $InsP_6$ degradation during gastrointestinal digestion and food processing and storage. Ins, lower inositol phosphates, and $InsP_6$ are involved in signal transduction in eukaryotic cells, and the main second messenger, Ins(1,4,5)P_3, has been extensively studied.[46] Stimulation of $InsP_3$ receptors located on the endoplasmic reticulum (ER) causes calcium release from the ER, which stimulates an array of cellular responses.[47] $InsP_3$ is rapidly converted to other InsPs by phosphorylation and dephosphorylation in a complex biochemical network participating in cell signaling regulation. Thus, a putative approach to address the roles of specific inositol phosphates has involved stabilized synthetic analogs.[144]

Ins and InsPs are demonstrate cancer chemopreventive and chemotherapeutic properties in cancer cells and animal cancer models.[58-62] Ins suppresses liver and lung carcinogenesis in mice.[63] Ins and InsPs were also found to be involved in Aβ aggregation in Alzheimer's disease.[70] More recently, other stereoisomers of Ins were reported to be of therapeutic importance for human neuropsychiatric disorders.[145] In cancer and pre-cancerous cells, degradation of $InsP_6$ to inositol and $InsP_1$-$InsP_5$ could enhance its activity,[79] however the underlying mechanisms are poorly understood and lower InsPs are hypothesized to play a role.[73, 80]

Although Ins and InsPs are significant in so many different areas including nutrition, physiology, and pharmacy, their rapid enzyme-mediated interconversion combined with a lack of selective and sensitive analysis methods suitable for complex biological sources limits advances in understanding relevant biological mechanisms. Analytical difficulties in separating and detecting InsPs relate to their low abundances, lack of spectrophotometric absorbances, and high charge states. High-performance

chromatographic techniques including anion-exchange chromatography,[146] gas chromatography after derivatization,[147] ion-pair chromatography,[148] and thin-layer chromatography[149] have been used to separate Ins and InsPs. Inositol phosphates are negatively charged, therefore flow injection-capillary zone electrophoresis can attain high separation efficiencies, but has limited sensitivity (~ 10 μM) and robustness for analyzing large sample sets.[150] A common strategy for detecting InsPs is colorimetric analysis of derivatives. Phosphates can be detected by molybdate staining followed by heating and UV detection. Although this method is simple and inexpensive, it is subject to interferences, and unsuitable for on-line detection.[149, 151] Tetravalent transition-metal ions can bind tightly to both cation-specific dye and polyanions, which can be used for InsP detection with very high sensitivity (picomolar range).[152-155] Radiolabelling is a sensitive approach for detecting Ins and InsP, but can be expensive and it involves radioactivity.[156, 157] Chemically suppressed conductivity and thermospray mass spectrometry are direct detection methods that avoid pre- or post-column derivization.[158-160] Ion-pair chromatography associated with inductively coupled plasma-sector field-mass spectrometry can individually measure $InsP_2$-$InsP_6$ with excellent selectivity and sensitivity by monitoring $^{31}P^+$ signals.[161] $InsP_5$ and $InsP_6$ have been measured in situ by ^{31}P nuclear magnetic resonance spectroscopy.[162] Recently there has been a greater focus on applying liquid chromatography-mass spectrometry (LC/MS) and LC-MS/MS for analyzing *myo*-inositol with limit of detections (LOD) down to 600 pg and 60 pg, respectively.[163, 164] Despite the range of analytical methods investigated, none are capable of measuring Ins and InsPs simultaneously. Because of the potential broad impacts of understanding Ins and InsPs abundances and distributions and their wide range of sources, general high-throughput methods to analyze inositol compounds are needed.

In this study, we report the development and validation of a quantitative high-performance anion exchange liquid chromatography tandem mass spectrometry (LC-MS/MS) method with electrospray ionization (ESI) for the simultaneous determination of *myo*-inositol and *myo*-inositol phosphates in biological samples. ESI has poor tolerance for the typically high salt levels in the eluant from ion-exchange chromatography, which has limited the interface of ion-exchange chromatography with mass spectrometry. To

address this problem, we use a volatile ammonium carbonate eluant buffer rather than extensive desalting steps prior to introducing samples into the ion source. This method does not require derivatization and is convenient, selective, and accurate. Using this assay, we measured inositol and inositol phosphates in nut/grain samples and in human cancer cells.

2. Experimental procedures

2.1 Chemicals and materials

Myo-inositol, ammonium carbonate, and adenosine 5′-monophosphate (AMP) were purchased from Sigma (St. Louis, MO), and D-*myo*-Inositol-1-monophosphate ammonium salt, D-*myo*-Inositol 4,5-biphosphate potassium salt, *myo*-inositol 1,4,5-triphosphate ammonium salt, D-*myo*-inositol 1,4,5,6-tetrakisphosphate potassium salt, *myo*-inositol 1,3,4,5,6-pentakisphosphate potassium salt, and *myo*-inositol hexakisphosphate sodium salt were purchased from AG scientific with purity 99% (San Diego, CA), and used for making analytical standards. The phytic acid sodium salt hydrate was purchased from Sigma (St. Louis, MO) and used for in-house reference sample preparation. The purity of commercial chemicals was greater than 99% and used as supplied. Glacial acetic acid, sodium hydroxide (pellet), and methanol (HPLC grade) was obtained from Fischer (Pittsburgh, PA). Deionized water was obtained from a Milli-Q system (Millipore, Milford, MA) and filtered through a 0.22 μM pore polystyrene membrane (Corning, Pittsburgh, PA). Raw almonds, hazelnuts and oats were purchased from Cub Foods supermarket (Minneapolis, MN). Hela and MCF-7 cancer cells lines were obtained from ATCC (Manassas, VA).

2.2 Instrumentation

2.2.1 Anion exchange chromatography

HPLC was carried out on an Agilent 1100 series capillary HPLC system equipped with an autosampler. The HPLC system was interfaced with either a TSQ Quantum Ultra AM or Discovery Max (Thermo Scientific, San Jose, CA) triple quadrupole mass spectrometer with an electrospray ionization (ESI) source. Data acquisition and analysis were performed with Xcalibur software (Version 2.0). All samples were transferred into a silanized autosampler vial with a fused 100 μL inset (ChromTech, Apple Valley, MN). Injection volume was 4 μL. The column and autosampler tray temperatures were set at 25 °C. A Biobasic AX 0.5 x 150 mm 5 μm anion-exchange column (Thermo) was used. The chromatography mobile phases were Solvent A: 200 mM aqueous $(NH_4)_2CO_3$ (pH 9.0), and Solvent B: methanol and water (5:95 v/v). A gradient solvent system was used starting with 100% Solvent B, and analytes were eluted by increasing the salt

concentration to 150 mM as indicated in Table 1. Total run time was 33 min, plus 10 min wash to clear the high salt levels from the column. Total pressure of the LC/MS/MS system was typically 70 bar.

2.2.2 Mass Spectrometry

The ESI source was operated in negative ion mode. To maximize instrument cleanliness, the elutant was diverted from the mass spectrometer to waste by an electronically controlled divert valve for the initial two minutes of each run. The ion source was set as follows: spray voltage, 5 kV; ion transfer capillary temperature, 330 °C; sheath gas (nitrogen), 31 (arbitrary units). Precursor and most abundant fragment ions were obtained by scanning each analyte separately in MS full-scan mode and MS/MS scan mode. Collision energy (CE) was optimized for each analyte by direct infusion of 1 μM standard solution. Analytes were monitored by selected reaction monitoring (SRM), for relevant ions at optimized collision energies (Table 2). A summary of parent, most prominent product ion, and optimal collision energy of each analyte is shown in Table 2.

2.3 Preparation of analytical standards

Separate individual solutions of each analyte were prepared in methanol/water (5:95 v/v), and from these a mixed standard solution (200 μM Ins and $InsP_1$-$InsP_6$) was prepared. The mixed standard solution and an internal standard solution (AMP in methanol/water 5:95 v/v) were combined and further diluted with methanol/water (5:95 v/v) to produce a series of standard solutions with the following concentration of analytes: 0.5 μM, 1.0 μM, 1.5 μM, 2.0 μM, 2.5 μM, 5.0 μM, 10 μM, 15 μM, 20 μM, 25 μM, 50 μM, 75 μM and 100 μM. The final concentration of the internal standard (AMP) was 125 μM in all samples.

An in-house reference standard solution of Ins and $InsP_1$-$InsP_6$ was prepared by a modification of a published procedure.[146, 165] Thus, phytic acid sodium salt (0.30 g, 0.45 mmol) was dissolved in acetic acid (100 mL, 3.2 M) in a glass tube under a positive pressure of nitrogen and sealed with a rubber septum. The solution was heated (140 °C, 3 hours then 60 °C for 12 hours), allowed to cool to 25 °C, and the resulting solution was dried under a stream of nitrogen. The resulting residue was reconstituted in 5 mL

methanol/water (5:95 v/v) and the pH of the solution was adjusted to 7.0 by adding NaOH (6 M). Aliquots were stored at -20 °C in 1.5 mL centrifuge tubes.

2.4 Sample preparation

Three plant samples were studied: almond, hazelnut and whole grain oat. Raw nut samples were peeled to remove the skins and then ground with a mortar and pestle. The powered sample (0.5 g) was suspended in acetic acid (3 mL of 3.2 M) and homogenized (IKEA Ultra-Turrax T25 homogenizer, Cincinnati, OH) at 24000 rpm 10 times × 10 s. The resulting suspension was shaken for 3 h at 25 °C, vortex-mixed, and centrifuged (5000 g, 20 min, 4 °C). Supernatant (1 mL) was removed and diluted with water to a final aqueous volume of 20 mL. Aqueous NaOH (0.5 mL, 1 M) was added to adjust the pH to 7.0. The solution was filtered through a 0.45 μM nylon syringe filter. To remove oils, a portion of the filtrate (5 mL) was extracted by adding hexane (5 mL) and vortex-mixing for 5 minutes to remove oils. After centrifugation (5000 g, 10 min), the hexane layer was removed using a glass pipet. The final solution was evaporated to dryness on a Savant Speed Vac System (Holbrook, NY). The residues were reconstituted in 100 μL 5% aqueous methanol, and filtered using a 0.22 μM nylon syringe filter. A portion of the reconstituted solution (70 μL) was combined with internal standard solution (10 μL) in a silanized autosampler vial with insert (100 μL) such that the final concentration of AMP was 125 μM, which is the same as used in analytical standards. The peeled skin was cut into small pieces and processed separately in the same manner.

Hela cells and MCF-7 cells were cultivated in Dulbecco's modified Eagle's medium and minimum essential medium (Invitrogen) supplemented with 10% heatinactivated fetal bovine serum (PAA Laboratories, Pasching, Austria), 2 mM glutamine (PAA Laboratories), and 100 units/ml penicillin/streptomycin (PAA Laboratories). The cells were cultured at 37 °C in an incubator with 90% humidified atmosphere containing 5% CO_2. Before harvesting, cells were washed with phosphate-buffered saline and then cells were lysed with cell lysis buffer (0.01% Triton X-100 and 1 mM EDTA in 20 mM Tris-HCl buffer) in the presence of protease inhibitor cocktail. After centrifugation (10000 g, 30 min), supernatant was collected and protein concentration was quantified using the Bradford assay.[166] A volume corresponding to 0.5-

2 mg of protein from each cell extract was processed following the same procedure as described for nut meats, beginning with acetic acid extraction.

2.5 Extraction efficiency

To evaluate the efficiency associated with acetic acid-extraction of Ins and InsPs, 10 μL and 30 μL of the in-house reference standard solution (concentration of the standard $InsP_6$ in-house reference, C_s) was extracted with acetic acid (3 mL, 3.2 M) and processed as described above. The concentration was determined with reference to the standard curves. Extraction efficiency (%) was determined by comparing the differential analyte-AMP peak area ratios in processed samples (concentration after processing, C_p) versus non-processed samples (C_s) using eq.1.

Extraction efficiency (%) = $(C_p/C_s) \times 100\%$ eq. 1

2.6 Matrix effects

In-house reference standard solutions (10 μL and 40 μL) were combined with plant samples immediately after they were suspended in acetic acid (3 mL, 3.2 M). The resulting suspensions were extracted in the usual manner and analyzed with reference to the standard curves. Recovery was determined by comparing the differential analyte-AMP peak area ratios in the samples with added in-house reference standard (C_p) and the samples without adding the in-house reference standard (C_b) versus the analyte concentration in the in-house reference standard (C_s).(eq.2)

Recovery (%) = $[(C_p - C_b)/C_s] \times 100\%$. eq. 2

2.7 Characteristics of the analytical method

The analytical method was evaluated for linearity, accuracy, and precision. The calibration curves were linear over a range of 0.5-100 μM, which was determined using 16 solutions of varying concentrations measured in triplicate. A linear regression equation was derived from standard calibration curves in which peak area ratios for target analyte versus the internal standard were plotted versus the nominal standard concentration. Each calibration curve was acquired in triplicate. The intra-day variability of the method was evaluated by analyzing five different solutions on the same day (3 replicates). The inter-day variability was evaluated at five concentrations on three consecutive days. Precision was evaluated by calculating relative standard deviation

(RSD) as a percentage from the ratio of the standard deviation of observed concentration versus the observed concentration. Accuracy, i.e. agreement of the calculated concentration with the nominal concentration, was examined at three concentration levels.

3. Results and discussion

3.1 Method development

InsPs are polyanionic compounds that are well-suited for separation by high performance anion-exchange chromatography.[143, 167] Ins and InsP are ionized efficiently by negative ion electrospray when aqueous solutions are directly infused, but ESI is not generally tolerant of the high salt levels in the mobile solvent used for anion exchange chromatography, therefore the eluant typically needs to be desalted before ESI injection.[168, 169] Alternatively, volatile mobile phase additives may be used in place of common non-volatile additives[170] such as Na_2SO_4 in Tris buffer, HCl, NaOH, and ammonium phosphate, which have been used to separate Ins and InsPs.[157, 161, 171, 172] We have found that ammonium carbonate is an optimal mobile phase additive for anion-exchange chromatography and direct coupling to the ESI. A variety of commercial weak and strong capillary anion-exchange columns were investigated, with the weak anion-exchange column (Biobasic AX 0.5 x 150 mm, Thermo Scientific) chosen for effectively separating analytes within the shortest runtime and with analytes eluting in the expected sequences, first with Ins at 7 min and finally $InsP_6$ at 23 min (Figure 2). The mobile phase pH was optimized to 9.0 for InsPs ionization and separation; repeated pH 9.0 runs with high buffer concentration did not alter column performance. The optimized concentration of ammonium carbonate solution was 200 mM, by which Ins and InsPs could be separated within 25 minutes (Figure 2). The flow rate was 10 μL/min, which kept the amount of salt injected into the ESI source low. Finally, increasing the methanol concentration from 5 % to 25 % did not alter the retention time of analytes.

Stable-isotope-labeled internal standards are ideal for quantitative analysis by LC-MS/MS, however, stable isotope-labeled inositol phosphates are not commercially available and would require unreasonably time and resource-consuming syntheses.[144] Therefore, we chose to use a common internal standard with similar chemical properties. Several candidate compounds were screened as possible internal standards (Chart 1), including glucose-6-phosphate, 3-chlorobenzoic acid, 3,5-dinitrobenzoic acid, 5,5'-dithiobis(2-nitrobenzoic acid), adenosine 5'-monophosphate (AMP), shikimic acid, 2-phospho-L-ascorbic acid, 4-methylumbelliferyl phosphate, and *O*-phospho-L-tyrosine.

Among these, 2-phospho-L-ascorbic acid, 3-chlorobenzoic acid, *O*-phospho-L-tyrosine and 4-methylumbelliferyl phosphate were difficult to fragment in negative ion mode. No eluting peaks were observed for 3,5-dinitrobenzoic acid and 5,5'-dithiobis(2-nitrobenzoic acid). Shikimic acid has a tendency to form mixed populations of monomers and dimers, leading to difficulties in accurate concentration determination. Glucose-1-monophosphate has the same retention time and fragmentation patterns as $InsP_1$. AMP was selected as the optimal standard and the level of endogenous AMP is undetectable after extraction. Its retention time is 10 min and it fragments by loss of the base to produce the major product ion ribose-5 phosphate (*m/z* 211). For analysis of standard solutions at several levels (5 pmol, 25 pmol, 250 pmol) with or without AMP, retention times and detection sensitivities were unchanged. However without using AMP as internal standard to normalize the acquired data, linear fits could not be achieved (data not shown).

The electrospray ionization source was operated in negative ion mode, which yields higher S/N ratios than positive-ion-detection mode for Ins.[163] The optimal MS/MS transition for each analyte was determined by examining product ion spectra (data not shown). Ins fragmentation produces a product ion *m/z* 161, corresponding to $[H_2O]^-$ loss (*m/z* 18). $InsP_1$ fragments by inositol ring loss (*m/z* 180), and the other inositol phosphates fragment by phosphate group $[H_3PO_4]^-$ loss (*m/z* 98). A mixture of the standards in the HPLC mobile phase was infused at the HPLC flow rate into the ion source during which the source conditions and collision energies were optimized by monitoring ion currents of these product ions to maximize sensitivity.

Using AMP as an internal standard, and inositol phosphate standards, calibration curves were constructed in which peak-area ratios were related to their concentration over the concentration range. Slopes, intercepts, r^2, and linear concentration ranges from these calibration curves are summarized in Table 3. The LOD for each analyte was 0.25pmol (S/N >10). However, in the 0.25-400 pmol range, the curves for $InsP_2$, $InsP_3$, and $InsP_6$ deviate slightly from linearity giving an $r^2 < 0.98$ (Figure 3). Thus we only analyzed within the ranges resulting in an $r^2>0.994$.

To determine intra-day precision, standard samples were analyzed in four replicates at three concentrations (Table 4), and RSD% values for all analytes are below 15%. Inter-

day precisions were measured at three concentrations on three consecutive days (Table 5). The inter-day RSD% values for Ins at 40 pmol and 300 pmol, and for $InsP_3$ and $InsP_6$ at 100 pmol were higher than 15%, and the others are within 15%.

3.2 Sample preparation

For LC-MS/MS analysis of components in complex matrices, sample clean up is important to minimize ion suppression and matrix effects and maintain cleanliness of the column, ion source and mass spectrometer. A further concern for Ins/InsPs is the stability of the analytes to sample preparation, as inositol phosphates can be interconverted rapidly. We compared a variety of solutions for acidic extraction, including HCl,[150] formic acid, TFA,[154] and acetic acid. With HCl, only lower InsPs were obtained and most higher InsPs were hydrolyzed, and using TFA, all the target compounds were lost. For acetic acid and formic acid, all Ins and InsPs were recovered, however, formic acid extraction was less efficient than acetic acid since the corresponding intensity for each analyte, especially higher InsPs, was lower than that obtained from acetic acid extraction. Extractions using basic buffer (200 mM NH_4HCO_3) or base (2 M NaOH) resulted in low recoveries of all target compounds. Thus, acetic acid (3.2 M) was adopted as the optimal extraction solution for Ins and InsPs.

The sample preparation process was evaluated by measuring extraction efficiency and determining the effect of sample matrices on analyte recoveries. The $InsP_6$ in-house reference, a mixture of the analytes obtained by partially hydrolyzing $InsP_6$,[146, 165] was dissolved in acetic acid (3.2 M) prior to homogenizing followed by the same procedure as sample preparation. After processing, Ins and InsPs levels were compared to those in the parent solution. This analysis was carried out at two reference-standard concentrations and these results are shown in Table 6. Extraction efficiencies at both concentrations were similar, with Ins having the lowest recovery of 64-79%. In previous reports involving the recovery analysis of Ins from rat brain tissue or urine and saliva samples, recoveries ranged from 72-88%,[163, 164] but the sample preparation procedures had fewer and simpler steps since the target was only Ins, i.e. maximizing the extraction efficiencies of InsPs may come at the expense of lower Ins recovery. The effect of matrices on recovery was evaluated by combining the $InsP_6$ in-house reference with three different

plant matrices at two concentration levels (~4 μmol/g and ~16 μmol/g, corresponding to Recovery 1 and Recovery 2, respectively, Table 7). A comparison of the peak responses of post-extraction spiked samples with those of the $InsP_6$ in-house reference suggested that matrix effects are small by this analysis method. The recoveries for most analytes were within the range of 80-120%. In the complex matrices, the recoveries are higher than from the extraction solvent, suggesting that the matrix components may prevent analyte hydrolysis and interconversion.

3.3 Relative Ins and InsPs levels in food and mammalian cells

Dietary administration of inositol and $InsP_6$ has chemopreventive and chemotherapeutic effects in experimental animals.[59, 61] The mechanisms accounting for these observations remain unclear, and studies suggest they may be mediated by other InsPs.[173] Human diet is an important source of cellular InsPs, and the major dietary forms of InsPs are $InsP_6$, which is widely distributed in nuts and legumes.[49] In this study, we evaluated the levels of Ins and InsPs in three food samples: almonds, hazelnuts, and oats (Table 7). Figure 4 shows a representative chromatogram obtained by analyzing an extracted almond sample by the procedure described in this study. Compared with the chromatograms of standard Ins and InsPs solutions, analyte retention times shift slightly, but their identities were all confirmed by co-injection with standards. In the $InsP_4$ channel, an unknown peak (10 min) is observed for both food and mammalian cell samples (Figure 2, Figure 4 to Figure 8). We hypothesize that this is an alternative isomer of $InsP_4$, consistent with the presence of a small amount of this material in the $InsP_6$ in-house reference. Commercially available $InsP_4$ isomers (Ins(1,4,5,6)P_4 and Ins(1,3,4,5)P_4) did not co-elute with the unknown peak and it was not included in the quantitative calculations.

Total Ins and InsP levels ranged from 3 μmol/g to 53 μmol/g. $InsP_4$, $InsP_5$, and $InsP_6$ were detected at higher abundance than Ins and the other InsPs for each sample. In almonds and hazelnuts, $InsP_6$ is the dominant form (Table 7). These values are of the same order of magnitude as reported in a capillary electrophoresis study of InsPs in nuts and legumes, in which $InsP_6$ levels in nuts were measured to be higher than that in legumes.[150] The $InsP_5$ content of the oat sample is high (5.17 μmol/g) relative to other

foods analyzed, which may result from autohydrolysis of $InsP_6$ in commercial processing.[165, 172] The levels of $InsP_1$, $InsP_2$, and $InsP_3$ in almond are 1.5, 3.8, and 1.8 μmol/g respectively, which are slightly higher (2-5 fold) than the published results, while their levels in hazelnuts and oats are comparable with literature results.[150, 161, 165] Differences in results may result from differences in sample processing, for example, for almond and hazelnut, the skin was peeled and analyzed separately, and the levels of Ins and InsPs in the skin are higher than in the pulp (date not shown).

Ins and InsPs are broadly distributed in mammalian tissues and cells, performing critical roles in signal transduction.[174] Ins homeostasis and InsP signaling may be changed in certain pathophysiological conditions. It has been reported that breast tumors and colon tumors contain significantly lower inositol levels, as measured by ^1H NMR, compared to the normal tissue.[175, 176] Increased levels of $InsP_6$ protect cells from tumor necrosis factor α- and fas-induced apoptosis.[60] Augmented inositol 1,4,5-trisphosphate-mediated Ca^{2+} signaling was observed in Alzheimer disease.[177] However, in these studies the levels of Ins and InsPs changed relative to control cells, but information regarding absolute amounts of these compounds was not obtained. Therefore, it is difficult to compare results across separate studies. To explore the utility of the analytical method for studying Ins/InsPs levels in cells, we assayed the Ins and InsPs concentrations in breast cancer MCF-7 and cervical cancer Hela cells. Figure 5 shows a representative chromatogram of a MCF-7 cell extract analysis. Results are tabulated as a function of protein concentration (Table 8). The percent distributions of $InsP_4$, $InsP_5$, and $InsP_6$ of Hela cells are comparable with the published results for mice embryonic stem cells in which the level of $InsP_4$ is about four fold higher than the lower InsPs and two fold higher than $InsP_6$.[178] In contrast, $InsP_4$ was not observed in MCF-7 cells analyzed in this study. The relative ratios of $InsP_1$ to Ins (0.43 for MCF-7 cell, 0.18 for Hela cell) are higher than that in quail fibroblasts (~0.016).[179] The level of $InsP_3$ measured in these cells is about two orders of magnitudes higher than the levels of Ins(1,4,5)P_3 in rat salivary gland and cerebral cortex.[180, 181] Higher InsP levels determined in this study compared to values obtained using other methods is likely related to the presence of isomer mixtures, which are not separated in this study.

4. Conclusion

Ins and InsPs were individually and simultaneously analyzed using a novel sensitive and selective LC/MS/MS-based approach. This analytical approach fills a need for an on-line HPLC method and should be amenable to high throughput analysis. Absolute and relative levels of these biomolecules were quantified in raw dietary samples and in human cells. A limitation of the current approach is that different isomers of inositol phosphates are not chromatographically resolved. Future development and optimization of anion exchange chromatography systems may have the potential to yield an advanced system in which isomeric distributions may be evaluated. The current findings are a significant advance because anion-exchange HPLC is successfully coupled with tandem mass spectrometry for separation and detection. The availability of this analytical approach has potential to expand our knowledge of exogenous and endogenous levels of inositol and inositol phosphates, which is important for understanding their respective roles in signal transduction and other physiological processes, and for understanding relative benefits of dietary sources of inositol phosphates.

Table 1. Mobile phase gradient program.

Time (min)	a (%)	b (%)
0	0	100
3	0	100
8	50	50
28	75	25
33	0	100

a: 200 mM $(NH_4)_2CO_3$, pH 9.0;

b: methanol/water (5:95 v/v)

Table 2. Parent and product ion masses and collision energies used to evaluate Ins, $InsP_1$, $InsP_2$, $InsP_3$, $InsP_4$, $InsP_5$, $InsP_6$ and the internal standard (AMP) by HPLC-MS/MS. Retention times are also displayed for each analyte.

Analyte	Parent Mass (*m/z*)	Product Mass (*m/z*)	Collision Energy (eV)	Retention Time (min)
Ins	179	161	16	7.7±0.1
$InsP_1$	259	79	24	10.3±0.3
$InsP_2$	339	241	24	16.9±0.1
$InsP_3$	419	321	19	18.2±0.1
$InsP_4$	499	401	16	19.3±0.1
$InsP_5$	579	481	24	20.4±0.2
$InsP_6$	659	561	24	23.9±0.6
AMP	346	211	24	10.9±0.3

Table 3. Linearity, correlation coefficients, slopes, and intercepts obtained from three replicates analysis.

Analyte	Slope ($\times 10^2$)	Intercept ($\times 10^2$)	R^2	Number of data points	Linear Range (pmol)
Ins	0.74	0.94	0.9988	16	0.25-400
$InsP_1$	1.20	3.86	0.9987	16	0.25-400
$InsP_2$	0.78	35.08	0.9967	7	40-400
$InsP_3$	1.79	67.88	0.9943	7	40-400
$InsP_4$	1.08	0.87	0.9969	16	0.25-400
$InsP_5$	1.95	-10.74	0.9971	16	0.25-400
$InsP_6$	3.18	-153.30	0.9968	6	60-400

Table 4. Intra-day precision for analysis of a standardized mixed inositol and inositol phosphates solution ($InsP_6$ in-house hydrolysis reference, n=3)

Analyte	20 pmol	120 pmol	400 pmol
	RSD%	RSD%	RSD%
Ins	12.4	12.3	13.7
$InsP_1$	9.2	6.6	0.8
$InsP_2$	14.6	13.7	1.2
$InsP_3$	1.7	11.6	12.0
$InsP_4$	14.5	14.0	12.7
$InsP_5$	13.9	2.7	10.0
$InsP_6$	6.6	11.1	7.2

Table 5. Inter-day precision for analysis of a standardized mixed inositol and inositol phosphates solution ($InsP_6$ in-house hydrolysis reference, n=3)

Analyte	40 pmol	100 pmol	300 pmol
	RSD (%)	RSD (%)	RSD (%)
Ins	15.7	2.0	15.5
$InsP_1$	4.3	7.1	7.1
$InsP_2$	7.8	9.9	4.2
$InsP_3$	14.2	17.1	2.1
$InsP_4$	13.9	8.5	7.1
$InsP_5$	13.7	12.8	2.5
$InsP_6$	14.0	24.1	7.5

Table 6. Recovery (%) of analytes from a standardized mixed inositol and inositol phosphates solution ($InsP_6$ in-house hydrolysis reference, n=6) carried through the standard extraction and analysis procedure at two different concentration levels.

Analyte	Amount added (pmol)	Amount detected (pmol)	Recovery (%)
Ins	9.93	6.32	63.6
	33.41	26.26	78.6
$InsP_1$	3.52	2.85	81.0
	12.98	13.61	104.9
$InsP_2$	11.45	9.80	85.6
	117.15	87.28	74.5
$InsP_3$	9.50	8.07	84.9
	96.25	87.25	90.9
$InsP_4$	15.30	14.50	94.8
	91.74	111.46	121
$InsP_5$	3.21	2.98	92.8
	31.53	35.58	113
$InsP_6$	14.60	12.01	82.3
	160.52	168.55	105

Table 7. Inositol and inositol phosphate levels in almond, hazelnut, and oat samples. Recoveries from the dietary samples at two concentration levels of a standardized mixed inositol and inositol phosphates solution: Recovery 1, ~4 μmol/g, Recovery 2, ~16 μmol/g ($InsP_6$ in-house hydrolysis reference, n=6).

Almond	Amount (μmol/g)	Distribution (%)	Recovery 1 (%)	Recovery 2 (%)
Ins	7.44±3.88	14.1	77.8	94.5
$InsP_1$	1.53±0.39	2.9	84.7	83.9
$InsP_2$	3.76±1.33	7.1	98.3	95.2
$InsP_3$	1.80±0.20	3.4	82.4	95.6
$InsP_4$	8.46±0.27	16.1	91.8	97.9
$InsP_5$	9.95±0.71	18.9	68.5	84.6
$InsP_6$	19.75±2.93	37.5	111.1	105.6
Total	52.7			
Oat				
Ins	0.21±0.05	7.2	131.9	108.0
$InsP_1$	0.05±0.02	1.7	69.8	92.4
$InsP_2$	0.15±0.04	5.1	64.1	91.0
$InsP_3$	0.12±0.06	4.1	101.8	100.4
$InsP_4$	0.64±0.36	21.8	119.6	104.9
$InsP_5$	1.13±0.28	38.6	97.1	99.3
$InsP_6$	0.63±0.21	21.5	77.0	94.2
Total	2.93			
Hazelnut				
Ins	1.08±0.10	22.6	72.7	93.2
$InsP_1$	0.003±0.002	0.1	87.6	96.9
$InsP_2$	0.05±0.01	1.0	114.5	103.6
$InsP_3$	0.012±0.01	0.3	101.5	100.4
$InsP_4$	1.06±0.73	22.3	96.1	99.1
$InsP_5$	0.36±0.05	7.5	96.1	99.0
$InsP_6$	2.21±0.53	46.3	82.8	95.7
Total	4.78			

Table 8. Inositol and Inositol phosphate levels in human cells. (n=3)

	MCF-7 (μmol/mg protein)	% distribution	Hela (μmol/mg protein)	% distribution
Ins	0.69±0.32	57.5	0.009±0.001	4.1
$InsP_1$	0.29±0.05	24.1	0.003±0.000	1.4
$InsP_2$	0.07±0.02	5.8	0.011±0.008	5.0
$InsP_3$	0.008±0.006	0.7	0.007±0.007	3.2
$InsP_4$	n.d.	0	0.083±0.010	38.1
$InsP_5$	0.11±0.03	9.2	0.070±0.038	32.1
$InsP_6$	0.033±0.014	2.7	0.035±0.027	16.1
Total	1.20		0.22	

Chart 1. The structure of compounds investigated as an internal standard.

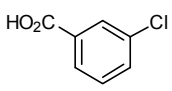

3-Chlorobenzoic acid

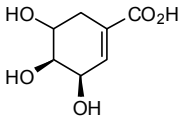

Shikimic acid

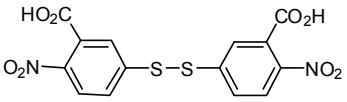

5,5′ -Dithiobis(2-nitrobenzoic acid)

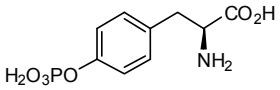

O-Phospho-L-Tyrosin

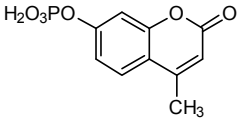

4-Methylumbelliferyl pohsphate

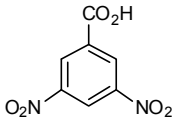

3,5-Dinitrobenzoic acid

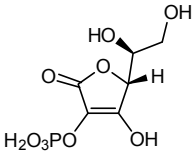

2-Phospho-L-Ascorbic acid

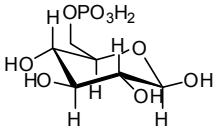

D-Glucose 6-phosphate

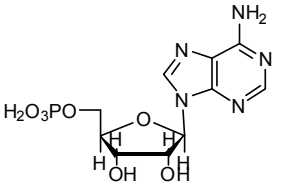

Adenosine 5′ -monophosphate

Figure 1. Structure of *myo*-inositol and *myo*-inositol phosphates.[182]

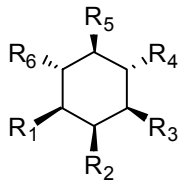

R= OH or $OPO(OH)_2$

Number of phosphate groups	Full name	Abbreviation
0	*myo*-inositol	Ins
1	*myo*-inositol monophospate[a]	$InsP_1$
2	*myo*-inositol bisphosphate[b]	$InsP_2$
3	*myo*-inositol triphosphate[c]	$InsP_3$
4	*myo*-inositol tetrakisphosphate[d]	$InsP_4$
5	*myo*-inositol pentakisphosphate[e]	$InsP_5$
6	*myo*-inositol hexakisphosphate	$InsP_6$

Isomers of known biological relevance: a, $Ins(1)P_1$, $Ins(3)P_1$, $Ins(4)P_1$; b, $Ins(4,5)P_2$, $Ins(1,4)P_2$; c, $Ins(1,4,5)P_3$, $Ins(1,3,4)P_3$; d, $Ins(1,4,5,6)P_4$, $Ins(1,3,4,5)P_4$; $Ins(1,3,4,5,6)P_5$.

Figure 2. Representative SRM chromatogram of a 120 pmol inositol phosphate mixture, the transition of each analyte is indicated in Table 2.

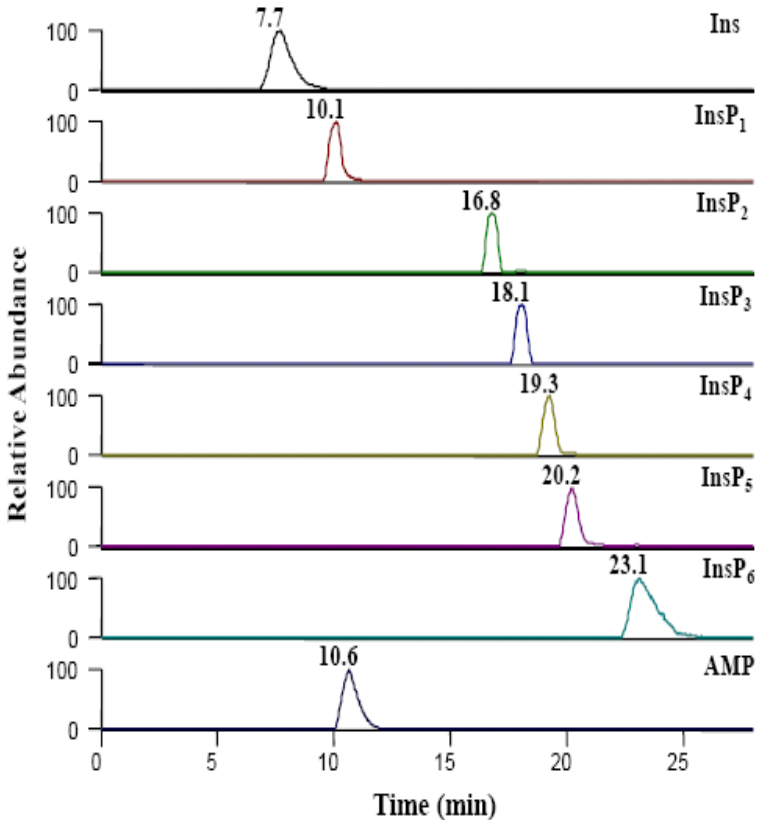

Figure 3. a, Multi-point standard calibration curve corresponding to the range resulting in $r^2 > 0.994$. b, Multi-point standard calibration curve for $InsP_2$, $InsP_3$ and $InsP_6$ in the range of 0.25-400 pmol

a. b.

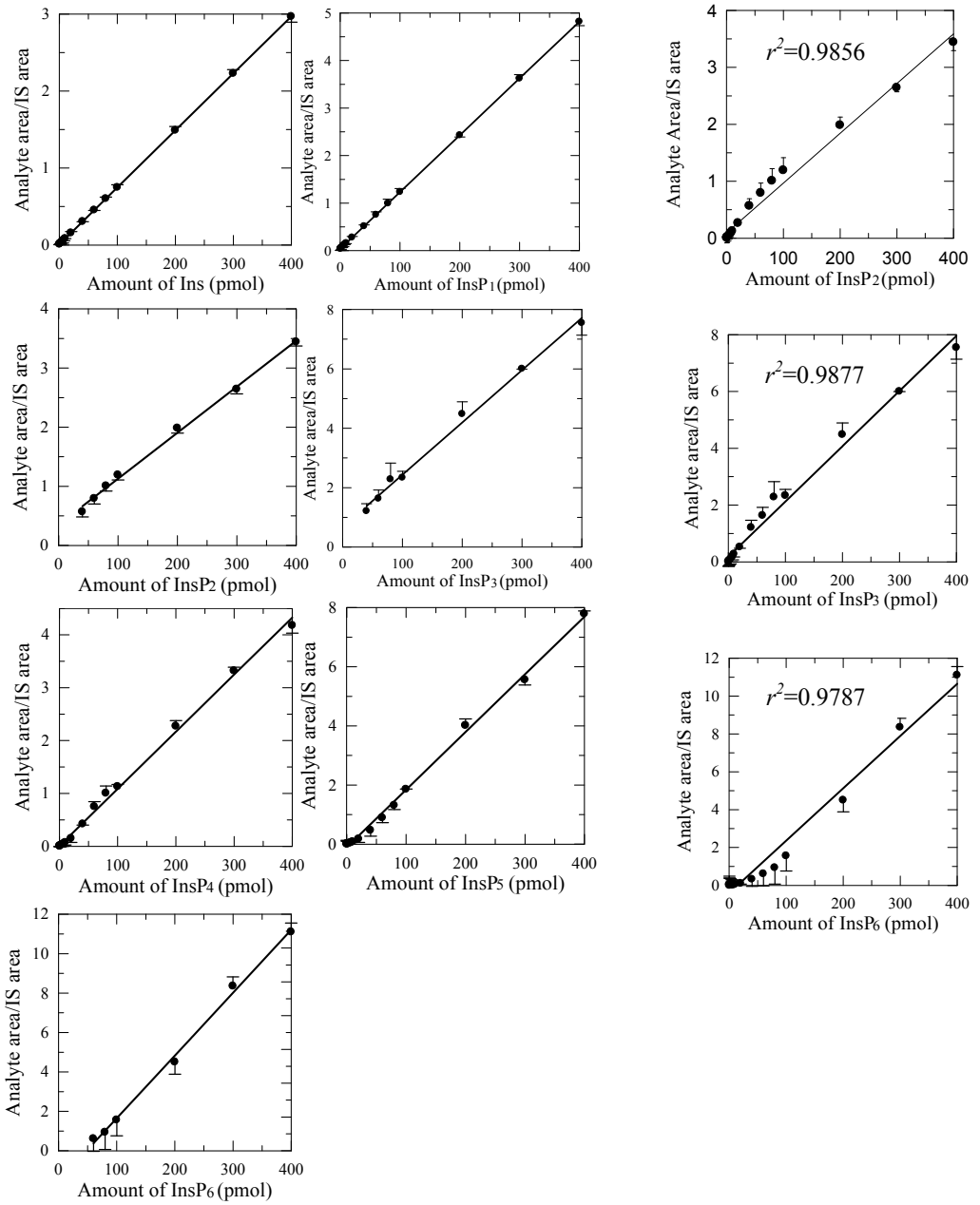

Figure 4. Representative chromatogram of extracted raw almonds.

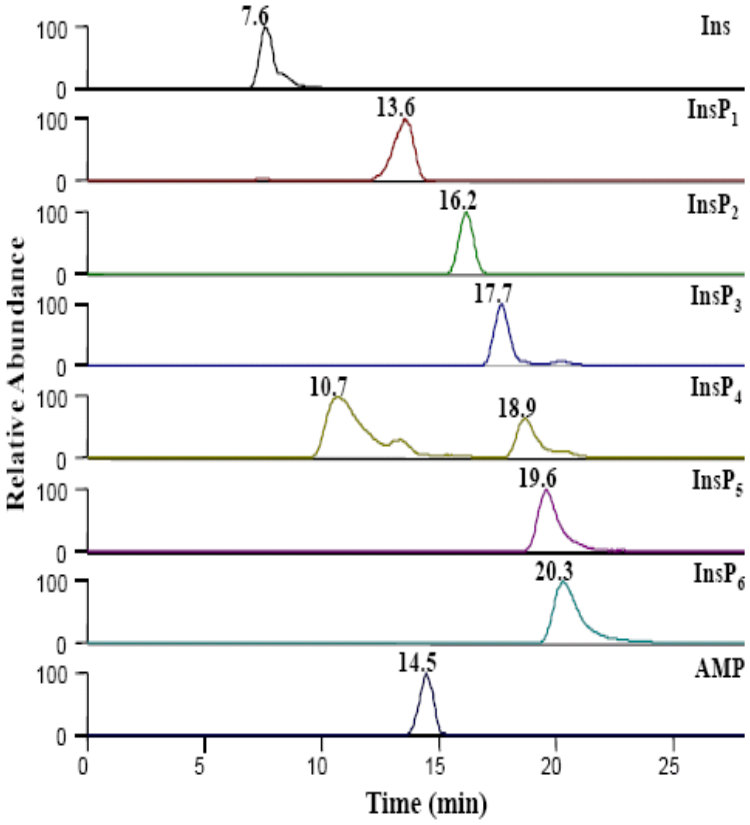

Figure 5. Representative chromatogram of extracted MCF-7 cells.

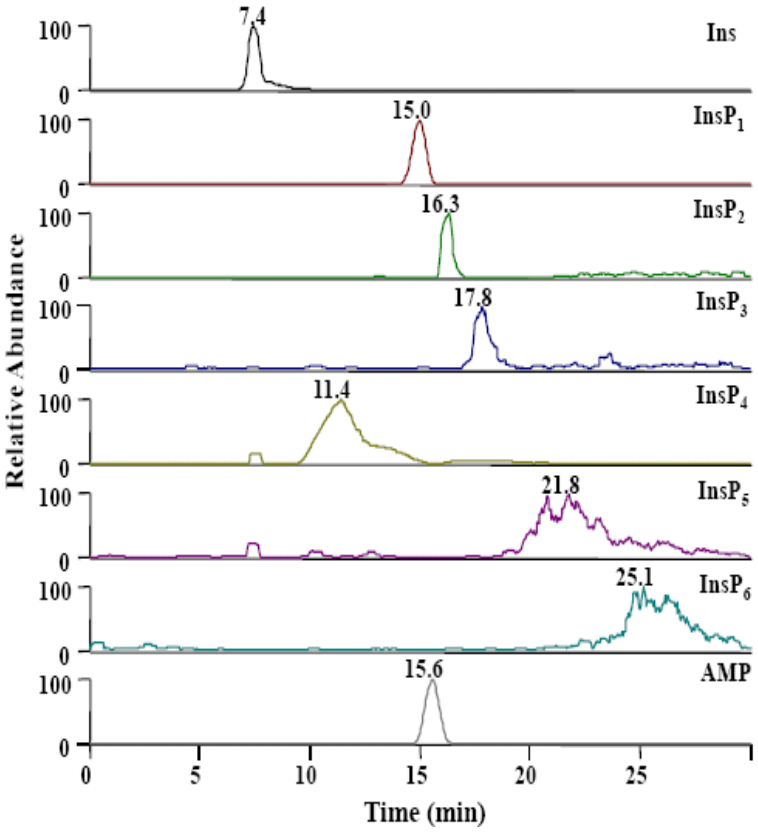

Figure 6. Representative chromatogram of extracted oats.

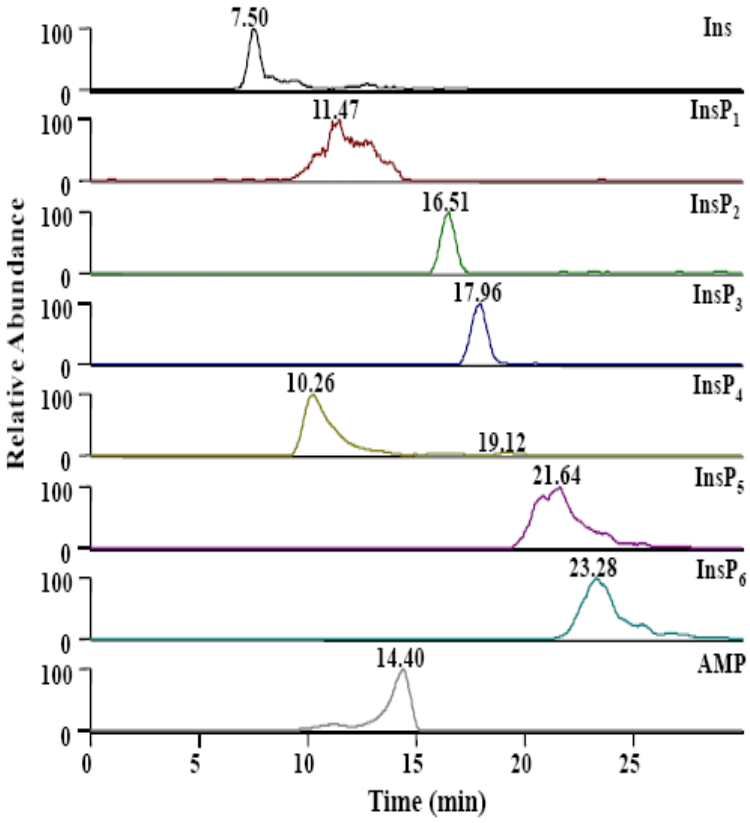

Figure 7. Representative chromatogram of extracted hazelnut.

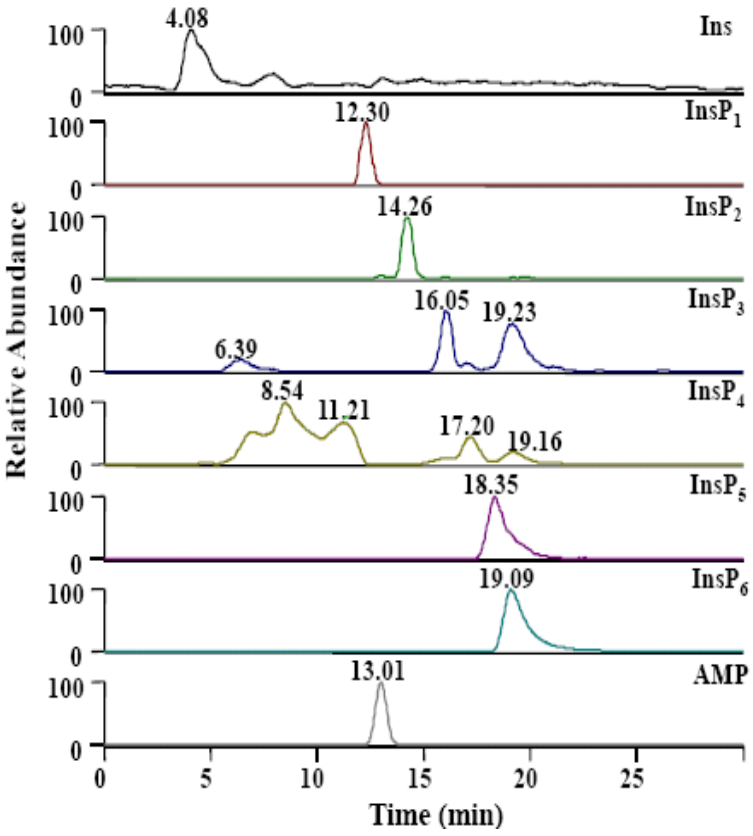

Figure 8. Representative chromatogram of extracted Hela cells.

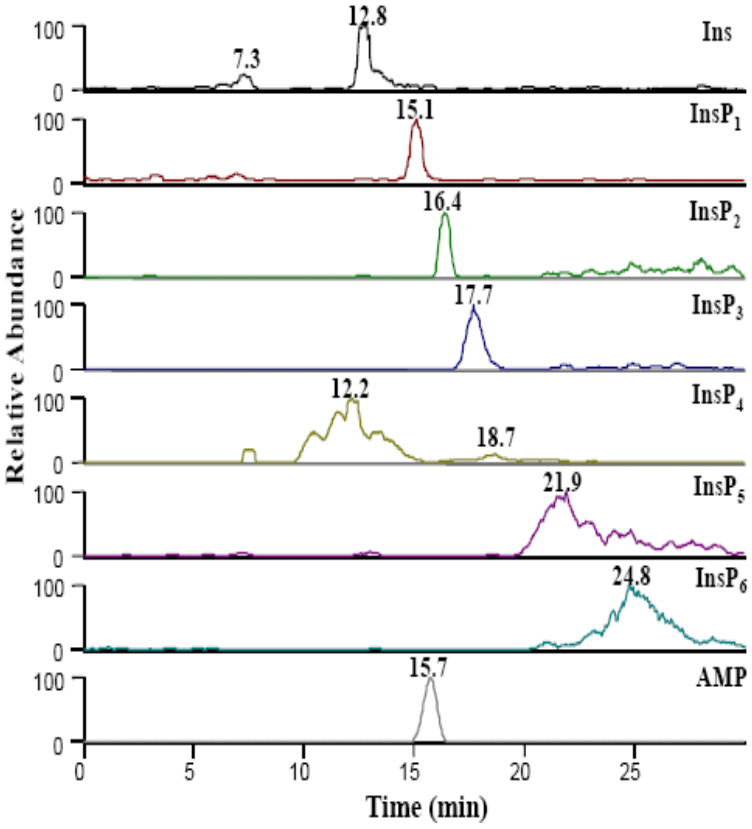

Chapter Three: Deoxygenated phosphorothioate inositol phosphate analogues: preparation and phosphatase stability[*]

[*] Portions reproduced with permission from Xiaodan Liu, Emily C. Moody, Stephen, S. Hecht, and Shana J. Sturla. (2008) Bioorg. Med. Chem. (16): 3419-3427.

1. Introduction

Myo-Inositol and its corresponding hexaphosphate ($InsP_6$, Chart 1) are widely distributed in plants and animals. Both have been shown to possess cancer preventive and therapeutic activity *in vitro* and in animal studies.[7, 62, 65, 183-187] In chemoprevention studies, these compounds were effective in reducing tumor number and size when given simultaneously with or after carcinogen exposure.[62, 65, 185-187] The biochemical mechanisms underlying the chemopreventive activity of inositol compounds are not known, but exogenously administered $InsP_6$ is rapidly dephosphorylated to lower inositol phosphates that participate in signal transduction pathways and affect the cell cycle.[173] Preclinical studies indicate that the combination of inositol with $InsP_6$ further enhances chemopreventive and anticancer effects and it has been suggested that this combination disproportionates to Ins(1,4,5)P_3, which normalizes the rate of cell division thus preventing tumor formation. The resulting hypothesis is that inositol phosphates with fewer than six phosphate groups, such as the biochemical second messenger Ins(1,4,5)P_3, may be responsible for the biological activity observed for inositol and $InsP_6$.[188-191]

There have been extensive studies of the roles of inositol and inositol phosphates in signal transduction and of the enzymes that catalyze the conversions between different inositol phosphates.[192-199] Among the various inositol phosphates, Ins(1,4,5)P_3 is the most understood; it is established as an important second messenger involved in many signaling pathways. After cleavage from the membrane-bound phosphatidyl inositol trisphosphate, Ins(1,4,5)P_3 binds to its corresponding receptor and stimulates the release of stored Ca^{2+} into the cytoplasm. This event triggers an array of cellular responses including glycogen breakdown, muscle contraction, and the release of neurotransmitters.[200-202] Ins(1,4,5)P_3 is rapidly deactivated by stepwise dephosphorylation to Ins(1,4)P_2, then to Ins-4-P_1 and finally *myo*-inositol.[203, 204] Alternatively, phosphorylation by Ins(1,4,5)P_3 3-kinase produces Ins(1,3,4,5)P_4.[205, 206] The metabolic instability and rapid clearance of Ins(1,4,5)P_3 make it difficult to probe directly the role of Ins(1,4,5)P_3 in biological events, such as those that may underlie mechanisms of inositol and $InsP_6$-mediated cancer chemoprevention. Thus the overall benefits of Ins(1,4,5)P_3 in cancer prevention and therapy remain controversial.

Inositol phosphate chemical analogs resistant to enzymatic degradation have potential for enhanced chemopreventive activity and mechanistic information obtained could serve as a starting point for medicinally focused approaches to develop improved agents for chemoprevention.[207-209] Furthermore, these compounds could serve as synthetic probes useful for investigating the role of inositol phosphates in biochemical signaling pathways that cannot be tested using current methods. As a step toward these goals, the primary aim of this study was to develop an enzyme-stable Ins(1,4,5)P_3 analog. The structural basis for its design involved structure-activity relationships previously established for Ins(1,4,5)P_3 receptor binding and Ca^{2+} release activity (Figure 1).[201, 210-215] Much of the information known regarding receptor binding specificity has been garnered from studies involving synthetic deoxy-analogs. Strategies for the syntheses of these compounds generally involve lengthy (i.e. on the order of 7-15 steps) modification of oxygenated carbohydrate precursors, including quebrachitol and D-galactopyranose.[216-218]The influence of deoxygenation at the 2- and 3- positions of the inositol framework was examined with 1D-3-deoxy and 1D-2,3-dideoxy-Ins(1,4,5)P_3,[217-219] which retain biological activity including receptor binding and Ca^{2+} mobilization. By contrast, analogs deoxygenated at the 6-position, such as 1D-2,3,6-trideoxy-Ins(1,4,5)P_3 and 1D-6-deoxy-Ins(1,4,5)P_3, displayed significantly lower binding affinity to the Ins(1,4,5)P_3 receptor.[217, 220]

Deoxygenation at specific positions of the inositol framework eliminates kinase phosphorylation sites,[217, 221] and replacement of phosphate groups with phosphorothioates retains key interactions between the molecules and Ins(1,4,5)P_3 receptors, but imparts phosphatase resistance.[222-224] We report here the synthesis of two novel inositol phosphate analogs, **5** and **6**, that on the basis of these design principles are expected to be enzyme-stable receptor-binding analogs. An evaluation of their chemical and biochemical properties, including binding affinities for the Ins(1,4,5)P_3 receptor and resistance to enzymatic hydrolysis is described.

2. Experimental procedures

2.1 General details

Tetrazole was obtained from Glen Research (Sterling, VI) as a saturated solution in anhydrous acetonitrile and used as provides. Ammonia was used from a lecture bottle, 99.9% pure, obtained from Aldrich. DEAE Sephadex A-25 anion exchange resin was obtained from Sigma Chemical Co. (St. Louis., MO), and was packed in a glass column with water. Alkaline Phosphatase was supplied from Sigma in a 50% glycerol solution with 5 mM $MgCl_2$ and 0.1 mM $ZnCl_2$; activity was assessed at 4900 units/mg protein with 11.2 mg protein/mL. Amicon Centricon YM-3 centrifuge filters were obtained from Millipore and were rinsed with 2 mL H_2O for 3 hours at 7000g prior to use. Ellman's reagent was prepared and used to detect phosphorothioate compounds in fractions after anion exchange chromatography as described previously.[166]

Direct injection mass spectrometry analysis was performed for compound characterization on an Agilent 1100 LC/MSD ion trap instrument (Agilent Technologies, Inc., Wilmington, DE) operating in negative-ion mode.

2.2 Synthesis of 1D-2,3-dideoxy-*myo*-inositol 1,4,5-trisphosphorothioate (6).

A 250 mL three-necked round bottom flask fitted with a condenser was flushed with N_2 and cooled to -78 ^oC. Ammonia (50 mL) was condensed into the flask at -78 ^oC. A solution of 1-D-6-*O*-benzyl-2,3-dideoxy-*myo*-inositol 1,4,5-tris[di-(2-cyanoethyl)-phosphorothioate] **11** (21 g, 25 mmol) in anhydrous dioxane (3 mL) was added dropwise while the solution was stirred. Na, stored in mineral oil, was slowly cut into small pieces, rinsed with Et_2O and immediately added to the reaction mixture. After one to two minutes, a color change to dark blue was observed and this solution was stirred at -78 ^oC for 10 min. The reaction was quenched by dropwise addition of MeOH (approx. 3 mL) and solvent was evaporated by warming to 23 ^oC under a N_2 purge. Crude residue was purified by aion exchange chromatography on DEAE Sephadex A-25 resin with a stepwise gradient starting with 0.3 mM triethylammonium bicarbonate (TEAB) to 0.7 mM TEAB. The presence of phosphorothioate in column fractions was detected by Ellman's reagent in column fractions, yielding 5.45 mg **6** was isolated (32%) as a yellowish white solid. ^1H NMR (D_2O) δ 4.21 (m, 2H), 3.63 (m, 1H), 2.21 (m, 2H), 1.47

(dd, J = 9.0, 2H); ^{31}P NMR (D_2O) δ 46.6, 48.8, 49.4; HRMS calculated for [C_6 H_{14} O_{10} P_3 S_3]: 434.8962, Found: 434.8963.

2.3 Reaction of 6 with alkaline phosphatase and HPLC/MS/MS analysis

In a volume of 300 μL, **6** (200 μmol) or Ins(1,4,5)P_3 (80 μmol) was incubated with alkaline phosphatase (6 μL, activity 62 units/μL) for 30 min at 37 ^{o}C. The resulting mixtures were first filtered by micro YW3000 (Micron Technology, Inc. CA.) at 4 °C, then centrifuged at 7000 rpm for 30 minutes to remove the enzyme. 4 microliters of the filtered solution per injection was introduced with an autosampler into the ESI source using a Biobasic AX 150 x 0.5 mm weak anion exchange capillary column. The flow rate was 10 μL/min, solvent A 95:5 mixture of water : methanol, solvent B 200 mM solution of $(NH_4)_2CO_3$. Initial solvent conditions (100% A) were changed with a linear gradient over the first 3 min to 50:50 B:A, then to 72:28 B:A over a course of 25 minutes, then returning to 100% A in 2 minutes. The retention times and molecular weights observed for compounds of interest are as follows: Ins(1,4,5)P_3, 17.9 min, $[M-1]^-$ 419, Inositol, 4.4 min, $[M-1]^-$ 179; $InsP_1$, 5.8 min, $[M-1]^-$ 259; $InsP_2$, 16.4 min, $[M-1]^-$ 339; **6**, 20.4 min, $[M-1]^-$ 435; hydrolyzed **6**, 16.8 min, $[M-1]^-$ 339; **12**, 15.9 min, $[M-1]^-$ 433; **13**, 6.3 min, $[M-1]^-$ 337. Negative ESI-MS/MS was performed using the following parameters: spray voltage 5.0 kV; sheath gas pressure, 31; capillary temperature, 330 °C; collision energy, 19 V; scan width, 0.3 amu; scan time, 0.25 s; Q1 peak width, 0.7 amu; Q3 peak width, 0.7 amu; Q2 gas pressure, 1.5 mTorr; source CID, -16 V; and tube lens offset, 59 V-69 V; MS/MS data were acquired and processed by Xcaliber software version 1.4 (Thermo Electron).

3. Results

3.1 Chemistry

1D-*myo*-inositol 4,5-bisphosphate analog **5** is a deoxygenated analog bearing two phosphorothioate groups in the 4- and 5-positions and retaining the 6-hydroxyl group, which is critical for the binding of Ins(1,4,5)P_3 to its receptor (Figure1, Chart1).[214, 215] While **5** is a putative Ins(4,5)P_2 analog, its synthesis was pursued primarily as a synthetic model and biochemical control substrate for investigating the Ins(1,4,5)P_3 analog **6**. Initially, we were interested in establishing chemistry needed to prepare and purify *trans*-vicinal phosphorothioates with a neighboring free alcohol.

Triol **10** was converted to the corresponding phosphates by treatment with bis(2-cyanoethyl)-*N,N*-diisopropyl phosphoramidite, followed by reaction with sulfur, and deprotection (Scheme 1). The final product was isolated as the triethylammonium salt after a short DEAE-Sephadex anion exchange column, eluting with an increasing gradient of triethylammonium bicarbonate (TEAB), and visualized by Ellman's reagent, which is used routinely as a sulfhydryl indicator (i.e. a visible yellow color is produced).[166] Analysis by HRMS displayed a molecular ion of 434.8963, consistent with the presence of three phosphorothioate moieties. Analysis by ^{31}P NMR displayed three resonances (46.6, 48.8, and 49.5), also consistent with the trisphosphorothioate structure. No ^{31}P resonances were observed in the 7.7-6.2 region,[217, 219] which would be expected for phosphate groups, and no mass corresponding to phosphate (rather than phosphorothioate) groups were observed. The synthesis involved 13 steps and the separation of a 1:1 mixture of isomers; **6** was obtained in 4% overall yield.

Storage of aqueous **6** solutions at low temperature (-20 ºC) for extended time (months) resulted in its partial decomposition, as indicated by MS analysis of aged samples in which a new peak with a negative ion *m/z* 433 was observed (Figure 2A). This decomposition product could be removed by repurification on a DEAE-Sephadex anion exchange column. Furthermore, it was found that when incubated with DL-dithiothreitol (DTT), a reagent useful for reducing disulfide bonds, the impurity with *m/z* 433 was completely re-converted to **6** (Figure 2B). This relationship was confirmed by MS analysis as indicated in Figure 2. These data suggest that the impurity resulted from the

formation of a disulfide bond between vicinal phosphorothioates. The corresponding equilibrium relationships and proposed structure **12** are illustrated in Scheme 2, and this material appeared to be stable to alkaline phosphatase-mediated hydrolysis (Figure 3C).

3.2 Biochemistry

The resistance of **6** to enzymatic degradation was addressed by reacting with alkaline phosphatase and analyzing the resulting mixture by LC/MS/MS using an electrospray ionization source (Figure 3B). As a positive control, Ins(1,4,5)P_3 (*m/z* 419) was extensively hydrolyzed by alkaline phosphatase (30 minutes, 37 °C), producing *myo*-inositol bisphosphate ($InsP_2$), *myo*-inositol monophosphate ($InsP_1$), and inositol (Figure 3A) with negatively charged $[M-H]^-$ ions *m/z* 339, 259, and 179, respectively. The identities of the inositol phosphates and inositol were verified by co-injection with authentic standards. To evaluate the stability of **6**, fragmentation data obtained for the products of Ins(1,4,5)P_3 incubation mixture were used to guide the anticipated product ions that would result from hydrolysis of **6**, for which authentic hydrolysis co-injection standards were not available. Thus, the products of the Ins(1,4,5)P_3 incubation mixture were selected for collision-induced dissociation (CID), and fragment ions for Ins(1,4,5)P_3 and $InsP_2$ of *m/z* 321 and 241, respectively, were observed (Figure 3A). These fragment ions correspond to loss of orthophosphoric acid (H_3PO_4). The fragment ion generated from $InsP_1$ (*m/z* 179) corresponds to phosphate loss, and water loss for inositol (*m/z* 161). Data from the LC/MS/MS analysis of incubates of **6** with alkaline phosphatase under identical conditions as the positive control, are shown in Figure 3B. The *m/z* values for the parent and fragment $[M-H]^-$ ions for **6** are 435 and 401, respectively. This fragmentation pattern is consistent with loss of SH_2. A product resulting from hydrolysis of **6** is expected to display *m/z* 339 and a fragment ion *m/z* 305, corresponding to loss of one phosphorothioate group. As indicated in Figure 3B, there is no evidence for the formation of this product under the phosphatase reaction conditions. As a further confirmation of the validity of the selected fragment, evidence for the putative hydrolyzed product (i.e. observation of a new MS peak with *m/z* 339 that fragments to *m/z* 305) was observed by carrying out the same MS analysis of **6** after prolonged storage (several months). Furthermore, the same behavior (i.e. the formation of hydrolysis

products) was observed for stored Ins(1,4,5)P_3. Finally, to determine whether **6** inhibits alkaline phosphatase, enzyme activity was monitored using a colorimetric assay with *p*-nitrophenyl phosphate (*p*NPP) as a substrate.[225] Phosphatase activity was determined at 37 °C by measuring the increase in absorbance at 405 nm that accompanies the hydrolysis of *p*NPP, and these data indicated that **6** does not inhibit alkaline phosphatase activity at high micromolar range(data not shown).

In studies carried out by Emily Moody, the binding affinity of **5** and **6** with respect to the Ins(1,4,5)P_3 receptor from bovine adrenal cortex was determined (Figure 4).[226] The strongest binding was demonstrated by Ins(1,4,5)P_3 (K_d 54 nM),. The binding constant for **6** was in the high nanomolar range (K_d 810 nM), while the binding of **5** was over three orders of magnitude higher.

4. Discussion

The design of the inositol phosphate analogs described in this study relied on known structure-activity relationships for Ins(1,4,5)P_3 (Figure 1), indicating that vicinal 4,5-phosphate groups are required for Ins(1,4,5)P_3 Ca^{2+}-releasing activity, and that the 1-phosphate acts as an enhancer.[47, 211] Replacing Ins(1,4,5)P_3´s phosphate groups by phosphorothioate groups has been found to provide resistance to phosphatase-catalyzed hydrolysis without greatly affecting binding properties,[224, 227] but the analog used in the study may still be phosphorylated at the 2- and 3-positions. Therefore, deoxygenation at these positions was a strategy utilized to block phosphorylation. 1D-2,3-dideoxy-Ins(1,4,5)P_3 maintains a relatively high affinity for the Ins(1,4,5)P_3 receptor and is a full agonist, releasing Ca^{2+} from permeabilized SH-SY5Y cells.[219] In human cells, phosphorylation of Ins(1,4,5)P_3 has been observed at the 3-position,[228] and the substrate of the known 6-kinase is not Ins (1,4,5)P_3, but Ins (1,3,4)P_3, which is formed by the hydrolysis of Ins(1,3,4,5)P_4.[229] In addition, 1D-6-deoxy-*myo*-Ins(1,4,5)P_3 was a full agonist, but is 70-fold less potent than Ins(1,4,5)P_3, indicating that the 6-hydroxyl group is important for receptor binding and Ca^{2+} release,[215, 220] and it is therefore present in **6**.

Inositol phosphate multikinases catalyze phosphorylation of the 3- and 6-hydroxyl groups of Ins(1,4,5)P_3, but in cells 3-phosphorylation is the dominant product.[230] Although known enzyme profiles indicate that **6** is expected to be kinase-stable, further studies are required to explicitly address the susceptibility toward phosphorylation by specific kinases. As a preliminary test of enzyme stability carried out in this study, we used alkaline phosphatase, which efficiently hydrolyzes Ins(1,4,5)P_3. In cells, Ins(1,4,5)P_3 5-phosphatase is the specific enzyme that hydrolyzes Ins(1,4,5)P_3, but it has low substrate-specificity compared with Ins(1,4,5)P_3 3-kinase.[231] Many synthetic inositol phosphates are high-K_i Ins(1,4,5)P_3 5-phosphatase inhibitors, such as *myo*-inositol 1,4,5-trisphosphorothioate [217, 219, 227, 231], suggesting that **6** is a potential Ins(1,4,5)P_3 5-phosphatase inhibitor. The current studies indicate that **6** is stable to general enzyme-mediated hydrolysis, but further studies with specific kinases and phosphatases and in the complex environment of the cell are required to determine the biological stability of **6**.

Thiophosphate **6** has a significant binding affinity (810 nM) for the Ins(1,4,5)P_3-receptor despite its structural modification. However, the presence of only the 4,5-phosphorothioates in **5** results in a dramatic decrease in binding affinity, consistent with the specificity of the ligand-receptor interaction. The X-ray structure of the Ins(1,4,5)P_3-binding domain of mouse type-I Ins(1,4,5)P_3 receptor with bound Ins(1,4,5)P_3 indicates interactions of specific Arg and Lys residues with the three phosphate groups,[232] and replacement by phosphorothioates therefore is expected to influence the interaction. Compared to other phosphatase-stable Ins(1,4,5)P_3 analogs, including 1L-(+)-*myo*-Ins(1,4,5)P_3,[227] 1D-6-deoxy-Ins(1,4,5)P_3S_3, and L-ch-Ins(2,3,5)P_3S_3,[233] **6** retains a notably high affinity for the Ins(1,4,5)P_3 receptor. Three closely related Ins(1,4,5)P_3-receptor subtypes have been characterized and they are differentially expressed and involved in physiological functions such as regenerating Ca^{2+} signals.[194] The previously reported analog 2-deoxy-1,4,5-Ins(1,4,5)P_3 had a slightly greater affinity for type 2 and type 3 receptors, whereas 3-deoxy-1,4,5-Ins(1,4,5)P_3 showed greater selectivity for type 3 receptor.[234] To define specific ligand-receptor binding interactions for **6**, further studies are needed to determine the selectivity of **6** for different Ins(1,4,5)P_3 receptors.

Techniques to assess the stabilities of inositol phosphates and analogs have included NMR, i.e. monitoring ^{31}P signals for enzymatic reactions performed in an NMR tube,[235] radioflow HPLC after incubation with [^{3}H]Ins(1,4,5)P_3,[215] or using a functional assay (i.e. measuring Ca^{2+} mobilization).[200] The requirement for large amounts of material and low sensitivity and accuracy are drawbacks for NMR analysis, and preparations of isotope-labeled analogs and tedious sample preparation are generally required for the radioflow methods. Finally, functional assays do not necessarily transfer for the analysis of structural analogs. To overcome limitations in these methods, we developed a new LC/MS/MS analytical method for inositol phosphate analog-enzyme incubations. This method is sensitive and fast, and sample preparation is easy. This method was used here to investigate analog stability toward phosphatase activity, but it has potential applications for further studies of inositol kinase activity and analysis of complex inositol mixtures.[236]

5. Conclusion

In conclusion, we have synthesized **5** and **6**, two novel deoxygenated phosphorothioate analogs of the inositol phosphates Ins(1,4,5)P_3 and Ins(4,5)P_2. Phosphorothioate **6** is stable to enzymatic hydrolysis, but a tendency of the vicinal phosphorothioates to form disulfide bonds was observed indicating limitations in its chemical stability. This analog specifically binds to Ins(1,4,5)P_3 receptor with a K_d of 810 nM, which compares favorably with previously reported Ins(1,4,5)P_3 phosphorothioate analogs.[227, 233] Future studies will be aimed at characterizing cellular responses to **6** and using it to probe the role of Ins(1,4,5)P_3 and its receptor in physiological processes.

Chart 1. Structures of D-*myo*-inositol (**1**), D-*myo*-inositol hexaphosphate (**2**), D-*myo*-inositol 4,5-bisphosphate (**3**), and D-*myo*-inositol 1,4,5-trisphosphate (**4**), 1D-1,2,3-trideoxy-*myo*-inositol 4,5-bisphosphorothioate (**5**), 1D-2,3-dideoxy-*myo*-inositol 1,4,5-trisphosphorothioate (**6**).

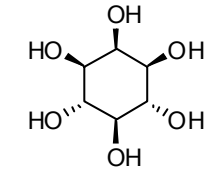

1, *myo*-Inositol

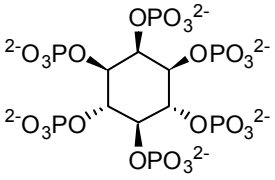

2, $InsP_6$

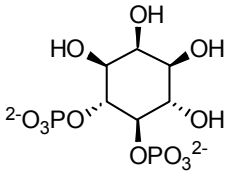

3, $Ins(4,5)P_2$

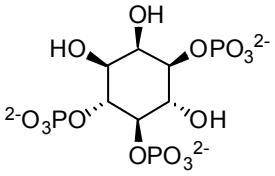

4, $Ins(1,4,5)P_3$

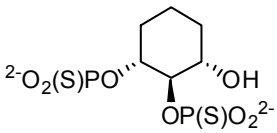

5, TD-$Ins(4,5)P_2S_2$

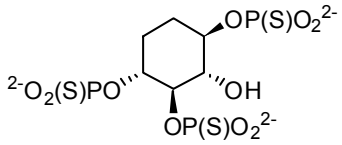

6, DD-$Ins(1,4,5)P_3S_3$

Figure 1. Previously established structure-activity relationships for Ins(1,4,5)P_3-receptor

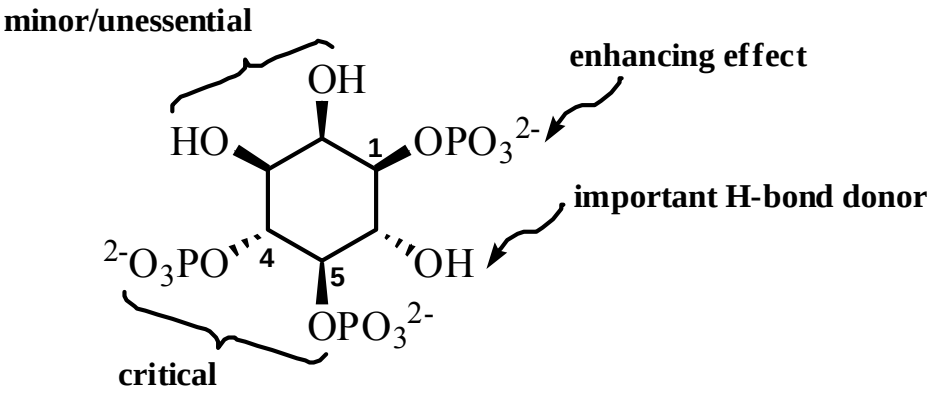

Figure 2. Full-scan MS of **12** after storage of **6** at -20 °C for one month, (A, *m/z* 432.9); and full-scan MS of the same material after treatment with excess of DTT, (B, *m/z* 434.9).

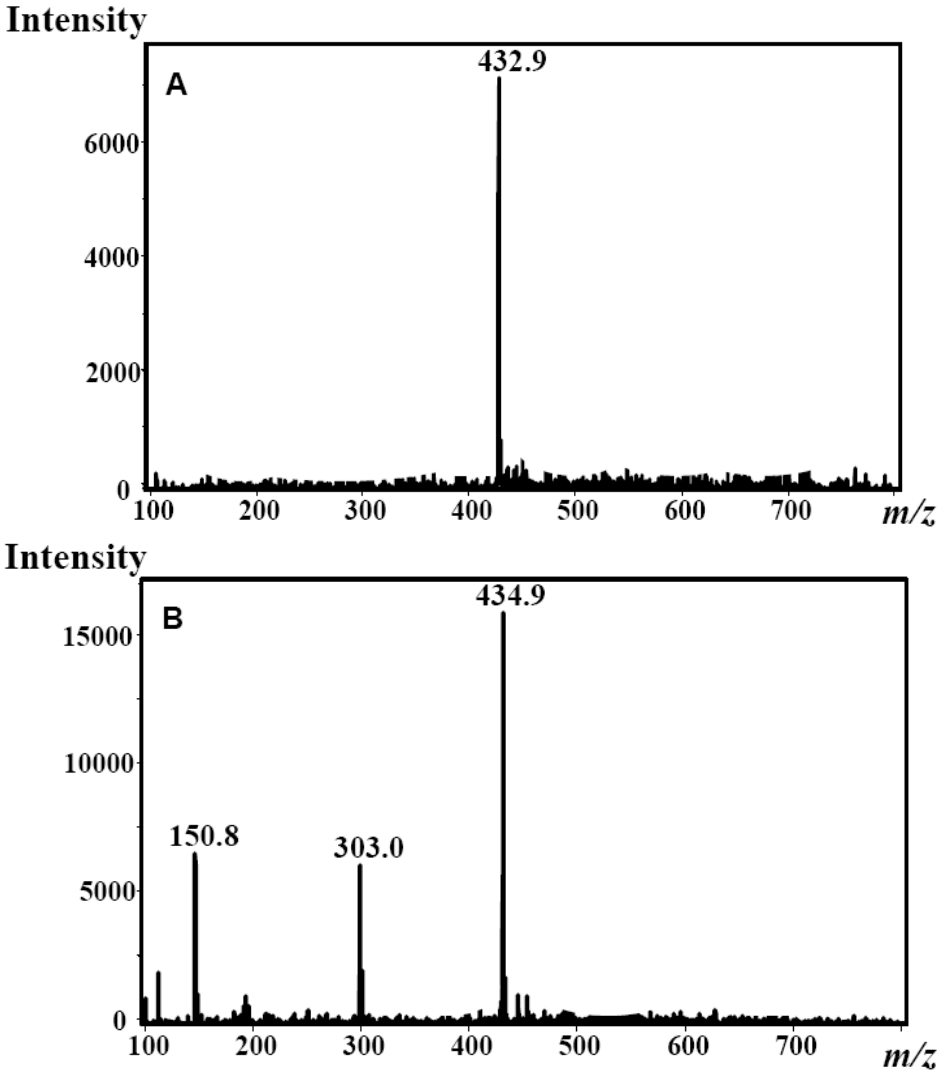

Figure 3. Effects of **5**, **6** and Ins(1,4,5)P_3 on equilibrium competition binding of [^{3}H]-Ins(1,4,5)P_3 to bovine adrenal cortical protein extracts.

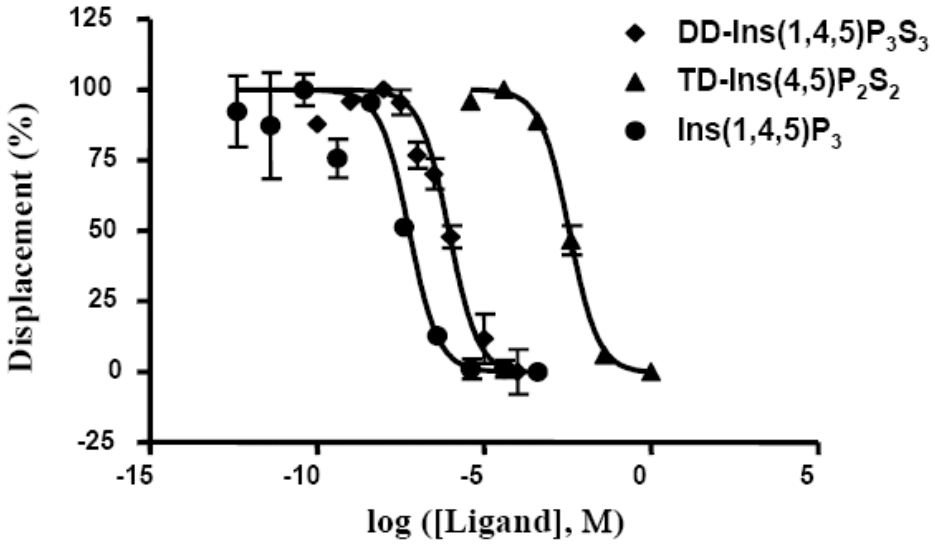

Figure 4 SRM chromatograms of reactions of Ins(1,4,5)P_3, **6,** or **12** with alkaline phosphatase. A, Ins(1,4,5)P_3 control (left, unreacted Ins(1,4,5)P_3; right, Ins(1,4,5)P_3 hydrolyzed to $InsP_2$, $InsP_1$, and inositol), a small amount of $InsP_1$ is detected with RT 5.77 min. B, **6** incubated with alkaline phosphatase. (left, unreacted **6**; right, sample after incubation indicates that starting compound remains intact, and there's no evidence for a hydrolysis product). C, **12** incubated with alkaline phosphatase. (left, unreacted **12**; right, sample after incubation indicates that starting compound remains intact, and there's no evidence for **13**. Monitored SRM transitions are indicated on the right for each channel.

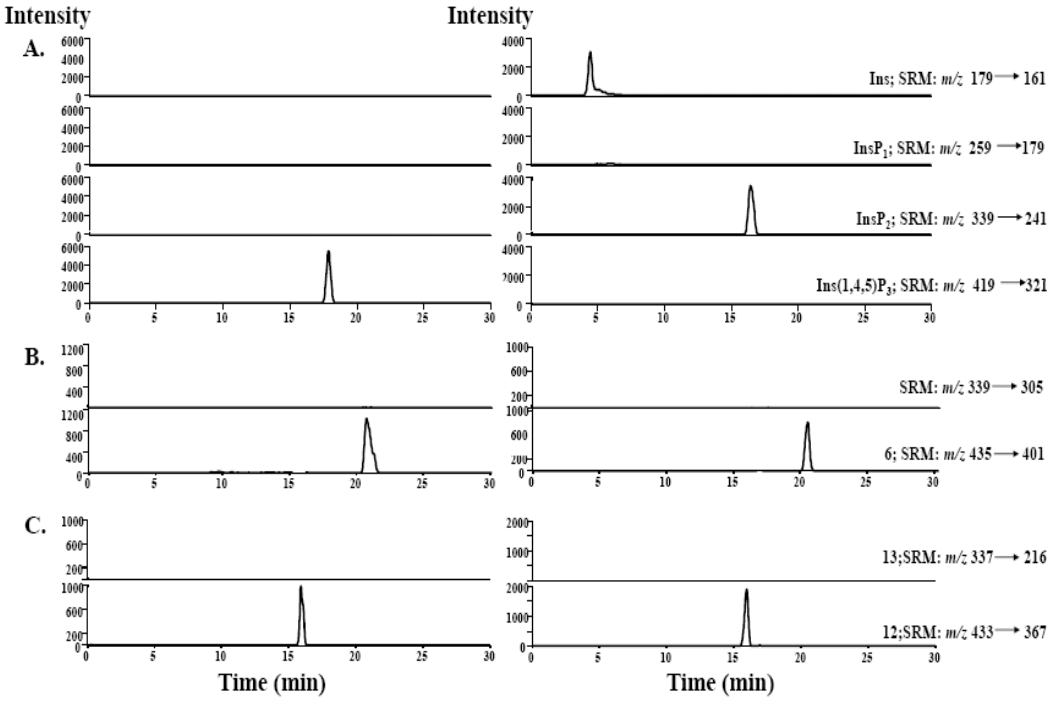

Scheme 1. Synthesis of the analog **6**. (i). Tetrazole, bis(2-cyanoethyl)-N, N-diisopropyl phosphoramidite; (ii). Sulfur, pyridine; (iii). Na, NH_3.

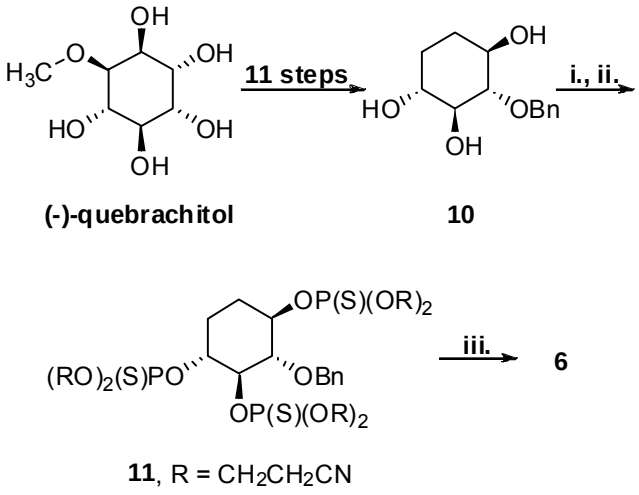

Scheme 2. Proposed decomposition pathway observed for **6** and proposed hydrolysis pathway. DTT, DL-dithiothreitol.

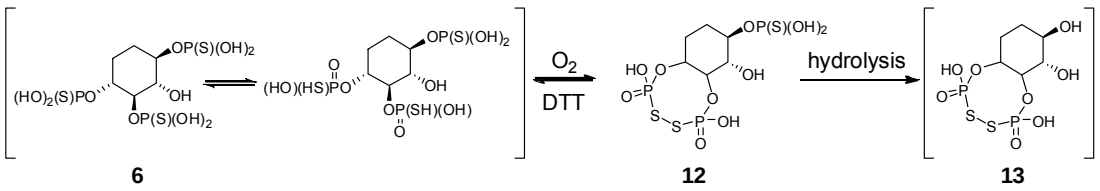

6 **12** **13**

Part II. Disruption of redox-regulating systems by illudin S and acylfulvenes

Acylfulvenes (AFs) are a class of antitumor agents with favorable cytotoxic selectivity profiles compared to their natural product precursor, illudin S. Illudin S readily reacts with thiol-containing small molecules such as cysteine, glutathione, and cysteine-containing peptides in slightly acidic pH (pH 6) in aqueous solution; reduced cellular glutathione levels can affect illudin S toxicity. However, AFs are less reactive towards these small thiols under the same conditions. By analogy, these compounds were proposed to have similar reactivity towards thiol-containing proteins, which may be responsible for AFs improved anticancer selectivity. The glutathione system (GSH and glutathione reductase (GR)) and thioredoxin system (thioredoxin reductase (TrxR) and thioredoxin (Trx)) are the major cellular redox-regulating systems that maintain cellular redox homeostasis, offering protection against oxidative stress. Disrupting this system will affect cell viability and lead to apoptosis. Furthermore, overexpression of thioredoxin and thioredoxin reductase in certain tumors is associated with higher proliferation capacities and lower apoptosis rates. The enzymes involved in these systems all have critical cysteine residues at the active site. The reactivities of illudin S and AFs toward these thiol-containing proteins were evaluated.

The inhibition potency of illudin S and AFs is in the same order for GR, TrxR, and Trx, which is opposite what was expected based on their reactivity with small thiols, i.e., HMAF > AF > illudin S, however, both AFs irreversibly inhibit TrxR and Trx by targeting the active site cysteines. For GR, HMAF is an irreversible inhibitor, while AF is a reversible inhibitor. GR and TrxR share great structural and activity similarity, but TrxR has a selenocysteine (Sec) at the active site, which makes TrxR more reactive toward electrophiles. The IC_{50}s for TrxR were in low micromolar range, while that for GR were hundred-fold higher. However, the presence of Sec is not the only reason in dictating the difference reactivity towards these two enzymes, since no covalent interaction occurs between AFs and glutathione peroxidase (Gpx), another redox-regulating enzyme containing Sec at active site. Furthermore, the inhibition of cellular GR and TrxR activity and reduction of Trx cellular protein level upon AFs treament suggest that they are AFs' cellular targets. Quenching of intrinsic fluorescence of GR and

Trx suggests extensive conformational changes of by illudin S and AFs, which may facilitate the interaction between AFs and enzymes, but not the same case for illudin S.

The differential reactivity of illudin S anda AFs towards these thiol-containing enzymes suggests that compared to small thiol-containing molecules, accessibility and reactivity of the enzyme active sites account for the inhibitory effects of AFs. The disruption of cellular redox systems by AFs may contribute to their improved anticancer selectivity compared to illudin S. The data obtained in this study are valuable in further understanding the role of modulating cellular redox enzymes in the anticancer effects of alkylating agents.

Chapter Four: Profiling patterns of glutathione reductase inhibition by the natural product illudin S and its acylfulvene analogues[*]

[*] Portions reproduced with permission from Xiaodan Liu and Shana J. Sturla. 2009 Mol. BioSyst. (5): 1013-1024.

1. Introduction

Fungal metabolism is a rich source of unique pharmacophore platforms, often exhibiting varying degrees of toxicity that may be detrimental to health or valuable for anti-infective or anticancer activity.[237, 238] Unlike modern target-directed drug development strategies, the structural complexity and bottom-up characteristics associated with natural product bioactivity, often translates to compounds with the capacity to interact with multiple cellular targets.[239] Understanding the range of contributing biochemical and chemical interactions and how they are interrelated may be a key for developing improved therapeutics or avoiding unwanted toxicities, and can also suggest new potential drug targets.

Acylfulvenes (AFs) are a class of antitumor agents derived from the naturally occurring sesquiterpenoid toxin illudin S, isolated from the Jack o'lantern mushroom (Chart 1).[240-243] Although illudin S is extremely cytotoxic to cancer cells, it exhibits low selectivity towards malignant cells versus normal cells and thus a narrow therapeutic window.[244] Semisynthetic analogues acylfulvene (AF) and hydroxymethylacylfulvene (HMAF) display improved therapeutic indices.[245, 246] Cellular assays suggest that illudin S and AFs covalently bind to DNA, as well as RNA and protein (Scheme 1).[247, 248] There is evidence that cytotoxicity is associated with bioactivation to a potent alkylating agent that reacts with DNA and interrupts DNA synthesis/repair (Scheme 1).[137, 247, 249-252] However, compared to conventional DNA alkylating agents, AFs display some unique activity profiles suggesting contributing interactions with other cellular targets and a distinct mechanism of action underlying cytotoxicity profiles.[134, 136] AFs also alkylate cellular proteins and react with thiols such as cysteine, glutathione or cysteine-containing peptides under slightly acidic conditions.[141, 142, 253, 254] Protein modification and protein binding are general modes of drug toxicity.[255] Furthermore, for many cellular proteins such as the glutathione reductase and thioredoxin reductase systems, cysteine thiol groups are particularly important to defend against oxidative stress and regulate the activity of cellular signaling proteins. However, the influence of AFs on critical cellular redox-regulating enzymes and their potential contributions to the cytotoxicities of AFs are not understood.

Glutathione reductase (GR, EC 1.6.4.2) is a dimeric FAD-containing enzyme with a redox-active disulfide at its active site. These two cysteine residues are different as the distal cysteine, which can interact with FAD domain, and proximal cysteine which does not. GR catalyzes the reduction of oxidized glutathione (GSSG) to reduced glutathione (GSH) at the expense of NADPH.[256, 257] The enzyme is responsible for maintaining a high intracellular ratio of GSH/GSSG which is critical in defending against oxidative stress. Known GR inhibitors such as isothiazol-3-one, can disrupt the GSH/GSSG balance and cellular reduction potentials.[258] While glutathione-drug conjugate formation may serve as a cellular detoxification route, the process of glutathione depletion may also disrupt redox homeostasis.[140, 259] Glutathione conjugation has been suggested to have a role in illudin S and AFs toxicology as a detoxification pathway. Pre-treating cells with *N*-ethylmaleimide or D,L-buthionine (*S, R*)-sulfoxime, which readily reacts with GSH or inhibits GSH synthesis, respectively, enhances cell sensitivity toward illudin S, while 2-oxothiazolidine-4-carboxylic acid pretreatment, which elevates GSH, is protective.[140] These studies were carried out for illudin S, which readily reacts with GSH, but AFs do not.[141, 142] Furthermore, there are various examples of GR inhibition for drug development strategy for antimalarials,[127] agents to decrease drug resistance,[128] and anticancer agents.[129] As a step toward mapping the overall biomolecular reactivity of AFs, and especially for understanding the potential role of interacting with redox-regulating enzymes on cytotoxic selectivities, we evaluated the influence of illudin S and AF on GR structure, activity and cellular properties.

In this study, we characterize for the first time the reactivities of illudin S and AFs toward purified yeast GR, revealing chemical structure-based differences in inhibition potencies and physical modes of the enzyme-drug interactions. The results of this study provide new information regarding how the cytotoxicities of illudin S and AF analogues may be mediated by influencing the cellular redox environment, and define chemical structure characteristics that differentiate reactivity profiles amongst this class of agents.

2. Experimental procedures

2.1 Chemicals and reagents

Illudin S was provided by MGI Pharma (Minneapolis, MN). Acylfulvene and HMAF were synthesized according to the published procedure with illudin S as starting material.[242, 243] Reduced nicotinamide adenine dinucleotide phosphate (NADPH) and oxidized glutathione (GSSG) were purchase from EMD chemicals (Gibbstown, NJ). Tris base, EDTA, BSA, and Carmustine (BCNU, 1,3-bis(2-chloroethyl)-1-nitroso-urea) were obtained from Sigma Chemical (Milwaukee, WI). Baker's yeast GR used for fluorescence evaluation was obtained from Sigma Chemical and GR for other experiments was obtained from MP Biomedicals (Cleveland, OH). Recombinant rAOR was expressed and purified as published previously.[260] Dulbecco's modified Eagle's medium (DMEM) was purchased from Mediatech (Herndon, VA). Fetal bovine serum (FBS) was purchased from Atlanta Biologicals (Lawrenceville, GA). Phosphate-buffered saline (PBS), 0.25% trypsin-EDTA, penicillin-streptomycin were obtained from Invitrogen (Carlsbad, CA). Tris-buffered saline was purchased from Biorad (Hercules, CA).

2.2 General considerations

GR, NADPH, GSSG, and bovine serum albumin (BSA) stock solutions were prepared in Tris-Cl buffer (50 mM, pH 7.2) containing EDTA (1 mM), i.e. TE buffer. All assays were carried out in TE buffer containing 0.3% (w/v) bovine serum albumin. Stock solutions of test compounds were prepared in DMSO, and aliquots of these solutions were added to the reaction mixture to yield a final DMSO concentration of 2% (v/v). GR activity was determined by measuring NADPH oxidation by monitoring change in UV absorbance at 340 nm with a Varian Cary 100 double-beam spectrophotometer.[256] All the measurements were performed in triplicates, and the data were presented as mean ± standard deviation. Fluorescence measurements were carried out on a Varian Cary spectrofluorometer at 90° in relation to the excitation source. Fluorescence was measured with excitation at 270 nm (bandpasses of 5 and 10 nm for excitation and emission respectively) and emission from 295 to 450 nm. HPLC analysis was carried out on an Agilent 1100 series instrument with diode array detector and autosampler. Analytes were

eluted with a solvent gradient involving, initially, 10% acetonitrile in water, linearly increasing to 50% acetonitrile in water over a course of 30 min, at a flow rate of 1 mL/min. A Phenomenex Luna 5 μm C_{18}(2) 100 Å 250 mm × 4.60 mm was used (Phenomenex, Torrance, CA).

Liquid chromatography-mass spectrometry (LC/MS) analyses were carried out on an Agilent 1100 capillary HPLC- iontrap mass spectrometer operated in positive ion mode; the HPLC was equipped with an autosampler. A Zorbax 300 SB-C3 column (150 mm×0.5 mm, 5 μm) was used. Analytes were eluted with a solvent gradient of 0.05% TFA in water (A) and 0.05% TFA in acetonitrile (B), at a flow rate of 15 μL/min: initial conditions, 30:70 B:A, were held 3 min followed by a linear increase to 80:20 B:A over a course of 20 min. Spectra were obtained by full scan data acquisition performed within *m/z* 100-1500. Mass deconvolution was performed with the Agilent ion trap analysis software.

LC/MS/MS analysis of peptide mixtures was performed on an Agilent 1100 capillary HPLC in line with an Agilent 1100 iontrap mass spectrometer operated in positive ion mode. An Agilent Zorbax SB-C18 column (150 mm× 0.5 mm, 5 μm) was used. Analytes were eluted with a gradient of solvent A (0.5% formic acid/0.01% TFA in water) and solvent B (0.5% formic acid/0.01% TFA in acetonitrile) at a flow rate of 15 μL/min: initial conditions, 3:97 B:A, were held constant for 3 min, and then increased to 5:95 B:A in 7 min and held for 10 min followed by linear increase to 35:65 B:A over a course of 95 min, and finally to 75:25 B:A in 10 min.

2.3 Substrate screening

To determine whether test compounds were GR substrates, each compound (AF and HMAF, 400 μM; Illudin S, 1 mM; reference blank, 2% DMSO) was combined individually with NADPH (200 μM) and GR (2.5 μM) in TE buffer with a final volume of 200 μL and allowed to react at 37 °C for 2 h. The resulting solution was extracted with ethyl acetate (EtOAc, 200 μL) and centrifuged for 5 min (6000 g). The supernatant was collected and EtOAc was evaporated under a stream of N_2. The dried material was reconstituted in 100 μL DMSO and 50 μL was injected and analyzed with the HPLC

method. As a positive control, the same procedure was carried out with AOR (2 μM) in place of GR.

2.4 Measurement of GR activity

GR inhibition assays were performed by combining NADPH (150 μM) and GR (5 nM) in TE buffer, total volume 200 μL in disposable acrylic cuvettes at 25 °C. GR was first treated with NADPH for 10 min before the addition of the test compound at the indicated concentration (AF, 62.5, 125, 250, 625, 750, 1000, 1250 μM; HMAF, 62.5, 125, 250, 625, 1250 μM; illudin S, 62.5, 125, 250, 625, 1250, 2000 μM) and further allowed to react for 30 min. GSSG (360 μL, 350 μM) and further allowed to react for 30 min. GSSG (360 μL, 350 μM) was then added and the decrease in absorbance at A_{340} was monitored over 3 min. Measurements were performed in triplicate. IC_{50} values were determined from a plot of relative activity v.s. compound concentration (Kaleidagraph). To evaluate the time-dependence of GR inhibition, GR was allowed to react with the test compounds (AF, 0, 500, 750, 1000 μM and 1250 μM; HMAF, 0, 125, 250, 500 and 1250 μM) in the same manner as described above and aliquots (200 μL) were taken at different time intervals (0, 2, 7, 13, 24, 30 min) and assayed as described above. To evaluate the effect of added substrate, i.e. GSSG on drug-mediated enzyme inhibition, GR was treated with test compounds in a total volume of 200 μL containing GSSG (250 μM or 1250 μM) for 30 min. Activity was determined by following A_{340} upon addition of 360 μL TE buffer containing GSSG (350 μM) and NADPH (100 μM) in the manner described above. To evaluate the effect of NADPH on GR inhibition, GR was allowed to react with compounds in the absence of NADPH for 30 min, and activity was measured in the same way as described for evaluating the effect of GSSG.

To determine the reversibility of inhibition, GR was allowed to react with AFs (AF, 250, 625, 750, 1000, 1250 μM; HMAF, 62.5, 125, 250, 625, 1250 μM) as described. After the 30 min reaction period, unbound compound was removed by gel-filtration with a size-exclusion micro bio-spin P6 pre-packed column according to the manufacturer's protocols. Briefly, the column was placed in 2 mL centrifuge tube to drain the excess packing buffer by gravity and the drained buffer was drained. The column was placed

back into the tube and centrifuged to remove the packing buffer (2 min, 1000 g). The column was placed in a clean centrifuge tube, and the reaction solution was loaded into two columns (100 μL/each) and the column was centrifuges for 4 min at 1000 g. The resulting solution was combined, and the activity was determined following the procedure described above.

2.5 Protein adduct analysis

GR (250 μg, 5 nmol) was allowed to react with AFs (1.25 mM) in a total volume of 1 mL TE buffer containing NADPH (1 mM) for 3 h at 25 °C. An aliquot (1 μL) of reaction solution was withdrawn and diluted to 200 μL; enzyme activity was determined as described above for measurement of GR activity. At 3 h, 50% GR activity was inhibited by HMAF, and 30% by AF. An Amicon ultra-4 centrifugal filter device (30,000 NMWL, Millipore, MA) was used to concentrate GR and remove unbound compound. GR was reconstituted in 1 mL TE buffer and re-treated in the same manner. After another 3 h incubation, GR activity was diminished 100% by HMAF, and 50% by AF. Modified GR was again concentrated with an Amicon filter, and unbound compound was further removed with a size exclusion micro Bio-spin P6 pre-packed column (6,000 NWML, Biorad, Hercules, CA). GR (250 μg, 5 nmol) was allowed to react with carmustine (0.25 mM) in a total volume of 1 mL TE buffer containing NADPH (1 mM) for 3 h at 25 °C. An Amicon ultra-4 centrifugal filter and micro bio-spin P6 pre-packed column were used to concentrate GR and remove unbound compound. The resulting solution was dried on a Speedvac concentrator (Savant, Waltham, MA). GR (20 μg in 8 μL TE buffer) was analyzed by LC/MS using method described in the general consideration. Both native and modified GR proteins eluted as a single peak with retention time 12.5 min.

2.6 Protein digestion and modified peptide analysis

Adducted protein samples obtained as described above (~200 μg, 4 nmol) were reconstituted in 20 μL guanidine-HCl (8 M, pH 7.2) containing 50 mM dithiothreitol (DTT) and heated at 95 °C for 15 min. Iodoacetamide (IAA, 5 μL, 0.5 M in TE buffer) was added and allowed to react for 30 min at 25 °C. Ammonium bicarbonate buffer (600 μL, pH 8), followed by trypsin (10 μg, ~0.43 nmol) was added. Proteolytic digestion was

allowed to occur at 37 °C for 24 h. Equal amount of the resulting mixtures were placed into two centrifuge tubes, and dried on a Speedvac concentrator and reconstituted in 200 μL of solvent A (0.5% formic acid/0.01% TFA in water). Modified peptides were analyzed by the general LC/MS/MS method.

2.7 Fluorescence analysis of GR

To evaluate conformational changes of GR in the presence of test compounds, GR (2 μM) was treated with test compounds in a total volume of 0.5 mL TE buffer at indicated conditions for 30 min at 25 °C. Changes in intrinsic fluorescence were evaluated by using the general method. To evaluate the effect of test compounds on GR, GR was treated with either AF or HMAF (0.01, 0.04, 0.2, 1 mM) or illudin S (0.02, 0.1, 0.4, 2 mM). To evaluate the effect of test compound on GR in the presence of GSSG, GR was treated with test compounds in the presence of GSSG (400 μM). To evaluate the effect of test compounds on NADPH-reduced GR, GR was pre-reduced by NADPH (100 μM) for 10 min followed by the compound treatment. GR was also pre-treated with both NADPH (100 μM) and GSSG (400 μM) for 10 min prior to addition of the test compounds.

2.8 Cell culture and cellular GR determination

Hela cells were maintained as monolayers in DMEM medium supplemented with 10% FBS and 1% penicillin-streptomycin in a humidified, 5% CO_2 atmosphere at 37 °C. Hela cells were subcultured in the medium described above for three days to reach 80% confluence (100 mm^2 plate, 2×10^6 cells/plate). Cells were treated with test compounds diluted with medium (0.1% final concentration of DMSO) for two or ten hours. After the treatment period cells were washed with PBS twice. Cells were collected as follows: 2 mL of 0.25% trypsin-EDTA was added and the cells were incubated for 5 min at 25 °C, and then cells were scratched off and divided evenly into three centrifuge tube (1.5 mL), and centrifuged (5 min, 1000g) followed by removal of the supernatant. Cells were resuspended in 0.2 mL of lysis buffer (50 mM Tris-HCl, pH 7.5; 1 mM EDTA; 0.1% Triton X-100; 1 mM phenylmethanesulfonyl fluoride; 1 mM benzamidine; 1.4 μM pepstatin A; and 2.0 μM leupeptin) and sonicated at 4 °C (5 s bursts). The resulting cell

lysate was centrifuged for 10 min (8000 g, 4 °C), and the supernatant was withdrawn for analysis. Cell cytosol containing 50 μg protein as determined by the bicinchoninic acid (BCA) protein assay reagent (Pierce, Rockford, IL) was incubated with 325 μL of 1 mM GSSG in TE buffer at 25 °C for 10 min. NADPH (150 μL, 1 mM) was added, and the rate of NADPH consumption was monitoring changes in absorbance at 340 nm for 5 min at 25 °C.

Cell cytosol containing 25 μg protein was analyzed by 4-12% SDS-PAGE according to the manufacturer's protocol (Invitrogen, Carlsbad, CA) and transferred onto a membrane (PVDF, Invitrogen, Carlsbad, CA) for 1 h at 33 V, 4 °C. Membranes were blocked with 5% (w/v) nonfat milk powder in tris-buffered saline (TBS)/Tween 20 (0.05%) overnight at 4 °C. The membrane was incubated with primary anti-GR (ABR, Rockford, IL) and anti-actin (Invitrogen, Carlsbad, CA) antibodies diluted 2000 times in TBS/Tween 20 (5 mL) for 1 h. The membrane was washed three times with TBS/Tween 20 (5mL, 5 min) and subject to incubation with 5 mL of secondary conjugated antibody (goat anti-rabbit IgG horseradish peroxidase, Biorad, Hercules, CA, 1:2000 dilution in TBS/Tween 20,) for 1 h. After four 5 min washes with TBS/Tween 20 (5 mL/each), enhanced chemiluminescence was measured with a western blotting analysis system (Pierce, Rockford, IL).

3. Results

3.1 Concentration and time-dependent inhibition of GR

To test the hypothesis that illudin S and AFs may inhibit GR and to compare their potencies as GR inhibitors, various concentrations of the test compounds were incubated with GR in the presence of NADPH for 30 min. Loss of enzyme activity was observed in a concentration-dependent manner for AFs (Figure 1A). Calculated IC_{50} values are 216 μM for HMAF and 871 μM for AF; 2 mM illudin S did not inhibit GR. As a positive control, under the same conditions, we measured a 71 μM IC_{50} for carmustine, which is consistent with published data (Figure 2).[110] On the basis of these data, four concentrations of AFs were selected to study the time-dependence of the observed inhibition. GR was incubated with varying HMAF concentrations for 30 min (Figure 1B and 1C). The enzyme activity decreased with time, characteristic of irreversible inhibition, and inhibitory parameters (K_i and k_{inact}) were determined.[261] Thus, the linear correlation derived from a plot of reciprocal of apparent inhibition rate constants (K_{app}) versus the reciprocal of HMAF concentration (Figure 1C inset), yields the inactivation rate constant k_{inact} (0.2 min^{-1}) and inhibitory constant K_i (180 μM) were derived on the basis of the following equations*:

$$\frac{1}{K_{app}} = \frac{1}{k_{inact}} + \frac{K_i}{k_{inact}} \frac{1}{[\text{HMAF}]}$$

$$\text{HMAF} + \text{GR} \overset{K_i}{\rightleftharpoons} \text{HMAF:GR*} \xrightarrow{k_{inact}} \text{HMAF-GR}$$

These data further confirm that GR inhibition by HMAF is irreversible.[261] The same experiment was carried out for AF, however, these data suggest a rapid initial loss of activity, then establishment of equilibrium. Such behaviour does not fit the same model,[261] indicating that the GR inhibition mechanisms for AF and HMAF are different from each other.

* [HMAF] is high relative to GR concentration at time 0, [GR_0]. HMAF:GR* is the HMAF:GR complex, and HMAF-GR is the inactivated enzyme

3.2 GR Substrate screening

To verify that there was no GR-mediated conversion of illudin S and AFs to their major cytosolic metabolites, we compared the released products of the reactions of test compounds and GR with those from AOR, a cytosolic enzyme that has been characterized with regard to its AF-bioactivating capacity (Scheme 1).[137, 138, 262, 263] In the AOR-catalyzed reduction of AF and HMAF with NADPH as a cofactor, one major metabolite was observed by HPLC analysis of the extracted reaction mixture, and this product had the same retention time and UV spectra as the synthetic standard M_A and M_H (Chart 1).[262, 263] Under the experimental conditions, no metabolites were observed to be formed from the reaction of AOR/NADPH with illudin S.[138, 264] Finally, no M_A, M_H or M_I was observed when illudin S and AFs were tested as possible substrates for GR-mediated conversion at a constant NADPH concentration and in the absence of GSSG (Figure 3).

3.3 Gel-filtration of inhibited GR

To determine whether GR inhibition by AFs is reversible, gel-filtration studies were conducted in which GR was allowed to react with AFs in the same way as described for studies carried out to determine the concentration-dependence of inhibition. Inactivated GR was passed through a size exclusion micro Bio-spin P6 gel-filtration column (NWML 6000) to remove non-covalently bound compounds. The results of this process were that the GR activity inhibited by AF was recovered, but not that inhibited by HMAF (Figure 4). These results indicate that AF is a reversible inhibitor and HMAF is an irreversible inhibitor.

3.4 Effect of GSSG on GR inhibition

To probe the nature of the AF-GR interaction with respect to the proximity of binding at or near the active site where the natural substrate GSSG interacts, a competitive inhibition assay was carried out in the presence of GSSG. A moderate protective effect against inhibition by HMAF was observed, which did not depend on GSSG concentration (Figure 5B). Thus, when GSSG concentration was equal to or less than the highest drug concentration (1250 μM), no protection towards GR inhibition was observed, suggesting that HMAF may be more competitive for the active site. However, the presence of GSSG did not protect GR from inhibition by AF (Figure 5A). These

results suggest that AF may bind to the GR at an allosteric site, but HMAF binds to the active site as well as other binding sites. In contrast, 250 μM GSSG protected GR from inhibition by carmustine (Figure 6), suggesting that carmustine only binds to GR active site.

3.5 Effect of NADPH on the inhibition of GR by AFs

NADPH reduces the disulfide bridge at the GR active site to generate two free cysteine thiols that in turn reduce GSSG to GSH through disulfide/dithiol exchange. To determine whether the reduced form of GR is required for GR inhibition by AFs, NADPH was omitted from the incubation solution and added only at the point of measuring GR activity (a requirement of the spectroscopic assay). In this study, GR inhibition by AFs was observed to be mildly attenuated. Thus, GR inhibition by 1000 μM and 1250 μM AF was reduced by 30%; GR inhibition by 625 μM and 1250 μM HMAF was reduced by 45% (Figure 7). In contrast, GR pre-reduction by NADPH is absolutely required for GR inhibition by carmustine (Figure 6), further illustrating differences in modes of enzyme interaction for AFs vs. carmustine, and suggesting that AFs may interact with portions of GR other than the active site, in a process that may contribute in part to enzyme inactivation.

3.6 Drug-induced intrinsic GR fluorescence quenching

Data obtained from the experiments described indicate that GR inhibition depends only mildly on active site protection by GSSG and pre-reduction by NADPH. We were therefore interested in determining whether drug binding induced any conformational changes in the enzyme and such changes therefore were probed by analyzing intrinsic GR fluorescence. Illudin S and AFs are inherently non-fluorescent molecules, and the buffer system does not have an appreciable effect on the intrinsic fluorescence of GR unless NADPH, which has fluorescence emission peak a 460 nm and causes reduction on GR intrinsic fluorescence, is present. As shown in Figure 8, all of the compounds tested caused significant decreases in GR fluorescence. Peak splitting in the 300-360 nm spectral region was observed regardless of whether GSSG or NADPH were present which may associated with GR unfolding.[265, 266] Thus, at micromolar concentrations, illudin S and AFs can completely eliminate the intrinsic GR fluorescence, suggesting

extensive binding interactions of these small molecules with GR, and that GR inhibition by AFs is at least partially due to a drug-induced GR conformational change. Carmustine can also induce a 50% decrease of GR fluorescence intensity, which is observed at 1 mM drug concentration, and does not cause peak shift and splitting as observed in illudin and AF-mediated fluorescence changes (Figure 9).

3.7 MS analysis of a whole protein adduct

On the basis of gel-filtration data, we established that GR inhibition by HMAF is irreversible, while for AF it is reversible. Therefore, LC/MS was used to obtain information regarding the chemical nature of HMAF-GR. In the control sample, i.e. enzyme treated with an equal amount of DMSO, a peak with *m/z* 51499 corresponding to the GR monomer was observed (Figure 10), which is consistent with published data in which the GR monomer *m/z* 51488, as well as the truncated monomer *m/z* 51719, was observed, with no GR homodimer detected.[267] A higher GR concentration (5 μM) was used for LC/MS sample preparation, such that GR incubated with 1 mM AFs in the presence of NADPH at a total volume of 1 mL for three hours at 25 °C, was not completely inactivated. GR was concentrated and unbound drug was removed with an Amicon Ultra-4 centrifuge filter (NWML 30,000). The concentrated enzyme was reconstituted and treated by the same procedure for three more hours, which resulted in total loss of GR activity by HMAF and 50% loss by AF. Filtered samples were analyzed by LC/MS, and the results are presented in Figure 10. The AF-treated GR was unchanged compared to the control, consistent with the expected lack of covalent adduction. After reaction with HMAF, however, the parent GR was completely absent, and a new peak with an *m/z* 51992, corresponding to the bis-adduct (GR monomer + 2×246 Da), was observed. In contrast, mono-adduct was observed for carmustine-treated GR (Figure 11), which is consistent with X-ray data previously obtained for carmustine-GR crystals.[268]

3.8 LC/MS/MS analysis of GR active site peptide modified by HMAF

The whole protein analysis data presented above indicates the formation of a bis-adduct between GR and HMAF. Further insight regarding identities of HMAF-modified amino acids was obtained by LC/MS/MS analysis of proteolytically digested GR. Modified and control samples were treated with trypsin after DTT reduction and IAA

alkylation to block cysteine disulfide formation.[269] For control GR, the observed full scan ion *m/z* 716.6 corresponds to the doubly charged active site peptide ALGGTC^{42}VNVGC^{47}VPK (calculated MW: 1430.2 Da, Figure 12A). When subjected to collision-induced dissociation (CID) in the ion trap mass spectrometer, the masses of *y* and *b* series ions[270] were in agreement with theoretical values for this peptide with cysteines modified by IAA (Figure 12A). The full scan ion *m/z* 716.6 was not observed in the LC/MS/MS spectrum of HMAF-treated GR. Instead a doubly charged peptide peak ion *m*/*z* 905.4 $[M + 2H]^{2+}$ was observed, and this mass corresponds to modification of the active-site peptide sequence with two equivalents of HMAF (calculated MW: 1808.8 Da, Figure 12B). This fragmentation signal is weak, and not all diagnostic *y* and *b* ions were detected. Furthermore, inherent in the peptide sequence, the calculated b_6-b_9 ion masses are the same as y_5-y_8 (Table 1.) Therefore, although these fragmentations were detected, it remains ambiguous which portion of the modified peptide these peaks represent. Significantly, b_{11} and y_9 with a mass increase by 2×246 were observed, suggesting adducts reside on both cysteines.

3.9 Cellular GR inhibition

Human cervical cancer cells (Hela) were used to determine whether the test compounds influence the cellular GR activity and GR protein levels. Due to the cytotoxicity of these compounds, concentrations causing less than 20% cell death were selected to treat cells. After exposure to equitoxic dose of illudin S and AFs for 2 h and 12 h respectively, cells were collected and cellular GR activities were measured. As shown in Figure 13A, 2 h treatment did not cause any significant inhibitory effect on cellular GR activity by illudin S or AFs, but 20-40% inhibition of GR activity was observed by carmustine treatment. Cellular GR activity was inhibited about 40% after 12 h exposure to 4 μM HMAF and 70% from 5 μM carmustine (Figure 13B). Thus, the relative magnitudes of cellular GR inhibition by HMAF and carmustine are comparable with their inhibition potencies in the cell-free system. AF did not inhibit cellular GR activity. Interestingly, after 12 h treatment illudin S inhibited GR activity by 50%, and in a concentration-independent manner. Western blotting analysis does not suggest any reduction in cellular GR protein levels (Figure 14), however, carmustine slightly reduces

the GR level and a new band was observed with a molecular weight close to the GR dimer which may be the crosslink adduct formed between carmustine and two GR monomers, or between carmustine, GR and some other cellular protein with similar molecular weight.

4. Discussion

DNA alkylation is thought to play a major role in illudin S and AF toxicity, however at equitoxic concentrations, the incorporation of AFs into genomic DNA in tumor cells is similar with that of illudin S, suggesting other cellular reactivity factors may play a role in distinguishing the improved therapeutic index of AFs versus illudin S.[247, 248] For example, reductase-mediated bioactivation has been shown to contribute in part to dictating differences in cytotoxicity profiles for AFs.[139] Further, the extreme toxicity of illudin S has been attributed to its reactivity towards thiols like GSH.[140] By analogy, it has been hypothesized that illudin S can react with thiol-containing enzymes, which may be expected to contribute to cytotoxicity.[140] Compared with illudin S, AFs are much less reactive towards small-molecule thiols.[142, 242] However, no studies have been carried out to test whether illudin S reacts with thiol-containing enzymes differently than AFs, in order to address the potential role of this process in their toxicity.[271] On the basis of data obtained in the present study, a proposed model accounting for differences in reactivity profiles of illudin S and AFs toward the critical thiol-containing GR, compared with the known GR inhibitor carmustine, is illustrated in Scheme 3.

In the current study, yeast GR, a key enzyme involved in cellular redox regulation, was selected as a model to profile relative reactivities of illudin S and its AF analogues toward enzymes containing critical thiols. Yeast GR is a homodimeric flavoenzyme that shares considerable sequence homology with human and *E. coli* GR. Human and yeast GR exhibit ~68% similarity with almost identical FAD-binding domain sequences that contain the critical redox-active dithiol.[272, 273] The dimeric forms of human and *E. coli* GR are important for catalysis, and the monomers are not enzymatically active.[274, 275] Mechanistic studies of dimer dissociation and unfolding of yeast GR, induced by acid and pressure,[266] or by a denaturing agent (i.e. guanidine hydrochloride),[265] were associated with changes in GR intrinsic fluorescence. In addition, unfolding can release more accessible cysteines compared to native GR.

Monitoring changes in intrinsic protein fluorescence is an approach to evaluate GR conformational changes with respect to the unfolding and possible dissociation of the GR homodimer.[265, 276] Not all reported GR inhibitors can induce fluorescence changes, but

for examples such as endogenous aldehydes, isocyanates, and trehalose, capacity to change GR intrinsic fluorescence correlates with GR binding and conformational changes.[277-279] In this study, we found that each test compound quenches GR intrinsic fluorescence to different extents. Micromolar illudin S and AFs significantly quench GR intrinsic fluorescence regardless of the presence or absence of GSSG and NADPH (Figure 8). Carmustine, however, does not affect GR fluorescence at micromolar concentration and quenches 50% GR fluorescence at 1 mM drug concentration (Figure 9). Together, these data suggest that the interactions between GR and illudin S or AFs are more extensive, i.e. involve physical interactions that may manifest in fluorescence change, than for carmustine, which has been reported to react with one cysteine residue at the GR active site.[268] There are 12 tyrosine, 4 tryptophan, and 13 phenylalanine residues on the solvent-accessible surface of GR. The observed fluorescence quenching for the interactions of AFs or illudin S with GR may reflect direct interaction of drug with these residues that quenches GR intrinsic fluorescence with or without an associated conformational changes.[280, 281] In addition, the peak splitting that causes the red and blue-shifts in the protein intrinsic fluorescence spectra may also reflect possible GR conformational change induced by the drugs. This hypothesis is also supported by the present observation that the GSSG-bound form of GR can still be inhibited by AFs (Figure 5). Without NADPH present, GR can also be inhibited by AFs, and this profile is similar to the reported inhibitor *O*-phthalaldehyde, which reacts with non-essential residues (Figure 7).[282] In contrast, NADPH is required for carmustine-mediated inhibition, and GSSG can completely block it (Figure 6). Although illudin S induces similar fluorescence changes, it does not inhibit enzyme activity (up to 2 mM illudin S was tested). The lack of planarity and additional substituents in the cyclopentane ring of illudin S compared to AFs may be contributing factors, i.e. steric hinderances, leading to the diminished reactivity of illudin S toward the enzyme active site vs. small-molecule thiols.

Results of this study indicate that AF is a reversible GR inhibitor and HMAF is an irreversible inhibitor. Mass spectrometry analysis of whole GR protein modified by HMAF, or carmustine as a positive control, reveals that HMAF forms a bis-adduct

(Figure 10) and carmustine forms a mono-adduct with GR (Figure 11). The presence of four-fold higher level of BSA in addition to GR, which contains 35 cysteine residues, does not interfere with the formation of the observed GR-HMAF adduct, suggesting that the alkylation process is selective towards GR active site and not a result of indiscriminant reactions with cysteine residues in the protein. When BSA was allowed to react with HMAF for two days at room temperature, mono-adduct can be observed with a mass increase by 229 which may be resulted from the direct replacement of the hydroxyl group by the thiol on the cysteine residue.

On the basis of published data and the protein fingerprint analysis, the purified GR used in this study contains four cysteine residues (refer to yeast GR sequence accession number BAA07109), and therefore studies were carried out to address whether there is any molecular specificity in the covalent interaction of HMAF with GR. Information regarding the drug-GR covalent adducts was obtained by LC-ESI-MS analysis of modified whole protein. We utilized LC-ESI-MS/MS and matrix-assisted laser desorption/ionization mass spectrometry (MALDI) to identify the modification sites. In such analyses, chemical modifications may significantly modulate peptide ionization efficiencies.[283] By MALDI, none of the intact or modified active site peptides (IAA- or HMAF) was detected, possibly due to the overall high hydrophobicity, since ESI tends to favor the ionization of hydrophobic peptides compared to MALDI.[284] However, the peptides containing the other two cysteines other than the active site cysteines were detected by MALDI and neither of them were modified after HMAF treatment, suggesting that the GR alkylation by HAMF does not occur at these two cysteines. By LC-ESI-MS/MS, fragments of control IAA-alkylated peptides exhibited a strong spectral signature in which most *y* and *b* fragment ions were detected (Figure 12); however, for the free active site sequence, the corresponding peptide peak (*m/z* 659.4) was not observed. The lack of a peak corresponding to the free peptide may be due to disulfide formation, or that IAA-alkylation may enhance ionization efficiencies of the active site peptides. By contrast, no IAA alkylated active site peptide (*m/z* 716.6) was observed in HMAF-modified GR digestion mixtures, indicating that the active site sequence has been modified by HMAF. The peptide observed after reaction with HMAF yields a MS

fragmentation pattern that is consistent with HMAF-induced alkylation of both active-site cysteines (Scheme 2). Key *y* and *b* ions were detected to locate the modified residues. Still, certain complexities in the mass spectra make some fragments hard to address.

On the basis of these results, we propose a model describing differences in patterns of GR interactions by small molecules comprised of the following steps: 1. Drug-enzyme binding (E:Drug); 2. Induction of a conformational change in GR (E*), reflected by a change in intrinsic fluorescence; 3. Enzyme inactivation, i.e. measured by loss of GSSG-reducing capacity; 4. Chemical reaction between the activated GR-drug complex and conversion to covalent adducts. In this process, illudin S only proceeds to the first stage and induces conformational changes that are not associated with activity loss. AF reacts with GR reversibly, and the binding of AF to GR is probably locating at sites other than the active site since the presence of GSSG does not protect GR activity. The interaction of GR with HMAF is more complicated. Initially as a reversible inhibitor, HMAF competes with GSSG for the active site, but also has other binding sites, consistent with our observation that GSSG can only partially block inhibition. Further, the absence of NADPH does not diminish GR inhibition, and this process may induce unfolding to expose the proximal cysteine. As an irreversible inhibitor, HMAF can proceed through all steps shown in scheme 3 and react with NADPH-reduced GR, leading to reactions with both cysteines at the active site and forming a bis-adduct. Finally, in comparison, carmustine may not induce conformational changes that facilitate the exposure of the proximal cysteine, and thus forms a mono-adduct at the distal cysteine.

To evaluate the influence of the test compounds on cellular GR at equitoxic concentrations, human cervical cancer cells (Hela), which are generally responsive towards AFs, were treated with test compounds at equitoxic concentrations that maintain 80% cell survival.[134] The data obtained indicates that AF does not inhibit cellular GR, which is consistent with the cell-free observations since the weak and reversible GR inhibition may be attenuated by other species in the context of the cellular environment. HMAF and carmustine both inhibit cellular GR with relative potencies that mirror their relative in *vitro* IC_{50}, suggesting that covalent modification contributes in a similar manner for these agents to the observed cellular enzyme inhibition. Interestingly, illudin

S was observed to inhibit cellular GR activity in a concentration-independent manner (Figure 13). This observation is difficult to explain, and may be related to illudin activation to a chemically reactive and GR-interactive species by cellular reductase or by GSH conjugation.[140, 264] Further studies are needed to reconcile the observed differences and elucidate the potential role of drug metabolism in modulating GR inhibition potency; however, preliminary studies have not been informative because of potential confounding protein-protein interactions between isolated reductase enzymes.

Cellular thiol-based redox regulation is tightly controled by antioxidant enzymes such as GR, as well as thioredoxin reductase, thioredoxin and glutathione S-peroxidase.[113, 115] The current study is the first step towards mapping illudin S and AFs reactivities towards these enzymes and potential cellular consequences, which will provide useful information regarding the mechanisms of small molecule cytotoxicity, and facilitate the design and synthesis of more potent antitumor derivatives. Furthermore, this study links the antitumor profiles of these cytotoxins with their interaction profiles for a representative enzyme containing key cysteine residues.

5. Conclusion

We have evaluated mechanisms of GR inhibition by the natural product illudin S and its AF analogues, and compared their activities with the known GR inhibitor carmustine. On the basis of results of experiments devised to evaluate enzyme inhibition, protein intrinsic fluorescence changes, reversibility of drug-enzyme interactions, covalent modification of whole proteins, and proteomic mapping of peptide covalent modification, a descriptive model accounting for structure-based differences in the reactivities of these molecules is proposed. Each of the test molecules exhibits some degree of interaction with the enzyme; however, illudin S does not inhibit GR, AF is a reversible inhibitor, and HMAF is an irreversible inhibitor that covalently modifies the protein at active site cysteine residues. In the complex environment of the cell, HMAF and illudin S inhibit GR, but do not reduce GR protein levels. Overall, the reactivities of illudin S and AF analogues toward GR are opposite what might be expected on the basis of reactivity towards thiol-containing molecules, emphasizing the importance of balancing chemical reactivity and molecular recognition in dictating biochemical responses. Furthermore, the minor impacts on cellular GR activity and expression suggest further studies needed to map reactivity profiles for illudin S and AFs toward additional cellular targets to better understand relative mechanisms of cytotoxicity. The data obtained in this study may be important in further development of alkylating agents as anticancer drugs, as we gain more information regarding the role of covalent protein modification in cytotoxicity.

Table 1. Mass of *y* and *b* ions from the IAA- and HMAF- modified GR active site sequence by trypsin digestion.

HMAF	IAA	b		Active site sequence		y	IAA	HMAF
			1	**A**	14			
	185.1	185.1	2	**L**	13	1246.6	1360.7	1738.6
	242.1	242.1	3	**G**	12	1133.5	1247.6	1625.5
	299.2	299.2	4	**G**	11	1076.5	1190.6	1568.5
	400.2	400.2	5	**T**	10	1019.5	1133.5	1511.5
749.2	560.2	503.2	6	**C**	9	918.5	1032.5	1410.5
848.3	659.3	602.3	7	**V**	8	815.4	872.5	1061.4
962.3	773.4	716.3	8	**N**	7	716.4	773.4	962.4
1061.4	872.4	815.4	9	**V**	6	602.3	659.4	848.3
1118.4	929.5	872.4	10	**G**	5	503.3	560.3	749.3
1467.4	1089.5	975.4	11	**C**	4	446.2	503.3	692.2
1566.5	1188.6	1074.5	12	**V**	3	343.2	343.2	
1663.6	1285.6	1171.6	13	**P**	2	244.2	244.2	
			14	**K**	1	147.1	147.1	

*Numbers in red represent corresponding *y* or *b* ion mass plus one molecular mass of IAA or HMAF.
Number in blue represent corresponding *y* or *b* ion mass plus two molecular masses of IAA or HMAF.

Chart 1. Structure of illudin S, acylfulvene analogues AF and HMAF, and their major metabolite, and carmustine (BCNU).

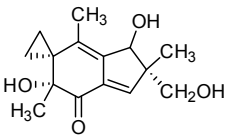

Illudin S

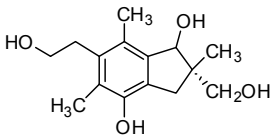

M_I

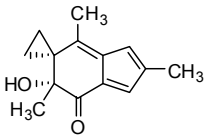

(-)-Acylfulvene (AF)

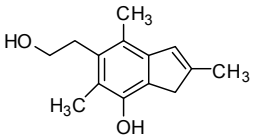

M_A

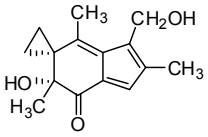

(-)-6-hydroxymethylacylfulvene (HMAF)

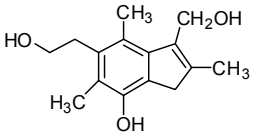

M_H

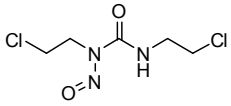

Carmustine (BCNU)

Figure 1. Inhibition of GR by AF, HMAF and illudin S. A, concentration-dependent inhibition of GR. GR (5 nM) was incubated with test compounds in the presence of NADPH (150 μM) for 30 min at 25 °C (AF (♦), 62.5, 125, 250, 625, 750, 1000, 1250 μM; HMAF (●) and Illudin S (▲), 62.5, 125, 250, 625, 1250 μM. B, time-dependent inhibition of GR by AF at 0 (●), 500 μM (♦), 750 μM (▲), 1000 μM (■), and 1250 μM (▼). C, time-dependent inhibition of GR by HMAF at 0 (●), 125 μM (■), 250 μM (▲), 500 μM (♦), and 1250 μM (▼). GR (5 nM) was incubated AFs, aliquots were withdrawn and assay for residual GR activity at different time intervals. The slopes of the lines representing apparent rate constants of inhibition (*K*app) were determined by linear regression analysis. The data were derived from a representative of two independent experiments. The inset is the Kitz and Wilson replotting of GR inhibition by HMAF: double reciprocal plot of *Kapp* vs HMAF concentration [I]. The *Ki* and k_{inact} values were determined to be 180 μM and 0.2 min^{-1} based on the following formula: $1/Kapp = 1/k_{inact} + (Ki/k_{inact}) \times 1/[I]$

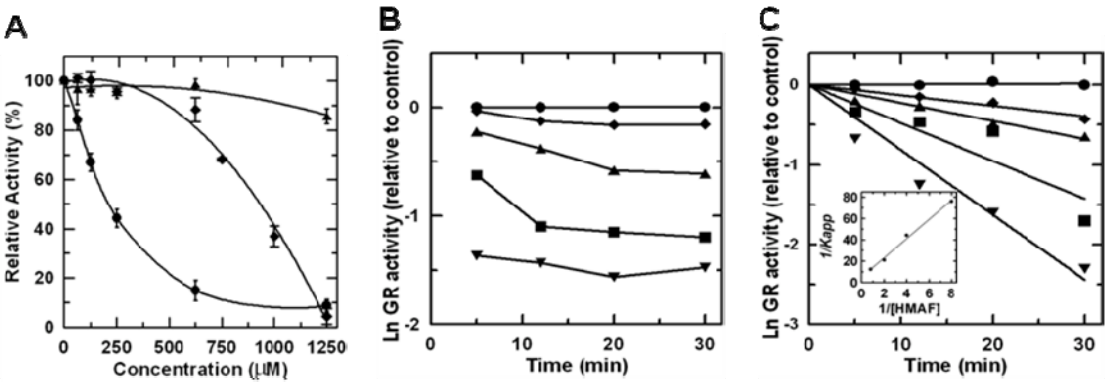

Figure 2. Inhibition of GR by carmustine. GR (5 nM) was incubated with carmustine in the presence of NADPH (150 μM) for 30 min at 25 °C, carmustine, 62.5, 125, 250, 625, 1250 μM.

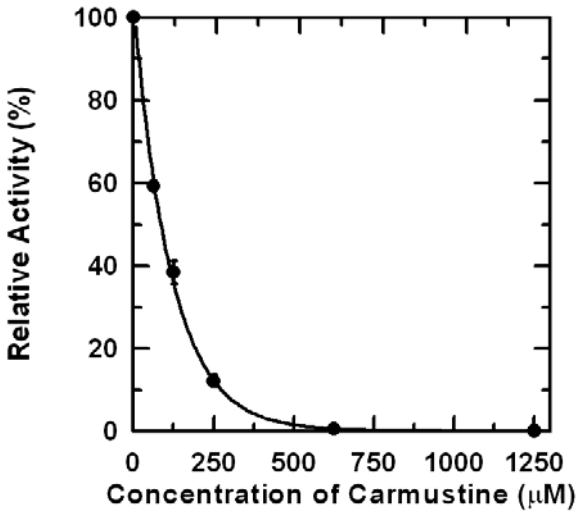

Figure 3. Substrate screening analysis for the potential conversion of illudin S and AFs to reduced metabolites by GR. Test compounds (AF, 400 μM; HMAF, 400 μM; illudin S, 1mM) were allowed to react with AOR (2 μM) or GR (2.5 μM) in TE buffer containing NADPH (200 μM) for 2 h at 37 °C, followed by EtOAc extraction and HPLC analysis. Control samples were incubated in buffer containing NADPH (200 μM) and extracted in the same manner. The peak at 5 min observed in each sample is DMSO. A. AF (26 min), M_A (21 min); A1. AF control; A2. AF-AOR; A3. AF-GR; B. HMAF (17 min), M_H (15 min); B1. HMAF control; B2. HMAF-AOR; B3. HMAF-GR; C. illudin S (13 min); C1. illudin S control; C2. illudin S-AOR; C3. illudin S-GR.

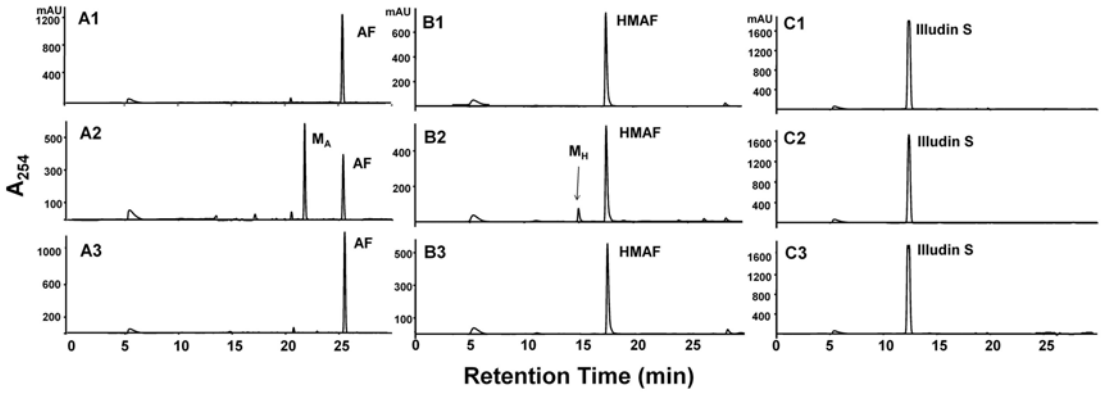

Figure 4. Gel-filtration analysis of AF and HMAF-inactivated GR. GR (5 nM) was incubated with test compounds (AF(●), 250, 625, 750, 1000, 1250 μM; HMAF(♦), 62.5, 125, 250, 625, 1250 μM) in the presence of NADPH (150 μM) in TE buffer for 30 min at 25 °C. Unbound compound was removed by micro bio-spin P6 pre-packed size exclusion columns (Biorad, Hercules, CA) with NWML 6000.

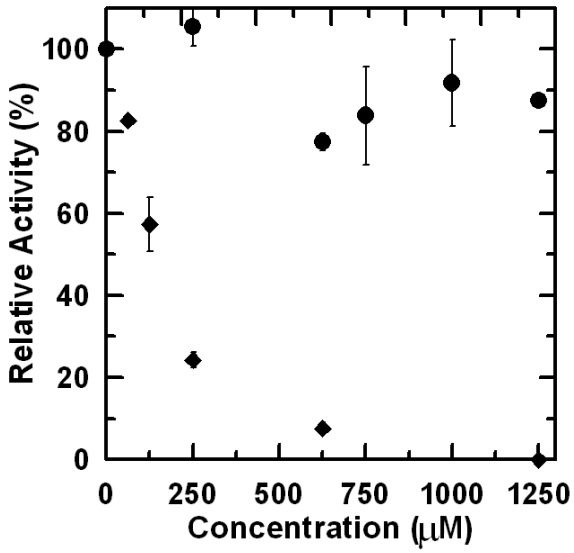

Figure 5. Effect of GSSG on the inhibition of GR by AFs. GR (5 nM) was incubated with AFs (A. AF, 250, 500, 750, 1000, 1250 μM; B. HMAF, 62.5, 125, 250, 625, 1250 μM) for 30 min in the presence of different concentration of GSSG [(●) 0, (♦) 250, (▲) 1250 μM] for 30 min, and then activity was measured.

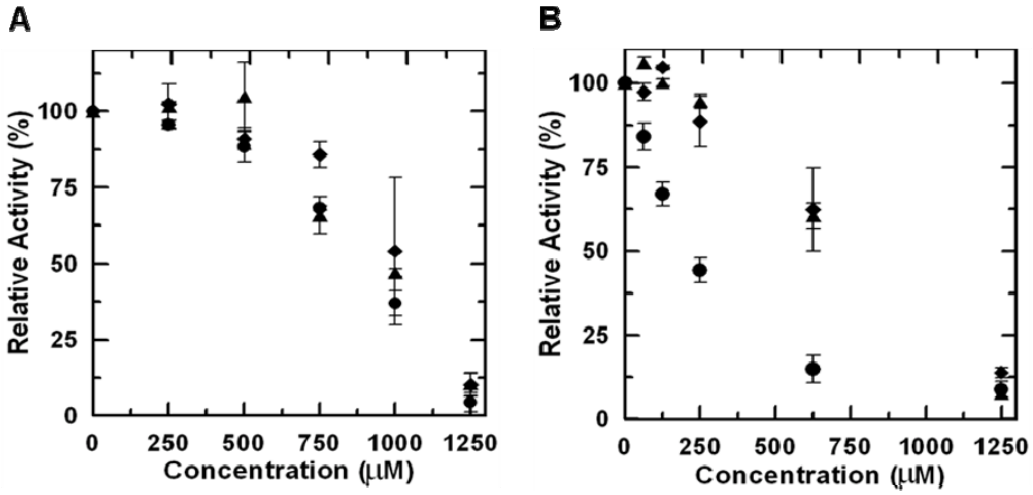

Figure 6. Effect of NADPH and GSSG on the GR Inhibition by carmustine. GR (5 nM) was incubated with carmustine (2.5, 12.5, 62.5, 250, 1000 μM) in the presence (●) and absence (♦) of NADPH (150 μM), or in the presence (▲) of GSSG (0.25 mM) for 30 min at 25 °C, and then the activity was measured.

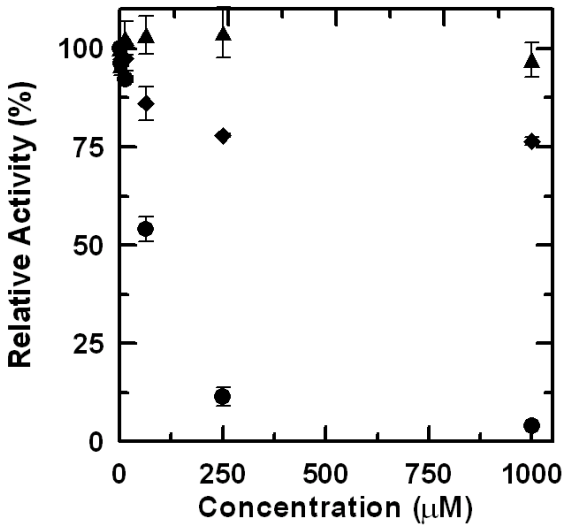

Figure 7. Effect of NADPH on GR Inhibition by AFs. GR (5 nM) was incubated with AFs (A. AF, 250, 500, 750, 1000, 1250 μM; B. HMAF, 62.5, 125, 250, 625, 1250 μM) in the presence (●) or absence (♦) of NADPH for 30 min at 25 °C, and then activity was measured.

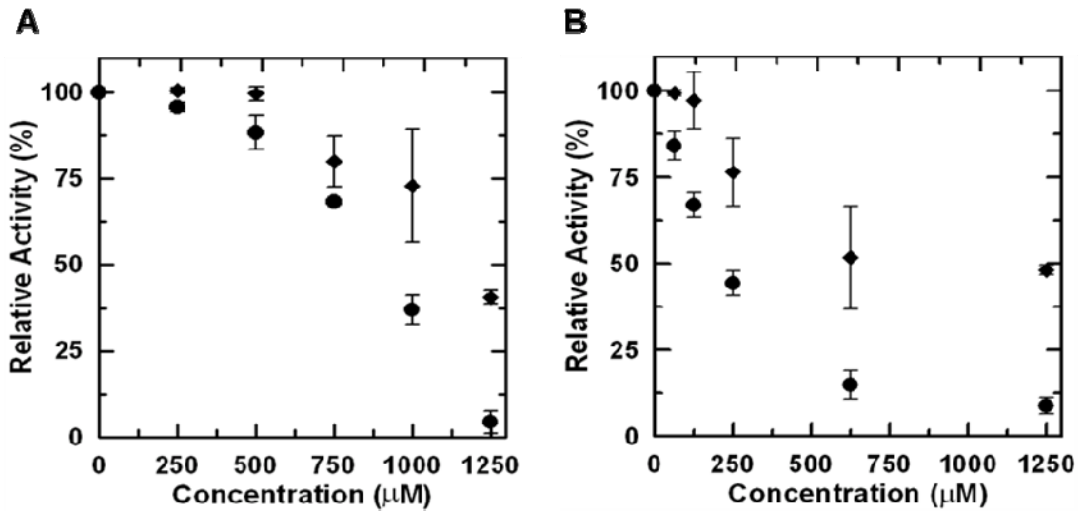

Figure 8. GR fluorescence spectrum changes in the presence of varying concentration of illudin S and AFs. Illudin S (20, 100, 400, 2000 μM) and AFs (10, 40, 200, 1000 μM) were incubated with GR (2 μM) in a total volume of 500 μL TE buffer for 30 min at 25 °C under different conditions: A. in the absence of NADPH; B. in the presence of NADPH (100 μM); C. in the absence of NADPH and in the presence of GSSG (400 μM); D. in the presence of NADPH (100 μM) and GSSG (400 μM).

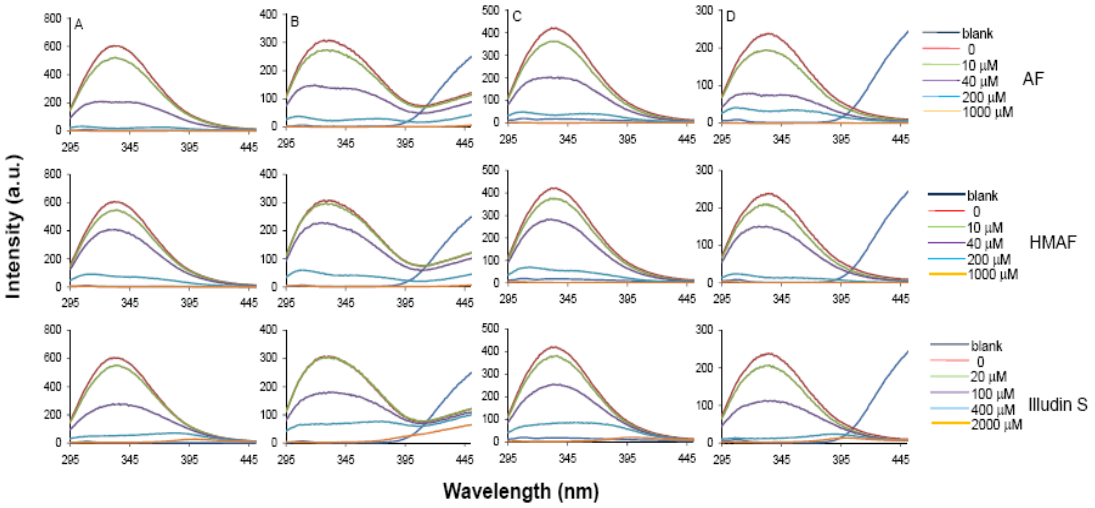

Figure 9. GR fluorescence spectrum changes in the presence of varying concentration of carmustine. Carmustine (0.01, 0.05, 0.20, 1.00 mM) was allowed to react with GR (2 μM) in a total volume of 500 μL TE buffer for 30 min at 25 °C under different conditions: a. the absence of NADPH; b. in the presence of NADPH (100 μM); c. in the absence of NADPH and in the presence of GSSG (400 μM); d. in the presence of NADPH (100 μM) and GSSG (400 μM).

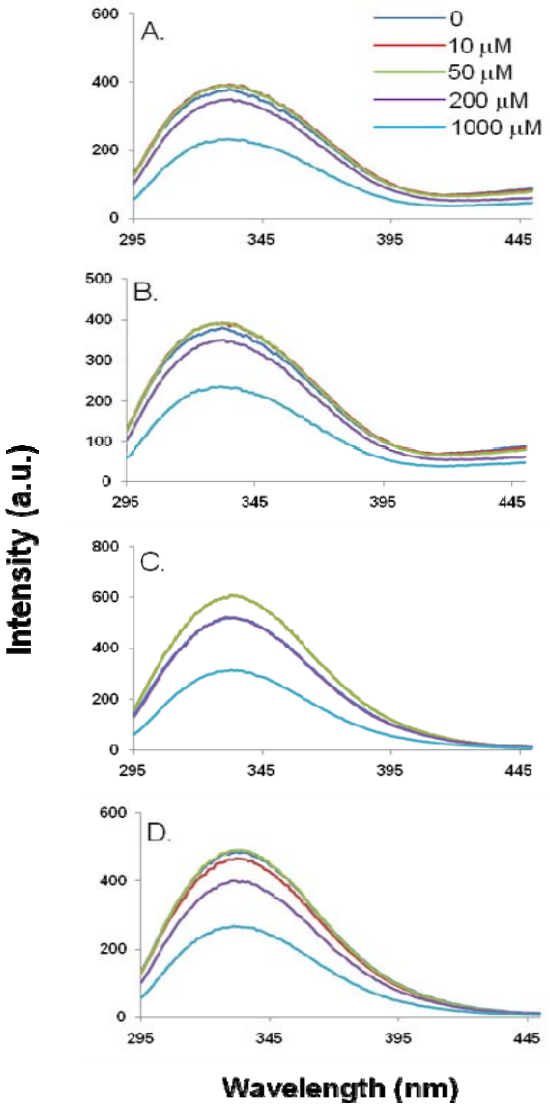

Figure 10. LC/MS spectra derived from GR samples. GR (5 nmol) was allowed to react with AFs (1.25 mM) in TE buffer containing NADPH (1 mM). Modified GR was then concentrated and unbound compound removed before LC/MS analysis.

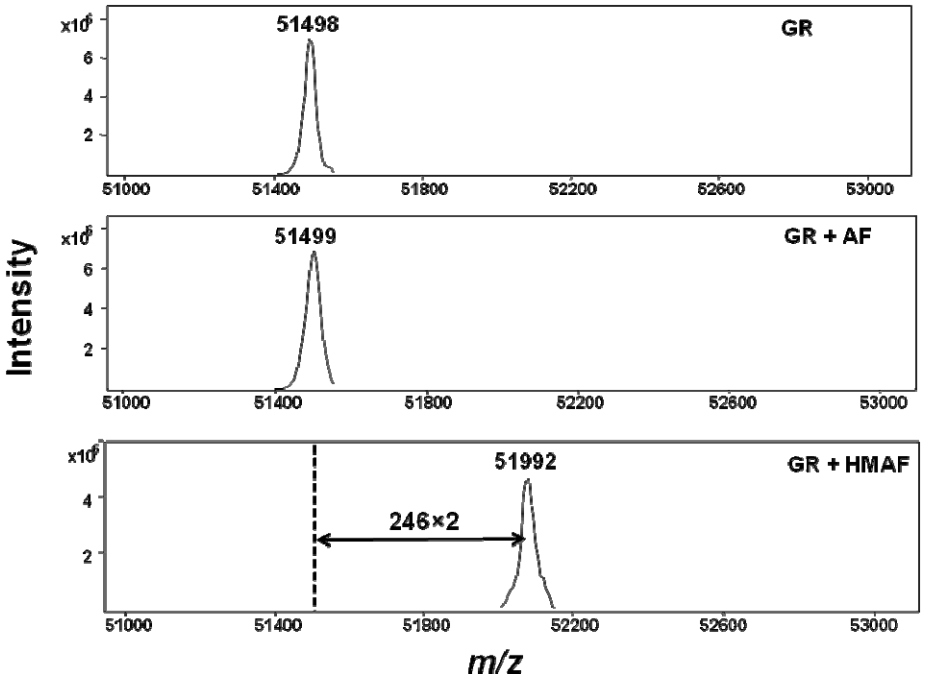

Figure 11. LC/MS spectra derived from GR-carmustine adduct. GR (5 nmol) was allowed to react with carmustine (0.25 mM) in 1 mL TE buffer containing NADPH (1 mM) for 3 h at 25 °C. Unbound compound was removed before LC/MS analysis.

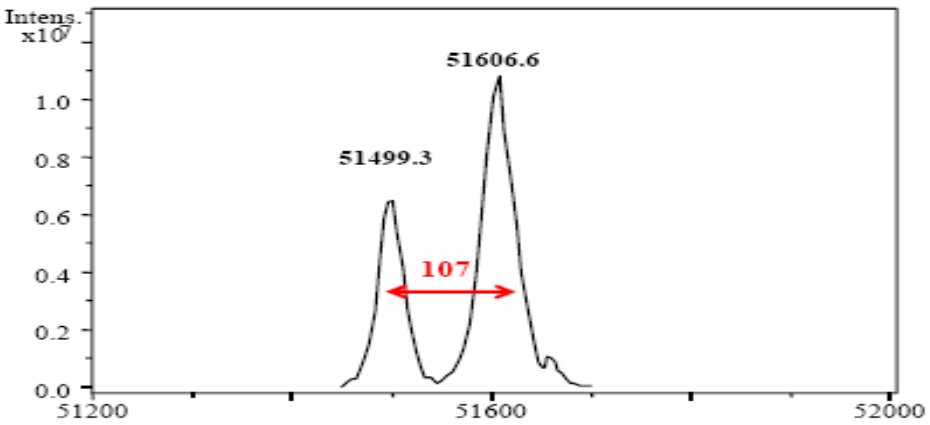

Figure 12. LC/MS/MS analysis of the GR active-site peptide. A. peptide from control GR with cysteine residues modified by iodoacetamide (*m/z* 716.6 $[M+2H]^{2+}$), B. peptide from GR-HMAF adduct (*m/z* 905.4 $[M+2H]^{2+}$). Other minor ions that appear, but are not labeled in the figure include: *m/z* 299.2 (b_4), 326.2 (y_3-NH_3), 944.1(b_8^*,y_7^*-H_2O), 1015.3(a_8^*-H2O), and 1301.5(MH^{+*}-NH_3).

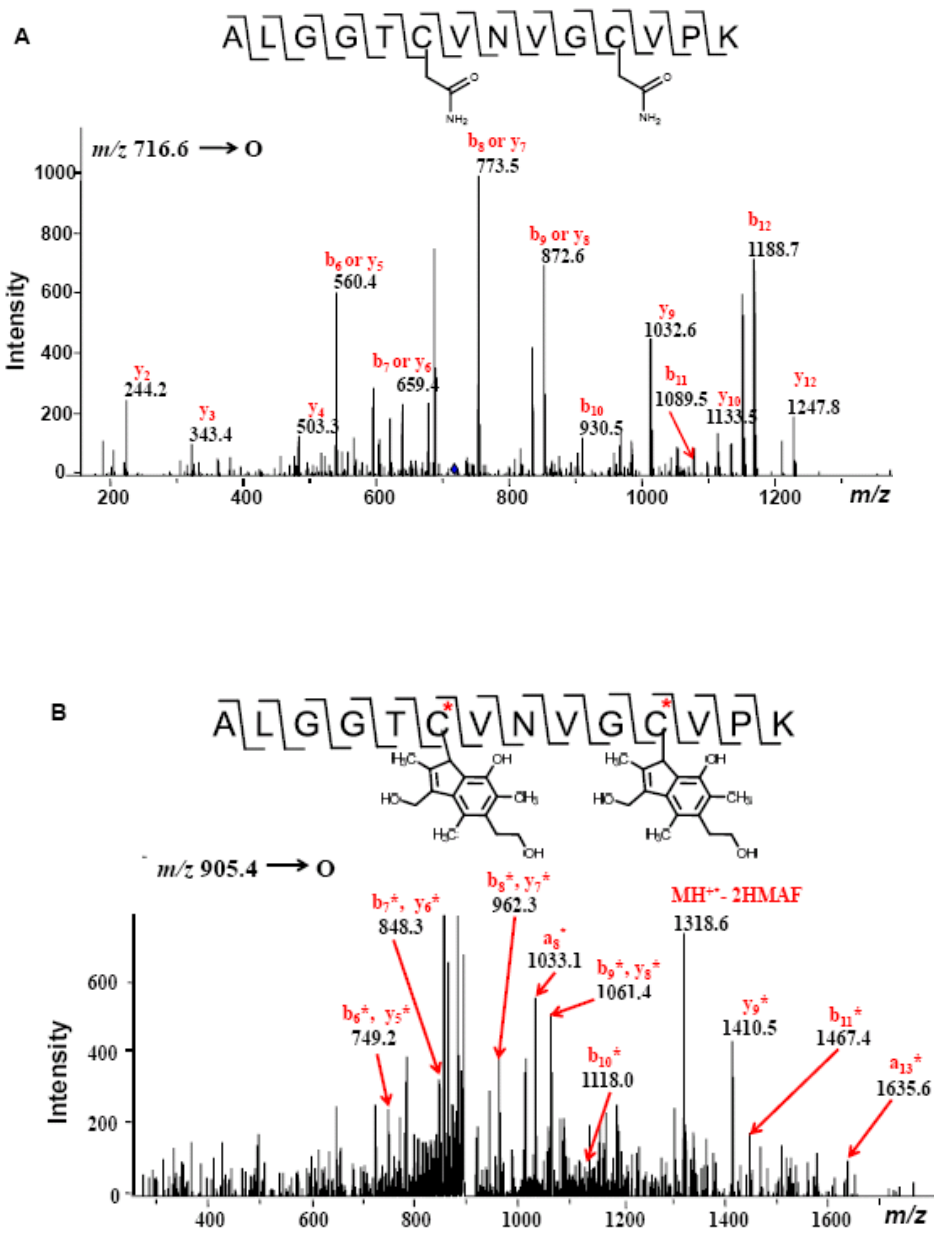

Figure 13. Inhibition of GR in Hela cells treated with illudin S, AFs and carmustine at equitoxic concentrations. Hela cells were exposed to test compounds (AF 0.2, 1.0, 4.0 μM; HMAF: 0.2, 1.0, 4.0 μM; illudin S: 0.02, 0.10, 0.40 μM; carmustine: 5, 20 μM) for 2 h (A) and 12 h (B), then cellular GR activity was measured. Each bar represents the mean and standard deviation of the results from four experiments. Asterisks represent significant difference relative to controls: * $p < 0.05$, ** $p < 0.01$.

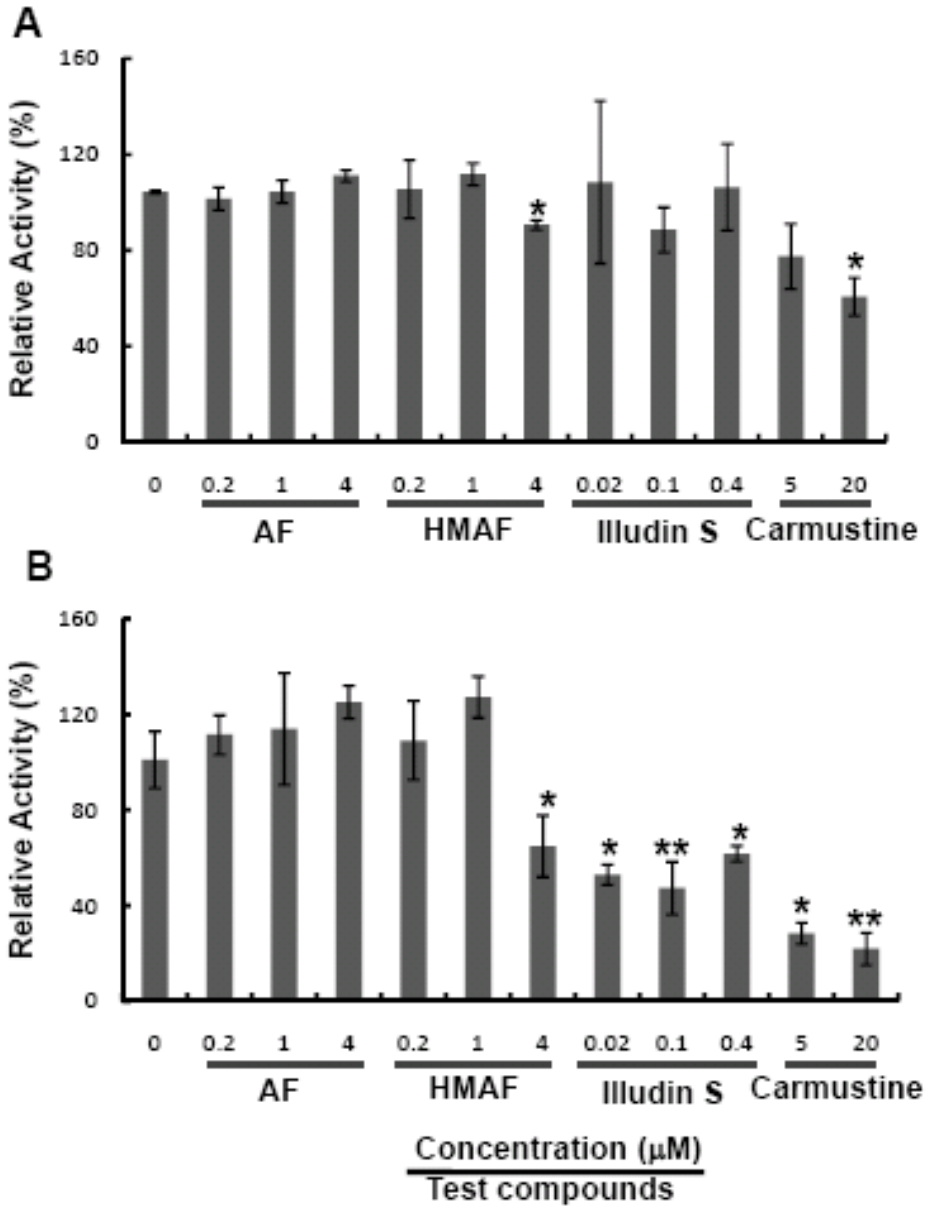

Figure 14. Influence on cellular GR protein levels after treatment by illudin S, AFs and carmustine. HeLa cells were exposed to test compounds (AF 0.2, 1.0, 4.0 μM; HMAF: 0.2, 1.0, 4.0 μM; illudin S: 0.02, 0.10, 0.40 μM; carmustine: 20 μM) for 2 h (A) and 12 h (B) respectively. Cellular GR was measured by western blotting, and 25 μg cell lysate protein corresponding to each treatment was analyzed by western blotting.

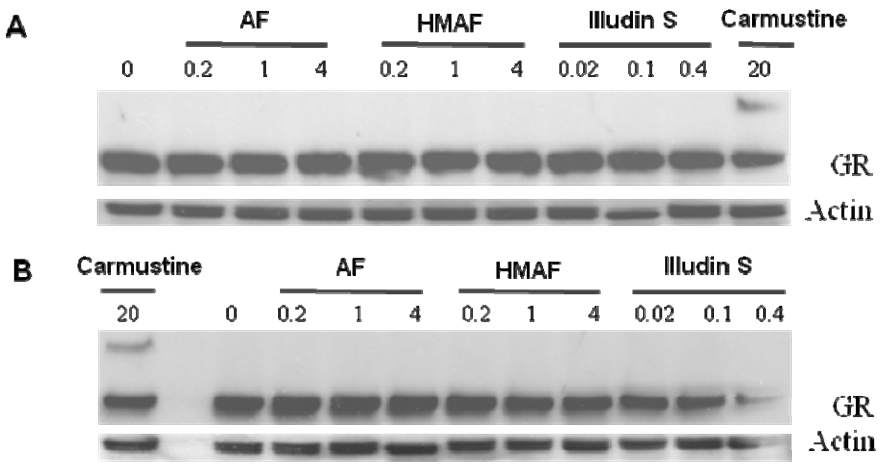

Scheme 1. Proposed mechanisms of biomolecular alkylation by AFs

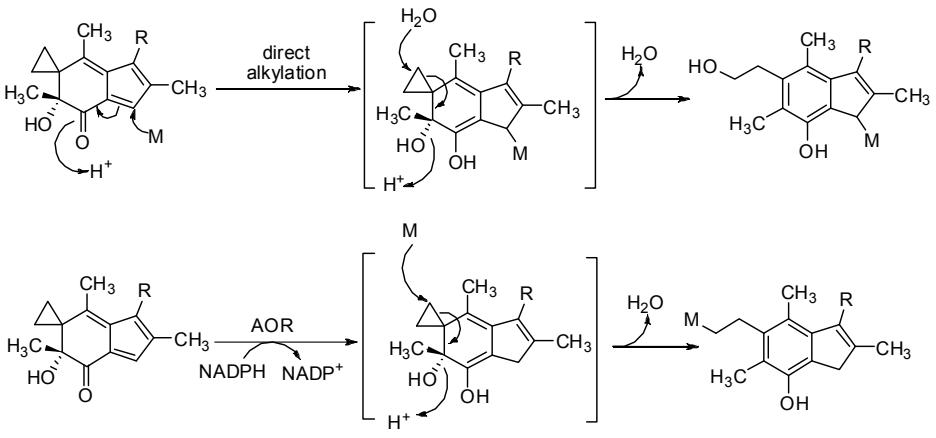

Scheme 2. Kinetic model for HMAF-induced GR inactivation. HMAF:GR is the noncovalent compelx of HMAF with enzyme and HMAF-GR represents the inactivated alkylated enzyme.

$$\text{HMAF} + \text{GR} \overset{K_i}{\rightleftharpoons} \text{HMAF:GR} \xrightarrow{k_{inact}} \text{HMAF-GR}$$

Scheme 3. Proposed chemical mechanism of GR inhibition by HMAF.

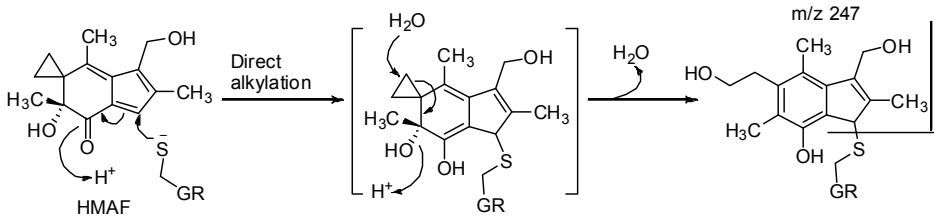

Chapter Five: Thioredoxin as an anticancer target: mechanism of inhibition by acylfulvenes

1. Introduction

Acquiring knowledge regarding pathological features of cancer and the mechanism of actions of anticancer drugs is a basis for developing more targeted cancer therapies.[285] While conventional chemotherapeutic drugs generally exhibit unwanted toxicities, they have established effectivities and are being increasingly combined with newer generation therapeutic agents as a means of maintaining potency while reducing general toxicities and providing individualized therapies.[43] In some cases, a single drug may be exquisitely selective for a given cellular target, but it is common that small molecules target multiple pathways. This is particularly true for natural product-derived chemotherapeutic drugs, which are generally selected for antitumor activity rather than target selection.[39] While there is debate regarding the merits of target selectivity and promiscuity balanced with number of agents in a combination therapy, it is undeniable that a clear understanding about the molecular targets of a single agent remains critical.

Natural products and their derivatives comprise over 60% of approved anticancer drugs since the 1980s.[25] However, relatively few of the isolated natural compounds proceed to become clinically useful drugs, whereas these unique molecules are valuable leads for the development of more efficacious analogs. Illudins, which are sesquiterpene compounds from the mushroom *Omphalotus illudens*, possess a cyclopropane ring and reactive α,β-unsaturated ketone group.[241] The main mode of action of acylfulvenes (AFs) is thought to be the alkylation of DNA, and while various multidrug resistant cancer cells are sensitive to illudins, they exhibit unfavorable toxicity profiles that prevent clinical application.[244, 286] McMorris and coworkers have prepared many semisynthetic illudin analogs, resulting in the invention of the AFs, which differ from illudin S in the functional groups on the five –membered ring (Chart 1) to improve therapeutic indices.[242, 243, 287-290] AFs provide a potential step toward new clinical candidates, but also unique small molecule probes for understanding chemical and biochemical reactivity profiles that determine cytotoxic selectivity for alkylating agents.

Both illudin S and acylfulvene derivatives, including AF and HMAF, react with glutathione through direct Michael-type addition, or undergo bioreductive activation with NADPH as cofactor to generate a highly reactive intermediate that can alkylate

macromolecules such as DNA, RNA and proteins.[138, 262-264] DNA damage associated with illudin S and HMAF is ignored by global genome repair systems but recognized by transcription-coupled nucleotide excision repair; the reasons for this unusual repair selectivity are not understood.[135, 250, 291] Acylfulvene is a primarily monofunctional DNA alkylator that forms elevated levels of 3-adenosine adducts in sensitive cells,[139, 292] inhibits DNA synthesis,[252] and induces apoptosis.[293, 294] The basis for the improved selectivities of acylfulvene analogs compared to illudin S is not yet clear; it is hypothesized to be connected with (1) tuning of susceptibility to reductase-mediated bioactivation to their corresponding reactive DNA-alkylating intermediates, and (2) relative potencies for reacting with key thiol-containing enzymes elevated in tumor cells.[247, 248, 295, 296] Illudin S readily reacts with Cys, glutathione, or Cys-containing peptide under mild conditions, but acylfulvenes are far less reactive towards these small thiols under similar conditions.[141, 142, 242, 254] By analogy, it has been hypothesized that proteins of the thiol–disulfide oxidoreductase family (CysXXCys active site sequences) react with illudins to a greater extent than acylfulvenes.[295]

Redox control plays an important role in regulating cellular function and viability. Cysteine residues are critical in redox regulation through the reversible thiol/disulfide exchange reaction that can be a switch for a protein conformation or activity. In another sense, they also may provide a chemical target for drug intervention.[255, 297] Disruptions of the redox state are characteristic of many diseases including cancer.[298] The redox-regulating glutathione reductase (GR) was selected to test the reactivity of illudin S and AFs with macromolecules, however, we observed that reactivity profiles are reverse of what might be expected, and only HMAF forms covalent adducts with GR.[299] Radiolabeled HMAF was found to form covalent adducts with thioredoxin (Trx) and thioredoxin reductase (TrxR), a cellular homolog of the GR system, and the extent of binding was roughly proportional to the number of Cys residues in each enzyme.[253] However, it is not known whether illudin S interacts with Trx system enzymes, nor whether the observed interaction of HMAF with the Trx system influences function.

Trx is a small protein (12 kDa) with a highly conserved active site (WCGPCK) among species from archaea to humans.[300-302] Two main isoforms of Trx have been

identified in mammalian cells depending on their cellular location: cytosolic (Trx1) and mitochondrial (Trx2). The Trx active site disulfide is reduced by the selenoenzyme thioredoxin reductase (TrxR) with NADPH as electron donor.[303] Reduced Trx then recognizes protein disulfides and undergoes two consecutive thiol-disulfide exchange reactions and releases reduced protein and oxidized Trx. Trx is involved in the redox regulation of a broad spectrum of processes in cells through dithiol-disulfide exchange reactions including DNA synthesis, apoptosis, signal transduction and antioxidative defense.[304-306] Trx inhibits apoptosis by negatively regulating of apoptosis signal-regulating kinase 1 (ASK-1), and activating transcription factors that mediate cell growth and survival.[304] In the nucleus, Trx regulates the DNA binding of redox-sensitive transcription factors such as NF-κB, p53, and HIF-1.[307-309] Trx overexpression has been associated with aggressive human cancers including lung, cervix, pancreatic, gastric and colon cancer.[119, 294, 310, 311] Moreover, elevated Trx limits sensitivity of cancer cells to conventional anticancer drugs such as cisplatinum, mitomycin C, and doxorubicin.[312, 313] The toxicity profile of HMAF suggests its mechanism of action and resistance is different from illudin S and AFs, and other alkylating drugs,[134] and there appears to be a positive correlation that can be drawn between cancer types with typically increased Trx levels and cancer types with high sensitivities towards HMAF.[117, 134] However, it has not been previously determined whether illudin S, AF or HMAF inhibit Trx or how their reactivities compare. This information is needed to evaluate whether this is a potential cellular target for these compounds, and if controlling interactions with the Trx system can contribute to improved therapeutic indices in chemotherapy.

In this study, we characterized the reactivity of illudin S and AFs toward E coli. Trx, which shares high similarity with human thioredoxin with respect to the overall structure and active site, as a model system.[314, 315] Experiments were carried out to evaluate the proximity of drug binding sites to the Trx active site, the influence of the drugs on Trx insulin-reducing activity, covalent protein modification, and cellular levels and localization of Trx. The results of this study provide new knowledge regarding cytotoxin-induced disruption of a redox-regulating enzyme and its potential contribution to anticancer selectivity.

2. Experimental procedures

2.1 Chemicals and reagents

Illudin S was provided by MGI Pharma (Minneapolis, MN). Acylfulvene and HMAF were synthesized according to a published procedure with illudin S as starting material.[242, 243] Purified E.coli Trx1 was purchased from Promega Corporation (Madison, WI). Insulin from bovine pancreas, Tris base, and EDTA were obtained from Sigma Chemical (Milwaukee, WI). Dithiothreitol (DTT) was obtained from Fisher Scientific Inc (Hanover Park, IL). Recombinant rAOR was expressed and purified as published previously.[260] *N*-biotinoyl-*N*-(iodoacetyl)ethylene diamine (BIAM) was purchased from Molecular Probes, Inc.(Eugene, OR). Dulbecco's modified Eagle's medium (DMEM) was purchased from Mediatech (Herndon, VA). Fetal bovine serum (FBS) was purchased from Atlanta Biologicals (Lawrenceville, GA). Phosphate-buffered saline (PBS), 0.25% trypsin-EDTA, penicillin-streptomycin were obtained from Invitrogen (Carlsbad, CA). Tris-buffered saline was purchased from Biorad (Hercules, CA)

2.2 General considerations

Trx and DTT stock solutions were prepared in Tris-Cl buffer (50 mM, pH 7.2) containing EDTA (1 mM), i.e. TE buffer. All assays were carried out in TE buffer containing. Stock solutions of test compounds were prepared in DMSO, and aliquots of these solutions were added to the reaction mixture to yield a final DMSO concentration of 2% (v/v). Trx activity was determined by measuring turbidity formed from reduction of insulin by monitoring UV absorbance at 650 nm with a 96-well plate reader (Biotek, Winooski, VT).

Fluorescence measurements were carried out on Varian Cary spectrofluorometer at 90° in relation to the excitation source. Fluorescence was measured with excitation at 280 nm (bandpasses of 5 and 10 nm for excitation and emission respectively) and emission from 295 to 450 nm.

HPLC analysis was carried out on an Agilent 1100 series instrument with diode array detector and autosampler. Analytes were eluted with a solvent gradient involving water (A) and acetonitrile (B), at a flow rate of 1 mL/min: initial conditions, 10:90 B:A, were held for 5 min followed by linear increase to 50:50 B:A over a course of 20 min and

held 5 min. For AF analysis, analytes were eluted with a solvent gradient involving water (A) and acetonitrile (B), at a flow rate of 1 mL/min: initial conditions, 10:90 B:A, were held for 5 min followed by linear increase to 50:50 B:A over a course of 20 min, and then further increase to 80:20 B:A in 20 min and held 5 min. Phenomenex Luna 5 μm C_{18}(2) 100 Å 250 mm × 4.60 mm was used (Phenomenex, Torrance, CA).

Liquid chromatography-mass spectrometry (LC/MS) analyses were carried out on an Agilent 1100 capillary HPLC-iontrap mass spectrometer operated in positive ion mode and the HPLC is equipped with an autosampler. A Zorbax 300 SB-C3 column (150 mm × 0.5 mm, 5 μm) was used. Analytes were eluted with the following solvent gradient involving 0.05% TFA in water (A) and 0.05% TFA in acetonitrile (B), at a flow rate of 15 μL/min: initial conditions, 30:70 B:A, were held 3 min followed by a linear increase to 80:20 B:A over a course of 20 min. Spectra were obtained by full scan data acquisition performed within *m/z* 100-1500. Mass deconvolution analysis was performed using the Agilent ion trap analysis software.

2.3 Fluorescence analysis

To evaluate conformational changes of Trx in the presence of test compounds, Trx (4 μM) was treated with test compounds in a total volume of 0.5 mL TE buffer at indicated conditions for 2 h at 25 °C. Changes in intrinsic fluorescence of Trx were evaluated with the general method. To evaluate the effect of test compounds on Trx, Trx was treated with AF (1.6, 8, 40, 200, 800 μM), or HMAF (2, 10, 40, 200, 100 μM), or illudin S (12.5, 50, 200, 500, 2000 μM) for different period of time in the presence of DTT (2 mM).

2.4 Reaction of compounds with Trx in the presence or absence of DTT

To determine whether test compounds were Trx substrates, each compound (AF and HMAF, 400 μM; Illudin S, 1 mM; reference blank, 2% DMSO) was combined individually with non-reduced Trx (4 μM) in the presence of DTT (2 mM), or pre-reduced Trx (4 μM) in TE buffer with a final volume of 200 μL and allowed to react at 25 °C for 2 h. The resulting solution was extracted with ethyl acetate (EtOAc, 200 μL) and centrifuged for 5 min (6000 g). The supernatant was collected and EtOAc was

evaporated on a Speedvac concentrator (Savant, Waltham, MA). The dried material was reconstituted in 100 μL DMSO, and 50 μL was injected and analyzed with the HPLC method. As a negative control, the same procedure was carried out with compound only or compound with DTT.

2.5 Trx activity assay

Reduced Trx was prepared from oxidized Trx by incubation of 60 μL Trx (450 μM) with 20 μL DTT (100 mM) at 25 °C for 20 min. DTT was subsequently removed with micro bio-spin P6 column (NMWL 6000, Bio-rad, Hercules, CA) pre-equilibrated with N_2-purged TE buffer. The absence of DTT in the collection was verified by the Ellman's reagent at 412 nm.[166] The reduced Trx was then diluted to final concentration at 4 μM with N_2-purged TE buffer. 5 μL of compound at various concentrations was then added to 195 μL of pre-reduced Trx diluted solution and allowed to react in 96-well plate at 25 °C for 2 h. The Trx activities were measured by its ability to reduce insulin with DTT as the electron donor by a published method.[316] Briefly, after incubation, 50 μL DTT (10 mM) and 60 μL insulin (10 mg/ml) was added, and the enzyme activity was measured at 25 °C by monitoring the increase of A_{650} due to the precipitation of reduced insulin. The blank contains all the reagents except Trx.

2.6 Protein adduct analysis

Trx (450 μM) was pre-reduced by DTT (100 mM) and DTT was subsequently removed with a micro bio-spin P6 column. 500 μL pre-reduced Trx (15 μM) was allowed to react with 5 μL compounds (100 mM) respectively at 25 °C for 2 h. A Microcon Y-10 filter device (10,000 NMWL, Millipore, MA) was used to concentrate drug-treated Trx to a final volume of 80 μL according to the manufacturer's protocol. Then a micro bio-spin P6 column was used to remove unbound compound. The resulting solution was dried on the Speedvac concentrator. Trx (3 μg in 8 μL TE buffer) was analyzed by LC/MS using the method described in the general considerations. Both native and modified Trx proteins eluted as a single peak with retention time 12.5 min.

2.7 Detection of the AFs modified residues in Trx

The potential modification of Trx by AFs at Cys was determined with the use of the thiol-reactive biotinylation reagent BIAM, which reacts selectively with reduced Cys in proteins and does not react with oxidized Cys.[317] Varying concentrations of acyfulvene were added to prereduced Trx (0.9 μM), which was then incubated at 25 °C for 2 h. The same amounts of DMSO were added to control experiments. After incubation, 1 μL of the reaction mixture was removed and added to new tubes containing 19 μL of 100 μM BIAM, followed by incubation at 25 °C for another 30 min to alkylate the remaining free -SH groups in the enzyme. A sample containing ten microliters of BIAM-modified enzyme was mixed with loading buffer (2.5 μL, Invitrogen, CA) and antioxidant reagents (1 μL, Invitrogen, CA), and the samples were subjected to SDS-PAGE on a 7.5% gel, and the separated proteins were transferred to a nitrocellulose membrane. Proteins labeled with BIAM were detected by horseradish peroxidase (HRP)-conjugated streptavidin and enhanced chemiluminescence (ECL) detection (Pierce, IL).

2.8 Western blotting

A total of 10^4 Hela or MCF-7 cells were plated out on six-well tissue culture plates. Cells were allowed to grow for three days, and then exposed to drugs for 12 h for Hela cells and 24 h for MCF-7 cells. After treatment, cells were washed twice with PBS. Cells were harvested and kept frozen at -80 °C until use. Lysed cells were assayed for protein content with a BCA-kit protocol according to manufacturer's instructions (Pierce, Rockford, IL), gel electrophoresed, and transferred via standard blotting techniques. Membrane was cut into two pieces according to the molecular weight marker. Blots were probed simultaneously with rabbit anti-human Trx1 antibody diluted 1:2000 followed by horseradish peroxidase (HRP)-conjugated goat anti-rabbit secondary antibody diluted 1:2000. Bands were analysed with an enhanced chemiluminescence protocol and visualized on radiographic film. Blots were probed with HRP-conjugated rabbit anti-human α-actin diluted 1:2000.

2.9 Fluorescence microscopy

Hela cells were seeded at 10^5 cells per well in 6-well plates that contained 22 cm glass coverslips coated with collagen (10 μg/mL) and incubated for 48 h at 37 °C. Cells

were incubated either with test compounds, cisplatin, or DMSO (0.2%) for 8 h. Afterward, the cells were washed twice with PBS (pH 7.4), and then fixed with 3.7% formaldehyde in PBS for 20 min. After two washes with PBS, the cells were permeabilized with 0.1% saponin in PBS and blocked with 3% (w/v) BSA in PBS for 1 h at 25 °C. The cells were then incubated for 2 h at 25 °C with the anti-thioredoxin-1 monoclonal antibody (BD Transduction Laboratories) in a solution containing 0.1% saponin and 3% BSA in PBS (1:500). The cells were washed three times with PBS and incubated for 1 h at 25°C in blocking buffer containing anti-mouse IgG FITC-conjugate (1:1000), and 4,6-diamidino-2-phenylindole (2.5 ng/mL in PBS) to stain the cellular nuclei (1:2000). The signals were observed under a Zeiss Axioscop 2 microscope equipped with a Zeiss Axiocam R2 digital camera and 100X objective. Images were captured using Zeiss Axiovision software release 3.1 (Carl Zeiss, Inc., Thornwood, NY).

3. Results

3.1 Trx does not catalyze the reduction of illudin S and AFs

To verify that there was no Trx-mediated conversion of illudin S and AFs to their major cytosolic metabolites (Chart 1), we compared the HPLC spectra of released products of reactions involving test compounds with non-reduced Trx in the presence of DTT, or with pre-reduced Trx (Figure 1). For AF treatments, only a single peak corresponding to AF was observed to elulte (26 min). No metabolites (Chart 1) were observed to be formed from the reaction of illudin S or HMAF under a variety of conditions as illustrated in Figure 1.[138, 264] However, we observed the formation of a single significant product peak (22 min) in reactions of HMAF and DTT regardless of the presence or absence of Trx (Figure 1, HMAF, B and C). Similarly, illudin S reacts with DTT, but the formation of only a small product peak was observed and it eluted after the peak corresponding to illudin S (11 min). The major HMAF-DTT product was purified by HPLC. Mass spectrometry analysis indicated it to be a dimer of a HMAF-DTT conjugate (*m/z* 764.2, Figure 2). The fragmentation pattern of the monomer (*m/z* 383.2) suggests the primary hydroxyl group of HMAF is being displaced by the hydroxyl (fragment *m/z* 244.9), and sulfuhydryl group of DTT (fragment *m/z* 261.0,), giving a rise to apparent mixture of isomers. Further work is required to determine whether they can be separated and individually characterized.

3.2 Illudin S and AFs quench Trx intrinsic fluorescence

Intrinsic tryptophan fluorescence is an optical indicator that reflects the redox status of the Trx active site.[318, 319] Active site disulfide reduction results in a large increase in fluorescence, indicating a conformational change in the environment of both Trx tryptophan residues (Trp 28 and Trp 31), which are close to the active site disulfide (Cys 32 and Cys 35).[319] Thus, we acquired differential fluorescence spectra at 350 nm to evaluate drug binding and proximity to the Trx active site. Trx fluorescence was significantly quenched in a concentration-dependent manner after incubation with illudin S, AF, or HMAF in the presence of DTT (Figure 3). Trx fluorescence was completely quenched by 1600 μM illudin S, or 400 μM AFs respectively. Furthermore, it was

associated with a redshift, which has been proposed to result from an increase in exposure of the tryptophan residue to the solvent.[320]

The observed intrinsic fluorescence quenching effect is independent of the DTT concentration as well as incubation time, but was also observed for HMAF-DTT (Figure 3). The same study was carried out for the metabolites of AFs (i.e. M_A and M_H). However, M_H does not quench Trx fluorescence significantly, and M_A itself is a strongly fluorescent molecule, so the data are inconclusive. The known Trx irreversible inhibitor 4-HNE was examined in the same way, and no quenching effect was observed under the same conditions.

3.3 AFs inhibit Trx insulin-reducing activity

A Trx/TrxR coupled insulin reduction assay has been reported previously as a means to evaluate whether a compound interacts with the redox-active Cys of Trx. In this assay, Trx is reduced by TrxR with NADPH as electron donor, and solution turbidity, associated with insulin oxidation, is monitored.[321] Our preliminary studies indicated that illudin S and AFs had inhibitory activity in this assay, however, on the basis of the potential reactivity of the compounds toward TrxR,[253] we used an assay in which Trx catalyzes the reduction of insulin disulfides by DTT.[316] The presence of DTT protects Trx from being inhibited by these compounds, thus no Trx inhibition was observed when test compounds were added to the reaction mixture without removing DTT. Therefore, excess DTT was removed from the reduced Trx prior to incubation with drugs. AFs were found to inactivate Trx in a dose-dependent manner (Figure 4). The Trx insulin-reducing activity was inhibited completely by 1250 μM AF or 250 μM HMAF. In contrast, illudin S at 2500 μM and M_A at 1mM) did not inactivate Trx activity; M_H slightly inhibits Trx activity about 50% at 2500 μM (data not shown).

3.4 Mass spectrometry analysis of Trx modification by AFs

LC/MS was used to probe the chemical nature of the AFs-Trx interaction. Analysis of a control sample, i.e. pre-reduced Trx treated with DMSO, gave rise to a major peak in the mass spectrum with *m/z* 11675 Da and a minor peak with *m/z* 11677 Da.The calculated MW for reduced Trx is 11675.3, thus the measured value of the major peak corresponds to oxidized Trx (Figure 6.). After 2 h treatment of reduced Trx with AF, two

new peaks were identified with MW 11887 and 12100 Da. The mass differences between these species and reduced Trx are 213 and 213×2, which correspond to one and two molecules of AF adducted to Trx. For HMAF-treated Trx, one additional peak appeared with *m/z* 12134 Da, consistent with the formation of a bis-adduct between HMAF and Trx. No adduct was observed without pre-reducing Trx with DTT, or without removing excess DTT. The same adducts were observed from AFs-Trx incubation in the presence or absence of AOR and NADPH in the incubation mixture. Similar experiments were carried out for illudin S and no adducts were observed between illudin S and Trx.

3.5 Trx is modified by AFs on active site Cysteines

Data presented above indicate that AF and HMAF directly covalently modify Trx, and that both inhibit the activity of Trx. Together these results suggest that the active site may be the target of modification. Further, E coli Trx only has two Cys residues (Cys^{32} and Cys^{35}), both located in the active site. Biotin-conjugated iodoacetamide (BIAM) is an alkylating agent that selectively labels the free thiols of Cys residues in proteins, and therefore can be used as an indicator of free thiols.[317] Pre-reduced Trx was treated with varying concentrations of AFs followed by BIAM, and was then analyzed by blotting. The biotin tag was recognized by streptavidin-horseradish peroxidase and detected with enhanced chemiluminescence (Pierce, Rockford, IL). With increasing drug concentration, the intensity of the band corresponding to BIAM-labeled protein diminished (Figure 7). With high AF concentration (250 and 1250 μM), the band intensity was reduced up to about half that of control, suggesting mono-alkylation of the protein by AF. The band almost disappeared completely at high HMAF concentration (250 μM), indicating alkylation on both Cys.

3.6 Influence of illudin S and AFs on cellular Trx levels

To further evaluate whether AFs also influence cellular Trx, the Trx levels in cells were measured after drug treatment. HeLa cells were treated with AFs, illudin S, or DMSO for 12 h, and cell lysates were prepared and analyzed for Trx by western blotting. A dose-dependent down-regulation of Trx was observed following treatment with either AF or HMAF. Cellular Trx levels were reduced by 30% upon treatment by 1 μM AFs,

and 70% by 4 μM AFs (Figure 8). Illudin S treatment also led to a reduction in cellular Trx level in a dose-independent manner. At a concentration of 1 μM, illudin S almost abolished the cellular Trx. Similar results were observed for MCF-7 cells in the case of 24h AF or HMAF exposure, however, there was no significant reduction in Trx levels of MCF-7 cells treated with illudin S.

3.7 Influence of illudin S or AFs on cellular localization of Trx

As a multifunctional protein, Trx exists in the extracellular milieu, cytoplasm, and nucleus, and has a different role in each location.[105, 322] Since cellular Trx levels decreased with AFs treatment, and Trx was covalently modified by AF in cell-free systems, we tested whether the interaction between Trx and AFs alters the cellular localization of Trx. Cisplatin has been observed to promote Trx nuclear translocation, which has been thought to play a role in cellular resistance to cisplatin.[323] As a positive control, HeLa cells were treated with cisplatin, and the reported nuclear accumulation was observed (Figure 9). Cells were treated with illudin S, AF, or HMAF, as well as DMSO, or the AF metabolites M_H and M_A. Trx intracellular localization in was visualized by indirect immune-fluorescence staining with an anti-Trx monoclonal antibody. In DMSO-treated cells, Trx was visualized in both cytoplasm and nucleus. In cells exposed to illudin S (0.5 μM), AF (2 μM), or HMAF (2 μM) for 10 h, Trx was visualized to exist mainly in the nucleus. As further confirmation of the specificity of AFs and illudin S in mediating Trx translocation, the cellular localization was not observed to be influenced by the metabolites of AFs (10 μM), which share some general chemical properties of the AFs, but do not appear to bind to the protein.

3.8 AOR has no effect on the inhibition of Trx by AFs

The NADPH-dependent alkenal/one reductase (AOR) catalyzes the reduction of the α,β-unsaturated double bond of illudin S and acylfulvene to generate an extremely unstable cyclohexadiene intermediate.[137, 138, 262, 263] To investigate if bioactivation potentiates the inhibitory potency of illudin S and AF, NADPH-reduced AOR was introduced into the reaction mixture of pre-reduced Trx and test compounds and the reaction was allowed to occur the same as for the inhibition experiment. Results indicate

the presence of AOR does not increase the potency of AFs toward Trx (data not shown). Furthermore, the same modification pattern of Trx by AFs was characterized by BIAM labeling and whole protein mass spectrometry analysis in the presence or absence of AOR (data not shown).

4. Discussion

DNA alkylation is thought to be the major mechanism of illudin S and AF toxicity. Reductase-mediated bioactivation has been shown to contribute in part to dictating differences in cytotoxicity profiles for AFs.[139] The evidences that the less cytotoxic illudin analogs are less reactive towards small thiols, together with the observation that cell sensitivity towards illudin S was modulated by cellular glutathione level, suggests that the differential toxicity may also result from the reaction with cellular thiol-containing enzymes.[140-142, 242, 254] Redox control plays an important role in regulating cellular function and viability. Cellular redox status is controlled by two major thiol-based antioxidant systems, the glutathione system and the thioredoxin system. Our study of their differential reactivity towards glutathione reductase, a redox-regulating enzyme with two Cys at the active site, reveals the reverse reactivity as expected.[299] HMAF was observed to form covalent adduct with Trx and TrxR.[253] Upregulation of Trx expression has been correlated with aggressive cancers and drug resistance.[324, 325] In this study, we compared the reaction potency of these compounds toward Trx and establish a link of the Trx-AFs interaction between the cell and cell-free system.

Trx is a small protein (12 kDa) with highly conserved structure and active site (WCGPCK) among species from E. coli to humans.[300, 314, 315] Human Trx contains three additional Cyss which are implicated in dimer formation and other potential regulation processes.[314] In this paper, we select E. coli Trx as a model to investigate the differential reactivity of illudin S and AFs towards thiols in macromolecules, since its active site is perfectly described with respect to the reductase activity and active site tryptophan-originated fluorescence.[316, 318, 319]

The active site of *E. coli* Trx is composed of Cys residues at positions 32 and 35, and it also has two tryptophan residues with one at position 28 and the other at position 31. Trp31 lies on the protein surface, whereas Trp28 is partially buried.[315] Reduction of the Trx catalytic disulfide has been shown to cause a significant increase in Trp fluorescence due to the introduction of a localized conformational change that releases Trp28.[319] Fluorescence changes have been associated with the binding of metal ions to Trx, such as Cd^{2+}.[326] In another study, GSSG was observed to extensively quench the Trp

fluorescence of human Trx (100 mM GSSG resulted in 85% reduction of Trx fluorescence), which was proposed to result from exposure of Trp to the solvent.[320] As a convenient preliminary indicator of whether illudin S or AFs react with Trx, in the present study, we tested the ability of illudin S and AFs to completely quench the fluorescence of reduced Trx. The fluorescence quenching of Trx by illudin S or AFs was associated with the red shift the emission peak, indicating extensive conformational changes. The quenching effect is initiated rapidly: the extent of quenching within 3 min is the same as that for 90 min. The quenching effect is independent of the DTT concentration in the mixture. The HMAF-DTT conjugate also quenched Trx intrinsic fluorescence, and at 200 μM, Trx intrinsic fluorescence was completely quenched. Mass analysis indicates the HMAF-DTT is a dimer. Since 200 μM conjugate contains 400 μM of the HMAF core, accounting for the concentration of monomeric unit, the quenching efficiency of HMAF and HMAF-DTT are comparable to each other. This observation may explain why DTT protect Trx inhibition by HMAF, i.e. the presence of DTT does not block the accessibility of Trx active site from HMAF, but DTT replaces Trx to react with HMAF. In contrast, the reported Trx covalent inhibitor 4-HNE didn't quench Trx fluorescence under the same experimental conditions, suggesting a different interaction mechanism with Trx which was also observed from GdnHCl treated Trx.[320]

The inactivation of Trx by illudin S and AFs was evaluated in a cell-free system. Trx activity was measured by an adaptation of a standard insulin reduction activity assay,[316] with DTT as electron donor. AFs do not inhibit Trx insulin-reduction when DTT is in the incubation mixture. Thus, it is necessary to remove excess DTT before adding test compounds to reduced Trx. An alternative experimental approach is to use thioredoxin reductase to reduce Trx with NADPH as electron donor.[321] However, data suggest that illudin S and AFs have the capacity to interact with TrxR, which is anticipated to confound inhibition data. It was reported that 25-fold molar excess DTT and GSSG reduce Trx-HMAF adduct formation,[327] it has not been experimentally addressed why this could happen. We analyzed reaction mixtures of illudin S, AF, or HMAF with Trx in the presence or absence of DTT and found that DTT efficiently and independently forms a conjugate with HMAF. In order to identify the conjugate, we

allowed 100 equivalents of DTT to react with 1 equivalent of HMAF under the same conditions. HMAF-DTT was isolated in 70% yield and was characterized as a mixture of hydroxyl- and sulfhydryl- HMAF adducts. Under similar conditions, we observed that a small amount of an illudin S-DTT adduct was observed, but the product was not isolated and characterized because of its low levels. The illudin S-DTT adduct may follow the same reaction scheme as illudin S with glutathione, i.e. the sulfurhydryl attack the α,β-unsaturated ketone followed by the opening of cyclopropane ring by water or chloride.[138] This reactivity pattern is opposite what was expected on the basis of previous studies regarding the reactivity of illudin S toward small thiols, affirming that the extent of reactivity depends not only on the identity of the electrophile, but also on the thiol structure.

The concentration of AFs at which Trx activity was completely inhibited correlated with the concentration at which Trx intrinsic fluorescence was completely quenched (Figure 5). For AF and illudin S, nonspecific binding that doesn't result in inactivation of Trx was observed, i.e. AF induces fluorescence quenching but does not inhibit insulin reduction capacity. On the other hand, for HMAF, protein binding effectively reflects activity inhibition. The core structure of the illudin S and AF analogs comprised of a tricyclic cyclopropane, cyclohexanone, and cyclophenone dictates their biological activity. They can covalently react with nucleophiles like free sulfhydryl by means of the conjugate addition reaction involving the bicyclic enone. The hydroxymethyl group in HMAF is important in improving efficacy and the displacement of the primary hydroxyl on HMAF with other groups significantly decreases its cytotoxicity.[142, 243, 254, 290] Considering the accessibility of the Trx active site,[315] together with the ability to form covalent adducts with AF, we propose that one possible mechanism underlying this correlation is one in which the induced conformational change may just facilitate the interaction of Trx with AFs, especially HMAF, but not illudin S.

Data from mass spectrometric analysis of whole Trx protein after incubation with AFs or illudin S suggest that HMAF forms a bis-adduct and AF mainly forms a mono-adduct with Trx. Illudin S does not form an adduct. However, no adducts were observed when the incubation was carried out in the presence of DTT. On the basis of the mass

change of HMAF-Trx adduct (*m/z* 2×229), and in analogy with previously observed reactions, we propose that adduct was formed via the displacement of the hydroxyl group on HMAF by the Cys thiol of Trx (Scheme 1). Metabolites of AFs or HMAF-DTT conjugate do not form adducts with Trx. Interestingly, when we follow the published procedure in which radiolabeled HMAF was allowed to react with Trx followd by washing with cold perchloric acid,[253] we also observed a Trx-HMAF adduct with similar mass change, but mainly mono-adduct. Briefly, we allowed Trx to react with HMAF in the presence of DTT followed by trichloroacetic acid (15%) precipitation and cold acetone wash. However, in the same manner without TCA precipitation and acetone washing, no adduct was observed. These results suggest that the adduct formed under these experimental conditions may be resulted from the acidic condition at which HMAF can readily lose the primary hydroxyl group to generate the stabilized intermediate which can be directly attacked by the thiol of Trx (Scheme 2).[142]

In the present study, adducts formed between AFs and Trx Cys were probed with the thiol-reactive compound BIAM, which reacts with free protein thiols. AFs were observed to block the two Cys residues, which are located in the active site, of E. coli Trx. Consistent with results from whole protein MS analysis indicating that the major adduct formed between AF and Trx is a mono-adduct, the intensity of the band corresponding to BIAM-labeled protein is about half of its original intensity when protein is reacted with high concentrations of AF (250 and 1250 μM). For HMAF, however, at a drug concentration of 250 μM, the BIAM-labeled protein band almost disappeared, suggesting that both Cys are modified in this case, consistent with the MS analysis indicating bis-adduct formation. For each of these experiments, we tested whether the bioactivating enzyme AOR could potentiate the inhibition of Trx by AFs or change the pattern of adduct formed between AFs and Trx. However, AOR was observed to have no influence on adduct formation, both on the basis of insulin-reductase activity, BIAM-labeled band intensities and MS analysis of treated whole protein samples.

Cyclopentenone prostaglandins involved in pro-oxidant effect owing to the electrophilic center were reported to covalently modify Trx both in cell and cell-free system.[328] Trx levels in SH-SY5Y were reduced upon treatment with biotinylated 15d-

prostaglandin J_2. In contrast, treatment of breast and colon cancer with quinones that also form covalent adducts with isolated hTrx did not result in reduction of cellular Trx.[329] In the present study, we found that cellular Trx levels were significantly reduced in a dose-dependent manner upon treatment of HeLa or MCF-7 cells with AF or HMAF. However, illudin S only caused Trx levels to decrease in HeLa cells, not MCF-7, and this effect was independent of the illudin S dose, which is consistent with our previous observations that cellular GR inhibition by illudin S is dose-independent. These data suggest a clear difference in the role, if any, of Trx or GR interactions of AFs vs. illudins in dictating cytotoxicity. Higher cellular Trx levels have been correlated with diminished cell sensitivity toward alkyalting drugs such as cisplatin and mitomycin C.[312] Interestingly, synergistic effects have been observed in the combinational therapy of HMAF with cisplatin or mitomycin C in cancer cell and a cancer xenograft model.[330, 331] Thus, the observed interactions of Trx with HMAF may contribute to enhancing the activity of the combined drug in these combination therapies.

In mammalian cells, Trx plays a distinct role in different locations. Outside the cell, Trx acts as a co-cytokine with chemokine-like activity.[332] Inside the cell, Trx functions as the major redox-regulating system and translocates into the nucleus to regulate other signaling proteins and gene expression in response to a variety of stresses such as oxidative stress, ionizing radiation,[333] and small molecules such as nitric oxide.[322] In the present study, AFs and illudin S were all found to stimulate nuclear accumulation of Trx, similar to what has been observed with cisplatin as previously reported.[323] It has been reported that more Trx in its reduced form in nucleus than that in the cystosol.[334]Since our results indicate that AFs can only react with reduced Trx, nuclear Trx more likely reacts with these compounds.

5. Conclusion

We have evaluated mechanisms of Trx inhibition by the natural product illudin S and its AF analogues. Experiments were carried out to evaluate enzyme inhibition, protein intrinsic fluorescence changes, covalent modification of whole proteins, and influence on the cellular Trx level and location. All three compounds quenched Trx intrinsic fluorescence significantly, suggesting that conformational changes are induced by illudin S and AFs. Illudin S does not inhibit insulin-reductase activity of pre-reduced Trx, and AFs are irreversible inhibitors that covalently modify the protein at active site cysteine residues. In the complex environment of the cell, AFs inhibit Trx protein level in a dose-dependent manner. The interaction between Trx and these test compounds promotes Trx nuclear accumulation. Overall, the reactivities of illudin S and AF analogues toward Trx are opposite to what might be expected on the basis of reactivity towards thiol-containing molecules and consistent with their reactivity towards glutathione reductase, further emphasizing the importance of balancing chemical reactivity and molecular recognition in dictating biochemical responses. Another observation made in this study is that HMAF reacts with DTT. However, AF does not react with DTT, and illudin S only does so to a minor extent. The HMAF-DTT adduct quenches Trx fluorescence with the same potency as HMAF, suggesting the adduct may play a role in protecting Trx from reaction with HMAF. Altogether, the data obtained in this study provide more insight into the role of protein alkylation in the cytotoxicity and anticancer selectivity of illudin S and acylfulvene derivatives.

Chart 1. Structures of illudin S, acylfulvene, hydroxymethylacylfulvene, and their corresponding metabolites.

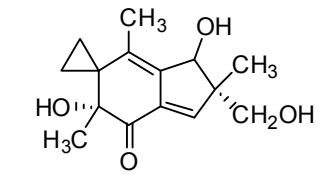

Illudin S

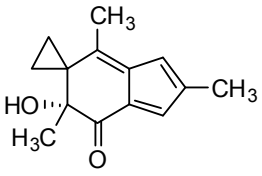

(-)-Acylfulvene (AF)

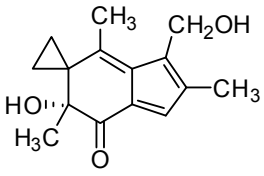

(-)-6-hydroxymethylacylfulvene (HMAF)

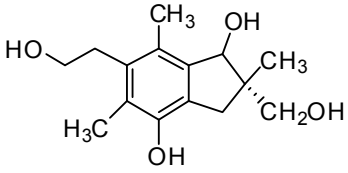

M_I

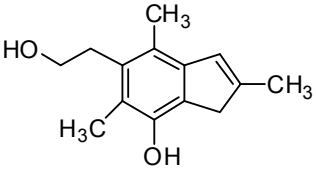

M_A

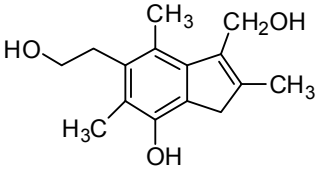

M_H

Figure 1. HPLC-UV analysis of the product from the reaction of of Trx with illudin S or AFs. Test compounds (AF, 400 μM; HMAF, 400 μM; illudin S, 1mM) were allowed to react with Trx (2 μM) in the presence of DTT (2 mM, row C) or in the absence of DTT, but with pre-reduced Trx (2 μM, row D) in TE buffer (500 μL) for 2 h at 25 °C, followed by EtOAC extraction and HPLC analysis. Control samples were incubated in buffer in the absence (row A) or presence of DTT (20 mM, row B) and extracted in the same manner. The peak at 5 min observed in each sample is DMSO. The retention times of AF, HMAF and illudin S are 26 min, 17 min, and 12 min respectively.

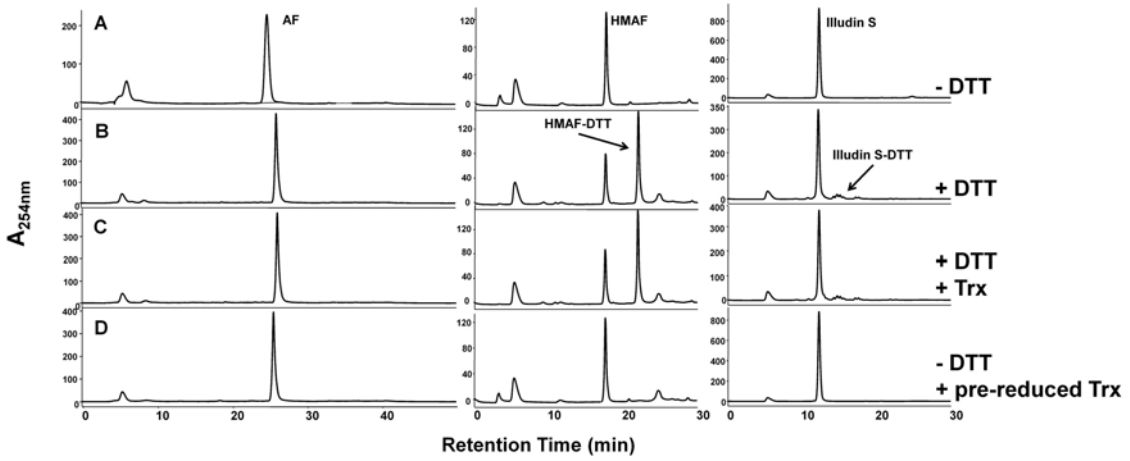

Figure 2. The MS/MS spectra of HMAF-DTT conjugate, MS2 spectra of HMAF-DTT monomer (top) and MS3 spectra of fragment 229 from MS2 (bottom).

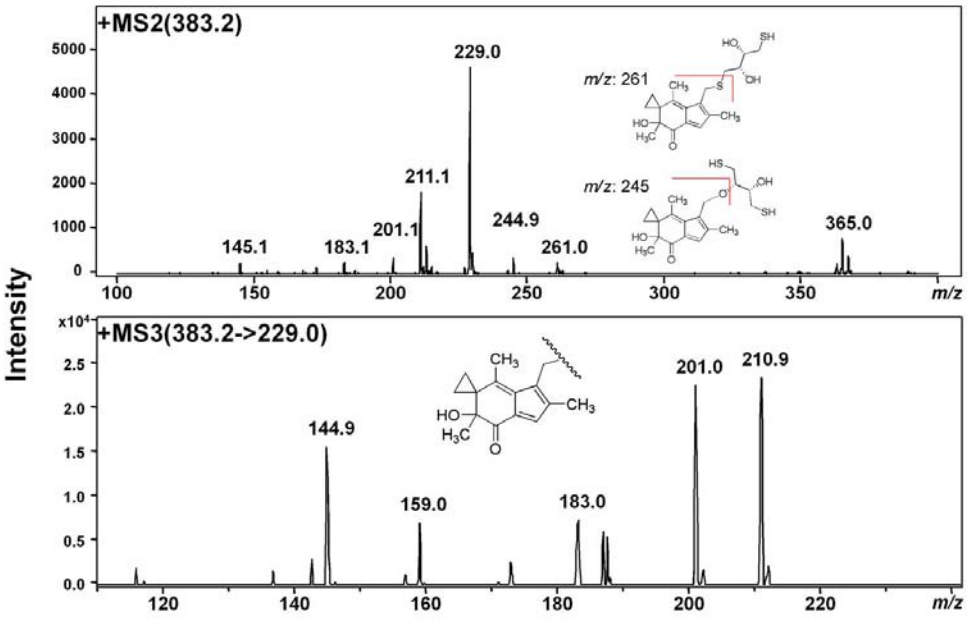

Figure 3. Inhibition of Trx Intrinsic fluorescence by compounds. Trx (9 μM) was combined with DTT (2 mM) in 500 μL of TE buffer for 10 min prior to the addition of varying concentration of compounds followed by incubation at 25 ºC for 90 min. Fluorescence was recorded with excitation at 280 nm. The inset is the plot of relative fluorescence intensity to the control versus the drug concentration.

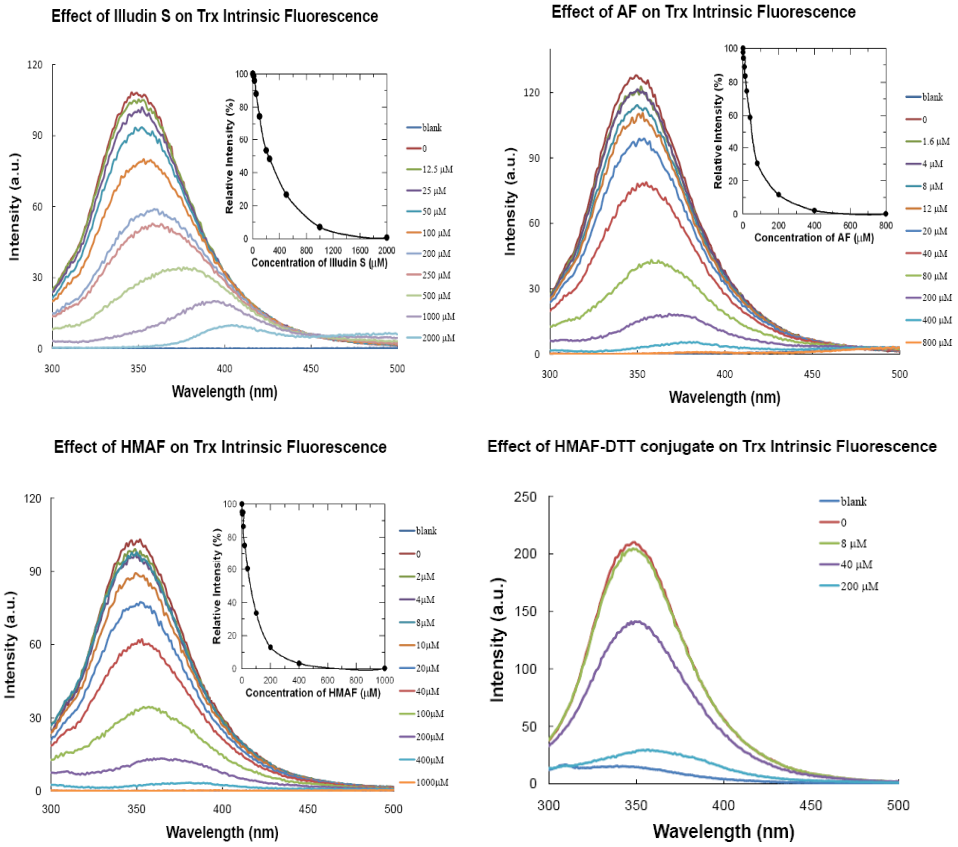

Figure 4. Inactivation of Trx by illudin S and AFs. Trx activity was measured by its ability to reduce insulin in the presence of DTT. Pre-reduced Trx was incubated with various concentrations of drugs for 2 h at 25ºC before addition of insulin and DTT. The precipitation of reduced insulin free chain was monitored at 650 nm.

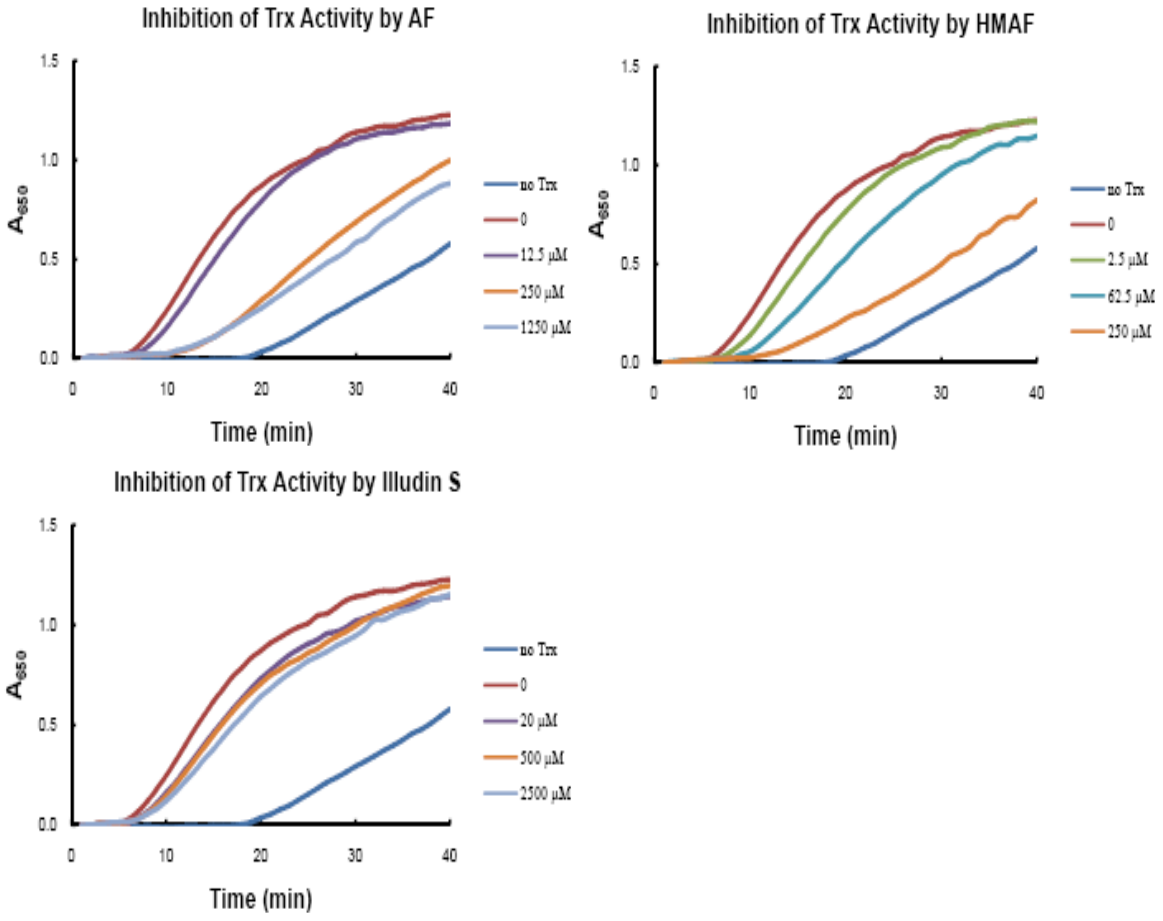

Figure 5. Relationship between concentration required to achieve complete fluorescence quenching and concentration required to achieve complete Trx inactivation by AF, HMAF, and illudin S

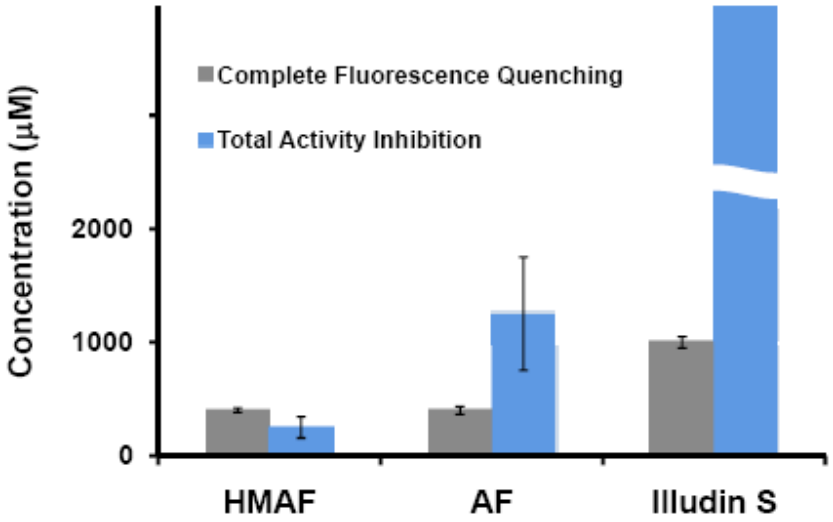

Figure 6. HPLC-ESI+-MS analysis of adducts formed between Trx and AFs. Total ion chromatogram of control Trx (Top panel). (A), ESI+ mass spectrum of the 14.6 min protein peak of control Trx; deconvoluted mass spectrum of the 14.5 min peak (inset, observed *m/z* = 11675 Da) (B), ESI+ mass spectrum of the protein peak of Trx following incubation with AF; deconvoluted mass spectrum(inset, observed adducts *m/z* = 11887 and 12100 respectively) (C), ESI+ mass spectrum of Trx following incubation with HMAF; deconvoluted mass spectrum (inset, observed adduct *m/z* = 12134).

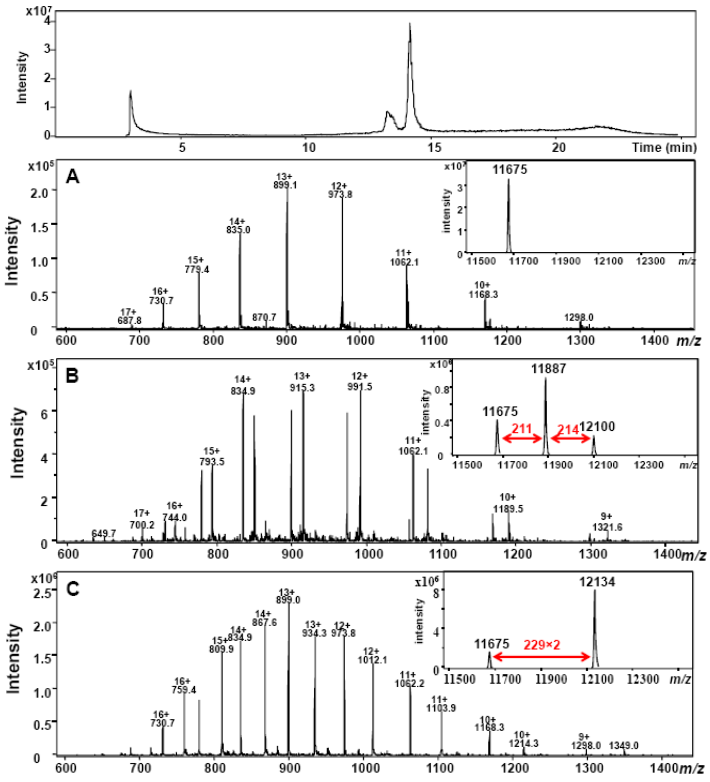

Figure 7. Trx Modification by AFs at Cys residue. Different concentrations of AFs were added to DTT pre-reduced Trx (0.9 μM) and incubated at 25 ºC for 2 h. BIAM was added to alkylate active site free Cys residues. Results are representative of two independent experiments.

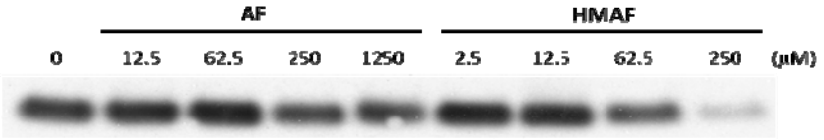

Figure 8. Inhibition of Cellular Trx level by AFs. HeLa cells and MCF-7 cells exposed to various concentrations of drugs for 12 h and 24 h respectively were lysed and proteins (20 μg) were separated on SDS-PAGE under reducing conditions.

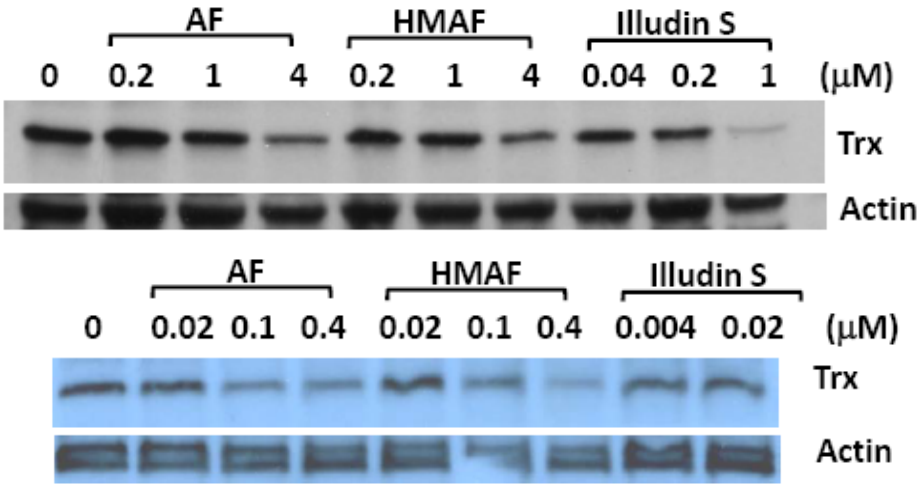

Figure 9. Indirect immunofluorescence analysis to determine Trx sub-cellular location in HeLa cells. Cells were treated with different compounds (AF, 2 μM, HMAF, 2 μM, illudin S 0.2 μM, cisplatin, 10 μM, MA, 10 μM, and MH, 10 μM) for 10 h and cellular Trx wasvisualized as described in the experimental section. Images shown represent data from three independent experiments.

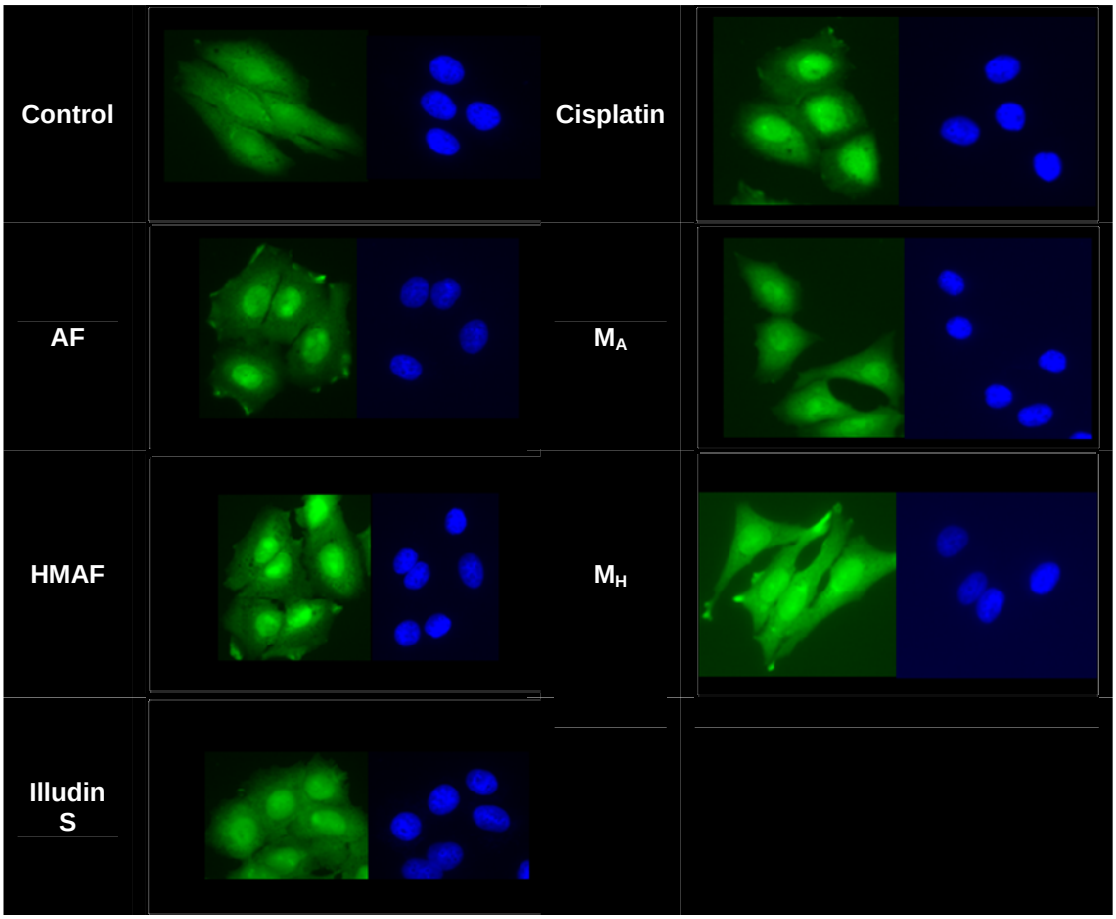

Scheme 1. Proposed Mechanism of Trx Inhibition by AFs

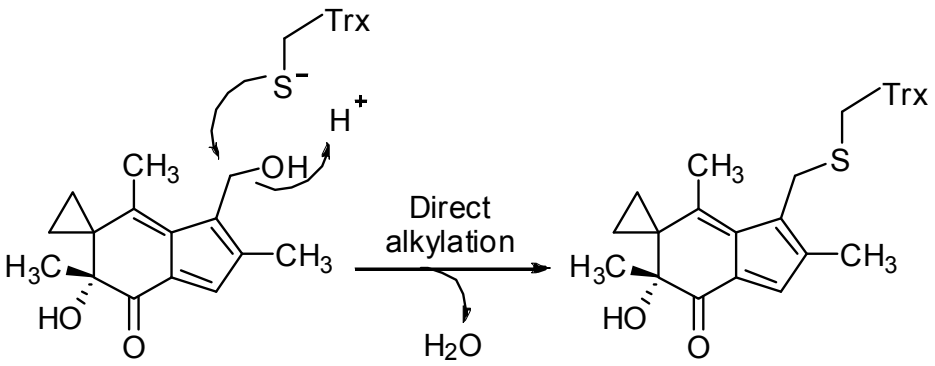

Scheme 2. Proposed decomposition pathway of HMAF under acidic condition

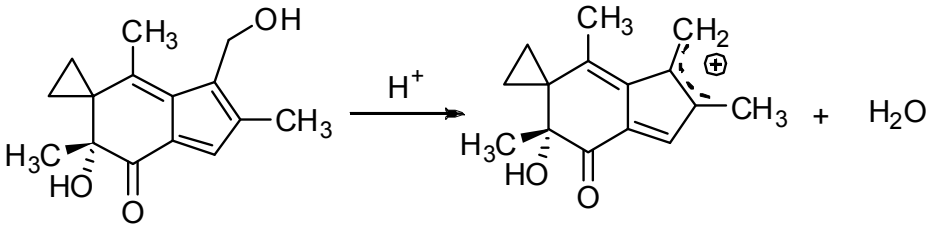

HMAF

Chapter Six: On the role of selenium-dependent antioxidant enzymes in cancer cells: alkylation and inhibition of thioredoxin reductase vs. glutathione peroxidase by anticancer acylfulvenes

1. Introduction

Selenium (Se), as a nutritional supplement, has been shown to inhibit tumor cell invasion and decrease the risk of some human cancers, such as prostate, lung, and colon cancer.[335, 336] The chemopreventive and chemotherapeutic effects of Se may result from modulation of cell differentiation and proliferation, which protects cells from carcinogenesis in both the early and late stages of cancer progression.[336] Se acts as an antioxidant when incorporated into proteins,[116] so the modulation of selenoenzyme levels may be an underlying mechanism for chemopreventive and chemotherapeutic effects observed for Se.[336, 337]

In human blood, Se levels vary between 0.8-1.4 μM.[338-341] Thioredoxin reductase (TrxR) and glutathione peroxidase (Gpx) contain selenium in the form of selenocystein (Sec), the naturally occurring selenium analog of cysteine regarded as the 21st amino acid.[342, 343] In TrxR, the Sec residue is located at the C-terminus active site as part of the tetrapeptide Gly-Cys-Sec-Gly motif.[342] TrxR has a broad range of substrates, including disulfide-containing proteins, such as thioredoxin, many small molecule thiols, such as 5,5'-dithiobis(2-nitrobenzoic) acid (DTNB), and even non-disulfide compounds such as vitamin K. The flexible C-terminus TrxR active site is exposed to the protein surface and is accessible to substrates and inhibitors. In addition, the Sec residue is more reactive than Cys towards electrophiles due to its lower pK_a. These features make TrxR highly susceptible to reactions with electrophilic compounds, and previous studies show that some alkylating agents strongly inhibit TrxR and its cellular homolog glutathione reductase.[110, 299] The Gpxs are a family of peroxidases that contain one essential active site Sec and, with glutathione as a co-substrate, catalyze the reduction of inorganic or organic peroxides. Gpx 1 is the most predominant Gpx isoform; it catalyzes the reduction of hydrogen peroxide and lipid peroxides to water and corresponding hydroxides. Nitric oxide-mediated modifications of the Gpx selenocysteine has been shown to inactivate the enzyme.[344] Upregulated TrxR and downregulated Gpx have been found in many types of cancers.[117, 345] TrxR over-expression is of particular interest as an anticancer drug target.[124, 125, 346]

Acylfulvenes (AFs) are a class of semisynthetic antitumor agents derived from the natural sesquiterpene cytotoxin illudin S, isolated from the Jack o'lantern mushroom (Chart 1).[240-243] Although illudin S kills various drug-resistant cancer cells, it exhibits low selectivity towards malignant cells versus normal cells and thus has limited practical application in cancer therapy.[244] Semisynthetic acylfulvene (AF) analogues, including hydroxymethylacylfulvene (HMAF), have improved cancer cell selectivity.[245, 246] Studies regarding their cellular accumulation suggest that illudin S and AFs covalently bind to cellular DNA, RNA, and protein (Scheme 1).[247, 248] There is evidence that cytotoxicity is associated with bioactivation to an unstable cyclohexadiene intermediate that more potently reacts with DNA and interrupts DNA synthesis/repair.[137, 247, 249-252] However, compared to conventional DNA alkylating agents, AFs display some unique activity profiles suggesting contributing interactions with other cellular targets, i.e. certain proteins, and a distinct mechanism of action underlying cytotoxicity profiles.[134, 136] The specificity and efficiency with which tumor-associated reductase enzymes activate AFs versus illudins appear to contribute in part to the selectivity of acylfulvene analogs compared to illudin S. However, an overall mechanism accounting for differences between these structurally related small molecules has not been established and is an important goal in building an understanding of chemical and biochemical factors that dictate drug toxicity. As part of a program aimed at elucidating the potential contributions of protein-drug interactions in dictating the toxicities of alkylating agents in a selective manner, we were interested in testing whether the high nucleophilicity and accessability of the Sec-containing enzymes TrxR and Gpx rendered them susceptible to illudin S and/or AF and whether there is any basis for chemical selection in this process.

Illudin S reacts with cysteine under mild conditions more readily in aqueous buffer at pH 6 than acylfulvenes.[141, 142, 242, 254] It has been hypothesized that the same reactivity might be observed for Cys-containing enzymes and could contribute to general toxicity. However, we found that for glutathione reductase (GR), an enzyme with a redox-active disulfide at its active site, acylfulvenes are more reactive as inhibitors that disrupt enzyme structure and inhibit GSSG reductase activity, and HMAF was found to covalently bind active site Cys residues.In contrast, illudin S did not inhibit glutathione reductase activity

although it also induced enzyme conformational changes.[299] To understand analogous reactivity patterns in the case of Sec-containing enzymes, and to address the standing question of cellular protein targets of acylfulvenes, we characterize the reactivities of illudin S and AFs toward TrxR and Gpx in this study. The results of this study reveal chemical- and structure-based differences in inhibition potencies, differential enzyme-drug interactions, as well as a correlation between selenium and drug sensitivity. These data suggest that cytotoxicities of illudin S and AF derivatives may be mediated in part by influencing the cellular redox environment by interacting with reactive selenoenzymes and that Se modulates the responses of cancer cells towards AFs. This information contributes to a broader understanding regarding chemical and biochemical factors involved in regulating cell sensitivity towards alkylating drugs.

2. Experimental procedures

2.1 Chemicals and reagents

Illudin S was provided by MGI Pharma (Bloomington, MN). Acylfulvene and HMAF were synthesized according to the published procedure with illudin S as the starting material.[242, 243] Purified rat thioredoxin reductase, glutathione peroxidase from bovine erythrocytes, Tris base, DTNB and EDTA were obtained from Sigma Chemical (Milwaukee, WI). Biotin-conjugated iodoacetamide was purchased from Invitrogen (BIAM, Carlsbad, CA). Reduced nicotinamide adenine dinucleotide phosphate (NADPH) was purchase from EMD chemicals (Gibbstown, NJ). Dulbecco's modified Eagle's medium (DMEM) was purchased from Mediatech (Herndon, VA). Fetal bovine serum (FBS) was purchased from Atlanta Biologicals (Lawrenceville, GA). Phosphate-buffered saline (PBS), 0.25% trypsin-EDTA, penicillin-streptomycin were obtained from Invitrogen (Carlsbad, CA). Tris-buffered saline was purchased from Biorad (Hercules, CA)

2.2 Enzyme Activity Assays

Drug stock solutions were prepared in DMSO. All other solutions used in the assay were prepared in TE buffer (50 mM Tris-Cl, 1 mM EDTA) at pH 7.2. The activity of enzyme was determined at room temperature using a UV/visible spectrophotometer (Varian Cary-100). TrxR (80 nM) was first reduced by incubation with excess NADPH (100 μM) in a total volume of 0.1 mL at room temperature for 10 min. Then appropriate amounts of compounds (prepared in DMSO) were added to the pre-reduced TrxR followed by incubating at room temperature for the appropriate time. The same amounts of DMSO were added to the control experiments. The enzyme activities were measured by DTNB reducing assay in which at the end of incubation, 0.4 mL of assay solution (2 mM DTNB and 200 μM NADPH in TE buffer) was added and the absorbance at 420 nm was monitored for 3 min.

To determine the reversibility of inhibition, TrxR was allowed to react with AFs as described. After the 2 h reaction period, unbound compound was removed by gel-filtration with a size-exclusion micro bio-spin P6 pre-packed column according to the manufacturer's protocols. Briefly, the column was placed in 2 mL centrifuge tube to

drain the excess packing buffer by gravity. The column was placed back into the tube and centrifuged to remove the packing buffer (2 min, 1000 g). Afterwards, the column was placed in a clean centrifuge tube, and the reaction solution was loaded into two columns (100 μL/each) followed by centrifugation for 4 min at 1000 g. The resulting solution was combined, and the activity was determined following the procedure described above.

2.3 Cell culture and cellular TrxR determination

HeLa cells were maintained as monolayers in DMEM medium supplemented with 10% FBS and 1% penicillin-streptomycin in a humidified, 5% CO_2 atmosphere at 37 °C. Hela cells were subcultured in the medium described above for three days to reach 80% confluence (100 mm^2 plate, 2×10^6 cells/plate). Cells were treated with test compounds diluted with medium (0.1% final concentration of DMSO) for two or ten hours. After the treatment period, cells were washed with PBS twice. Cells were collected as follows: 2 mL of 0.25% trypsin-EDTA was added and the cells were incubated for 5 min at 25 °C, and then cells were scratched off and divided evenly into three centrifuge tube (1.5 mL), and centrifuged (5 min, 1000g) followed by removal of the supernatant. Cells were resuspended in 0.2 mL of lysis buffer (50 mM Tris-HCl, pH 7.5; 1 mM EDTA; 0.1% Triton X-100; 1 mM phenylmethanesulfonyl fluoride; 1 mM benzamidine; 1.4 μM pepstatin A; and 2.0 μM leupeptin) and sonicated at 4 °C (5 s bursts). The resulting cell lysate was centrifuged for 10 min (8000 g, 4 °C), and the supernatant was withdrawn for analysis. Cell cytosol containing 50 μg protein as determined by the bicinchoninic acid (BCA) protein assay reagent (Pierce, Rockford, IL) was incubated with 80 μL of reaction mixture containing insulin (1 mg/mL) and NADPH (200 μM) in TE buffer at 25 °C for 10 min. Trx (50 μL, 1 mg/mL) was added, and the rate of NADPH consumption was monitoring changes in absorbance at 340 nm for 5 min at 25 °C.

Cell cytosol containing 50 μg protein was analyzed by 4-12% SDS-PAGE according to the manufacturer's protocol (Invitrogen, Carlsbad, CA) and transferred onto a membrane (PVDF, Invitrogen, Carlsbad, CA) for 1 h at 33 V, 4 °C. Membranes were blocked with 5% (w/v) nonfat milk powder in tris-buffered saline (TBS)/Tween 20 (0.05%) overnight at 4 °C. The membrane was incubated with primary anti-TrxR (ABR,

Rockford, IL) and anti-actin (Invitrogen, Carlsbad, CA) antibodies diluted 2000 times in TBS/Tween 20 (5 mL) for 1 h. The membrane was washed three times with TBS/Tween 20 (5mL, 5 min) and subject to incubation with 5 mL of secondary conjugated antibody (goat anti-rabbit IgG horseradish peroxidase, Biorad, Hercules, CA, 1:2000 dilution in TBS/Tween 20,) for 1 h. After four 5 min washes with TBS/Tween 20 (5 mL/each), enhanced chemiluminescence was measured with a western blotting analysis system (Pierce, Rockford, IL).

2.4 Cell viability assay

The cytotoxicity was determined by Promega CellTiter 96 Aqueous One Solution Cell Proliferation Assay. Briefly, cells were seeded on 96-well plate with a beginning density at 1000 cells/well in either regular medium or medium containing 1 μM sodium selenite for 3 days. The exponentially growing cells were then exposed to varying drug concentration for a period of time. The drug-containing medium was exchanged with fresh regular medium. Cellular viability was determined by exposing cells to MTS solution for 2 h at 37 °C, and the formation of formazan was measured at 490 nm by using microplate reader. All experiments were carried out in triplicate.

2.5 Detection of the AFs-modified sites

NADPH-reduced TrxR (0.9 μM) and different concentrations of AFs were incubated at 37 °C for 2 h. The same amounts of DMSO were added to the control experiments. After incubation, 1 μl of the reaction mixture was taken out and added to new tubes containing 19 μL of BIAM (100 μM, pH 6.5 and 8.5 in TE buffer) further incubated at 37 °C for another 30 min to allow the alkylation at the remaining free -SeH and –SH groups in the enzyme. Fifteen microliters of BIAM-modified enzyme were mixed with 5 μL of loading buffer (Invitrogen), 20 μL of the samples were subjected to SDS-PAGE on a 4-12% gel, and the separated proteins were transferred to nitrocellulose membrane. Proteins labeled with BIAM were detected with horseradish peroxidase-conjugated streptavidin and enhanced chemiluminescence detection.

2.6 Trypsin-mediated digestion and LC/MS analysis of AF-modified TrxR

TrxR (50 μg, 1 nmol) was allowed to react with AFs (1.25 mM) in a total volume of 0.2 mL TE buffer containing NADPH (1 mM) for 2 h at 25 °C. An aliquot (1 μL) of reaction solution was withdrawn and diluted to a total volume of 300 μL; enzyme activity was determined as described above for measurement of TrxR activity. After 2 h, TrxR activity was inhibited by AFs completely. Incubation solutions were diluted to a volume of 1 mL by adding 0.8 mL TE buffer followed by trypsin in 0.1 M HCl (0.2 μg/μL). Proteolytic digestion was allowed to occur at 37 °C for 24 h. The resulting mixture was divided into two equal portions, placed into centrifuge tubes, concentrated to dryness on a Speedvac concentrator, and reconstituted by adding 20 μL of solvent A (0.5% formic acid/0.01% TFA in water) to each tube. The resulting samples were analyzed by LC/MS.

LC/MS analysis of peptide mixtures was performed on an Agilent 1100 capillary HPLC in line with an Agilent 1100 iontrap mass spectrometer operated in positive ion mode. An Agilent Zorbax SB-C18 column (150 mm× 0.5 mm, 5 μm) was used. Analytes were eluted with a gradient of solvent A (0.5% formic acid/0.01% TFA in water) and solvent B (0.5% formic acid/0.01% TFA in acetonitrile) at a flow rate of 15 μL/min: initial conditions, 3:97 B:A, were held constant for 3 min, and then increased to 5:95 B:A in 7 min and held for 10 min followed by linear increase to 35:65 B:A over a course of 95 min, and finally to 75:25 B:A in 10 min.

2.7 LC/MS analysis of Gpx modification by AFs

Gpx (20 μg, 0.9 nmol) was allowed to react with AFs (1.25 mM) in a total volume of 0.1 mL TE buffer for 2 h at 25 °C. A micro bio-spin P6 column (10,000 NMWL, Biorad, CA) was used to remove unbound compound. Collected solution was then dried on speedvac and reconstituted in water (30 μL). 8 μL samples were analyzed by LC/MS.

LC/MS analyses were carried out on an Agilent 1100 capillary HPLC- iontrap mass spectrometer operated in positive ion mode; the HPLC was equipped with an autosampler. A Zorbax 300 SB-C3 column (150 mm×0.5 mm, 5 μm) was used. Analytes were eluted with a solvent gradient of 0.05% TFA in water (A) and 0.05% TFA in acetonitrile (B), at a flow rate of 15 μL/min: initial conditions, 30:70 B:A, were held 3 min followed by a linear increase to 80:20 B:A over a course of 20 min. Spectra were

obtained by full scan data acquisition performed within *m/z* 100-1500. Mass deconvolution was performed with the Agilent ion trap analysis software.

3. Results

3.1 Illudin S and AFs inhibit TrxR in a dose- and time-dependent manner

When NADPH-reduced TrxR was treated with illudin S and AFs, its DNTB reduction activity was inhibited in a dose-dependent manner (Figure 1). The IC_{50} values were determined to be 257 μM for illudin S, 7.3 μM for AF, and 0.4 μM for HMAF respectively. Without pre-reducing TrxR, no inhibition was observed for illudin S, and the IC_{50} values for AFs increase to millimolar ranges (Figure 2). The inhibition of TrxR by AFs is time-dependent; within five minutes, over 60% of TrxR activity was inhibited by 50 μM AF and 7.5 μM HMAF respectively (Figure 3), suggesting a rapid reaction between TrxR and AFs. Further, the relative inhibition potencies of AF and HMAF towards TrxR in the absence of pre-reduction are similar, suggesting the inhibition of TrxR by AFs mainly results from interactions of AF with the TrxR active site. Some other interactions may also partially account for the inhibition.

3.2 TrxR inhibition by AFs is irreversible

To determine whether TrxR inhibition by AFs is reversible, gel-filtration studies were conducted. TrxR was allowed to react with AFs in the same manner as described for studies carried out to determine the concentration-dependence of inhibition. The resulting inactivated TrxR was passed through a size exclusion micro Bio-spin P6 gel-filtration column (NWML 6000) to remove non-covalently bound compounds and the re-isolated enzyme was assayed for DNTB reduction capacity. The native TrxR activity was not recovered after removing the AFs from the incubation solution (Figure 4), suggesting AFs are irreversible inhibitors of TrxR.

3.3 Alkylation of cysteines at TrxR active site

An affinity assay involving selective BIAM-alkylation of free Cys residues was carried out for the AF-Trx interaction to determine whether active site Cys in TrxR were chemically modified by AFs. The enzyme was allowed to react with varying concentrations of AFs before labeling with BIAM which only selectively reacts with the cysteine residues at the active site. Due to the difference in pK_as of the TrxR active site residues Cys 497 (pKa 8.3) and Sec 498 (pKa 5.2),[347] only Sec is modified at pH 6.5 and both residues will be modified at pH 8.5. At pH 6.5, the labeling intensity was weaker

with increasing concentrations of AFs, suggesting modification of Sec by AFs (Figure 5). At pH 8.5, the labeling intensity of TrxR at the highest treatment concentration of AFs (125 μM AF and 25 μM HMAF) was almost abolished, suggesting both Cys and Sec at the active site were modified by AFs.

3.4 Identification of the covalent adduct between AF and TrxR

Since AF irreversibly inhibited the DNTB reduction activity of TrxR, and the modification appears to occur at the C-terminus active site, we analyzed the trypsin digest of the covalently modified TrxR by LC/MS to evaluate the chemical pathway involved. A singly charged ion corresponding to the active site peptide product of the tryptic digest was observed by ion trap MS analysis (*m/z* 1142.4, Figure 6A). Due to the presence of selenium in the peptide sequence (SGGDILQSGCysSecG), the isotope envelope is uniquely diagnostic. Singly charged ions corresponding to AF-mediated mono-alkylation of the active site tryptic peptide was observed (*m/z* 1358.6, Figure 6B), and the associated mass change (*m/z* 216) is consistent with formation of an adduct via direct conjugate addition to the α,β-unsaturated carbonyl. Due to poor ionization efficiency, the HMAF-modified peptide could not be identified.

3.5 Evidence for TrxR inhibition by AFs in whole cells

Human cervical cancer cells (HeLa) are highly sensitive to AFs, with a reported IC_{50} of 20 ng/mL for HMAF in a three day continuous treatment strategy.[134] To test whether TrxR might be involved in the observed HeLa cell sensitivity toward AFs, the cells were treated with equitoxic concentrations of illudin S, AF, or HMAF for 12 h. After washing and cell lysis, residual TrxR activity was determined. A dose-dependent loss of TrxR activity resulted from each of the compounds tested (Figure 7), with about a 50% reduction observed with 1 μM illudin S, 4 μM AF, and 1 μM HMAF. These data, i.e. relative potencies for reducing cellular TrxR activity, mirror inhibition potencies in a cell-free system, however, illudin S is relatively more potent in cells. This observation may result from the more efficient cellular uptake of illudin S vs. AFs.[247, 248, 296]

3.6 Selenite-enhanced sensitivity of cells towards AFs

It has been reported that culture medium supplemented with selenite will induce the cellular TrxR level in breast cancer MCF-7 cells and liver cancer HepG2 cells.[348, 349] In

the present study, HeLa cells were cultured in media containing 1 μM sodium selenite for three consecutive days. By western blotting analysis and measurement of cellular TrxR activity after selenite induction, cellular TrxR protein levels were found to have increased 3.6-fold (Figure 8A) and TrxR activity increased 4.2-fold (Figure 8B). The changes in cell sensitivity toward illudin S and AFs under different levels of TrxR were investigated. Results indicated that increasing the cellular level of TrxR sensitizes cells toward AFs, but not toward illudin S (Figure 8C), suggesting that TrxR is a cellular target of AFs. After induction by 1 μM selenite for three continuous days, HeLa cell sensitivity towards 100 μM AFs was increased about 50% compared to the cell sensitivity without selenite induction.

3.7 AFs do not covalently modify Gpx

Gpx was incubated with AFs for 3 h and then unbound compound was removed with a microcon Y-10 centrifuge filter (NMWL 10,000). Whole protein mass spectrometry analysis indicates that no covalent adduct was formed between the compound and Gpx (Figure 9).

4. Discussion:

Illudin S is isolated from *Lampteromyces japonicas* and is the major toxic ingredient responsible for the poisoning effect of this basidiomycete.[350] Although illudin S is highly effective against many types of drug resistant cancers, it does not discriminate between cancerous cells and normal cells, which has restricted its clinical application.[244, 286] Structural modifications of illudin S have resulted in some analogs with greatly improved selectivity such as AF and HMAF.[242, 243] AFs maintains the same key structural features as illudin S, which is unrelated to commonly used therapeutic agents. With the novel structure, including a cyclopropane ring and an α,β-unsaturated ketone, illudin S and AFs can undergo direct Michael-type addition by nucleophiles as well as metabolic bioactivation by NADPH-dependent reductase followed by nucleophilic attack at the cyclopropane ring (Scheme 1).[137, 247, 249-252] DNA alkylation is thought to be a major mechanism of action, however, at equitoxic concentrations, no significant difference was observed with respect to the incorporation of illudin S or AFs into genomic DNA, suggesting other cellular reactivity factors may play a role in improving the therapeutic index of AFs.[247, 248] For example, reductase-mediated bioactivation has been shown to contribute in part to dictating differences in cytotoxicity profiles for AFs.[139] Further, the better reactivity of illudin S than AFs towards thiols like GSH, cysteine and thiol-containing peptides was hypothesized to be responsible for its extreme toxicity.[140-142, 253, 254] Although lowering cellular GSH level makes cells more sensitive towards illudin S, considering the large pool of small thiols in cells and nanomolar IC_{50}s associated with illudin S, it may not be that reasonable to conclude the changed sensitivity is exclusively caused by the cellular GSH levels. By analogy, it has been hypothesized that illudin S can react with thiol-containing enzymes, which may be expected to contribute to cytotoxicity.[140] Protein modification and protein binding are general modes of drug toxicity.[255] In correlation with their reactivity with small thiols, illudin S and AFs were expected to have the same reactivity potency towards thiol-containing enzymes. However, the study of the interaction between these compounds with glutathione reductase, a critical cellular redox-regulating enzyme, reveals that AFs are much more reactive with GR than illudin S. Selenocysteine is more reactive towards electrophiles

than cysteine due to its lower pK_a value,[347] thus it will be helpful to understand the mechanism of AFs' action by probing their interaction with critical cellular selenoenzymes.

Although the biochemical mechanism of Se chemopreventive and chemo-therapeutic effects against cancer is still unclear, the function of Se has been mainly attributed to its presence in seleno proteins and the correlation of selenium administration and level of selenoenzymes has been extensively studied.[335, 345, 351-356] Se is incorporated into selenoproteins in the form of selenocysteine either during protein synthesis or through post-translational process.[88] Selenoproteins such as thioredoxin reductase and glutathione peroxidase are involved in cellular antioxidant defense and redox signaling.

The thioredoxin system, comprised of TrxR, its protein substrate thioredoxin, and NADPH, together with the homologous glutathione system, comprised of GR, NADPH, and GSH, is the major regulator of intracellular redox balance, exerting a wide range of activities in oxidant defense, cell viability, and proliferation. TrxR is very similar in both structure and mechanism to GR.[357] They both use NADPH as a cofactor to reduce the conserved internal disulfide center. TrxR is distinct from GR by the presence of a C-terminus redox center (Gly-Cys-Sec-Cys) which is functionally equal to GR's substrate GSSG.[358, 359] The flexibility of the C-terminus redox center not only allows TrxR to have a broad range of substrates, but also makes it extraordinarily reactive towards electrophiles due to the reactive and solvent accessible selenocysteine. The selenocysteine was reported to be targeted by many anti-cancer compounds, such as curcumin, motexafin gadolinium, flavonoids, and quinines.[125, 346] TrxR regulates cell proliferation by controlling DNA systhesis and antioxidant defense with reduced thioredoxin. In normal cells, TrxR is critical for maintaining intracellular proteins in their reduced states and defending against oxidative stress. In malignant cells, however, TrxR supports tumor growth and progression. Elevated levels of TrxR were found in many types of cancer cell lines, especially ovarian and prostate cancer, which are both very sensitive to HMAF.[117, 134] Our previous study indicate that GR can be inhibited by AFs with varying potencies and mechanisms, but not by illudin S.[299] In this paper, we further investigate the influence of TrxR by illudin S and AFs.

NADPH-reduced TrxR was inhibited by AFs with low micromolar IC_{50}s, but the IC_{50} of illudin S is 100-fold higher (Figure 1), which is consistent with their relative potencies for inhibiting GR. Reduced TrxR is more susceptive to AFs inhibition than non-reduced TrxR (Figure 2, ~1000-fold higher). Thus, we hypothesize that there may be some interactions other than the direct interaction with the TrxR active site, ansd similar observation was made on GR inhibition by AFs.[299] The reversibility study reveals that both AFs are irreversible TrxR inhibitors (Figure 4), however, only HMAF is an irreversible GR inhibitor, which may be explained by the higher reactivity of Sec. The results of a BIAM labeling experiment further supports that the Sec was selectively targeted by both AFs at low concentrations. Peptide mass spectrometry analysis suggests the adduct was formed following a direct alkylation pathway (mass change *m/z* 216), which is also consistent with the proposed formation of a HMAF-GR adduct by direct 1, 4 – addition to the α,β-unsaturated ketone followed by opening of the cyclopropane ring by water. Although blotting results suggest that the neighbouring cysteine was also modified by higher concentrations of AFs, no ions corresponding to a bis-adducts were observed. This may be due to the poor ionization efficiency of HMAF-modified peptides as previously discussed.[299] We only observed singly charged ions corresponding to the unmodified active peptide (SGGDILQSCysSecG, *m/z* 1142.4) and a mono-adduct of AF by ion trap mass spectrometry. Because the unique isotopic distribution of Se, it is easy to confirm the identity of correponding peptides. Similar observations were made during the analysis of a 4-hydroxynonenal modified TrxR active site, in which also only a singly charged modified peptide mass peak was identified with the Se-specific isotopic mass distribution.[121]

TrxR expression is upregulated by up to 10-fold in cancer cells compared with normal cells.[342, 360] Se has been reported to induce TrxR 10-30 fold alone or in combination with sulforaphane.[348, 349] 3.6-fold induction of TrxR protein level in HeLa cells by 1 μM selenite is associated with a 4.2-fold increase in activity. We also compared induction efficiency for the combination of Se and sulforaphane (Figure 10). Results suggest that in HeLa cells, TrxR basal levels are already high and there is no significant increase when co-induced by Se and sulforaphane. In the case of MCF-7 cells,

however, basal levels of TrxR are much lower, and co-induction resulted in a 10 fold TrxR expression increase. Interestingly, although sulforaphane induces TrxR expression, it also inhibits celluar TrxR activity significantly.[361] Therefore, we used Se to induce TrxR, and cells are more sensitive to AFs, but not to illudin S. These results suggest that cancer cells with elevated TrxR are more sensitive, indicating that TrxR is targeted by AFs, but not by illudin S. This profile also is consistent with their relative TrxR inhibitory potencies in a cell-free system. Enhance antitumor activity was observed for combination therapy of selenium compounds and anticancer drugs taxol, doxorubincin, irinotecan, platinum agents, 5-FU and campthotecin.[362-364] Some, including cisplatin and doxorubincin,[110] have been characterized as TrxR inhibitors, suggesting increasing TrxR levels with Se may enhance cell sensitivity towards current danticancer drugs. Conversely, normal cells with lower TrxR level are less sensitive toward anticancer drugs that are potent TrxR inhibitors.

Gpx is a homotetrametic enzyme with two asymmetric unites containing two dimers. Each dimer has two selenocysteines at the active sites which are in the form of Se^- in the resting state and directly participate in the process of hydroperoxide reduction of Gpx. Unlike the flexible C-terminus active site of TrxR, the active site of Gpx located at the N-terminal ends of long α-helices, surrounded by aromatic side-chains, may protect selenocysteine from AFs.[365] Additional knowledge about the influence of hydroperoxide reduction activity of Gpx by AFs is needed to better understand the interaction of Gpx with AFs.

5. Conclusion

We evaluated inhibition potencies of TrxR by the natural product illudin S and its AF analogues. The inhibitory results obtained in this study are in one way consistent with the results obtained for GR, but in another quite different from that. The inhibition potency of illudin S and AFs is in the same order for GR and TrxR, i.e., HMAF > AF > illudin S, however, both AFs irreversibly inhibit TrxR by targeting the active site Sec and Cys with a much lower IC_{50}s than that for GR. That combined with the observation that no covalent interaction occurs between Gpx and AFs, suggests that the accessibility and reactivity of the enzyme active sites account for the inhibitory effects of AFs. In both cases, illudin S was the weakest inhibitor, which is opposite to their reactivity toward small molecule thiols, suggesting that polarity (illudin S > HMAF > AF) and stereochemistry may play a role in the binding of these compounds to the enzymes. Furthermore, the inhibition of cellular TrxR activity and increased sensitivity to AFs suggest that cellular TrxR is targeted. The data obtained in this study are valuable in further understanding the role of modulating cellular redox enzymes in the anticancer effects of alkylating agents.

Chart 1. Structure of illudin S and acylfulvene derivatives.

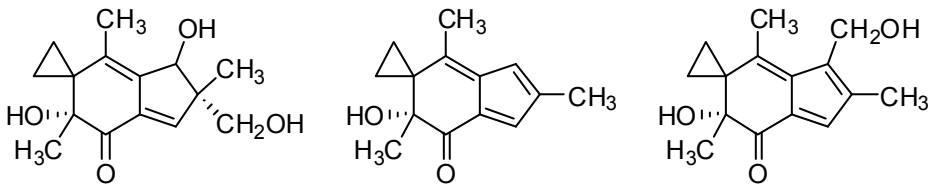

Illudin S Acylfulvene HMAF

Figure 1. Dose-dependent inhibition of pre-reduced TrxR by illudin S and AFs. TrxR (80 nM) was first incubated with NADPH (100 μM) at 25ºC for 10 min followed by the addition of test compounds and further incubated for 2 h at 25 °C (A, Illudin S, 62.5, 125, 250, 500, 1000, 2500 μM; B, AF, 2.5, 5, 12.5, 25, 50 μM; C, HMAF, 0.125, 0.25, 0.5, 1, 1.5, 2.5 μM). The residual activity was measured with DTNB assay described in the experimental details.

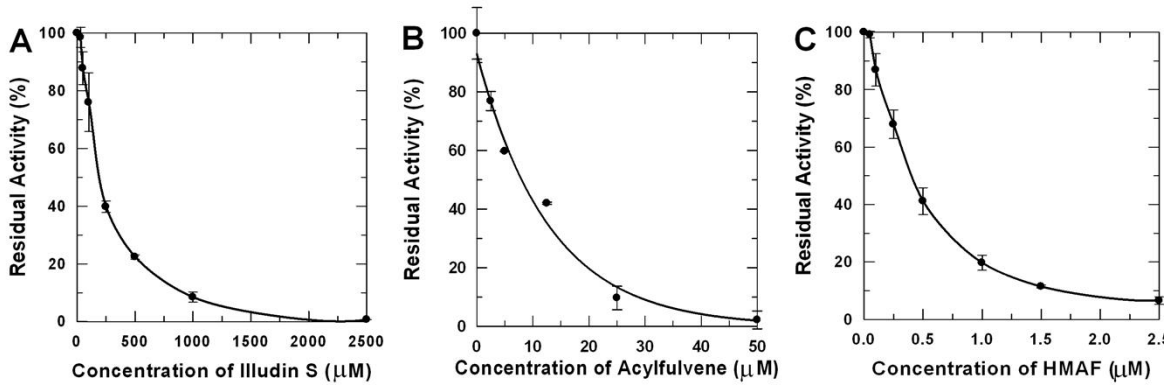

Figure 2. Inhibition of non-reduced TrxR by AF and HMAF. TrxR (80 nM) was incubated with the test compounds for 2 h at 25 °C (AF, 0.25, 0.5, 1.0, 2.5 mM; HMAF, 0.25, 0.5, 1.0, 2.5, 3.6, 5 mM). The residual activity was measured with DTNB assay described in the experimental details.

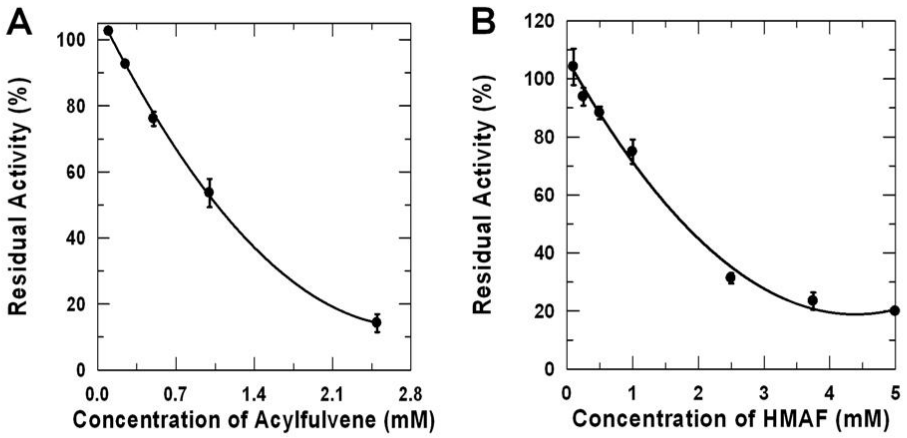

Figure 3. Time-dependent inhibition of TrxR by AFs. TrxR (80 nM) was first incubated with NADPH (100 μM) at 25ºC for 10 min followed by the addition of test compounds (A. AF 50 μM and B. HMAF 7.5 μM) at 25 °C. To assay the enzyme activity, 100 μL of the incubation solution was taken out at different time intervals and the residual activity was measured with DTNB assay described in the experimental details. Each data points represent an average of two measurements.

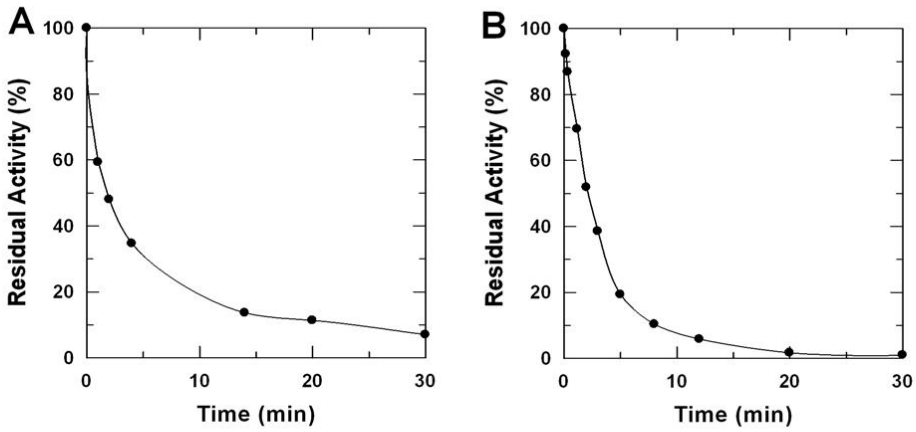

Figure 4. Gel-filtration analysis of AF and HMAF-inactivated TrxR. TrxR (80 nM) was first incubated with NADPH (100 μM) at 25ºC for 10 min followed by the addition of test compounds and further incubation for 2 h at 25 °C (A, AF, 3.3, 6.7, 16.7, 33.3, 66.7 μM; C, HMAF, 0.13, 0.27, 0.53, 1.33, 2.67 μM). Unbound compound was removed by micro bio-spin P6 pre-packed size exclusion columns (Biorad, Hercules, CA) with NWML 6000. The residual activity was measured with DTNB assay described in the experimental details.

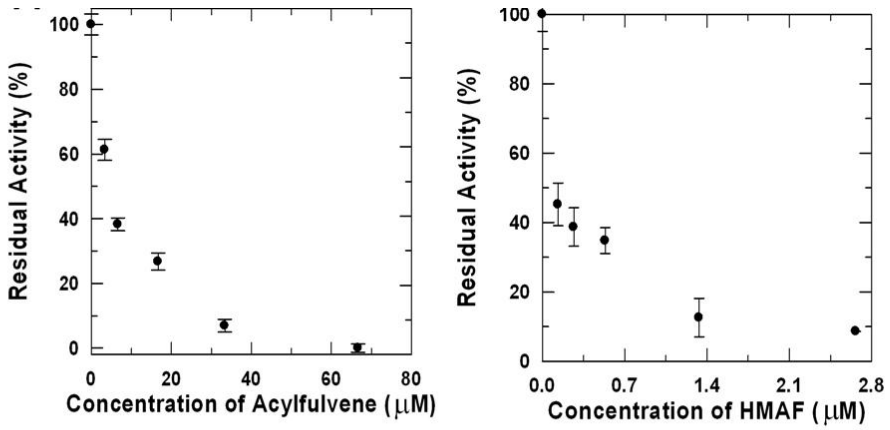

Figure 5. The C-terminus redox-active site cysteines of TrxR were targets of AFs alkylation. Different concentrations of AFs were added to NADPH (200 μM) pre-reduced TrxR (0.9 μM) and incubated at 25ºC for 2 h. BIAM was added to alkylate active site free Sec at pH 6.5 and free Cys and Sec at pH 6.5. Results are representative of three independent experiments.

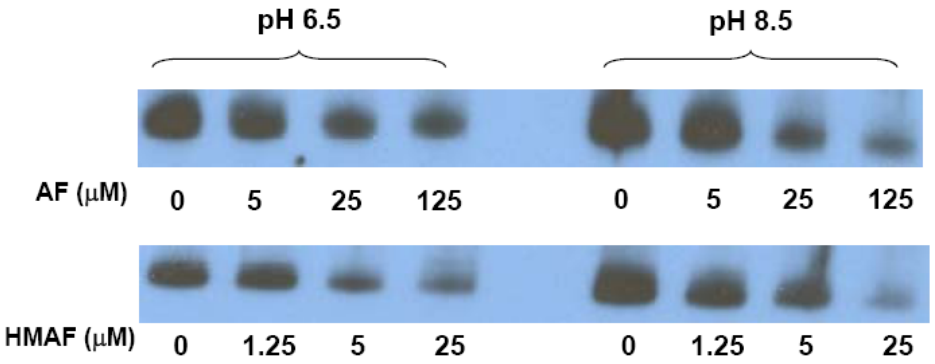

Figure 6. LC/MS analysis of AF- modified active peptide (SGGDILQSGCysSecG). The mono-isotopic mass for the unmodified peptide is 1138.3, and that for the AF-modified peptide is 1354.4. The mass change (*m/z* 216) equals the addition of one molecule of AF.

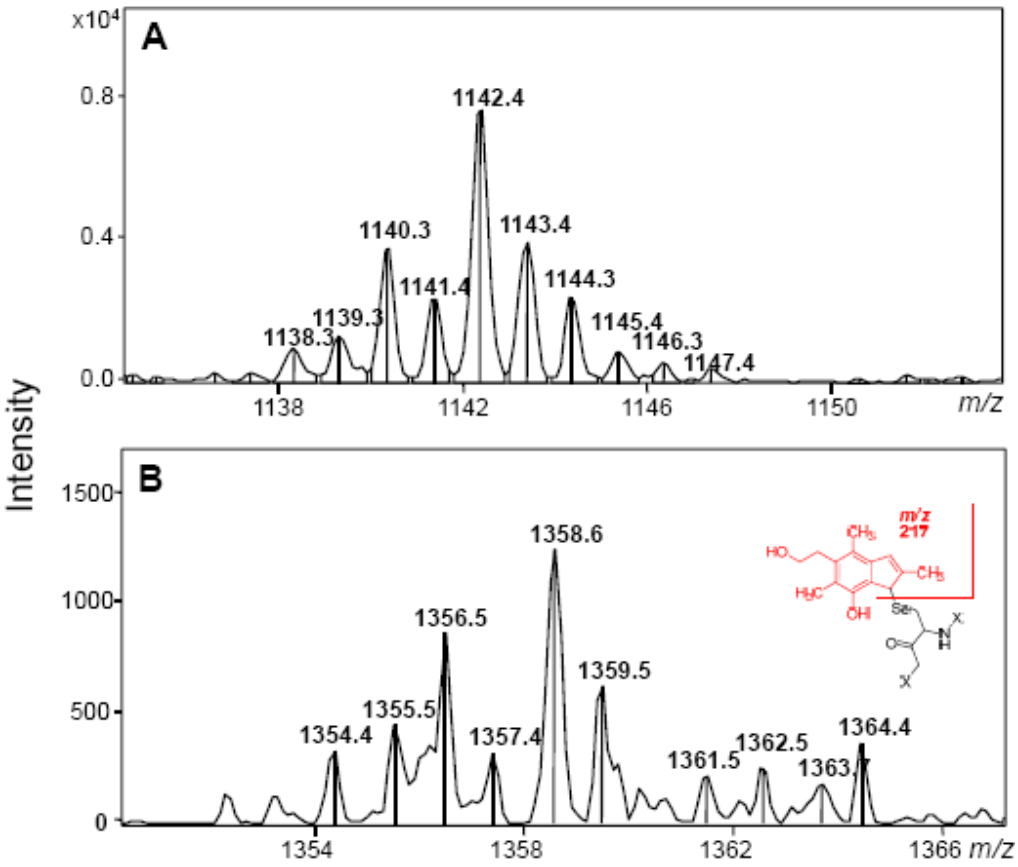

Figure 7. Inhibition of TrxR in HeLa cells by illudin S and AFs. HeLa cells were exposed to individual compound (illudin S: 0.04, 0.20, 1.00 μM; AF 0.2, 1.0, 4.0 μM; HMAF: 0.2, 1.0, 4.0 μM) for 12 h and then cellular TrxR activity was measured. Asterisks represent a significant difference relative to controls: * $p < 0.05$, ** $p < 0.01$.

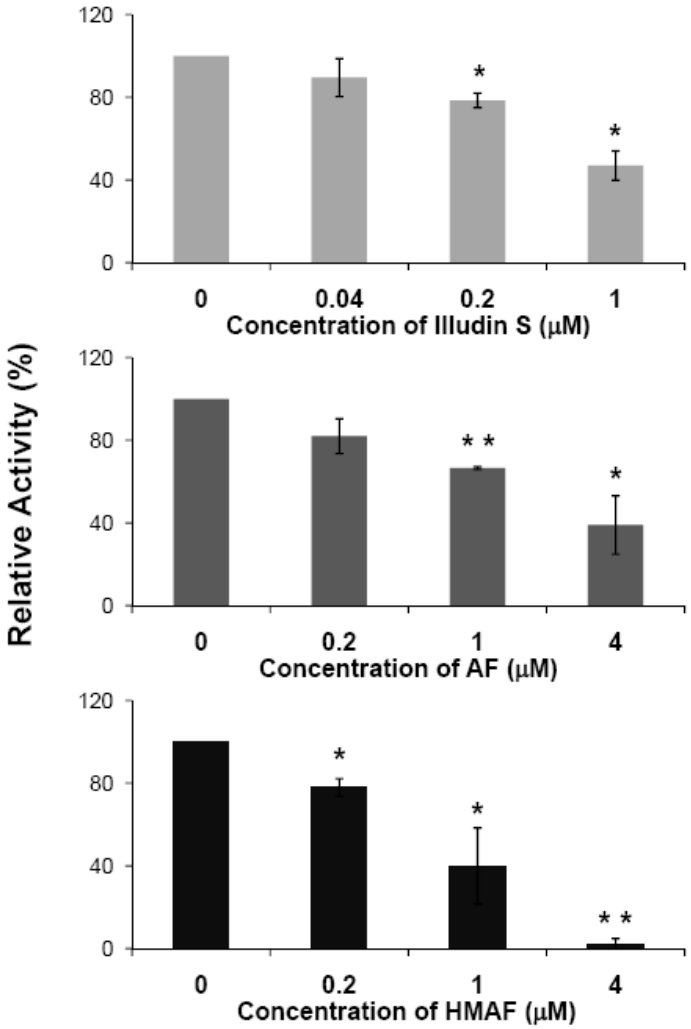

Figure 8. Induction of cellular TrxR by selenite (Na_2SeO_4) and differential sensitivity of HeLa cells towards illudin S and AFs. HeLa cells were cultured in medium with or without addition of sodium selenite (1 μM) for three continuous days. The cellular TrxR protein level (A) and activity (B) were determined. HeLa cells were seeded on 96-well plates (1000 cells/well) and cultured in medium with or without addition of sodium selenite (1 μM) for three continuous days and then changed with medium containing test compounds (illudin S, 0.2, 0.5, 1, 2 μM; AFs, 10, 20, 50, 100 μM) for 12 h. Cytotoxicity was measured with MTS assay (Promega, WI). Asterisks represent a significant difference between cytotoxicities resulting from no selenite and 1 μM selenite medium: * $p < 0.05$, ** $p < 0.01$.

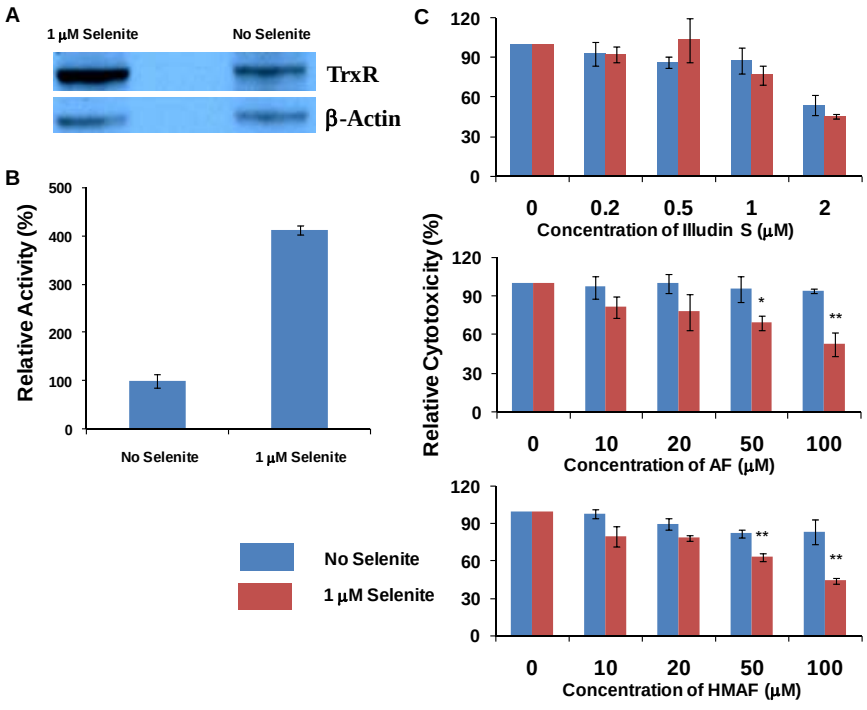

Figure 9. LC/MS spectra derived from AFs treated Gpx. Gpx (1.6 nmol) was allowed to react with AFs (1.25 mM) in TE buffer. Gpx samples were then concentrated and unbound compound removed before LC/MS analysis.

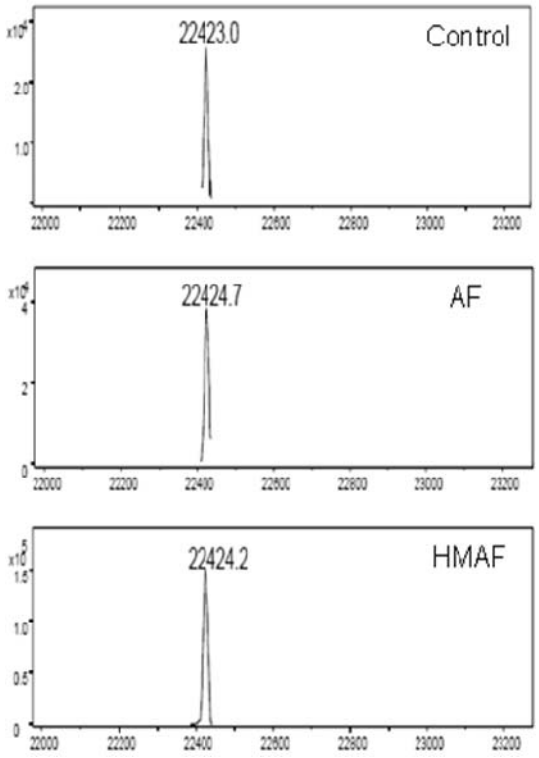

Figure 10. Induction of cell TrxR by selenite (1 μM) and combination of selenite (1 μM) and different concentration of sulforaphane.

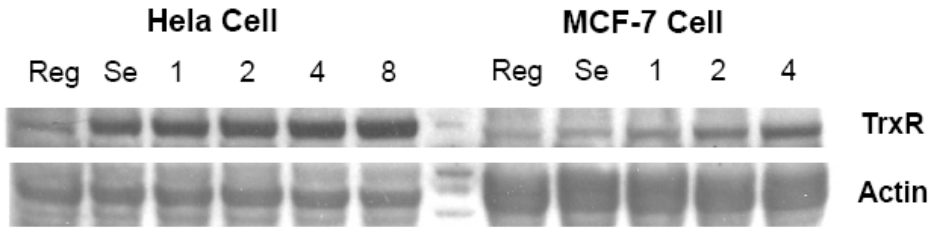

Chapter Seven: Summary and outlook

1. Ins and InsPs

Ins and InsPs have critical functions in biological systems and are of interest in a variety of areas including pharmaceutical and nutritional science, either as a single compound or as part of complex networks. Although Ins is a relatively simple molecule, its stereochemical complexity and distribution of phosphates results in a total of 63 isomers. The structural diversity, together with the lack of a chromophore makes the analysis of these compounds difficult. The rapid turnover of InsPs in biological events makes it difficult to address the role of individual InsP. Therefore, this complex situation has been of particular interest to analytical chemists in the past two decades, and many analytical methods have been developed for these compounds, including separation with various chromatographic techniques and electrophoresis, and photospectrometry detection following colorimetric derivation, radioactivity counting, P NMR, and mass spectrometry. We developed a sensitive and selective anion exchange HPLC/MS/MS method for the simultaneous or individual analysis of the absolute and relative levels of Ins and InsPs ($InsP_1$ to $InsP_6$). The limit of detection is in the picomolar range for all analytes and this method has been applied to analyze Ins and InsPs in food samples and cancer cells. This analytical approach fills a need for an on-line HPLC method and should be amenable to high throughput analysis. One limitation of this approach is that different isomers of inositol phosphates are not chromatographically resolved. Future development and optimization of anion exchange chromatography systems may have the potential to yield an advanced system in which isomeric distributions may be evaluated. The availability of this analytical approach has potential to expand our knowledge of exogenous and endogenous levels of inositol and inositol phosphates, which is important for understanding their respective roles in signal transduction and other physiological processes, and for understanding relative benefits of dietary sources of inositol phosphates.

The metabolism of InsPs is rapid and catalyzed by a network of reactions catalyzed by kinases and phosphates. The rapid turnover of InsPs makes it difficult to address the role of individual chemical species in biological events. Therefore, enzyme-stable analogues with similar biological activities are of importance as probes to investigate

Ins/InsP functions. We synthesized phosphorothioate analogs of the inositol phosphates Ins(1,4,5)P_3 and Ins(4,5)P_2. The InsP_3 analog is stable to phosphatase-mediated hydrolysis and lacks hydroxyl group kinase-mediated phosphorylation sites, but a tendency of the vicinal phosphorothioates to form disulfide bonds was observed, indicating limitations in its chemical stability. An additional limitation of the developed analogues is that they involve a lengthy synthesis. The InsP_3 analog 1D-2,3-dideoxy-*myo*-inositol 1,4,5-trisphosphorothioate specifically binds the Ins(1,4,5)P_3 receptor with a K_d of 810 nM, which compares favorably with previously reported Ins(1,4,5)P_3 phosphorothioate analogs.[233] Future studies can be aimed at characterizing cellular responses to this analog and using it to probe the role of Ins(1,4,5)P_3 in cancer chemoprevention and biochemical processes.

2. Illudin S and AFs

Compared to the natural product illudin S, acylfulvene derivatives have improved anticancer selectivity. The α,β-unsaturated ketone and a cyclopropane ring, together with the observations that they bind DNA and cause DNA synthesis inhibition, make these compounds regarded as alkylating agents. The formation of acylfulvene-DNA adducts and their susceptibility to repair and ability to inhibit DNA synthesis have been studied. However, a unifying mechanism for the improved cytotoxic selectivities of AFs over illudins is still unclear. It has been proposed that reactions of illudins with thiol-containing macromolecules contribute to the high general cytotoxicity of illudins S. To test the role of this pathway, we evaluated the reactivity of these compounds towards several critical redox-regulating enzymes that all have cysteine residues at the catalytic active site.

The study with glutathione reductase as an enzyme target indicates that each compound exhibits some degree of interaction with the enzyme reflected by the changes in GR intrinsic fluorescence, however, illudin S does not inhibit GR, AF is a reversible inhibitor, and HMAF is an irreversible inhibitor that covalently modifies the protein at active site cysteine residues. Further mechanistic studies with respect to the proximity of binding to the active site occupied by its natural substrate GSSG and reducing status of GR by AFs suggest AFs undergo a different mechanism of inhibition, in which HMAF

mainly reacts with the active site and AF interacts with GR on sites other than the active site.

We evaluated inhibition potencies of illudins S, AF, and HMAF toward the Trx system. The inhibitory results for TrxR and Trx are consistent with results obtained for GR in that inhibition potencies of illudin S and AFs rank similarly for GR or TrxR, i.e., HMAF>AF>illudin S, suggesting that polarity (illudin S>HMAF>AF) may play a role in the binding of these compounds to the enzymes. All three compounds non-covalently bind Trx, detectable by significant quenching of Trx intrinsic fluorescence upon treatment with the test compounds. However, both AFs irreversibly inhibit TrxR and Trx by alkylating the active site cysteine residues. In comparison, we investigated the reactivity of these compounds with another Sec-containing enzyme glutathione peroxidase, but no evidence for covalent interactions between Gpx and AFs was observed. Cellular TrxR activity was diminished in AFs-treated cells, and cells had increased sensitivity towards AFs when TrxR was induced by selenium. Trx levels and its nuclear translocation were influenced after treatment with AFs such that the nuclear Trx accumulated upon AFs treatment. Taken together these observations suggest that the Trx system is the cellular target of AFs.

In this body of work, we selected several redox-regulating thiol-containing enzymes to investigate the differential activity of illudin S and acylfulvenes. Although these enzymes are critical in cellular function and become abnormal in cancer cells, they still cannot represent the global interactions of these compounds with thiol-containing cellular proteins. Therefore, further investigation of the influence on the thiol-containing proteins by illudin S and AFs on a more global scale may be helpful in determining the role of reacting with thiols of cellular macroproteins in AFs improved anticancer selectivity.[255, 271] Although the result is indicative of modifications on active site cysteine residues by AFs based on the mass spectrometry analysis of GR and Trx adducts, it does not provide enough information to confirm the chemical structure of the adducts. Further investigation with other techniques such as crystallographic analysis of GR-HMAF, Trx-AF and Trx-HMAF adducts, may provide more useful information for future

optimization on these analogs to yield more specific inhibitors towards individual enzymes.

The data described here are valuable in further understanding the role of modulating cellular redox enzymes in the anticancer effects by alkylating agents. Overall, the reactivities of illudin S and AF analogues toward GR are opposite to what might be expected on the basis of reactivity towards thiol-containing molecules, suggesting this differential reactivity may be involved in AFs' increased selectivities, i.e. as a target for AFs in sensitive cells, rather than an indiscriminant target of illudins S in all cells. These differential activities emphasize the importance of balancing chemical reactivity and molecular recognition in dictating biochemical responses.

3. Other preliminary observations

3.1 Weak inhibition of hamster-NAT2 by AFs

Arylamine *N*-acetyltransferases (NAT, EC 2.3.1.5) catalyze the AcCoA-dependent acetylation of various aromatic amines, hydrazines, and hydrazides, and also catalyze the formation of highly electrophilic agents by acetylating the hydroxyl group of arylhydroxylamines and arylhydroxamic acids.[366] The DNA damage caused by the NAT-generated electrophiles upon exposure to arylamines is thought to be the major mechanism for their mutagenic and carcinogenic effects.[367] During NAT catalysis, a conserved cysteine residue (Cys 68) plays a critical role by accepting an acetyl group from AcCoA, which is then transferred to the substrate.[368] We studied the inhibitory effects of illudin S and AFs on hamster NAT2; the results indicate that AFs, but not illudins S, inhibit NAT2 (Figure 1A.). Mass spectrometry analysis of AFs-treated NAT2 suggests that AF and HMAF covalently modify NAT2 and that the product peak results from the same mass change (*m/z* 205) (Figure 1B.). The corresponding inhibition potencies are in the high micromolar range and much weaker compared to other NAT inhibitors such as 4-nitrosobiphenyl with IC_{50}s in the nanomolar range.[369] The conserved cysteine residue is very susceptible to attack by electrophilic agents, which is usually associated with the inactivation of the transferase activity.[370] However, AFs are not potent NAT inhibitors even though they can covalently modify the enzyme. Further studies are required to determine if the modification is on the active site cysteine or not,

which will be helpful to explain the low inhibition potency. If the modification does occur at the active site, the accessibility of this conserved cysteine may be responsible for the weak inhibition by AFs. In addition, the mass change (*m/z* 205) does not correspond to any previously characterized adducts formed between thiols with AFs,[142] so further studies are required to identify the chemical transformation that gives rise to this adduct.

3.2 AOR-mediated enhancement of TrxR and GR activity

NADPH-dependent alkenal/one oxidoreductase (AOR) is a reductive enzyme that appears to contribute at least in part to bioactivating illudin S and AFs to a more potent alkylating agent, which have been shown to alkylate cellular DNA. AOR catalyzes the reduction of the double bond of the α,β-unsaturated ketone to generate an extremely unstable electrophilic cytohexadiene intermediate, which is then attacked by DNA nucleophiles at the cyclopropyl group, leading to adduct formation. Overexpressed cellular AOR was observed to increase cell sensitivity towards AFs. We hypothesized that the presence of AOR might therefore potentiate the potency of AFs as inhibitors of TrxR and GR. To our surprise, the presence of AOR not only abolishes the inhibition of GR by AFs, but also activates GR activity regardless of the presence of AFs (Figure 2). The same observation was made in the case of the TrxR-HMAF interaction (data not shown), and TrxR activity can be activated about three fold by AOR in a dose-dependent manner (Figure 3). These observations suggest there may be protein-protein interactions between AOR and TrxR or GR. Due to the observed activating effects on GR and TrxR by AOR, we could not obtain results regarding the influences of bioactivation of AFs on the their inhibition potency. To further probe the hypothesis that the activated intermediates of AFs may be more potent inhibitors, a chemically activated version of AFs would be a necessary model to obviate the copresence of AOR and GR or TrxR.

Figure 1. Inhibition of NAT2 by illudin S and AFs. A, dose-dependent inhibition on AcCoA transferase activity of Hamster NAT2 by illudin S and AFs. B, the mass spectra of hamster NAT2 treated with AFs. The NAT2 assay was carried out with PNPA as the acetyl donor and PABA as the acetyl acceptor. NAT2 (0.5 μg/mL, 14.6 nM) was incubated with various concentration of compounds in MOPS buffer (100 mM, pH 7.0, 150 mM NaCl, 0.1 mM DTT) in a final volume of 200 μL at 25 °C for 2 h. Then MOPS buffer (300 mL) and PABA (10 mL, 100 mM) were added at the end of incubation. The reaction was initiated by addition of PNPA (5 mL, 50 mM, prepared in DMSO) The rate of the reaction was determined by monitoring the linear increase in absorbance at 400 nm due to the formation of *p*-nitrophenol.[371] NAT2 (5 nmol) was allowed to react with AFs (1 mM) in 0.5 mL MOPS buffer at 25 °C for 2 h. Then micro bio-spin P6 column (NMWL 6000) was used to remove unbound compound. The resulting solution was dried on the Speedvac concentrator. NAT2 (10 μg in 8 μL TE buffer) was analyzed by LC/MS using method described in the general consideration of Chapter 4. Both native and modified NAT2 proteins eluted as a single peak with retention time 14 min.

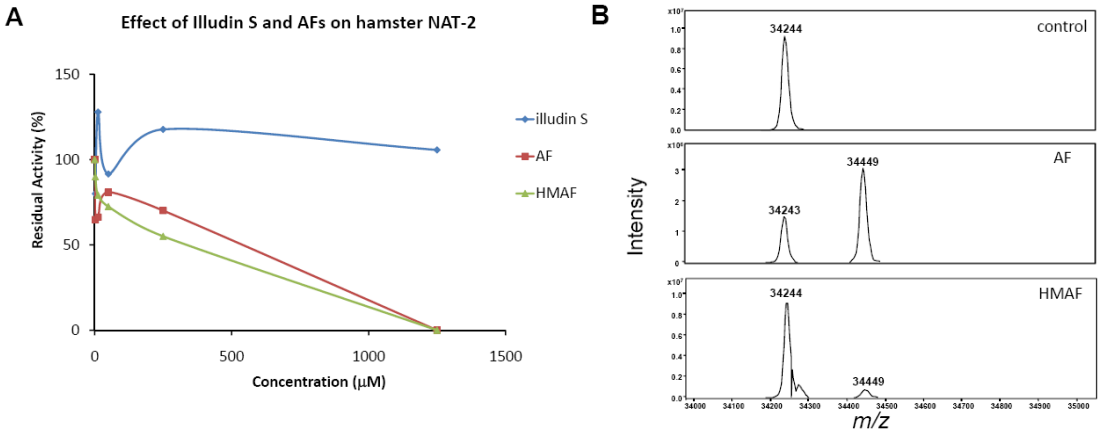

Figure 2. Activation of GR activity by AOR in the presence of AFs. GR assays were performed by combining NADPH (150 μM) and GR (5 nM) in TE buffer, total volume 100 μL in disposable acrylic cuvettes at 25 °C. Compounds (prepared in DMSO) were combined with AOR (10 μg/ml) and NADPH (100 μM), total volume 100 μL, and incubated at 25 °C for 10 min. These two solutions were combined and further allowed to react for 2 h at 37. °C. GSSG (360 μL, 350 μM) was then added and the decrease in absorbance at A_{340} was monitored over 3 min.

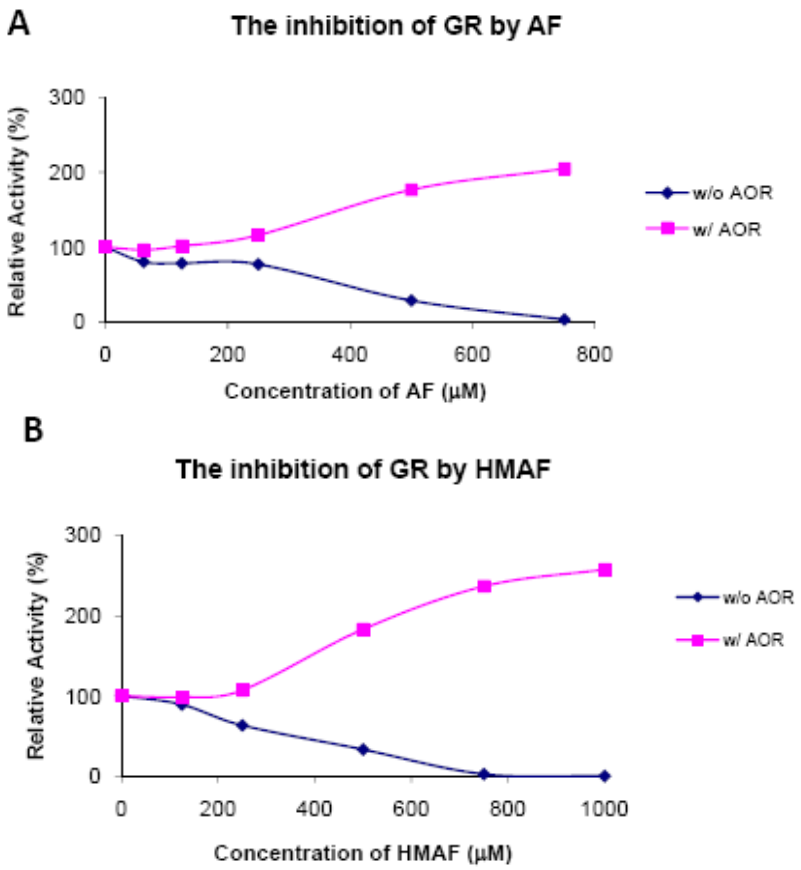

Figure 3. Activation of TrxR DTNB-reductase activity by AOR. A, dose-dpendent activation of TrxR by AOR. B, activated TrxR activity by 15 μg/mL AOR. Each point is the average of two runs and error bars represent the range in measurements. TrxR was first reduced by incubation with excess NADPH (100 μM) in a total volume of 0.1 mL at 25 °C for 10 min. Compounds (prepared in DMSO) were combined with AOR and NADPH (100 μM), total volume 100 μL, and incubated at 25 °C for 10 min. These two solutions were combined and further allowed to react for 2 h at 37. °C. The same amounts of DMSO were added to the control experiments. The enzyme activities were measured by DTNB reducing assay in which at the end of incubation, 0.4 mL of assay solution (2 mM DTNB and 200 μM NADPH in TE buffer) was added and the absorbance at 420 nm was monitored for 3 min.

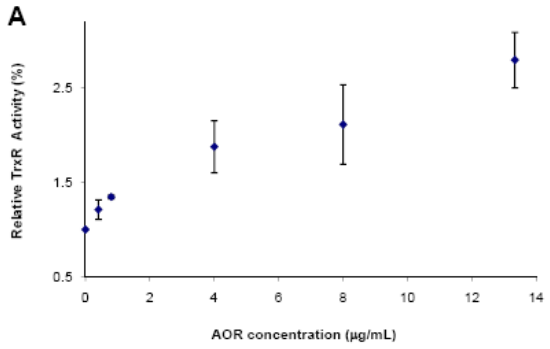

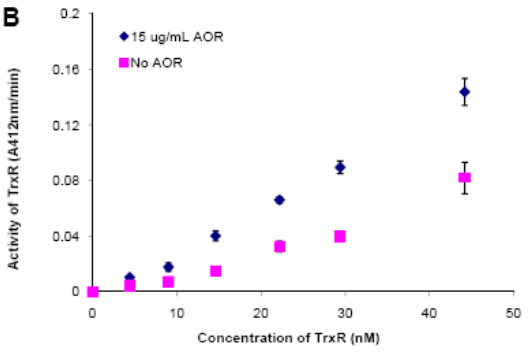

References

1. Stat bite: Changes in the U.S. death rate by cause, 1950 and 2002, *J. Natl. Cancer Inst.* **2005**, *97*, 1244.
2. Parkin, D. M. Global cancer statistics in the year 2000, *Lancet Oncol.* **2001**, *2*, 533-543.
3. ARMITAGE, P.; DOLL, R. The age distribution of cancer and a multi-stage theory of carcinogenesis, *Br. J. Cancer* **1954**, *8*, 1-12.
4. Hakama, M. Epidemiologic evidence for multi-stage theory of carcinogenesis, *Int. J. Cancer* **1971**, *7*, 557-564.
5. Armitage, P.; Doll, R. The age distribution of cancer and a multi-stage theory of carcinogenesis, *Br. J. Cancer* **2004**, *91*, 1983-1989.
6. Bean, K. B. Colorectal cancer: preventable, treatable, and beatable! *Gastroenterol. Nurs.* **2005**, *28*, 1-2.
7. Lam, S.; McWilliams, A.; LeRiche, J.; MacAulay, C.; Wattenberg, L.; Szabo, E. A phase I study of myo-inositol for lung cancer chemoprevention, *Cancer Epidemiol. Biomarkers Prev.* **2006**, *15*, 1526-1531.
8. Luo, H.; Tang, L.; Tang, M.; Billam, M.; Huang, T.; Yu, J.; Wei, Z.; Liang, Y.; Wang, K.; Zhang, Z. Q.; Zhang, L.; Wang, J. S. Phase IIa chemoprevention trial of green tea polyphenols in high-risk individuals of liver cancer: modulation of urinary excretion of green tea polyphenols and 8-hydroxydeoxyguanosine, *Carcinogenesis* **2006**, *27*, 262-268.
9. Cheng, A. L.; Hsu, C. H.; Lin, J. K.; Hsu, M. M.; Ho, Y. F.; Shen, T. S.; Ko, J. Y.; Lin, J. T.; Lin, B. R.; Ming-Shiang, W.; Yu, H. S.; Jee, S. H.; Chen, G. S.; Chen, T. M.; Chen, C. A.; Lai, M. K.; Pu, Y. S.; Pan, M. H.; Wang, Y. J.; Tsai, C. C.; Hsieh, C. Y. Phase I clinical trial of curcumin, a chemopreventive agent, in patients with high-risk or pre-malignant lesions, *Anticancer Res.* **2001**, *21*, 2895-2900.
10. Athar, M.; Back, J. H.; Tang, X.; Kim, K. H.; Kopelovich, L.; Bickers, D. R.; Kim, A. L. Resveratrol: a review of preclinical studies for human cancer prevention, *Toxicol. Appl. Pharmacol.* **2007**, *224*, 274-283.
11. Perabo, F. G.; Von Low, E. C.; Ellinger, J.; von Rucker, A.; Muller, S. C.; Bastian, P. J. Soy isoflavone genistein in prevention and treatment of prostate cancer, *Prostate Cancer. Prostatic Dis.* **2008**, *11*, 6-12.
12. Bunker, C. H.; McDonald, A. C.; Evans, R. W.; de la Rosa, N.; Boumosleh, J. M.; Patrick, A. L. A randomized trial of lycopene supplementation in Tobago men with high prostate cancer risk, *Nutr. Cancer* **2007**, *57*, 130-137.
13. Surh, Y. J.; Kundu, J. K.; Na, H. K.; Lee, J. S. Redox-sensitive transcription factors as prime targets for chemoprevention with anti-inflammatory and antioxidative phytochemicals, *J. Nutr.* **2005**, *135*, 2993S-3001S.
14. Zhang, Y.; Talalay, P. Mechanism of differential potencies of isothiocyanates as inducers of anticarcinogenic Phase 2 enzymes, *Cancer Res.* **1998**, *58*, 4632-4639.
15. Hou, D. X.; Fukuda, M.; Fujii, M.; Fuke, Y. Induction of NADPH:quinone oxidoreductase in murine hepatoma cells by methylsulfinyl isothiocyanates: methyl chain length-activity study, *Int. J. Mol. Med.* **2000**, *6*, 441-444.

16. Sellam, A.; Poupard, P.; Simoneau, P. Molecular cloning of AbGst1 encoding a glutathione transferase differentially expressed during exposure of Alternaria brassicicola to isothiocyanates, *FEMS Microbiol. Lett.* **2006**, *258*, 241-249.
17. Sun, C.; Liu, X.; Chen, Y.; Liu, F. Anticancer effect of curcumin on human B cell non-Hodgkin's lymphoma, *J. Huazhong Univ. Sci. Technolog Med. Sci.* **2005**, *25*, 404-407.
18. Sun, C. Y.; Liu, X. Y.; Chen, Y.; Liu, F.; Wang, Y. Experimental study on anticancer effect of curcumin on Raji cells in vitro, *Zhongguo Zhong Xi Yi Jie He Za Zhi* **2004**, *24*, 1003-1006.
19. Aggarwal, B. B.; Kumar, A.; Bharti, A. C. Anticancer potential of curcumin: preclinical and clinical studies, *Anticancer Res.* **2003**, *23*, 363-398.
20. Dhillon, N.; Aggarwal, B. B.; Newman, R. A.; Wolff, R. A.; Kunnumakkara, A. B.; Abbruzzese, J. L.; Ng, C. S.; Badmaev, V.; Kurzrock, R. Phase II trial of curcumin in patients with advanced pancreatic cancer, *Clin. Cancer Res.* **2008**, *14*, 4491-4499.
21. Vucenik, I.; Kalebic, T.; Tantivejkul, K.; Shamsuddin, A. M. Novel anticancer function of inositol hexaphosphate: inhibition of human rhabdomyosarcoma in vitro and in vivo, *Anticancer Res.* **1998**, *18*, 1377-1384.
22. McMillan, B.; Riggs, D. R.; Jackson, B. J.; Cunningham, C.; McFadden, D. W. Dietary influence on pancreatic cancer growth by catechin and inositol hexaphosphate, *J. Surg. Res.* **2007**, *141*, 115-119.
23. Weglarz, L.; Parfiniewicz, B.; Orchel, A.; Dzierzewicz, Z. Anti-proliferative effects of inositol hexaphosphate and verapamil on human colon cancer Caco-2 and HT-29 cells, *Acta Pol. Pharm.* **2006**, *63*, 443-445.
24. Farnsworth, N. R.; Akerele, O.; Bingel, A. S.; Soejarto, D. D.; Guo, Z. Medicinal plants in therapy, *Bull. World Health Organ.* **1985**, *63*, 965-981.
25. Newman, D. J.; Cragg, G. M. Natural products as sources of new drugs over the last 25 years, *J. Nat. Prod.* **2007**, *70*, 461-477.
26. Vater, J.; Gao, X.; Hitzeroth, G.; Wilde, C.; Franke, P. "Whole cell"--matrix-assisted laser desorption ionization-time of flight-mass spectrometry, an emerging technique for efficient screening of biocombinatorial libraries of natural compounds-present state of research, *Comb. Chem. High Throughput Screen.* **2003**, *6*, 557-567.
27. Tang, Z. M.; Wang, Z. Y.; Kang, J. W. Screening of acetylcholinesterase inhibitors in natural extracts by CE with electrophoretically mediated microanalysis technique, *Electrophoresis* **2007**, *28*, 360-365.
28. Boer, A. R.; Hokke, C. H.; Deelder, A. M.; Wuhrer, M. General microarray technique for immobilization and screening of natural glycans, *Anal. Chem.* **2007**, *79*, 8107-8113.
29. Yu, L. H.; Li, Y. J.; Sun, L.; Shang, J.; Xu, J. G. Application of fingerprint of active part on extraction techniques for Vernonia anthelmintica, *Zhong Yao Cai* **2007**, *30*, 1589-1591.
30. Mao, C. N.; He, W.; Li, Y.; Yuan, W. R. Studies on extraction of active fraction from Rhizoma et Radix Ligustici by supercritical CO2 extraction, *Zhong Yao Cai* **2008**, *31*, 1559-1562.

31. Jiang, H.; Randlett, C.; Junga, H.; Jiang, X.; Ji, Q. C. Using supported liquid extraction together with cellobiohydrolase chiral stationary phases-based liquid chromatography with tandem mass spectrometry for enantioselective determination of acebutolol and its active metabolite diacetolol in spiked human plasma, *J. Chromatogr. B. Analyt Technol. Biomed. Life. Sci.* **2009***, 877*, 173-180.
32. Hirose, T.; Sunazuka, T.; Sugawara, A.; Endo, A.; Iguchi, K.; Yamamoto, T.; Ui, H.; Shiomi, K.; Watanabe, T.; Sharpless, K. B.; Omura, S. Chitinase inhibitors: extraction of the active framework from natural argifin and use of in situ click chemistry, *J. Antibiot. (Tokyo)* **2009***, 62*, 277-282.
33. Zhao, C.; Furukawa, S.; Ohki, Y. A novel collagenase-assisted extraction of active pharmaceutical ingredients from gelatin products for quantitative analysis by high performance liquid chromatography, *J. Chromatogr. A* **2009***, 1216*, 4524-4528.
34. Wolfender, J. L.; Ndjoko, K.; Hostettmann, K. Liquid chromatography with ultraviolet absorbance-mass spectrometric detection and with nuclear magnetic resonance spectroscopy: a powerful combination for the on-line structural investigation of plant metabolites, *J. Chromatogr. A* **2003***, 1000*, 437-455.
35. Qu, J.; Wang, Y. H.; Li, J. B.; Yu, S. S.; Li, Y.; Liu, Y. B. Rapid structural determination of new trace cassaine-type diterpenoid amides in fractions from Erythrophleum fordii by liquid chromatography-diode-array detection/electrospray ionization tandem mass spectrometry and liquid chromatography/nuclear magnetic resonance, *Rapid Commun. Mass Spectrom.* **2007***, 21*, 2109-2119.
36. Qu, J.; Hu, Y. C.; Li, J. B.; Wang, Y. H.; Zhang, J. L.; Abliz, Z.; Yu, S. S.; Liu, Y. B. Structural characterization of constituents with molecular diversity in fractions from Lysidice brevicalyx by liquid chromatography/diode-array detection electrospray ionization tandem mass spectrometry and liquid chromatography nuclear magnetic resonance, *Rapid Commun. Mass Spectrom.* **2008***, 22*, 755-765.
37. Sugai, T.; Habano, W.; Jiao, Y. F.; Tsukahara, M.; Takeda, Y.; Otsuka, K.; Nakamura, S. Analysis of molecular alterations in left- and right-sided colorectal carcinomas reveals distinct pathways of carcinogenesis: proposal for new molecular profile of colorectal carcinomas, *J. Mol. Diagn.* **2006***, 8*, 193-201.
38. Teixeira, M. R.; Heim, S. Multiple numerical chromosome aberrations in cancer: what are their causes and what are their consequences? *Semin. Cancer Biol.* **2005***, 15*, 3-12.
39. Goel, A.; Jhurani, S.; Aggarwal, B. B. Multi-targeted therapy by curcumin: how spicy is it? *Mol. Nutr. Food Res.* **2008***, 52*, 1010-1030.
40. Liu, Y.; Veena, C. K.; Morgan, J. B.; Mohammed, K. A.; Jekabsons, M. B.; Nagle, D. G.; Zhou, Y. D. Methylalpinumisoflavone inhibits hypoxia-inducible factor-1 (HIF-1) activation by simultaneously targeting multiple pathways, *J. Biol. Chem.* **2009***, 284*, 5859-5868.
41. Rajabalian, S. Methanolic extract of Teucrium polium L. potentiates the cytotoxic and apoptotic effects of anticancer drugs of vincristine, vinblastine and doxorubicin against a panel of cancerous cell lines, *Exp. Oncol.* **2008***, 30*, 133-138.
42. Haranaka, K.; Sakurai, A.; Satomi, N.; Ono, T.; Haranaka, R. Combination therapy with traditional Chinese medicines and Streptococcus pyogenes products (OK 432)

for endogenous tumor necrosis factor therapy. A preliminary report, *Cancer Biother.* **1995***, 10*, 131-138.
43. Segota, E.; Bukowski, R. M. The promise of targeted therapy: cancer drugs become more specific, *Cleve. Clin. J. Med.* **2004***, 71*, 551-560.
44. Shears, S. B. The versatility of inositol phosphates as cellular signals, *Biochim. Biophys. Acta* **1998***, 1436*, 49-67.
45. Zhang, X.; Majerus, P. W. Phosphatidylinositol signalling reactions, *Semin. Cell Dev. Biol.* **1998***, 9*, 153-160.
46. Irvine, R. F.; Schell, M. J. Back to the Water: the Return of the Inositol Phosphates, *Nature Reviews: Molecular Cell Biology* **2001***, 2*, 327-328-338.
47. Berridge, M. J. Inositol trisphosphate and calcium signalling, *Nature* **1993***, 361*, 315-325.
48. Shears, S. B.; Yang, L.; Qian, X. Cell signaling by a physiologically reversible inositol phosphate kinase/phosphatase, *Adv. Enzyme Regul.* **2004***, 44*, 265-277.
49. Phillippy, B. Q. Inositol Phosphates in Foods, *Advances in Food and Nutrition Research* **2003***, 45*, 1-2-59.
50. Lonnerdal, B.; Sandberg, A. S.; Sandstrom, B.; Kunz, C. Inhibitory effects of phytic acid and other inositol phosphates on zinc and calcium absorption in suckling rats, *J. Nutr.* **1989***, 119*, 211-214.
51. Simpson, C. J.; Wise, A. Binding of zinc and calcium to inositol phosphates (phytate) in vitro, *Br. J. Nutr.* **1990***, 64*, 225-232.
52. Sandstrom, B.; Cederblad, A.; Stenquist, B.; Andersson, H. Effect of inositol hexaphosphate on retention of zinc and calcium from the human colon, *Eur. J. Clin. Nutr.* **1990***, 44*, 705-708.
53. Sandstrom, B.; Sandberg, A. S. Inhibitory effects of isolated inositol phosphates on zinc absorption in humans, *J. Trace Elem. Electrolytes Health Dis.* **1992***, 6*, 99-103.
54. Sandberg, A. S.; Brune, M.; Carlsson, N. G.; Hallberg, L.; Skoglund, E.; Rossander-Hulthen, L. Inositol phosphates with different numbers of phosphate groups influence iron absorption in humans, *Am. J. Clin. Nutr.* **1999***, 70*, 240-246.
55. Skoglund, E.; Lonnerdal, B.; Sandberg, A. S. Inositol phosphates influence iron uptake in Caco-2 cells, *J. Agric. Food Chem.* **1999***, 47*, 1109-1113.
56. Einat, H.; Belmaker, R. H. The effects of inositol treatment in animal models of psychiatric disorders, *J. Affect. Disord.* **2001***, 62*, 113-121.
57. Kim, H.; McGrath, B. M.; Silverstone, P. H. A review of the possible relevance of inositol and the phosphatidylinositol second messenger system (PI-cycle) to psychiatric disorders--focus on magnetic resonance spectroscopy (MRS) studies, *Hum. Psychopharmacol.* **2005***, 20*, 309-326.
58. Rizvi, I.; Riggs, D. R.; Jackson, B. J.; Ng, A.; Cunningham, C.; McFadden, D. W. Inositol hexaphosphate (IP6) inhibits cellular proliferation in melanoma, *J. Surg. Res.* **2006***, 133*, 3-6.
59. Lee, H. J.; Lee, S. A.; Choi, H. Dietary administration of inositol and/or inositol-6-phosphate prevents chemically-induced rat hepatocarcinogenesis, *Asian Pac. J. Cancer. Prev.* **2005***, 6*, 41-47.

60. Verbsky, J.; Majerus, P. W. Increased levels of inositol hexakisphosphate (InsP6) protect HEK293 cells from tumor necrosis factor (alpha)- and Fas-induced apoptosis, *J. Biol. Chem.* **2005**, *280*, 29263-29268.
61. Vucenik, I.; Shamsuddin, A. M. Cancer inhibition by inositol hexaphosphate (IP6) and inositol: from laboratory to clinic, *J. Nutr.* **2003**, *133*, 3778S-3784S.
62. Midorikawa, K.; Murata, M.; Oikawa, S.; Hiraku, Y.; Kawanishi, S. Protective effect of phytic acid on oxidative DNA damage with reference to cancer chemoprevention, *Biochem. Biophys. Res. Commun.* **2001**, *288*, 552-557.
63. Nishino, H.; Murakoshi, M.; Masuda, M.; Tokuda, H.; Satomi, Y.; Onozuka, M.; Yamaguchi, S.; Bu, P.; Tsuruta, A.; Nosaka, K.; Baba, M.; Takasuka, N. Suppression of lung and liver carcinogenesis in mice by oral administration of myo-inositol, *Anticancer Res.* **1999**, *19*, 3663-3664.
64. Wattenberg, L. W.; Estensen, R. D. Chemopreventive effects of myo-inositol and dexamethasone on benzo[a]pyrene and 4-(methylnitrosoamino)-1-(3-pyridyl)-1-butanone-induced pulmonary carcinogenesis in female A/J mice, *Cancer Res.* **1996**, *56*, 5132-5135.
65. Wattenberg, L. W.; Wiedmann, T. S.; Estensen, R. D.; Zimmerman, C. L.; Galbraith, A. R.; Steele, V. E.; Kelloff, G. J. Chemoprevention of pulmonary carcinogenesis by brief exposures to aerosolized budesonide or beclomethasone dipropionate and by the combination of aerosolized budesonide and dietary myo-inositol, *Carcinogenesis* **2000**, *21*, 179-182.
66. Vucenik, I.; Sakamoto, K.; Bansal, M.; Shamsuddin, A. M. Inhibition of rat mammary carcinogenesis by inositol hexaphosphate (phytic acid). A pilot study, *Cancer Lett.* **1993**, *75*, 95-102.
67. Vucenik, I.; Yang, G. Y.; Shamsuddin, A. M. Comparison of pure inositol hexaphosphate and high-bran diet in the prevention of DMBA-induced rat mammary carcinogenesis, *Nutr. Cancer* **1997**, *28*, 7-13.
68. Zhang, Z.; Song, Y.; Wang, X. L. Inositol hexaphosphate-induced enhancement of natural killer cell activity correlates with suppression of colon carcinogenesis in rats, *World J. Gastroenterol.* **2005**, *11*, 5044-5046.
69. Marks, G.; Aydos, R. D.; Fagundes, D. J.; Pontes, E. R.; Takita, L. C.; Amaral, E. G.; Rossini, A.; Ynouye, C. M. Modulation of transforming growth factor beta2 (TGF-beta2) by inositol hexaphosphate in colon carcinogenesis in rats, *Acta Cir. Bras.* **2006**, *21 Suppl 4*, 51-56.
70. McLaurin, J.; Franklin, T.; Chakrabartty, A.; Fraser, P. E. Phosphatidylinositol and inositol involvement in Alzheimer amyloid-beta fibril growth and arrest, *J. Mol. Biol.* **1998**, *278*, 183-194.
71. Ullah, A.; Shamsuddin, A. M. Dose-dependent inhibition of large intestinal cancer by inositol hexaphosphate in F344 rats, *Carcinogenesis* **1990**, *11*, 2219-2222.
72. Shamsuddin, A. M.; Yang, G. Y. Inositol hexaphosphate inhibits growth and induces differentiation of PC-3 human prostate cancer cells, *Carcinogenesis* **1995**, *16*, 1975-1979.

73. Yang, G. Y.; Shamsuddin, A. M. IP6-induced growth inhibition and differentiation of HT-29 human colon cancer cells: involvement of intracellular inositol phosphates, *Anticancer Res.* **1995***, 15*, 2479-2487.
74. Tantivejkul, K.; Vucenik, I.; Eiseman, J.; Shamsuddin, A. M. Inositol hexaphosphate (IP6) enhances the anti-proliferative effects of adriamycin and tamoxifen in breast cancer, *Breast Cancer Res. Treat.* **2003***, 79*, 301-312.
75. Vucenik, I.; Ramakrishna, G.; Tantivejkul, K.; Anderson, L. M.; Ramljak, D. Inositol hexaphosphate (IP6) blocks proliferation of human breast cancer cells through a PKCdelta-dependent increase in p27Kip1 and decrease in retinoblastoma protein (pRb) phosphorylation, *Breast Cancer Res. Treat.* **2005***, 91*, 35-45.
76. Somasundar, P.; Riggs, D. R.; Jackson, B. J.; Cunningham, C.; Vona-Davis, L.; McFadden, D. W. Inositol hexaphosphate (IP6): a novel treatment for pancreatic cancer, *J. Surg. Res.* **2005***, 126*, 199-203.
77. Diallo, J. S.; Betton, B.; Parent, N.; Peant, B.; Lessard, L.; Le Page, C.; Bertrand, R.; Mes-Masson, A. M.; Saad, F. Enhanced killing of androgen-independent prostate cancer cells using inositol hexakisphosphate in combination with proteasome inhibitors, *Br. J. Cancer* **2008***, 99*, 1613-1622.
78. Guido, M.; Fagundes, D. J.; Ynouye, C. M.; Pontes, E. R.; Takita, L. C.; Siufi do Amaral, E. G.; Teruya, R.; Paes, M. C.; Brasileiro, J. L.; Aydos, R. D. Apoptotic effects of inositol hexaphosphate on biomarker Itpr3 in induced colon rat carcinogenesis, *Acta Cir. Bras.* **2008***, 23*, 157-164.
79. Shamsuddin, A. M.; Vucenik, I.; Cole, K. E. IP6: a novel anti-cancer agent, *Life Sci.* **1997***, 61*, 343-354.
80. Shamsuddin, A. M. Metabolism and cellular functions of IP6: a review, *Anticancer Res.* **1999***, 19*, 3733-3736.
81. Yodoi, J.; Nakamura, H.; Masutani, H. Redox regulation of stress signals: possible roles of dendritic stellate TRX producer cells (DST cell types), *Biol. Chem.* **2002***, 383*, 585-590.
82. Kwon, Y. W.; Masutani, H.; Nakamura, H.; Ishii, Y.; Yodoi, J. Redox regulation of cell growth and cell death, *Biol. Chem.* **2003***, 384*, 991-996.
83. Trachootham, D.; Lu, W.; Ogasawara, M. A.; Nilsa, R. D.; Huang, P. Redox regulation of cell survival, *Antioxid. Redox Signal.* **2008***, 10*, 1343-1374.
84. Lander, H. M.; Milbank, A. J.; Tauras, J. M.; Hajjar, D. P.; Hempstead, B. L.; Schwartz, G. D.; Kraemer, R. T.; Mirza, U. A.; Chait, B. T.; Burk, S. C.; Quilliam, L. A. Redox regulation of cell signalling, *Nature* **1996***, 381*, 380-381.
85. Martinez-Ruiz, A.; Lamas, S. Signalling by NO-induced protein S-nitrosylation and S-glutathionylation: convergences and divergences, *Cardiovasc. Res.* **2007***, 75*, 220-228.
86. Fomenko, D. E.; Marino, S. M.; Gladyshev, V. N. Functional diversity of cysteine residues in proteins and unique features of catalytic redox-active cysteines in thiol oxidoreductases, *Mol. Cells* **2008***, 26*, 228-235.
87. Sun, Q. A.; Gladyshev, V. N. Redox regulation of cell signaling by thioredoxin reductases, *Methods Enzymol.* **2002***, 347*, 451-461.
88. Lu, J.; Holmgren, A. Selenoproteins, *J. Biol. Chem.* **2009***, 284*, 723-727.

89. Winterbourn, C. C.; Hampton, M. B. Thiol chemistry and specificity in redox signaling, *Free Radic. Biol. Med.* **2008**, *45*, 549-561.
90. Zhang, Z. Y.; Dixon, J. E. Active site labeling of the Yersinia protein tyrosine phosphatase: the determination of the pKa of the active site cysteine and the function of the conserved histidine 402, *Biochemistry* **1993**, *32*, 9340-9345.
91. Jez, J. M.; Noel, J. P. Mechanism of chalcone synthase. pKa of the catalytic cysteine and the role of the conserved histidine in a plant polyketide synthase, *J. Biol. Chem.* **2000**, *275*, 39640-39646.
92. Guengerich, F. P.; Fang, Q.; Liu, L.; Hachey, D. L.; Pegg, A. E. O6-alkylguanine-DNA alkyltransferase: low pKa and high reactivity of cysteine 145, *Biochemistry* **2003**, *42*, 10965-10970.
93. Gallogly, M. M.; Starke, D. W.; Mieyal, J. J. Mechanistic and Kinetic Details of Thiol-Disulfide Exchange by Glutaredoxins and Potential Mechanisms of Regulation, *Antioxid. Redox Signal.* **2009**.
94. Aracena-Parks, P.; Goonasekera, S. A.; Gilman, C. P.; Dirksen, R. T.; Hidalgo, C.; Hamilton, S. L. Identification of cysteines involved in S-nitrosylation, S-glutathionylation, and oxidation to disulfides in ryanodine receptor type 1, *J. Biol. Chem.* **2006**, *281*, 40354-40368.
95. Little, C.; O'Brien, P. J. Mechanism of peroxide-inactivation of the sulphydryl enzyme glyceraldehyde-3-phosphate dehydrogenase, *Eur. J. Biochem.* **1969**, *10*, 533-538.
96. Drincovich, M. F.; Andreo, C. S. Redox regulation of maize NADP-malic enzyme by thiol-disulfide interchange: effect of reduced thioredoxin on activity, *Biochim. Biophys. Acta* **1994**, *1206*, 10-16.
97. Atmane, N.; Dairou, J.; Paul, A.; Dupret, J. M.; Rodrigues-Lima, F. Redox regulation of the human xenobiotic metabolizing enzyme arylamine N-acetyltransferase 1 (NAT1). Reversible inactivation by hydrogen peroxide, *J. Biol. Chem.* **2003**, *278*, 35086-35092.
98. Koehler, C. M.; Tienson, H. L. Redox regulation of protein folding in the mitochondrial intermembrane space, *Biochim. Biophys. Acta* **2009**, *1793*, 139-145.
99. Chen, C. Y.; Willard, D.; Rudolph, J. Redox regulation of SH2-domain-containing protein tyrosine phosphatases by two backdoor cysteines, *Biochemistry* **2009**, *48*, 1399-1409.
100. Graf, P. C.; Martinez-Yamout, M.; VanHaerents, S.; Lilie, H.; Dyson, H. J.; Jakob, U. Activation of the redox-regulated chaperone Hsp33 by domain unfolding, *J. Biol. Chem.* **2004**, *279*, 20529-20538.
101. Winter, J.; Linke, K.; Jatzek, A.; Jakob, U. Severe oxidative stress causes inactivation of DnaK and activation of the redox-regulated chaperone Hsp33, *Mol. Cell* **2005**, *17*, 381-392.
102. Choi, H. I.; Lee, S. P.; Kim, K. S.; Hwang, C. Y.; Lee, Y. R.; Chae, S. K.; Kim, Y. S.; Chae, H. Z.; Kwon, K. S. Redox-regulated cochaperone activity of the human DnaJ homolog Hdj2, *Free Radic. Biol. Med.* **2006**, *40*, 651-659.
103. Xanthoudakis, S.; Curran, T. Redox regulation of AP-1: a link between transcription factor signaling and DNA repair, *Adv. Exp. Med. Biol.* **1996**, *387*, 69-75.

104. Akamatsu, Y.; Ohno, T.; Hirota, K.; Kagoshima, H.; Yodoi, J.; Shigesada, K. Redox regulation of the DNA binding activity in transcription factor PEBP2. The roles of two conserved cysteine residues, *J. Biol. Chem.* **1997***, 272*, 14497-14500.
105. Hirota, K.; Murata, M.; Sachi, Y.; Nakamura, H.; Takeuchi, J.; Mori, K.; Yodoi, J. Distinct roles of thioredoxin in the cytoplasm and in the nucleus. A two-step mechanism of redox regulation of transcription factor NF-kappaB, *J. Biol. Chem.* **1999***, 274*, 27891-27897.
106. Kalinina, E. V.; Chernov, N. N.; Saprin, A. N. Involvement of thio-, peroxi-, and glutaredoxins in cellular redox-dependent processes, *Biochemistry (Mosc)* **2008***, 73*, 1493-1510.
107. Holmgren, A.; Johansson, C.; Berndt, C.; Lonn, M. E.; Hudemann, C.; Lillig, C. H. Thiol redox control via thioredoxin and glutaredoxin systems, *Biochem. Soc. Trans.* **2005***, 33*, 1375-1377.
108. Arner, E. S.; Holmgren, A. Physiological functions of thioredoxin and thioredoxin reductase, *Eur. J. Biochem.* **2000***, 267*, 6102-6109.
109. Fujiwara, N.; Fujii, T.; Fujii, J.; Taniguchi, N. Roles of N-terminal active cysteines and C-terminal cysteine-selenocysteine in the catalytic mechanism of mammalian thioredoxin reductase, *J. Biochem. (Tokyo)* **2001***, 129*, 803-812.
110. Witte, A. B.; Anestal, K.; Jerremalm, E.; Ehrsson, H.; Arner, E. S. Inhibition of thioredoxin reductase but not of glutathione reductase by the major classes of alkylating and platinum-containing anticancer compounds, *Free Radic. Biol. Med.* **2005***, 39*, 696-703.
111. Hansen, R. E.; Roth, D.; Winther, J. R. Quantifying the global cellular thiol-disulfide status, *Proc. Natl. Acad. Sci. U. S. A.* **2009***, 106*, 422-427.
112. Brandes, N.; Schmitt, S.; Jakob, U. Thiol-Based Redox Switches in Eukaryotic Proteins, *Antioxid. Redox Signal.* **2008**.
113. Berndt, C.; Lillig, C. H.; Holmgren, A. Thiol-based mechanisms of the thioredoxin and glutaredoxin systems: implications for diseases in the cardiovascular system, *Am. J. Physiol. Heart Circ. Physiol.* **2007***, 292*, H1227-36.
114. Nakamura, H.; Bai, J.; Nishinaka, Y.; Ueda, S.; Sasada, T.; Ohshio, G.; Imamura, M.; Takabayashi, A.; Yamaoka, Y.; Yodoi, J. Expression of thioredoxin and glutaredoxin, redox-regulating proteins, in pancreatic cancer, *Cancer Detect. Prev.* **2000***, 24*, 53-60.
115. Jaeger, T.; Flohe, L. The thiol-based redox networks of pathogens: unexploited targets in the search for new drugs, *Biofactors* **2006***, 27*, 109-120.
116. Bellinger, F. P.; Raman, A. V.; Reeves, M. A.; Berry, M. J. Regulation and function of selenoproteins in human disease, *Biochem. J.* **2009***, 422*, 11-22.
117. Berggren, M.; Gallegos, A.; Gasdaska, J. R.; Gasdaska, P. Y.; Warneke, J.; Powis, G. Thioredoxin and thioredoxin reductase gene expression in human tumors and cell lines, and the effects of serum stimulation and hypoxia, *Anticancer Res.* **1996***, 16*, 3459-3466.
118. Soini, Y.; Kahlos, K.; Napankangas, U.; Kaarteenaho-Wiik, R.; Saily, M.; Koistinen, P.; Paaakko, P.; Holmgren, A.; Kinnula, V. L. Widespread expression of

thioredoxin and thioredoxin reductase in non-small cell lung carcinoma, *Clin. Cancer Res.* **2001***, 7*, 1750-1757.
119. Kakolyris, S.; Giatromanolaki, A.; Koukourakis, M.; Powis, G.; Souglakos, J.; Sivridis, E.; Georgoulias, V.; Gatter, K. C.; Harris, A. L. Thioredoxin expression is associated with lymph node status and prognosis in early operable non-small cell lung cancer, *Clin. Cancer Res.* **2001***, 7*, 3087-3091.
120. Yoo, M. H.; Xu, X. M.; Carlson, B. A.; Gladyshev, V. N.; Hatfield, D. L. Thioredoxin reductase 1 deficiency reverses tumor phenotype and tumorigenicity of lung carcinoma cells, *J. Biol. Chem.* **2006***, 281*, 13005-13008.
121. Cassidy, P. B.; Edes, K.; Nelson, C. C.; Parsawar, K.; Fitzpatrick, F. A.; Moos, P. J. Thioredoxin reductase is required for the inactivation of tumor suppressor p53 and for apoptosis induced by endogenous electrophiles, *Carcinogenesis* **2006***, 27*, 2538-2549.
122. Sakurai, A.; Yuasa, K.; Shoji, Y.; Himeno, S.; Tsujimoto, M.; Kunimoto, M.; Imura, N.; Hara, S. Overexpression of thioredoxin reductase 1 regulates NF-kappa B activation, *J. Cell. Physiol.* **2004***, 198*, 22-30.
123. Marzano, C.; Gandin, V.; Folda, A.; Scutari, G.; Bindoli, A.; Rigobello, M. P. Inhibition of thioredoxin reductase by auranofin induces apoptosis in cisplatin-resistant human ovarian cancer cells, *Free Radic. Biol. Med.* **2007***, 42*, 872-881.
124. Lu, J.; Chew, E. H.; Holmgren, A. Targeting thioredoxin reductase is a basis for cancer therapy by arsenic trioxide, *Proc. Natl. Acad. Sci. U. S. A.* **2007***, 104*, 12288-12293.
125. Fang, J.; Lu, J.; Holmgren, A. Thioredoxin reductase is irreversibly modified by curcumin: a novel molecular mechanism for its anticancer activity, *J. Biol. Chem.* **2005***, 280*, 25284-25290.
126. Lu, J.; Papp, L. V.; Fang, J.; Rodriguez-Nieto, S.; Zhivotovsky, B.; Holmgren, A. Inhibition of Mammalian thioredoxin reductase by some flavonoids: implications for myricetin and quercetin anticancer activity, *Cancer Res.* **2006***, 66*, 4410-4418.
127. Deharo, E.; Barkan, D.; Krugliak, M.; Golenser, J.; Ginsburg, H. Potentiation of the antimalarial action of chloroquine in rodent malaria by drugs known to reduce cellular glutathione levels, *Biochem. Pharmacol.* **2003***, 66*, 809-817.
128. Vanhoefer, U.; Yin, M. B.; Harstrick, A.; Seeber, S.; Rustum, Y. M. Carbamoylation of glutathione reductase by N,N-bis(2-chloroethyl)-N- nitrosourea associated with inhibition of multidrug resistance protein (MRP) function, *Biochem. Pharmacol.* **1997***, 53*, 801-809.
129. Bauer, H.; Fritz-Wolf, K.; Winzer, A.; Kuhner, S.; Little, S.; Yardley, V.; Vezin, H.; Palfey, B.; Schirmer, R. H.; Davioud-Charvet, E. A fluoro analogue of the menadione derivative 6-[2'-(3'-methyl)-1',4'-naphthoquinolyl]hexanoic acid is a suicide substrate of glutathione reductase. Crystal structure of the alkylated human enzyme, *J. Am. Chem. Soc.* **2006***, 128*, 10784-10794.
130. Galmarini, C. M. Drug evaluation: the thioredoxin inhibitor PX-12 in the treatment of cancer, *Curr. Opin. Investig Drugs* **2006***, 7*, 1108-1115.

131. Mori, H.; Sugie, S.; Hirono, I.; Yamada, K.; Niwa, H.; Ojika, M. Genotoxicity of ptaquiloside, a bracken carcinogen, in the hepatocyte primary culture/DNA-repair test, *Mutat. Res.* **1985***, 143*, 75-78.
132. Potter, D. M.; Baird, M. S. Carcinogenic effects of ptaquiloside in bracken fern and related compounds, *Br. J. Cancer* **2000***, 83*, 914-920.
133. Freitas, R. N.; O'Connor, P. J.; Prakash, A. S.; Shahin, M.; Povey, A. C. Bracken (Pteridium aquilinum)-induced DNA adducts in mouse tissues are different from the adduct induced by the activated form of the Bracken carcinogen ptaquiloside, *Biochem. Biophys. Res. Commun.* **2001***, 281*, 589-594.
134. Poindessous, V.; Koeppel, F.; Raymond, E.; Comisso, M.; Waters, S. J.; Larsen, A. K. Marked activity of irofulven toward human carcinoma cells: comparison with cisplatin and ecteinascidin, *Clin. Cancer Res.* **2003***, 9*, 2817-2825.
135. Kelner, M. J.; McMorris, T. C.; Estes, L.; Starr, R. J.; Rutherford, M.; Montoya, M.; Samson, K. M.; Taetle, R. Efficacy of Acylfulvene Illudin analogues against a metastatic lung carcinoma MV522 xenograft nonresponsive to traditional anticancer agents: retention of activity against various mdr phenotypes and unusual cytotoxicity against ERCC2 and ERCC3 DNA helicase-deficient cells, *Cancer Res.* **1995***, 55*, 4936-4940.
136. Hidalgo, M.; Izbicka, E.; Eckhardt, S. G.; MacDonald, J. R.; Cerna, C.; Gomez, L.; Rowinsky, E. K.; Weitman, S. D.; Von Hoff, D. D. Antitumor activity of MGI 114 (6-hydroxymethylacylfulvene, HMAF), a semisynthetic derivative of illudin S, against adult and pediatric human tumor colony-forming units, *Anticancer Drugs* **1999***, 10*, 837-844.
137. Dick, R. A.; Yu, X.; Kensler, T. W. NADPH alkenal/one oxidoreductase activity determines sensitivity of cancer cells to the chemotherapeutic alkylating agent irofulven, *Clin. Cancer Res.* **2004***, 10*, 1492-1499.
138. Tanaka, K.; Inoue, T.; Kadota, S.; Kikuchi, T. Metabolism of illudin S, a toxic principle of Lampteromyces japonicus, by rat liver. I. Isolation and identification of cyclopropane ring-cleavage metabolites, *Xenobiotica* **1990***, 20*, 671-681.
139. Gong, J.; Neels, J. F.; Yu, X.; Kensler, T. W.; Peterson, L. A.; Sturla, S. J. Investigating the role of stereochemistry in the activity of anticancer acylfulvenes: synthesis, reductase-mediated bioactivation, and cellular toxicity, *J. Med. Chem.* **2006***, 49*, 2593-2599.
140. McMorris, T. C.; Kelner, M. J.; Wang, W.; Moon, S.; Taetle, R. On the mechanism of toxicity of illudins: the role of glutathione, *Chem. Res. Toxicol.* **1990***, 3*, 574-579.
141. Tanaka, K.; Inoue, T.; Tezuka, Y.; Kikuchi, T. Michael-type addition of illudin S, a toxic substance from Lampteromyces japonicus, with cysteine and cysteine-containing peptides in vitro, *Chem. Pharm. Bull. (Tokyo)* **1996***, 44*, 273-279.
142. McMorris, T. C.; Yu, J. Reaction of antitumor hydroxymethylacylfulvene (HMAF) with thiols, *Tetrahedron* **1997***, 53*, 14579-14580-14590.
143. Kasim, A. B.; Edwards, H. M. Analysis for inositol phosphate forms in feed ingredients, *J. SCI. Food. Agric.* **1998***, 76*, 1-2-9.

144. Liu, X.; Moody, E. C.; Hecht, S. S.; Sturla, S. J. Deoxygenated phosphorothioate inositol phosphate analogs: synthesis, phosphatase stability, and binding affinity, *Bioorg. Med. Chem.* **2008**, *16*, 3419-3427.
145. McLaurin, J.; Golomb, R.; Jurewicz, A.; Antel, J. P.; Fraser, P. E. Inositol stereoisomers stabilize an oligomeric aggregate of Alzheimer amyloid beta peptide and inhibit abeta -induced toxicity, *J. Biol. Chem.* **2000**, *275*, 18495-18502.
146. Chen, Q. Determination of phytic acid and inositol pentakisphosphates in foods by high-performance ion chromatography, *J. Agric. Food Chem.* **2004**, *52*, 4604-4613.
147. Hirvonen, M. R.; Lihtamo, H.; Savolainen, K. A gas chromatographic method for the determination of inositol monophosphates in rat brain, *Neurochem. Res.* **1988**, *13*, 957-962.
148. Hamada, J. S. Scale-up potential of ion-pair high-performance liquid chromatography method to produce biologically active inositol phosphates, *J. Chromatogr. A* **2002**, *944*, 241-248.
149. Hatzack, F.; Rasmussen, S. K. High-performance thin-layer chromatography method for inositol phosphate analysis, *J. Chromatogr. B Biomed. Sci. Appl.* **1999**, *736*, 221-229.
150. Simonet, B. M.; Rios, A.; Grases, F.; Valcarcel, M. Determination of myo-inositol phosphates in food samples by flow injection-capillary zone electrophoresis, *Electrophoresis* **2003**, *24*, 2092-2098.
151. BANDURSKI, R. S.; AXELROD, B. The chromatographic identification of some biologically important phosphate esters, *J. Biol. Chem.* **1951**, *193*, 405-410.
152. Mayr, G. W. A novel metal-dye detection system permits picomolar-range h.p.l.c. analysis of inositol polyphosphates from non-radioactively labelled cell or tissue specimens, *Biochem. J.* **1988**, *254*, 585-591.
153. Hatzack, F.; Hubel, F.; Zhang, W.; Hansen, P. E.; Rasmussen, S. K. Inositol phosphates from barley low-phytate grain mutants analysed by metal-dye detection HPLC and NMR, *Biochem. J.* **2001**, *354*, 473-480.
154. Casals, I.; Villar, J. L.; Riera-Codina, M. A straightforward method for analysis of highly phosphorylated inositols in blood cells by high-performance liquid chromatography, *Anal. Biochem.* **2002**, *300*, 69-76.
155. Guse, A. H.; Goldwich, A.; Weber, K.; Mayr, G. W. Non-radioactive, isomer-specific inositol phosphate mass determinations: high-performance liquid chromatography-micro-metal-dye detection strongly improves speed and sensitivity of analyses from cells and micro-enzyme assays, *J. Chromatogr. B. Biomed. Appl.* **1995**, *672*, 189-198.
156. Taylor, G. S.; Garcia, J. G.; Dukes, R.; English, D. High-performance liquid chromatographic analysis of radiolabeled inositol phosphates, *Anal. Biochem.* **1990**, *188*, 118-122.
157. Tao, L.; Li, W. Rapid and sensitive anion-exchange high-performance liquid chromatographic determination of radiolabeled inositol phosphates and inositol trisphosphate isomers in cellular systems, *J. Chromatogr.* **1992**, *607*, 19-24.

158. Talamond, P.; Doulbeau, S.; Rochette, I.; Guyot, J. P. Anion-exchange high-performance liquid chromatography with conductivity detection for the analysis of phytic acid in food, *J. Chromatogr. A* **2000**, *871*, 7-12.
159. Smith, R. E.; MacQuarrie, R. A.; Jope, R. S. Determination of inositol phosphates and other anions in rat brain, *J. Chromatogr. Sci.* **1989**, *27*, 491-495.
160. Hsu, F. F.; Sherman, W. R. Performing high salt concentration gradient elution ion-exchange separations using thermospray mass spectrometry, *J. Chromatogr.* **1989**, *479*, 437-440.
161. Helfrich, A.; Bettmer, J. Determination of phytic acid and its degradation products by ion-pair chromatography (IPC) coupled to inductively coupled plasm-sector field-mass spectrometry (ICP-SF-MS), *J. Anal. At. Spectrom.* **2004**, 1330-1331-1334.
162. Kemme, P. A.; Lommen, A.; De Jonge, L. H.; Van der Klis, J. D.; Jongbloed, A. W.; Mroz, Z.; Beynen, A. C. Quantification of inositol phosphates using (31)P nuclear magnetic resonance spectroscopy in animal nutrition, *J. Agric. Food Chem.* **1999**, *47*, 5116-5121.
163. Kindt, E.; Shum, Y.; Badura, L.; Snyder, P. J.; Brant, A.; Fountain, S.; Szekely-Klepser, G. Development and validation of an LC/MS/MS procedure for the quantification of endogenous myo-inositol concentrations in rat brain tissue homogenates, *Anal. Chem.* **2004**, *76*, 4901-4908.
164. Perello, J.; Isern, B.; Costa-Bauza, A.; Grases, F. Determination of myo-inositol in biological samples by liquid chromatography-mass spectrometry, *J. Chromatogr. B. Analyt Technol. Biomed. Life. Sci.* **2004**, *802*, 367-370.
165. Lehrfeld, J. HPLC Separation and Quantitation of Phytic Acid and Some Inositol Phosphates in Foods: Problems and Solutions, *J. Agric. Food Chem.* **1994**, *42*, 2726-2727-2731.
166. Ellman, G. L. Tissue sulfhydryl groups. *Archives of Biochemistry and Biophysics* **1959**, *82*, 70.
167. Chen, Q. C.; Li, B. W. Separation of phytic acid and other related inositol phosphates by high-performance ion chromatography and its applications, *J. Chromatogr. A* **2003**, *1018*, 41-52.
168. Walters, J. J.; Grayson, M. A.; Gross, M. L.; Hughes, M.; Shearer, G.; Kohl, D. H.; Bashkin, J. Ion-exchange chromatography followed by ESI-MS for quantitative analysis of sugar monophosphates from glucose catabolism, *J. Am. Soc. Mass Spectrom.* **2006**, *17*, 104-107.
169. Richardson, S.; Cohen, A.; Gorton, L. High-performance anion-exchange chromatography-electrospray mass spectrometry for investigation of the substituent distribution in hydroxypropylated potato amylopectin starch, *J. Chromatogr. A* **2001**, *917*, 111-121.
170. Collins, R. N.; Onisko, B. C.; McLaughlin, M. J.; Merrington, G. Determination of metal--EDTA complexes in soil solution and plant xylem by ion chromatography-electrospray mass spectrometry, *Environ. Sci. Technol.* **2001**, *35*, 2589-2593.

171. Heathers, G. P.; Juehne, T.; Rubin, L. J.; Corr, P. B.; Evers, A. S. Anion exchange chromatographic separation of inositol phosphates and their quantification by gas chromatography, *Anal. Biochem.* **1989***, 176*, 109-116.
172. Hull, S. R.; Gray, J. S.; Montgomery, R. Autohydrolysis of phytic acid, *Anal. Biochem.* **1999***, 273*, 252-260.
173. Shamsuddin, A. M.; Vucenik, I. IP6 & inositol in cancer prevention and therapy, *Current Cancer Therapy Reviews* **2005***, 1*, 259-260-269.
174. Berridge, M. J.; Irvine, R. F. Inositol phosphates and cell signalling, *Nature* **1989***, 341*, 197-205.
175. Moreno, A.; Arust, C. Quantitative and Qualitative Characterization of ^{1}H NMR Spectra of Colon Tumors, Normal Mucosa and their Perchloric Acid Extracts: Decreased Levels of Myo-inositol in Tumours can be Detected in Intact Biopsies, *NMR in Biomedicine* **1996***, 8*, 33-34-45.
176. Gribbestad, I. S.; Fjosne, H. E.; Haugen, O. A.; Nilsen, G.; Krane, J.; Petersen, S. B.; Kvinnsland, S. In vitro proton NMR spectroscopy of extracts from human breast tumours and non-involved breast tissue, *Anticancer Res.* **1993***, 13*, 1973-1980.
177. Ito, E.; Oka, K.; Etcheberrigaray, R.; Nelson, T. J.; McPhie, D. L.; Tofel-Grehl, B.; Gibson, G. E.; Alkon, D. L. Internal Ca2+ mobilization is altered in fibroblasts from patients with Alzheimer disease, *Proc. Natl. Acad. Sci. U. S. A.* **1994***, 91*, 534-538.
178. Frederick, J. P.; Mattiske, D.; Wofford, J. A.; Megosh, L. C.; Drake, L. Y.; Chiou, S. T.; Hogan, B. L.; York, J. D. An essential role for an inositol polyphosphate multikinase, Ipk2, in mouse embryogenesis and second messenger production, *Proc. Natl. Acad. Sci. U. S. A.* **2005***, 102*, 8454-8459.
179. Diringer, H.; Koch-Kallnbach, M. E.; Friis, R. R. Quantitative determination of myoinositol, inositol 1-phosphate, inositol cyclic 1 : 2-phosphate and glycerylphosphoinositol in normal and Rous-sarcoma-virus-transformed quail fibroblasts under different growth conditions, *Eur. J. Biochem.* **1977***, 81*, 551-555.
180. Meek, J. L. Inositol bis-, tris-, and tetrakis(phosphate)s: analysis in tissues by HPLC, *Proc. Natl. Acad. Sci. U. S. A.* **1986***, 83*, 4162-4166.
181. Challiss, R. A.; Batty, I. H.; Nahorski, S. R. Mass measurements of inositol(1,4,5)trisphosphate in rat cerebral cortex slices using a radioreceptor assay: effects of neurotransmitters and depolarization, *Biochem. Biophys. Res. Commun.* **1988***, 157*, 684-691.
182. Turner, B. L.; Richardson, A. E.; Mullaney, E. J., Eds.; In *Inositol Phosphates - Linking Agriculture and the Environment;* CAB International: Wallingford, UK, 2007; , pp 304.
183. Shamsuddin, A. M.; Ullah, A.; Chakravarthy, A. K. Inositol and inositol hexaphosphate suppress cell proliferation and tumor formation in CD-1 mice, *Carcinogenesis* **1989***, 10*, 1461-1463.
184. Jyonouchi, H.; Sun, S.; Iijima, K.; Wang, M.; Hecht, S. S. Effects of anti-7,8-dihydroxy-9,10-epoxy-7,8,9,10-tetrahydrobenzo[a]pyrene on human small airway

epithelial cells and the protective effects of myo-inositol, *Carcinogenesis* **1999**, *20*, 139-145.
185. Witschi, H.; Espiritu, I.; Uyeminami, D. Chemoprevention of tobacco smoke-induced lung tumors in A/J strain mice with dietary myo-inositol and dexamethasone, *Carcinogenesis* **1999**, *20*, 1375-1378.
186. Wattenberg, L. W. Chemoprevention of pulmonary carcinogenesis by myo-inositol, *Anticancer Res.* **1999**, *19*, 3659-3661.
187. Hecht, S. S.; Kenney, P. M.; Wang, M.; Upadhyaya, P. Dose-response study of myo-inositol as an inhibitor of lung tumorigenesis induced in A/J mice by benzo, *Cancer Lett.* **2001**, *167*, 1-6.
188. Grases, F.; Simonet, B. M.; Vucenik, I.; Perello, J.; Prieto, R. M.; Shamsuddin, A. M. Effects of exogenous inositol hexakisphosphate (InsP(6)) on the levels of InsP(6) and of inositol trisphosphate (InsP(3)) in malignant cells, tissues and biological fluids, *Life Sci.* **2002**, *71*, 1535-1546.
189. Ferry, S.; Matsuda, M.; Yoshida, H.; Hirata, M. Inositol hexakisphosphate blocks tumor cell growth by activating apoptotic machinery as well as by inhibiting the Akt/NFkappaB-mediated cell survival pathway, *Carcinogenesis* **2002**, *23*, 2031-2041.
190. Shamsuddin, A. M.; Baten, A.; Lalwani, N. D. Effects of inositol hexaphosphate on growth and differentiation in K-562 erythroleukemia cell line, *Cancer Lett.* **1992**, *64*, 195-202.
191. York, J. D.; Odom, A. R.; Murphy, R.; Ives, E. B.; Wente, S. R. A phospholipase C-dependent inositol polyphosphate kinase pathway required for efficient messenger RNA export, *Science* **1999**, *285*, 96-100.
192. Ho, M. W.; Kaetzel, M. A.; Armstrong, D. L.; Shears, S. B. Regulation of a human chloride channel. a paradigm for integrating input from calcium, type ii calmodulin-dependent protein kinase, and inositol 3,4,5,6-tetrakisphosphate, *J. Biol. Chem.* **2001**, *276*, 18673-18680.
193. Yang, X.; Rudolf, M.; Carew, M. A.; Yoshida, M.; Nerreter, V.; Riley, A. M.; Chung, S. K.; Bruzik, K. S.; Potter, B. V.; Schultz, C.; Shears, S. B. Inositol 1,3,4-trisphosphate acts in vivo as a specific regulator of cellular signaling by inositol 3,4,5,6-tetrakisphosphate, *J. Biol. Chem.* **1999**, *274*, 18973-18980.
194. Miyakawa, T.; Maeda, A.; Yamazawa, T.; Hirose, K.; Kurosaki, T.; Iino, M. Encoding of Ca2+ signals by differential expression of IP3 receptor subtypes, *EMBO J.* **1999**, *18*, 1303-1308.
195. Yang, X.; Shears, S. B. Multitasking in signal transduction by a promiscuous human Ins(3,4,5,6)P(4) 1-kinase/Ins(1,3,4)P(3) 5/6-kinase, *Biochem. J.* **2000**, *351 Pt 3*, 551-555.
196. Renstrom, E.; Ivarsson, R.; Shears, S. B. Inositol 3,4,5,6-tetrakisphosphate inhibits insulin granule acidification and fusogenic potential, *J. Biol. Chem.* **2002**, *277*, 26717-26720.
197. Mattingly, R. R.; Wasilenko, W. J.; Woodring, P. J.; Garrison, J. C. Selective amplification of endothelin-stimulated inositol 1,4,5-trisphosphate and calcium

signaling by v-src transformation of rat-1 fibroblasts, *J. Biol. Chem.* **1992**, *267*, 7470-7477.
198. Iino, M.; Tsukioka, M. Feedback control of inositol trisphosphate signalling bycalcium, *Mol. Cell. Endocrinol.* **1994**, *98*, 141-146.
199. Norris, F. A.; Wilson, M. P.; Wallis, T. S.; Galyov, E. E.; Majerus, P. W. SopB, a protein required for virulence of Salmonella dublin, is an inositol phosphate phosphatase, *Proc. Natl. Acad. Sci. U. S. A.* **1998**, *95*, 14057-14059.
200. Berridge, M. J.; Irvine, R. F. Inositol trisphosphate, a novel second messenger in cellular signal transduction, *Nature* **1984**, *312*, 315-321.
201. Taylor, C. W.; Berridge, M. J.; Brown, K. D.; Cooke, A. M.; Potter, B. V. DL-myo-inositol 1,4,5-trisphosphorothioate mobilizes intracellular calcium in Swiss 3T3 cells and Xenopus oocytes, *Biochem. Biophys. Res. Commun.* **1988**, *150*, 626-632.
202. Gorczynska-Fjalling, E. The role of calcium in signal transduction processes in Sertoli cells, *Reprod. Biol.* **2004**, *4*, 219-241.
203. Foster, P. S.; Hogan, S. P.; Hansbro, P. M.; O'Brien, R.; Potter, B. V.; Ozaki, S.; Denborough, M. A. The metabolism of D-myo-inositol 1,4,5-trisphosphate and D-myo-inositol 1,3,4,5-tetrakisphosphate by porcine skeletal muscle, *Eur. J. Biochem.* **1994**, *222*, 955-964.
204. Speed, C. J.; Neylon, C. B.; Little, P. J.; Mitchell, C. A. Underexpression of the 43 kDa inositol polyphosphate 5-phosphatase is associated with spontaneous calcium oscillations and enhanced calcium responses following endothelin-1 stimulation, *J. Cell. Sci.* **1999**, *112 (Pt 5)*, 669-679.
205. Irvine, R. F.; Letcher, A. J.; Heslop, J. P.; Berridge, M. J. The inositol tris/tetrakisphosphate pathway--demonstration of Ins(1,4,5)P3 3-kinase activity in animal tissues, *Nature* **1986**, *320*, 631-634.
206. Nilsson, H.; Torndal, U. B.; Eriksson, L. C. Inositol 1,4,5-trisphosphate turnover enzymes--activities and subcellular distribution in hepatocarcinogenesis, *Carcinogenesis* **1997**, *18*, 2447-2451.
207. Primiano, T.; Egner, P. A.; Sutter, T. R.; Kelloff, G. J.; Roebuck, B. D.; Kensler, T. W. Intermittent dosing with oltipraz: relationship between chemoprevention of aflatoxin-induced tumorigenesis and induction of glutathione S-transferases, *Cancer Res.* **1995**, *55*, 4319-4324.
208. Pasquali, D.; Rossi, V.; Bellastella, G.; Bellastella, A.; Sinisi, A. A. Natural and synthetic retinoids in prostate cancer, *Curr. Pharm. Des.* **2006**, *12*, 1923-1929.
209. Gou, D. M.; Shieh, W. R.; Lu, P. J.; Chen, C. S. D-myo-inositol 1,4,5-trisphosphate analogues as useful tools in biochemical studies of intracellular calcium mobilization, *Bioorg. Med. Chem.* **1994**, *2*, 7-13.
210. Strupish, J.; Cooke, A. M.; Potter, B. V.; Gigg, R.; Nahorski, S. R. Stereospecific mobilization of intracellular Ca2+ by inositol 1,4,5-triphosphate. Comparison with inositol 1,4,5-trisphosphorothioate and inositol 1,3,4-trisphosphate, *Biochem. J.* **1988**, *253*, 901-905.
211. Nahorski, S. R.; Potter, B. V. Molecular recognition of inositol polyphosphates by intracellular receptors and metabolic enzymes, *Trends Pharmacol. Sci.* **1989**, *10*, 139-144.

212. Liu, C.; Potter, B. V. Synthesis of 3-Position-Modified Analogues of myo-Inositol 1,4,5-Trisphosphate, Tools for Investigation of the Polyphosphoinositide Pathway of Cellular Signaling, *J. Org. Chem.* **1997***, 62*, 8335-8340.
213. Willcocks, A. L.; Potter, B. V.; Cooke, A. M.; Nahorski, S. R. Myo-inositol(1,4,5)trisphosphorothioate binds to specific [3H]inositol(1,4,5)trisphosphate sites in rat cerebellum and is resistant to 5-phosphatase, *Eur. J. Pharmacol.* **1988***, 155*, 181-183.
214. Wilcox, R. A.; Nahorski, S. R.; Sawyer, D. A.; Liu, C.; Potter, B. V. The role of the 2- and 3-hydroxyl groups of 1D-myo-inositol 1,4,5-trisphosphate in the mobilisation of calcium from permeabilised human 1321N1 astrocytoma cells, *Carbohydr. Res.* **1992***, 234*, 237-246.
215. Hirata, M.; Watanabe, Y.; Yoshida, M.; Koga, T.; Ozaki, S. Roles for hydroxyl groups of D-myo-inositol 1,4,5-trisphosphate in the recognition by its receptor and metabolic enzymes, *J. Biol. Chem.* **1993***, 268*, 19260-19266.
216. Almeida, M. V.; Dubreull, D.; Cleophax, J.; Verre-Sebrie, C.; Pipelier, M.; Prestat, G.; Vass, G.; Gero, S. D. Stereoselective Synthesis of Inositol Mono, Bis and Trisphosphate Analogues From 6-Deoxy-D-lnositol Precursors. *Tetrahedron* **1999***, 55*, 7251-7252-7270.
217. Kozikowski, A. P.; Ognyanov, V. I.; Fauq, A. H.; Nahorski, S. R.; Wilcox, R. A. Synthesis of 1D-3-Deoxy-, 1D-2,3-Dideoxy-, and 1D-2,3,6-Trideoxy-*myo*-inositol 1,4,5-Trisphosphate from Quebrachitol, Their Binding Affinities, and Calcium Release Activity. *J. Am. Chem. Soc.* **1993***, 115*, 4429-4430, 4431, 4432, 4433, 4434.
218. Seewald, M. J.; Aksoy, L. A.; Powis, G.; Fauqb, A. H.; Kozikowski, A. P. Synthesis of D-3-Deoxy-myo-lnositol 1,4,5-Trisphosphate and its Effect on Ca2+ Release in NIH 3T3 Cells, *J. Am. Chem. Soc. Commun.* **1990**, 1638-1639.
219. Kozikowski, A. P.; Ognyanov, V. I.; Chen, C.; Fauq, A. H.; Safrany, S. T.; Wilcox, R. A.; Nahorski, S. R. Deoxygenated inositol 1,4,5-trisphosphate analogues and their interaction with metabolic enzymes. (1R,2R,4R)-cyclohexane-1,2,4-tris(methylenesulfonate): a potent selective 5-phosphatase inhibitor, *J. Med. Chem.* **1993***, 36*, 3035-3038.
220. Safrany, S. T.; Wojcikiewicz, R. J.; Strupish, J.; Nahorski, S. R.; Dubreuil, D.; Cleophax, J.; Gero, S. D.; Potter, B. V. Interaction of synthetic D-6-deoxy-myo-inositol 1,4,5-trisphosphate with the Ca2(+)-releasing D-myo-inositol 1,4,5-trisphosphate receptor, and the metabolic enzymes 5-phosphatase and 3-kinase, *FEBS Lett.* **1991***, 278*, 252-256.
221. Holmes, W.; Jogl, G. Crystal structure of inositol phosphate multikinase 2 and implications for substrate specificity, *J. Biol. Chem.* **2006***, 281*, 38109-38116.
222. Mills, S. J.; Potter, B. V. Synthesis of potent Ins(1,4,5)P3 5-phosphatase inhibitors by modification of myo-inositol 1,3,4,6-tetrakisphosphate, *Bioorg. Med. Chem.* **2003***, 11*, 4245-4253.
223. Taylor, C. W.; Berridge, M. J.; Cooke, A. M.; Potter, B. V. Inositol 1,4,5-trisphosphorothioate, a stable analogue of inositol trisphosphate which mobilizes intracellular calcium, *Biochem. J.* **1989***, 259*, 645-650.

224. Cooke, A. M.; Gigg, R.; Potter, B. V. L. *myo*-Inositol 1,4,5-Trisphosphorothioate: A Novel Analogue of a Biological Second Messenger. *J. Am. Chem. Soc. Commun.* **1987***, 10*, 1525-1526.
225. Walter, K.; Schutt, C. In *Alkaline phosphatase;* Bergmeyer, H. U., Ed.; in Methods of Enzymatic Analysis; Academic Press, Inc.: NY, 1974; Vol. II, pp 860-861, 862, 863, 864.
226. Challiss, R. A.; Chilvers, E. R.; Willcocks, A. L.; Nahorski, S. R. Heterogeneity of [3H]inositol 1,4,5-trisphosphate binding sites in adrenal-cortical membranes. Characterization and validation of a radioreceptor assay, *Biochem. J.* **1990***, 265*, 421-427.
227. Lampe, D.; Liu, C.; Potter, B. V. Synthesis of selective non-Ca(2+)-mobilizing inhibitors of D-myo-inositol 1,4,5-trisphosphate 5-phosphatase, *J. Med. Chem.* **1994***, 37*, 907-912.
228. Verbsky, J. W.; Chang, S. C.; Wilson, M. P.; Mochizuki, Y.; Majerus, P. W. The pathway for the production of inositol hexakisphosphate in human cells, *J. Biol. Chem.* **2005***, 280*, 1911-1920.
229. Chang, S. C.; Majerus, P. W. Inositol polyphosphate multikinase regulates inositol 1,4,5,6-tetrakisphosphate, *Biochem. Biophys. Res. Commun.* **2006***, 339*, 209-216.
230. Nalaskowski, M. M.; Deschermeier, C.; Fanick, W.; Mayr, G. W. The human homologue of yeast ArgRIII protein is an inositol phosphate multikinase with predominantly nuclear localization, *Biochem. J.* **2002***, 366*, 549-556.
231. Polokoff, M. A.; Bencen, G. H.; Vacca, J. P.; deSolms, S. J.; Young, S. D.; Huff, J. R. Metabolism of synthetic inositol trisphosphate analogs, *J. Biol. Chem.* **1988***, 263*, 11922-11927.
232. Bosanac, I.; Alattia, J. R.; Mal, T. K.; Chan, J.; Talarico, S.; Tong, F. K.; Tong, K. I.; Yoshikawa, F.; Furuichi, T.; Iwai, M.; Michikawa, T.; Mikoshiba, K.; Ikura, M. Structure of the inositol 1,4,5-trisphosphate receptor binding core in complex with its ligand, *Nature* **2002***, 420*, 696-700.
233. Safrany, S. T.; Wilcox, R. A.; Liu, C.; Dubreuil, D.; Potter, B. V.; Nahorski, S. R. Identification of partial agonists with low intrinsic activity at the inositol-1,4,5-trisphosphate receptor, *Mol. Pharmacol.* **1993***, 43*, 499-503.
234. Nerou, E. P.; Riley, A. M.; Potter, B. V.; Taylor, C. W. Selective recognition of inositol phosphates by subtypes of the inositol trisphosphate receptor, *Biochem. J.* **2001***, 355*, 59-69.
235. Hamblin, M. R.; Flora, J. S.; Potter, B. V. myo-Inositol phosphorothioates, phosphatase-resistant analogues of myo-inositol phosphates. Synthesis of DL-myo-inositol 1,4-bisphosphate and DL-myo-inositol 1,4-bisphosphorothioate, *Biochem. J.* **1987***, 246*, 771-774.
236. Xiaodan, L.; Shana J, S. Simultaneous determination of inositol and inositol phosphates level by liquid chromatography with tandem mass spectrometry, *Rapid Communications in Mass Spectrometry* **2007**.
237. Zhou, X.; Gong, Z.; Su, Y.; Lin, J.; Tang, K. Cordyceps fungi: natural products, pharmacological functions and developmental products, *J. Pharm. Pharmacol.* **2009***, 61*, 279-291.

238. Saleem, M.; Ali, M. S.; Hussain, S.; Jabbar, A.; Ashraf, M.; Lee, Y. S. Marine natural products of fungal origin, *Nat. Prod. Rep.* **2007***, 24*, 1142-1152.
239. Lam, K. S. New aspects of natural products in drug discovery, *Trends Microbiol.* **2007***, 15*, 279-289.
240. Anchel, M.; Hervey, A.; Robbins, W. J. Antibiotic substances from Basidiomycetes+. VII. Clitocybe illudens, *Proc. Natl. Acad. Sci. U. S. A.* **1950***, 36*, 300-305.
241. McMorris, T. C.; Anchel, M. Fungal Metabolites. the Structures of the Novel Sesquiterpenoids Illudin-S and -M, *J. Am. Chem. Soc.* **1965***, 87*, 1594-1600.
242. McMorris, T. C.; Kelner, M. J.; Wang, W.; Diaz, M. A.; Estes, L. A.; Taetle, R. Acylfulvenes, a new class of potent antitumor agents, *Experientia* **1996***, 52*, 75-80.
243. McMorris, T. C.; Kelner, M. J.; Wang, W.; Yu, J.; Estes, L. A.; Taetle, R. (Hydroxymethyl)acylfulvene: an illudin derivative with superior antitumor properties, *J. Nat. Prod.* **1996***, 59*, 896-899.
244. Kelner, M. J.; McMorris, T. C.; Taetle, R. Preclinical evaluation of illudins as anticancer agents: basis for selective cytotoxicity, *J. Natl. Cancer Inst.* **1990***, 82*, 1562-1565.
245. Kelner, M. J.; McMorris, T. C.; Estes, L.; Wang, W.; Samson, K. M.; Taetle, R. Efficacy of HMAF (MGI-114) in the MV522 metastatic lung carcinoma xenograft model nonresponsive to traditional anticancer agents, *Invest. New Drugs* **1996***, 14*, 161-167.
246. MacDonald, J. R.; Muscoplat, C. C.; Dexter, D. L.; Mangold, G. L.; Chen, S. F.; Kelner, M. J.; McMorris, T. C.; Von Hoff, D. D. Preclinical antitumor activity of 6-hydroxymethylacylfulvene, a semisynthetic derivative of the mushroom toxin illudin S, *Cancer Res.* **1997***, 57*, 279-283.
247. Kelner, M. J.; McMorris, T. C.; Montoya, M. A.; Estes, L.; Uglik, S. F.; Rutherford, M.; Samson, K. M.; Bagnell, R. D.; Taetle, R. Characterization of acylfulvene histiospecific toxicity in human tumor cell lines, *Cancer Chemother. Pharmacol.* **1998***, 41*, 237-242.
248. Kelner, M. J.; McMorris, T. C.; Montoya, M. A.; Estes, L.; Uglik, S. F.; Rutherford, M.; Samson, K. M.; Bagnell, R. D.; Taetle, R. Characterization of MGI 114 (HMAF) histiospecific toxicity in human tumor cell lines, *Cancer Chemother. Pharmacol.* **1999***, 44*, 235-240.
249. Gong, J.; Vaidyanathan, V. G.; Yu, X.; Kensler, T. W.; Peterson, L. A.; Sturla, S. J. Depurinating acylfulvene-DNA adducts: characterizing cellular chemical reactions of a selective antitumor agent, *J. Am. Chem. Soc.* **2007***, 129*, 2101-2111.
250. Jaspers, N. G.; Raams, A.; Kelner, M. J.; Ng, J. M.; Yamashita, Y. M.; Takeda, S.; McMorris, T. C.; Hoeijmakers, J. H. Anti-tumour compounds illudin S and Irofulven induce DNA lesions ignored by global repair and exclusively processed by transcription- and replication-coupled repair pathways, *DNA Repair (Amst)* **2002***, 1*, 1027-1038.
251. Koeppel, F.; Poindessous, V.; Lazar, V.; Raymond, E.; Sarasin, A.; Larsen, A. K. Irofulven cytotoxicity depends on transcription-coupled nucleotide excision repair

and is correlated with XPG expression in solid tumor cells, *Clin. Cancer Res.* **2004**, *10*, 5604-5613.
252. Amato, R. J.; Perez, C.; Pagliaro, L. Irofulven, a novel inhibitor of DNA synthesis, in metastatic renal cell cancer, *Invest. New Drugs* **2002**, *20*, 413-417.
253. Herzig, M. C.; Arnett, B.; MacDonald, J. R.; Woynarowski, J. M. Drug uptake and cellular targets of hydroxymethylacylfulvene (HMAF), *Biochem. Pharmacol.* **1999**, *58*, 217-225.
254. McMorris, T. C.; Yu, J.; Ngo, H. T.; Wang, H.; Kelner, M. J. Preparation and biological activity of amino acid and peptide conjugates of antitumor hydroxymethylacylfulvene, *J. Med. Chem.* **2000**, *43*, 3577-3580.
255. Liebler, D. C. Protein damage by reactive electrophiles: targets and consequences, *Chem. Res. Toxicol.* **2008**, *21*, 117-128.
256. Massey, V.; Williams, C. H.,Jr On the reaction mechanism of yeast glutathione reductase, *J. Biol. Chem.* **1965**, *240*, 4470-4480.
257. Sweet, W. L.; Blanchard, J. S. Human erythrocyte glutathione reductase: chemical mechanism and structure of the transition state for hydride transfer, *Biochemistry* **1991**, *30*, 8702-8709.
258. Arning, J.; Dringen, R.; Schmidt, M.; Thiessen, A.; Stolte, S.; Matzke, M.; Bottin-Weber, U.; Caesar-Geertz, B.; Jastorff, B.; Ranke, J. Structure-activity relationships for the impact of selected isothiazol-3-one biocides on glutathione metabolism and glutathione reductase of the human liver cell line Hep G2, *Toxicology* **2008**, *246*, 203-212.
259. Paci, A.; Rezai, K.; Deroussent, A.; De Valeriola, D.; Re, M.; Weill, S.; Cvitkovic, E.; Kahatt, C.; Shah, A.; Waters, S.; Weems, G.; Vassal, G.; Lokiec, F. Pharmacokinetics, metabolism, and routes of excretion of intravenous irofulven in patients with advanced solid tumors, *Drug Metab. Dispos.* **2006**, *34*, 1918-1926.
260. Dick, R. A.; Kwak, M. K.; Sutter, T. R.; Kensler, T. W. Antioxidative function and substrate specificity of NAD(P)H-dependent alkenal/one oxidoreductase. A new role for leukotriene B4 12-hydroxydehydrogenase/15-oxoprostaglandin 13-reductase, *J. Biol. Chem.* **2001**, *276*, 40803-40810.
261. KITZ, R.; WILSON, I. B. Esters of methanesulfonic acid as irreversible inhibitors of acetylcholinesterase, *J. Biol. Chem.* **1962**, *237*, 3245-3249.
262. McMorris, T. C.; Elayadi, A. N.; Yu, J.; Hu, Y.; Kelner, M. J. Metabolism of antitumor hydroxymethylacylfulvene by rat liver cytosol, *Drug Metab. Dispos.* **1999**, *27*, 983-985.
263. McMorris, T. C.; Elayadi, A. N.; Yu, J.; Kelner, M. J. Metabolism of antitumor acylfulvene by rat liver cytosol, *Biochem. Pharmacol.* **1999**, *57*, 83-88.
264. Tanaka, K.; Inoue, T.; Kadota, S.; Kikuchi, T. Metabolism by rat liver cytosol of illudin S, a toxic substance of Lampteromyces japonicus. II. Characterization of illudin S-metabolizing enzyme, *Xenobiotica* **1992**, *22*, 33-39.
265. Louzada, P. R.; Sebollela, A.; Scaramello, M. E.; Ferreira, S. T. Predissociated Dimers and Molten Globule Monomers in the Equilibrium Unfolding of Yeast Glutathione Reductase, *Biophysical journal* **2003**, *85*, 3255-3256-3261.

266. Morais, A. C. S.; Chapeaurouge, A.; Ferreira, S. T. Acid- and pressure-induced (un)folding of yeast glutathione reductase: Competition between protein oligomerization and aggregation, *The international journal of biochemistry & cell biology* **2005***, 37*, 1890-1891-1899.
267. Seefeldt, T.; Zhao, Y.; Chen, W.; Raza, A. S.; Carlson, L.; Herman, J.; Stoebner, A.; Hanson, S.; Foll, R.; Guan, X. Characterization of a novel dithiocarbamate glutathione reductase inhibitor and its use as a tool to modulate intracellular glutathione, *J. Biol. Chem.* **2009***, 284*, 2729-2737.
268. Karplus, P. A.; Krauth-Siegel, R. L.; Schirmer, R. H.; Schulz, G. E. Inhibition of human glutathione reductase by the nitrosourea drugs 1,3-bis(2-chloroethyl)-1-nitrosourea and 1-(2-chloroethyl)-3-(2-hydroxyethyl)-1-nitrosourea. A crystallographic analysis, *Eur. J. Biochem.* **1988***, 171*, 193-198.
269. Sechi, S.; Chait, B. T. Modification of cysteine residues by alkylation. A tool in peptide mapping and protein identification, *Anal. Chem.* **1998***, 70*, 5150-5158.
270. Johnson, R. S.; Martin, S. A.; Biemann, K.; Stults, J. T.; Watson, J. T. Novel fragmentation process of peptides by collision-induced decomposition in a tandem mass spectrometer: differentiation of leucine and isoleucine, *Analytical Chemistry* **1987***, 59*, 2621-2622-2625.
271. Dennehy, M. K.; Richards, K. A.; Wernke, G. R.; Shyr, Y.; Liebler, D. C. Cytosolic and nuclear protein targets of thiol-reactive electrophiles, *Chem. Res. Toxicol.* **2006***, 19*, 20-29.
272. Gisela, K. E.; SCHIRMER, R. H.; Renate, U. G. Glutathione Reductase from Human Erythrocytes, *European journal of biochemistry / FEBS* **1981***, 120*, 407-408-419.
273. Jones, E. T.; Williams, C. H.,Jr The sequence of amino acid residues around the oxidation-reduction active disulfide in yeast glutathione reductase, *J. Biol. Chem.* **1975***, 250*, 3779-3784.
274. Arscott, L. D.; Drake, D. M.; Williams, C. H.,Jr Inactivation-reactivation of two-electron reduced Escherichia coli glutathione reductase involving a dimer-monomer equilibrium, *Biochemistry* **1989***, 28*, 3591-3598.
275. Arscott, L. D.; Drake, D. M.; Williams, C. H.,Jr The structure of the flavoenzyme glutathione reductase, *Nature* **1978***, 273*, 120-121-124.
276. Rendon, J. L.; Mendoza-Hernandez, G. Unfolding kinetics of glutathione reductase from cyanobacterium Spirulina maxima, *Arch. Biochem. Biophys.* **2001***, 387*, 265-272.
277. Sebollela, A.; Louzada, P. R.; Sola-Penna, M.; Sarone-Williams, V.; Coelho-Sampaio, T.; Ferreira, S. T. Inhibition of yeast glutathione reductase by trehalose: possible implications in yeast survival and recovery from stress, *Int. J. Biochem. Cell Biol.* **2004***, 36*, 900-908.
278. Vander Jagt, D. L.; Hunsaker, L. A.; Vander Jagt, T. J.; Gomez, M. S.; Gonzales, D. M.; Deck, L. M.; Royer, R. E. Inactivation of glutathione reductase by 4-hydroxynonenal and other endogenous aldehydes, *Biochem. Pharmacol.* **1997***, 53*, 1133-1140.

279. Baylor, K. J.; Shine, C. M.; Heffron, J. J.; McIntosh, J. Isocyanate binding to yeast glutathione reductase measured by fluorescence spectroscopy, *Biochem. Soc. Trans.* **1997***, 25*, 47S.
280. Karplus, P. A.; Schulz, G. E. Refined structure of glutathione reductase at 1.54 A resolution, *J. Mol. Biol.* **1987***, 195*, 701-729.
281. Mittl, P. R.; Schulz, G. E. Structure of glutathione reductase from Escherichia coli at 1.86 A resolution: comparison with the enzyme from human erythrocytes, *Protein Sci.* **1994***, 3*, 799-809.
282. Pandey, A.; Katiyar, S. S. Inactivation of yeast glutathione reductase by O-phthalaldehyde, *J. Enzyme Inhib.* **1996***, 11*, 141-149.
283. Dongre, A. R.; Jones, A. L.; Somogyi, A.; Wysocki, V. H. Influence of Peptide Composition, Gas-Phase Basicity, and Chemical Modification on Fragmentation Efficiency: Evidence for the Mobile Proton Model, *J. Am. Chem. Soc.* **1996***, 118*, 8365-8366-8374.
284. Stapels, M. D.; Barofsky, D. F. Complementary use of MALDI and ESI for the HPLC-MS/MS analysis of DNA-binding proteins, *Anal. Chem.* **2004***, 76*, 5423-5430.
285. Lippman, S. M.; Heymach, J. V. The convergent development of molecular-targeted drugs for cancer treatment and prevention, *Clin. Cancer Res.* **2007***, 13*, 4035-4041.
286. Kelner, M. J.; McMorris, T. C.; Beck, W. T.; Zamora, J. M.; Taetle, R. Preclinical evaluation of illudins as anticancer agents, *Cancer Res.* **1987***, 47*, 3186-3189.
287. Schobert, R.; Biersack, B.; Knauer, S.; Ocker, M. Conjugates of the fungal cytotoxin illudin M with improved tumour specificity, *Bioorg. Med. Chem.* **2008***, 16*, 8592-8597.
288. Knauer, S.; Biersack, B.; Zoldakova, M.; Effenberger, K.; Milius, W.; Schobert, R. Melanoma-specific ferrocene esters of the fungal cytotoxin illudin M, *Anticancer Drugs* **2009***, 20*, 676-681.
289. McMorris, T. C.; Yu, J.; Hu, Y.; Estes, L. A.; Kelner, M. J. Design and Synthesis of Antitumor Acylfulvenes, *J. Org. Chem.* **1997***, 62*, 3015-3018.
290. McMorris, T. C.; Yu, J.; Lira, R.; Dawe, R.; MacDonald, J. R.; Waters, S. J.; Estes, L. A.; Kelner, M. J. Structure-activity studies of antitumor agent irofulven (hydroxymethylacylfulvene) and analogues, *J. Org. Chem.* **2001***, 66*, 6158-6163.
291. Kelner, M. J.; McMorris, T. C.; Estes, L.; Rutherford, M.; Montoya, M.; Goldstein, J.; Samson, K.; Starr, R.; Taetle, R. Characterization of illudin S sensitivity in DNA repair-deficient Chinese hamster cells. Unusually high sensitivity of ERCC2 and ERCC3 DNA helicase-deficient mutants in comparison to other chemotherapeutic agents, *Biochem. Pharmacol.* **1994***, 48*, 403-409.
292. Neels, J. F.; Gong, J.; Yu, X.; Sturla, S. J. Quantitative correlation of drug bioactivation and deoxyadenosine alkylation by acylfulvene, *Chem. Res. Toxicol.* **2007***, 20*, 1513-1519.
293. Woynarowski, J. M.; Napier, C.; Koester, S. K.; Chen, S. F.; Troyer, D.; Chapman, W.; MacDonald, J. R. Effects on DNA integrity and apoptosis induction by a novel antitumor sesquiterpene drug, 6-hydroxymethylacylfulvene (HMAF, MGI 114), *Biochem. Pharmacol.* **1997***, 54*, 1181-1193.

294. Woynarowska, B. A.; Woynarowski, J. M.; Herzig, M. C.; Roberts, K.; Higdon, A. L.; MacDonald, J. R. Differential cytotoxicity and induction of apoptosis in tumor and normal cells by hydroxymethylacylfulvene (HMAF), *Biochem. Pharmacol.* **2000**, *59*, 1217-1226.
295. McMorris, T. C. Discovery and development of sesquiterpenoid derived hydroxymethylacylfulvene: a new anticancer drug, *Bioorg. Med. Chem.* **1999**, *7*, 881-886.
296. Kelner, M. J.; McMorris, T. C.; Montoya, M. A.; Estes, L.; Rutherford, M.; Samson, K. M.; Taetle, R. Characterization of cellular accumulation and toxicity of illudin S in sensitive and nonsensitive tumor cells, *Cancer Chemother. Pharmacol.* **1997**, *40*, 65-71.
297. Giles, G. I. The redox regulation of thiol dependent signaling pathways in cancer, *Curr. Pharm. Des.* **2006**, *12*, 4427-4443.
298. Ogasawara, M. A.; Zhang, H. Redox Regulation and its Emerging Roles in Stem Cells and Stem-Like Cancer Cells, *Antioxid. Redox Signal.* **2008**.
299. Liu, X.; Sturla, S. J. Profiling patterns of glutathione reductase inhibition by the natural product illudin S and its acylfulvene analogues, *Mol. Biosyst* **2009**, *5*, 1013-1024.
300. Eklund, H.; Gleason, F. K.; Holmgren, A. Structural and functional relations among thioredoxins of different species, *Proteins* **1991**, *11*, 13-28.
301. LAURENT, T. C.; MOORE, E. C.; REICHARD, P. Enzymatic Synthesis of Deoxyribonucleotides. Iv. Isolation and Characterization of Thioredoxin, the Hydrogen Donor from Escherichia Coli B, *J. Biol. Chem.* **1964**, *239*, 3436-3444.
302. Holmgren, A. Thioredoxin and glutaredoxin systems, *J. Biol. Chem.* **1989**, *264*, 13963-13966.
303. Mustacich, D.; Powis, G. Thioredoxin reductase, *Biochem. J.* **2000**, *346 Pt 1*, 1-8.
304. Saitoh, M.; Nishitoh, H.; Fujii, M.; Takeda, K.; Tobiume, K.; Sawada, Y.; Kawabata, M.; Miyazono, K.; Ichijo, H. Mammalian thioredoxin is a direct inhibitor of apoptosis signal-regulating kinase (ASK) 1, *EMBO J.* **1998**, *17*, 2596-2606.
305. Powis, G.; Mustacich, D.; Coon, A. The role of the redox protein thioredoxin in cell growth and cancer, *Free Radic. Biol. Med.* **2000**, *29*, 312-322.
306. Nadeau, P. J.; Charette, S. J.; Toledano, M. B.; Landry, J. Disulfide Bond-mediated multimerization of Ask1 and its reduction by thioredoxin-1 regulate H(2)O(2)-induced c-Jun NH(2)-terminal kinase activation and apoptosis, *Mol. Biol. Cell* **2007**, *18*, 3903-3913.
307. Welsh, S. J.; Bellamy, W. T.; Briehl, M. M.; Powis, G. The redox protein thioredoxin-1 (Trx-1) increases hypoxia-inducible factor 1alpha protein expression: Trx-1 overexpression results in increased vascular endothelial growth factor production and enhanced tumor angiogenesis, *Cancer Res.* **2002**, *62*, 5089-5095.
308. Qin, J.; Clore, G. M.; Kennedy, W. M.; Huth, J. R.; Gronenborn, A. M. Solution structure of human thioredoxin in a mixed disulfide intermediate complex with its target peptide from the transcription factor NF kappa B, *Structure* **1995**, *3*, 289-297.

309. Ueno, M.; Masutani, H.; Arai, R. J.; Yamauchi, A.; Hirota, K.; Sakai, T.; Inamoto, T.; Yamaoka, Y.; Yodoi, J.; Nikaido, T. Thioredoxin-dependent redox regulation of p53-mediated p21 activation, *J. Biol. Chem.* **1999**, *274*, 35809-35815.
310. Grogan, T. M.; Fenoglio-Prieser, C.; Zeheb, R.; Bellamy, W.; Frutiger, Y.; Vela, E.; Stemmerman, G.; Macdonald, J.; Richter, L.; Gallegos, A.; Powis, G. Thioredoxin, a putative oncogene product, is overexpressed in gastric carcinoma and associated with increased proliferation and increased cell survival, *Hum. Pathol.* **2000**, *31*, 475-481.
311. Denko, N.; Schindler, C.; Koong, A.; Laderoute, K.; Green, C.; Giaccia, A. Epigenetic regulation of gene expression in cervical cancer cells by the tumor microenvironment, *Clin. Cancer Res.* **2000**, *6*, 480-487.
312. Yokomizo, A.; Ono, M.; Nanri, H.; Makino, Y.; Ohga, T.; Wada, M.; Okamoto, T.; Yodoi, J.; Kuwano, M.; Kohno, K. Cellular levels of thioredoxin associated with drug sensitivity to cisplatin, mitomycin C, doxorubicin, and etoposide, *Cancer Res.* **1995**, *55*, 4293-4296.
313. Kim, S. J.; Miyoshi, Y.; Taguchi, T.; Tamaki, Y.; Nakamura, H.; Yodoi, J.; Kato, K.; Noguchi, S. High thioredoxin expression is associated with resistance to docetaxel in primary breast cancer, *Clin. Cancer Res.* **2005**, *11*, 8425-8430.
314. Weichsel, A.; Gasdaska, J. R.; Powis, G.; Montfort, W. R. Crystal structures of reduced, oxidized, and mutated human thioredoxins: evidence for a regulatory homodimer, *Structure* **1996**, *4*, 735-751.
315. Katti, S. K.; LeMaster, D. M.; Eklund, H. Crystal structure of thioredoxin from Escherichia coli at 1.68 A resolution, *J. Mol. Biol.* **1990**, *212*, 167-184.
316. Holmgren, A. Thioredoxin catalyzes the reduction of insulin disulfides by dithiothreitol and dihydrolipoamide, *J. Biol. Chem.* **1979**, *254*, 9627-9632.
317. Kim, J. R.; Yoon, H. W.; Kwon, K. S.; Lee, S. R.; Rhee, S. G. Identification of proteins containing cysteine residues that are sensitive to oxidation by hydrogen peroxide at neutral pH, *Anal. Biochem.* **2000**, *283*, 214-221.
318. Stryer, L.; Holmgren, A.; Reichard, P. Thioredoxin. A localized conformational change accompanying reduction of the protein to the sulfhydryl form, *Biochemistry* **1967**, *6*, 1016-1020.
319. Holmgren, A. Tryptophan fluorescence study of conformational transitions of the oxidized and reduced form of thioredoxin, *J. Biol. Chem.* **1972**, *247*, 1992-1998.
320. Ado, K.; Taniguchi, Y. Pressure effects on the structure and function of human thioredoxin, *Biochim. Biophys. Acta* **2007**, *1774*, 813-821.
321. Holmgren, A. Enzymatic reduction-oxidation of protein disulfides by thioredoxin, *Methods Enzymol.* **1984**, *107*, 295-300.
322. Arai, R. J.; Masutani, H.; Yodoi, J.; Debbas, V.; Laurindo, F. R.; Stern, A.; Monteiro, H. P. Nitric oxide induces thioredoxin-1 nuclear translocation: possible association with the p21Ras survival pathway, *Biochem. Biophys. Res. Commun.* **2006**, *348*, 1254-1260.
323. Chen, X. P.; Liu, S.; Tang, W. X.; Chen, Z. W. Nuclear thioredoxin-1 is required to suppress cisplatin-mediated apoptosis of MCF-7 cells, *Biochem. Biophys. Res. Commun.* **2007**, *361*, 362-366.

324. Ceccarelli, J.; Delfino, L.; Zappia, E.; Castellani, P.; Borghi, M.; Ferrini, S.; Tosetti, F.; Rubartelli, A. The redox state of the lung cancer microenvironment depends on the levels of thioredoxin expressed by tumor cells and affects tumor progression and response to prooxidants, *Int. J. Cancer* **2008**, *123*, 1770-1778.
325. Kuo, M. T. Redox regulation of multidrug resistance in cancer chemotherapy: molecular mechanisms and therapeutic opportunities, *Antioxid. Redox Signal.* **2009**, *11*, 99-133.
326. Rollin-Genetet, F.; Berthomieu, C.; Davin, A. H.; Quemeneur, E. Escherichia coli thioredoxin inhibition by cadmium: two mutually exclusive binding sites involving Cys32 and Asp26, *Eur. J. Biochem.* **2004**, *271*, 1299-1309.
327. Woynarowska, B. A.; Woynarowski, J. M.; Liang, H.; Herzig, M. C. S.; Leal, B. Z.; Vallejo, M.; Moyer, M. P.; Waters, S. J. Irofulven binding and inactivation of purified and cellular redox-controlling proteins, 2004.
328. Shibata, T.; Yamada, T.; Ishii, T.; Kumazawa, S.; Nakamura, H.; Masutani, H.; Yodoi, J.; Uchida, K. Thioredoxin as a molecular target of cyclopentenone prostaglandins, *J. Biol. Chem.* **2003**, *278*, 26046-26054.
329. Bradshaw, T. D.; Matthews, C. S.; Cookson, J.; Chew, E. H.; Shah, M.; Bailey, K.; Monks, A.; Harris, E.; Westwell, A. D.; Wells, G.; Laughton, C. A.; Stevens, M. F. Elucidation of thioredoxin as a molecular target for antitumor quinols, *Cancer Res.* **2005**, *65*, 3911-3919.
330. Kelner, M. J.; McMorris, T. C.; Rojas, R. J.; Trani, N. A.; Estes, L. Enhanced antitumor activity of irofulven in combination with thiotepa or mitomycin C, *Cancer Chemother. Pharmacol.* **2002**, *49*, 412-418.
331. Poindessous, V.; Koeppel, F.; Raymond, E.; Cvitkovic, E.; Waters, S. J.; Larsen, A. K. Enhanced antitumor activity of irofulven in combination with 5-fluorouracil and cisplatin in human colon and ovarian carcinoma cells, *Int. J. Oncol.* **2003**, *23*, 1347-1355.
332. Bertini, R.; Howard, O. M.; Dong, H. F.; Oppenheim, J. J.; Bizzarri, C.; Sergi, R.; Caselli, G.; Pagliei, S.; Romines, B.; Wilshire, J. A.; Mengozzi, M.; Nakamura, H.; Yodoi, J.; Pekkari, K.; Gurunath, R.; Holmgren, A.; Herzenberg, L. A.; Herzenberg, L. A.; Ghezzi, P. Thioredoxin, a redox enzyme released in infection and inflammation, is a unique chemoattractant for neutrophils, monocytes, and T cells, *J. Exp. Med.* **1999**, *189*, 1783-1789.
333. Karimpour, S.; Lou, J.; Lin, L. L.; Rene, L. M.; Lagunas, L.; Ma, X.; Karra, S.; Bradbury, C. M.; Markovina, S.; Goswami, P. C.; Spitz, D. R.; Hirota, K.; Kalvakolanu, D. V.; Yodoi, J.; Gius, D. Thioredoxin reductase regulates AP-1 activity as well as thioredoxin nuclear localization via active cysteines in response to ionizing radiation, *Oncogene* **2002**, *21*, 6317-6327.
334. Watson, W. H.; Jones, D. P. Oxidation of nuclear thioredoxin during oxidative stress, *FEBS Lett.* **2003**, *543*, 144-147.
335. Rayman, M. P. Selenium in cancer prevention: a review of the evidence and mechanism of action, *Proc. Nutr. Soc.* **2005**, *64*, 527-542.
336. Zeng, H.; Combs, G. F.,Jr Selenium as an anticancer nutrient: roles in cell proliferation and tumor cell invasion, *J. Nutr. Biochem.* **2008**, *19*, 1-7.

337. Lu, J.; Jiang, C. Selenium and cancer chemoprevention: hypotheses integrating the actions of selenoproteins and selenium metabolites in epithelial and non-epithelial target cells, *Antioxid. Redox Signal.* **2005***, 7*, 1715-1727.
338. Hac, E.; Krechniak, J.; Szyszko, M. Selenium levels in human plasma and hair in northern Poland, *Biol. Trace Elem. Res.* **2002***, 85*, 277-285.
339. Hincal, F.; Basaran, N.; Yetgin, S.; Gokmen, O. Selenium status in Turkey. II. Serum selenium concentration in healthy residents of different ages in Ankara, *J. Trace Elem. Electrolytes Health Dis.* **1994***, 8*, 9-12.
340. Korunova, V.; Skodova, Z.; Dedina, J.; Valenta, Z.; Parizek, J.; Pisa, Z.; Styblo, M. Serum selenium in adult Czechoslovak (central Bohemia) population, *Biol. Trace Elem. Res.* **1993***, 37*, 91-99.
341. Sen'kevich, O. A.; Golubkina, N. A.; Kliuchnikova, N. F.; Kliuchnikov, P. F.; Sirotina, Z. V.; Koval'skii, I. The human selenium status in the Far East of Russia, *Vopr. Pitan.* **2008***, 77*, 67-71.
342. Gladyshev, V. N.; Jeang, K. T.; Stadtman, T. C. Selenocysteine, identified as the penultimate C-terminal residue in human T-cell thioredoxin reductase, corresponds to TGA in the human placental gene, *Proc. Natl. Acad. Sci. U. S. A.* **1996***, 93*, 6146-6151.
343. Forstrom, J. W.; Zakowski, J. J.; Tappel, A. L. Identification of the catalytic site of rat liver glutathione peroxidase as selenocysteine, *Biochemistry* **1978***, 17*, 2639-2644.
344. Asahi, M.; Fujii, J.; Takao, T.; Kuzuya, T.; Hori, M.; Shimonishi, Y.; Taniguchi, N. The oxidation of selenocysteine is involved in the inactivation of glutathione peroxidase by nitric oxide donor, *J. Biol. Chem.* **1997***, 272*, 19152-19157.
345. Esworthy, R. S.; Baker, M. A.; Chu, F. F. Expression of selenium-dependent glutathione peroxidase in human breast tumor cell lines, *Cancer Res.* **1995***, 55*, 957-962.
346. Hashemy, S. I.; Ungerstedt, J. S.; Zahedi Avval, F.; Holmgren, A. Motexafin gadolinium, a tumor-selective drug targeting thioredoxin reductase and ribonucleotide reductase, *J. Biol. Chem.* **2006***, 281*, 10691-10697.
347. Huber, R. E.; Criddle, R. S. Comparison of the chemical properties of selenocysteine and selenocystine with their sulfur analogs, *Arch. Biochem. Biophys.* **1967***, 122*, 164-173.
348. Gallegos, A.; Berggren, M.; Gasdaska, J. R.; Powis, G. Mechanisms of the regulation of thioredoxin reductase activity in cancer cells by the chemopreventive agent selenium, *Cancer Res.* **1997***, 57*, 4965-4970.
349. Zhang, J.; Svehlikova, V.; Bao, Y.; Howie, A. F.; Beckett, G. J.; Williamson, G. Synergy between sulforaphane and selenium in the induction of thioredoxin reductase 1 requires both transcriptional and translational modulation, *Carcinogenesis* **2003***, 24*, 497-503.
350. TADA, M.; YAMADA, Y.; BHACCA, N. S.; NAKANISHI, K.; OHASHI, M. Structure and Reactions of Illudin-S (Lampterol), *Chem. Pharm. Bull. (Tokyo)* **1964***, 12*, 853-855.

351. Yu, S. Y.; Ao, P.; Wang, L. M.; Huang, S. L.; Chen, H. C.; Lu, X. P.; Liu, Q. Y. Biochemical and cellular aspects of the anticancer activity of selenium, *Biol. Trace Elem. Res.* **1988**, *15*, 243-255.
352. Novoselov, S. V.; Calvisi, D. F.; Labunskyy, V. M.; Factor, V. M.; Carlson, B. A.; Fomenko, D. E.; Moustafa, M. E.; Hatfield, D. L.; Gladyshev, V. N. Selenoprotein deficiency and high levels of selenium compounds can effectively inhibit hepatocarcinogenesis in transgenic mice, *Oncogene* **2005**, *24*, 8003-8011.
353. Gundimeda, U.; Schiffman, J. E.; Gottlieb, S. N.; Roth, B.; Gopalakrishna, R. Negation of the cancer-preventive actions of selenium by overexpression of protein kinase C{epsilon} and selenoprotein thioredoxin reductase, *Carcinogenesis* **2009**.
354. Allmang, C.; Wurth, L.; Krol, A. The selenium to selenoprotein pathway in eukaryotes: More molecular partners than anticipated, *Biochim. Biophys. Acta* **2009**.
355. Renko, K.; Hofmann, P. J.; Stoedter, M.; Hollenbach, B.; Behrends, T.; Kohrle, J.; Schweizer, U.; Schomburg, L. Down-regulation of the hepatic selenoprotein biosynthesis machinery impairs selenium metabolism during the acute phase response in mice, *FASEB J.* **2009**, *23*, 1758-1765.
356. Karunasinghe, N.; Ferguson, L. R.; Tuckey, J.; Masters, J. Hemolysate thioredoxin reductase and glutathione peroxidase activities correlate with serum selenium in a group of New Zealand men at high prostate cancer risk, *J. Nutr.* **2006**, *136*, 2232-2235.
357. Arscott, L. D.; Gromer, S.; Schirmer, R. H.; Becker, K.; Williams, C. H.,Jr The mechanism of thioredoxin reductase from human placenta is similar to the mechanisms of lipoamide dehydrogenase and glutathione reductase and is distinct from the mechanism of thioredoxin reductase from Escherichia coli, *Proc. Natl. Acad. Sci. U. S. A.* **1997**, *94*, 3621-3626.
358. Williams, C. H.; Arscott, L. D.; Muller, S.; Lennon, B. W.; Ludwig, M. L.; Wang, P. F.; Veine, D. M.; Becker, K.; Schirmer, R. H. Thioredoxin reductase two modes of catalysis have evolved, *Eur. J. Biochem.* **2000**, *267*, 6110-6117.
359. Zhong, L.; Holmgren, A. Essential role of selenium in the catalytic activities of mammalian thioredoxin reductase revealed by characterization of recombinant enzymes with selenocysteine mutations, *J. Biol. Chem.* **2000**, *275*, 18121-18128.
360. Tamura, T.; Stadtman, T. C. A new selenoprotein from human lung adenocarcinoma cells: purification, properties, and thioredoxin reductase activity, *Proc. Natl. Acad. Sci. U. S. A.* **1996**, *93*, 1006-1011.
361. Hu, Y.; Urig, S.; Koncarevic, S.; Wu, X.; Fischer, M.; Rahlfs, S.; Mersch-Sundermann, V.; Becker, K. Glutathione- and thioredoxin-related enzymes are modulated by sulfur-containing chemopreventive agents, *Biol. Chem.* **2007**, *388*, 1069-1081.
362. Vadgama, J. V.; Wu, Y.; Shen, D.; Hsia, S.; Block, J. Effect of selenium in combination with Adriamycin or Taxol on several different cancer cells, *Anticancer Res.* **2000**, *20*, 1391-1414.
363. Fakih, M.; Cao, S.; Durrani, F. A.; Rustum, Y. M. Selenium protects against toxicity induced by anticancer drugs and augments antitumor activity: a highly selective,

new, and novel approach for the treatment of solid tumors, *Clin. Colorectal Cancer.* **2005***, 5*, 132-135.
364. Rudolf, E.; Radocha, J.; Cervinka, M.; Cerman, J. Combined effect of sodium selenite and campthotecin on cervical carcinoma cells, *Neoplasma* **2004***, 51*, 127-135.
365. Ladenstein, R.; Epp, O.; Bartels, K.; Jones, A.; Huber, R.; Wendel, A. Structure analysis and molecular model of the selenoenzyme glutathione peroxidase at 2.8 A resolution, *J. Mol. Biol.* **1979***, 134*, 199-218.
366. Hanna, P. E. N-acetyltransferases, O-acetyltransferases, and N,O-acetyltransferases: enzymology and bioactivation, *Adv. Pharmacol.* **1994***, 27*, 401-430.
367. Meerman, J. H.; van de Poll, M. L. Metabolic activation routes of arylamines and their genotoxic effects, *Environ. Health Perspect.* **1994***, 102 Suppl 6*, 153-159.
368. Zhang, N.; Liu, L.; Liu, F.; Wagner, C. R.; Hanna, P. E.; Walters, K. J. NMR-based model reveals the structural determinants of mammalian arylamine N-acetyltransferase substrate specificity, *J. Mol. Biol.* **2006***, 363*, 188-200.
369. Liu, L.; Wagner, C. R.; Hanna, P. E. Human arylamine N-acetyltransferase 1: in vitro and intracellular inactivation by nitrosoarene metabolites of toxic and carcinogenic arylamines, *Chem. Res. Toxicol.* **2008***, 21*, 2005-2016.
370. Wang, H.; Guo, Z.; Vath, G. M.; Wagner, C. R.; Hanna, P. E. Chemical modification of hamster arylamine N-acetyltransferase 2 with isozyme-selective and nonselective N-arylbromoacetamido reagents, *Protein J.* **2004***, 23*, 153-166.
371. Wang, H.; Liu, L.; Hanna, P. E.; Wagner, C. R. Catalytic mechanism of hamster arylamine N-acetyltransferase 2, *Biochemistry* **2005***, 44*, 11295-11306.